
REVERSAL OF OXALIPLATIN
RESISTANCE BY NEW ZEALAND
MANUKA HONEY EXTRACTS IN
GASTROINTESTINAL CANCER CELLS

Wei (Vivi) Lu
School of Science

September 2024

*A thesis submitted in complete fulfilment of the requirements for the degree of
Doctor of Philosophy, Auckland University of Technology, 2024*

Abstract

Gastrointestinal (GI) cancers remain among the leading causes of cancer-related deaths worldwide. GI cancer is one of the leading causes of cancer mortality in New Zealand with over 4,000 new cases and more than 1,000 deaths by GI cancers reported annually in NZ. Therefore, GI cancer is a big health burden to the health system. Although oxaliplatin-based chemotherapy has been widely adopted as the standard and preferred regimen for treating GI cancers including colorectal cancer (CRC), tumour resistance is one of the major limitations for many patients in clinical practice. Recently, our team has reported that MRP2 (a member of ATP-Binding Cassete (ABC) transporter protein) confers oxaliplatin resistance and a phytochemical MRP2 inhibitor myricetin increased cellular platinum accumulation and oxaliplatin cytotoxicity in several human GI cancer cell lines (Biswas et al., 2019; Khine et al., 2019). However, myricetin is not a potent MRP2 inhibitor and it only marginally enhanced oxaliplatin sensitivity in tumour xenograft mouse model (Khine et al., 2019). Manuka honey is produced from the nectar of the Manuka tree (*Leptospermum scoparium*), a native of New Zealand. Previous studies have shown that the content of Manuka honey contains more phenolic and flavonoid antioxidants in comparison to other types of honey worldwide. The strong antioxidant capacities of Manuka honey make them promising sources for further extraction/development of anticancer and chemopreventive compounds. Treatment with Manuka honey alone resulted in significant inhibition of colorectal tumour growth (Maria, Rkia, & Fawaz et al., 2013). Our team and others also discovered the anti-proliferation effects of NZ Manuka honey in several CRC cell lines but not in normal cells (Chan, 2016). However, the exact anti-cancer compound(s) in NZ Manuka honey remain unknown. Given the fact that NZ Manuka honey contains abundant myricetin analogues and more than 90% of ABC transporter inhibitors are derived from phytochemicals, this project aims to identify novel and potent MRP2 inhibitors/modulators from NZ Manuka honey.

In Chapter 3, a comprehensive LC–MS/MS method has been developed and validated for the relative quantitation of 14 fingerprint phenolic compounds. NZ Manuka honey contains a significant amount of quercetin, methyl syringate, DL-3-phenyllactic acid, chlorogenic acid, chrysin, myricetin, and 2-hydroxy-3-(4-methoxyphenyl) propanoic acid. A Mass Spectrometry Data Independent AnaLysis (MS-DIAL) approach was also explored to identify novel phytochemicals by aligning with the data from MS/MS libraries. To evaluate potential interactions between MRP2 and the NZ Manuka honey-derived fingerprint phenolic compounds, three-dimensional molecular docking of multiple ligands with MRP2 using an AutoDock Vina software was undertaken to identify MRP2 inhibitors based on the binding affinity and hydrogen bond interactions

(Chapter 4). AutoDock Vina-based *in silico* screening identified chrysin as a potential MRP2 inhibitor. To further build on *in silico* findings, heterogeneous expression systems using human embryonic kidney 293 cells (HEK293) overexpressing MRP2 were adapted in Chapter 5. The isogenic pair was employed to identify whether ligands that showed low binding affinities (Chapter 4) can inhibit the MRP2-mediated transport of a model substrate CDCF and reverse MRP2-conferred oxaliplatin resistance. Our results demonstrated that chrysin (10 μ M) increased the accumulation of CDCF and enhanced oxaliplatin cytotoxicity, in HEK-MRP2 cells, but not in HEK293 cells.

In Chapter 6, further studies were carried out to evaluate the concentration-dependant effect of chrysin on the cellular accumulation of CDCF *in vitro* in two GI cancer cell lines, Caco-2 and PANC-1, which overexpress ABCC2 (MRP2) endogenously. Chrysin reversed MRP2-mediated oxaliplatin resistance in both GI lines tested but only enhanced oxaliplatin-induced apoptosis in Caco-2 cell line. The findings provide critical insights into the mechanisms of chemoresistance in GI cancers and suggest potential strategies for enhancing oxaliplatin efficacy by combination treatment with chrysin. In conclusion, chrysin exerted concentration-dependent sensitization of oxaliplatin on ABCC2-expressing GI cancer cell lines (endogenously in Caco-2 and PANC-1) and these results may broaden our options to develop a novel combination therapy to sensitise tumour MDR in patients with GI cancers.

Acknowledgements

First and foremost, I would like to express my deepest gratitude to my primary supervisor, Associate Professor Yan Li, for his invaluable guidance and mentorship throughout the course of my doctoral journey. His continuous support, encouragement, and trust over the past four years have been instrumental in my growth and the completion of this project. As someone new to the biomedical field, I faced numerous challenges, but Prof. Li's unwavering belief in my potential inspired me to persevere. I am deeply thankful for his patience in teaching me new concepts and his insightful approach to cancer pharmacology, which has significantly shaped my understanding of the subject. Prof. Li's dedication to challenging and nurturing his students was a constant source of motivation, and I am truly grateful for the opportunity to learn under his supervision. His guidance in the lab, especially with unfamiliar instruments and procedures, has been invaluable. I am honoured to have been one of his students and appreciate all he has done to make me a better researcher.

I would also like to extend my heartfelt thanks to my co-supervisors, Dr. Rothman Kam and Associate Professor Brent Seal, for their unwavering support and willingness to share their expertise. Their thoughtful feedback and consistent availability have greatly contributed to the progress of my work. I truly appreciate their faith in allowing me to take on challenges and their readiness to assist whenever I needed guidance with my reports.

A special thank you goes to the members of the Biomedical lab: Sajeevani, Reem, Leo, and all my fellow lab mates. Your insights and support, both in scientific endeavours and day-to-day lab work, have been invaluable throughout my PhD. I am equally grateful to my dear friends Riya, Arthur, and Tracy, whose understanding and encouragement have made this journey more manageable. A special mention to my sister, Tracy, for her love, care, and for always being there to help me, from cooking to keeping my space organized—I appreciate you deeply.

Lastly, I wish to acknowledge the unwavering support of my family. To my parents and my daughter, your love and understanding have been my constant source of strength. Mum and Dad, thank you for your financial support and for always being just a phone call away, providing the comfort and encouragement I needed to push through. To my

daughter, even though you are too young to fully understand, your love has been my greatest motivation. I am sorry I couldn't always be there for you, but your affection and care, even at such a young age, have kept me going.

In closing, I want to reflect on the personal challenges I faced during this journey. From the struggles of the COVID-19 lockdown to personal hardships, including my battle with depression and the heartbreak of a broken relationship, this path was far from easy. But despite it all, I made it through, and I am proud to have come out stronger.

Attestation of Authorship

“I hereby declare that this submission is my own work and that, to the best of my knowledge and belief, it contains no material previously published or written by another person (except where explicitly defined in the acknowledgements), nor used artificial intelligence tools or generative artificial intelligence tools (unless it is clearly stated, and referenced, along with the purpose of use), nor material which to a substantial extent has been submitted for the award of any other degree or diploma of a university or other institution of higher learning.”

Signed: Date: 16th September, 2024

Contents

List of Figure	12
List of Table.....	15
Chapter 1 General Introduction	19
1.1. Overview of cancer and Gastrointestinal (GI) cancer	19
1.1.1. Cancer incidence in the world.....	20
1.1.2. Cancer incidence in New Zealand.....	20
1.1.3. GI Cancer and Colorectal Cancer.....	22
1.1.4. Gut microbiome and probiotics.....	27
1.2. Cancer chemotherapy regiments	29
1.2.1. Chemotherapy in colon cancer treatment.....	29
1.2.2. Chemotherapy in pancreatic cancer treatment	30
1.2.3. Platinum-based drugs.....	30
1.3. Anti-cancer drug resistance and ABC transporters.....	39
1.3.1. ABC transporters.....	43
1.3.2. Oxaliplatin uptake and ABC transporters	51
1.4. MRP2: Multidrug resistance-associated protein 2.....	55
1.4.1. MRP2 Transporter: A Key Player in Drug Metabolism, Detoxification, and Xenobiotic Defence.....	56
1.4.2. MRP2 Expression in Human Cancers: Implications for Chemoresistance and Potential as a Biomarker	57
1.4.3. Genetic Variants in the MRP2 Transporter (ABCC2): Implications for Dubin-Johnson Syndrome and Cancer Chemotherapy	58
1.4.4. The Role of MRP2 Transporters in Multidrug Resistance and Clinical Outcomes of Gastrointestinal Cancers: Implications for Platinum-Based Chemotherapy	59
1.5. Phytochemical inhibitors of ABC transporters	60
1.6. Manuka Honey	63

1.7. Hypothesis and aim of the thesis.....	66
Chapter 2 Materials and Methodology	69
2.1. Chemicals and equipment	69
2.2. Cell lines and cell culture.....	72
2.2.1. Human cell lines	72
2.2.2. Thawing cells	73
2.2.3. Cell maintenance and sub-culture	73
2.2.4. Cell counting.....	74
2.3. Cell viability Assay	74
2.3.1. Sample preparation	75
2.3.2. MTT assay	75
2.3.3. PrestoBlue™ Cell Viability	76
2.4. LC-MS/MS	76
2.4.1. LC-MS/MS Method Development.....	76
2.4.2. Method validation for myricetin quantification by LC-MS/MS.....	79
2.5. Western Blotting	80
2.5.1. Cell lysate preparation.....	81
2.5.2. DC Protein Assay.....	81
2.5.3. Sample Preparation	82
2.5.4. SDS PAGE.....	82
2.5.5. Transferring the protein from the gel to the membrane.....	82
2.5.6. Antibody Staining	83
2.5.7. Western Blotting Imaging and Data Analysis.....	83
2.6. Platinum cell accumulation by inductively coupled plasma spectrometry (ICP-MS).....	84
2.6.1. Protein concentration determination	84
2.6.2. Accumulation study of oxaliplatin	85

2.6.3. ICP-MS method validation for platinum quantification.....	85
2.7. Effect of chrysin on oxaliplatin-induced apoptosis in Caco-2 and PANC-1 cells by using Flow cytometry.....	87
2.7.1. Drug treatment	88
2.7.2. Sample preparation and flow cytometric analysis.....	89
2.8. Cell immunostaining of MRP2-Surface staining.....	89
2.8.1. MRP2 surface expression in HEK cell lines	90
2.8.2. Flow cytometry data analysis.....	91
2.9. Flow cytometry analysis-Beckman Coulter Kaluza software.....	92
2.10. Statistical analysis	93
Chapter 3 LC-MS/MS	94
3.1. Introduction.....	94
3.1.1. Machine and column information	94
3.1.2. Phenolics functions in Manuka Honey	95
3.2. Materials and methods.....	98
3.2.1. Chemicals and Standards	98
3.2.2. Standard Solutions	99
3.2.3. Extraction Procedure	99
3.2.4. LC-MS Method development by using myricetin-known phenolic....	100
3.2.5. Method Validation.....	100
3.2.6. LC-MS Analysis	101
3.2.7. MS-DIAL	102
3.2.8. Data analysis	102
3.3. LC-MS Analysis for Phenolics in Manuka Honey extract	102
3.2.1. Solid Phase Extraction (SPE) Sample Preparation.....	102
3.2.2. Phenolics LC-MS Total Ion Chromatogram (TIC) Scan in Manuka honey extract and MS-DIAL analysis	103

3.4. MRM validation for major phenolic compounds	107
3.5. Identification of Phenolic Compounds in Manuka Honey Extract ..	114
3.6. Summary	117
Chapter 4 In Silico Screening of MRP2 Inhibitors using AutoDock Vina ...	119
4.1. Introduction	119
4.2. Methods	121
4.2.1. Protein preparation	122
4.2.2. Ligand preparation	122
4.2.3. Docking runs	122
4.2.4. Data analysis	123
4.3. Results	123
4.3.1. Docking simulations	123
4.3.2. Interacting residues	124
4.4. Discussion	133
4.4.1. Binding Affinity	133
4.4.2. Non-Covalent Interactions	134
4.4.3. Chrysin, Genistein, Naringin and Silymarin	135
4.4.4. Limitations	137
4.4.5. Recommendations for future studies	137
4.5. Conclusion	137
Chapter 5 HEK293 cell line studies	Error! Bookmark not defined.
5.1. Introduction	Error! Bookmark not defined.
5.2. Materials and Methods	Error! Bookmark not defined.
5.2.1. Chemicals and equipment	Error! Bookmark not defined.
5.2.2. Cell culture	Error! Bookmark not defined.
5.2.3. Western blotting on HEK-MRP2 and HEK293	Error! Bookmark not defined.

defined.

5.2.4. Cell viability assays.....**Error! Bookmark not defined.**

5.2.5. CDCF [5(6)-carboxy-2,'7'-dichlorofluorescein] accumulation and efflux assays**Error! Bookmark not defined.**

5.2.6. Statistical analysis**Error! Bookmark not defined.**

5.3. Results.....Error! Bookmark not defined.

5.3.1. Characterisation of HEK-MRP2 cells...**Error! Bookmark not defined.**

5.3.2. The effect of chrysin on inhibition of MRP2 transporter**Error! Bookmark not defined.**

5.4. Discussion.....Error! Bookmark not defined.

5.5 ConclusionError! Bookmark not defined.

Chapter 6 Human gastrointestinal cancer cell line studies Error! Bookmark not defined.

6.1. Introduction.....Error! Bookmark not defined.

6.2. Materials and MethodsError! Bookmark not defined.

6.2.1. Chemicals and equipment.....**Error! Bookmark not defined.**

6.2.2. Cell culture**Error! Bookmark not defined.**

6.2.3. Cell Viability Assay (MTT assay/ Presto-Blue) with Manuka honey or Chrysin**Error! Bookmark not defined.**

6.2.4. Chrysin effects on cellular accumulation of CDCF in Caco-2 cell lines**Error! Bookmark not defined.**

6.2.5. Effect of chrysin on oxaliplatin-induced apoptosis in Caco-2 and PANC-1 cells.....**Error! Bookmark not defined.**

6.2.6. Statistical analysis**Error! Bookmark not defined.**

6.3. Results.....Error! Bookmark not defined.

6.3.1. The effect of Manuka honey on inhibition of MRP2 transporter....**Error! Bookmark not defined.**

6.3.2. The effect of chrysin on inhibition of MRP2 transporter in Caco-2 and

PANC-1 cancer cell lines	Error! Bookmark not defined.
6.3.3. Chrysin effects on oxaliplatin cellular accumulation of CDCF in GI cancer cells.....	Error! Bookmark not defined.
6.3.4. Effect of chrysin on oxaliplatin-induced apoptosis in Caco-2 and PANC-1 cells.....	Error! Bookmark not defined.
6.4. Discussion.....	Error! Bookmark not defined.
6.5. Conclusion.....	Error! Bookmark not defined.
Chapter 7 General Discussion	174
7.1. Introduction.....	174
7.2. Summary of the findings	174
7.2.1. MRP2 (multidrug resistance-associated protein 2) in gastrointestinal (GI) cancer resistance	175
7.2.2. Phytochemicals as MRP2 Inhibitors	176
7.2.3 Oxaliplatin-Induced Apoptosis	177
7.2.4. Clinical Relevance	177
7.3. Future studies	178
7.3.1. Animal (<i>in vivo</i>) study.....	178
7.3.2. Inhibition of other signalling pathways.....	178
7.3.3. Inhibition of other efflux transporters	179
7.3.4. Nanotechnology-based drug delivery.....	180
7.3.5. Development of Experimental Model for Analysing Oxaliplatin Resistance in GI Cancer.....	182
7.4. Final conclusions	184
References	185

List of Figure

FIGURE 1- 1 CANCER DEATHS BY TYPE GLOBALLY IN 2017 (SOURCE: IHME, GLOBAL BURDEN OF DISEASE (GBD))	23
FIGURE 1- 2 CANCER DEATHS BY TYPE IN NZ IN 2017 (SOURCE: IHME, GLOBAL BURDEN OF DISEASE (GBD))	25
FIGURE 1- 3 TUMOUR INVASION AND METASTATIC	27
FIGURE 1- 4 STRUCTURES OF THE CLINICALLY IMPORTANT PLATINUM DRUGS	31
FIGURE 1- 5 BIOTRANSFORMATION OF OXALIPLATIN	36
FIGURE 1- 6 MECHANISM OF ANTICANCER DRUGS EFFLUX BY ABC TRANSPORTERS	42
FIGURE 1- 7 STRUCTURE OF ABC MEMBRANE TRANSPORTERS.....	45
FIGURE 1- 8 ILLUSTRATES THE FUNCTION OF ABC TRANSPORTERS.....	47
FIGURE 1- 10 MYRICETIN STRUCTURE	65
FIGURE 2- 1 STANDARD CALIBRATION CURVE	79
FIGURE 2- 2 PROPER LAYERING OF THE ASSEMBLED TRANSFER PACK	83
FIGURE 2- 3 MRP2 WESTERN BLOTTING IMAGE BY IMAGEQUANT LAS 500.....	84
FIGURE 2- 4 CELL SURFACE STAINING PROTOCOL	91
FIGURE 2- 5 A REPRESENTATIVE EXAMPLE OF DATA ACQUISITION USING THE XDP MOFLOW.	92
FIGURE 3- 1 SCHEMATIC OF A TRIPLE QUADRUPOLE MASS SPECTROMETER	95
FIGURE 3- 2 MYRICETIN STRUCTURE.....	97
FIGURE 3- 3 LINEAR CURVE OF CHRYSIN.....	100
FIGURE 3- 4 REF: EURACHEM GUIDE: THE FITNESS FOR PURPOSE OF ANALYTICAL METHODS – A LABORATORY GUIDE TO METHOD VALIDATION AND RELATED TOPICS, (2ND ED. 2014). ISBN 978-91-87461-59-0. AVAILABLE FROM WWW.EURACHEM.ORG.....	101
FIGURE 3- 5 PHENOLICS POSITIVE TIC SCAN IN MANUKA HONEY.....	104
FIGURE 3- 6 PHENOLICS NEGATIVE TIC SCAN IN MANUKA HONEY	104
FIGURE 3- 7 UV CHROMATOGRAM AT THE WAVELENGTH OF 254NM.....	104
FIGURE 3- 8 UV CHROMATOGRAM AT THE WAVELENGTH OF 278NM.....	105
FIGURE 3- 9 UV CHROMATOGRAM AT THE WAVELENGTH OF 300NM.....	105
FIGURE 3- 10 LC-MS CALIBRATION CURVE OF METHYL SYRINGATE.....	115
FIGURE 3- 11 LC-MS CALIBRATION CURVE OF DL-3-PHENYLLACTIC ACID.	115
FIGURE 3- 12 LC-MS CALIBRATION CURVE OF 2-HYDROXY-3-(4-METHOXYPHENYL) PROPANOIC ACID.....	116
FIGURE 3- 13 LC-MS CALIBRATION CURVE OF QUERCETIN.....	116
FIGURE 3- 14 LC-MS CALIBRATION CURVES OF CHRYSIN.....	117
FIGURE 4- 1 THE PROTEIN STRUCTURE OF MRP2 (ABCC2) IS DOWNLOADED FROM ALPHAFOLD	

AND DEPICTED IN RIBBON FORM.	120
FIGURE 4- 2 SUB-STRUCTURES OF MRP2 MOLECULE. A: STRUCTURE 1, TARGET REGION 636-865; B: STRUCTURE 2, TARGET REGION 967-1531; C: STRUCTURE 3, TARGET REGION 43-158.	123
FIGURE 4- 3 INTERACTIONS WITHIN THE MRP2 (SUBSTRUCTURE 1)-LIGAND (A, CHRYSIN; B, GENISTEIN; C, NARINGIN; D, SILYMARIN) COMPLEX. BLACK DASHED LINES REPRESENT HYDROGEN BONDS, GREEN SPLINES REPRESENT HYDROPHOBIC CONTACTS, AND GREEN DASHED LINES REPRESENT π -STACKING.	127
FIGURE 4- 4 INTERACTIONS WITHIN THE MRP2 (SUBSTRUCTURE 2)-LIGAND (A, CHRYSIN; B, GENISTEIN; C, NARINGIN; D, SILYMARIN) COMPLEX. BLACK DASHED LINES REPRESENT HYDROGEN BONDS, GREEN SPLINES REPRESENT HYDROPHOBIC CONTACTS, AND GREEN DASHED LINES REPRESENT π -STACKING.	130
FIGURE 4- 5 INTERACTIONS WITHIN THE MRP2 (SUBSTRUCTURE 3)-LIGAND (A, CHRYSIN; B, GENISTEIN; C, NARINGIN; D, SILYMARIN) COMPLEX. BLACK DASHED LINES REPRESENT HYDROGEN BONDS, GREEN SPLINES REPRESENT HYDROPHOBIC CONTACTS, AND GREEN DASHED LINES REPRESENT π -STACKING.	132
FIGURE 4- 6 INTERACTIONS WITHIN THE MRP2 (SUBSTRUCTURE 1)-LIGAND (DAIDZEIN) COMPLEX. BLACK DASHED LINES REPRESENT HYDROGEN BONDS, GREEN SPLINES REPRESENT HYDROPHOBIC CONTACTS, AND GREEN DASHED LINES REPRESENT π -STACKING.	133
FIGURE 5- 1 PRESTO-BLUE CELL VIABILITY ASSAY STANDARD CURVE.....	143
FIGURE 5- 2 IMMUNOSTAINING OF MRP2 PROTEIN WAS DETECTED IN THE CYTOPLASMIC AND MEMBRANE REGIONS OF HEK-ABCC2 CELLS, BUT NOT IN HEK293 CELLS.	145
FIGURE 5- 3 WESTERN BLOT IMAGE OF MRP2 IN HEK293 AND HEK-ABCC2 CELL LINES	145
FIGURE 5- 4 CELL VIABILITY VALUE OF OXALIPLATIN OR CHRYSIN AND OXALIPLATIN COMBINATION ON HEK-ABCC2 CELL LINES.....	146
FIGURE 5- 5 CELL VIABILITY VALUE OF OXALIPLATIN OR CHRYSIN AND OXALIPLATIN COMBINATION ON HEK293 CELL LINES	147
FIGURE 5- 6 IC50 VALUE OF OXALIPLATIN OR CHRYSIN AND OXALIPLATIN COMBINATION ON HEK-ABCC2 AND HEK293 CELL LINES.....	147
FIGURE 5- 7 A PILOT STUDY OF CDCF ACCUMULATION IN HEK-ABCC2 CELLS IN THE PRESENCE AND ABSENCE OF CHRYSIN (10 AND 60 μ M) AND CA (50 μ M).....	149
FIGURE 5- 8 CELLULAR ACCUMULATION OF CDCF IN HEK-ABCC2 AND HEK293 CELL LINES	150
FIGURE 5- 9 REPRESENTATIVE FLOW CYTOMETRIC HISTOGRAM OF CDCF ACCUMULATION IN HEK293 AND HEK-ABCC2 CELL LINES, WITH RED LINE SHOWING CONTROL PANEL (CDCF ONLY), GREEN AND BLACK LINES SHOWING CDCF IN THE PRESENCE OF 10 AND 60 CHRYSIN, RESPECTIVELY.....	150

FIGURE 6- 1 DC PROTEIN ASSAY LINEAR CURVE.	159
FIGURE 6- 2 CELL VIABILITY VALUE OF OXALIPLATIN OR MANUKA HONEY AND OXALIPLATIN COMBINATION ON CACO-2 CELL LINES.....	160
FIGURE 6- 3 CELL VIABILITY VALUE OF OXALIPLATIN OR CHRYSIN AND OXALIPLATIN COMBINATION ON PANC-1 CANCER CELL LINES	162
FIGURE 6- 4 CELL VIABILITY VALUE OF OXALIPLATIN OR CHRYSIN AND OXALIPLATIN COMBINATION ON CACO-2 CANCER CELL LINES.....	162
FIGURE 6- 5 IC50 VALUE OF OXALIPLATIN OR CHRYSIN AND OXALIPLATIN COMBINATION ON PANC-1 AND CACO-2 CELL LINES	163
FIGURE 6- 6 FLUORESCENCE INTENSITY OF CDCF IN PANC-1 CANCER CELL LINES FOR INCREASING CONCENTRATION OF CHRYSIN.....	164
FIGURE 6- 7 FLUORESCENCE INTENSITY OF CDCF IN CACO-2 CANCER CELL LINES FOR INCREASING CONCENTRATION OF CHRYSIN.....	165
FIGURE 6- 8 APOPTOTIC CHANGES IN CACO-2 CANCER CELL LINES AND THEIR TREATMENT WITH CHRYSIN AND OXALIPLATIN.	169
FIGURE 6- 9 APOPTOTIC CHANGES IN PANC-1 CANCER CELL LINES AND THEIR TREATMENT WITH CHRYSIN AND OXALIPLATIN.	170
FIGURE 7- 1 CACO-2 CELL AND PROBIOTICS OR/AND CHRYSIN CO-CULTURE.....	183

List of Table

TABLE 2- 1 LIST OF CHEMICALS USED IN THIS STUDY WITH THEIR SOURCES	69
TABLE 2- 2 LIST OF EQUIPMENT USED IN THIS STUDY WITH THEIR SOURCES	70
TABLE 2- 3 CHARACTERISTICS OF HUMAN CELL LINES USED IN THE EXPERIMENT	72
TABLE 2- 4 METHODS COMPARATION TABLE	77
TABLE 2- 5 OPTIMIZED PARAMETERS FOR MYRICETIN	78
TABLE 2- 6 PREPARATION OF PLATINUM STANDARD IN CELL LYSATE WITH THALLIUM INTERNAL STANDARD	85
TABLE 3- 1 LIST OF CHEMICALS USED IN THIS CHAPTER.....	98
TABLE 3- 2 LIST OF PHENOLICS STANDARDS WOULD BE USED IN THIS CHAPTER	98
TABLE 3- 3 MAJOR COMPOUND ID NEGATIVE SCAN EXTRACT FROM MS-DIAL	106
TABLE 3- 4 MRM TRANSITIONS CONDITION FOR MAIN PHENOLICS COMPOUNDS CONFIRMED BY STANDARD	107
TABLE 3- 5 COMPARATION OF THE STANDARDS IN ETHANOL EXTRACT AND WATER EXTRACT-1.....	108
TABLE 3- 6 COMPARATION OF THE STANDARDS IN ETHANOL EXTRACT AND WATER EXTRACT-2.....	110
TABLE 3- 7 COMPARATION OF THE TWO MAJOR COMPOUNDS' CONTENT IN MANUKA HONEY AND THYME HONEY: 2-HYDROXY-3-(4-METHOXYPHENYL)PROPANOIC ACID; AND DL-3- PHENYLACTIC ACID, AND CHRYSIN QUANTITATIVE ANALYSIS.	112
TABLE 3- 8 COMPARATION OF THE OTHER MAJOR COMPOUND'S CONTENT IN MANUKA HONEY AND THYME HONEY: METHYL SYRINGATE	113
TABLE 4- 1 BEST BINDING MODES OF LIGANDS WITH MRP2 STRUCTURES 1, 2, AND 3.	124
TABLE 4- 2 HYDROGEN BOND AND HYDROPHOBIC BOND OF THE LIGANDS WITH MRP2 STRUCTURES 1 AND 2.	125
TABLE 5- 1 DRUG TREATMENTS AND INCUBATION TIME USED IN CELL VIABILITY ASSAYS	142
TABLE 6- 1 DRUG TREATMENTS AND INCUBATION TIME USED IN CELL VIABILITY ASSAYS	157
TABLE 6- 2 DATA ANALYSIS OF APOPTOSIS ASSAY WITH OXALIPLATIN TREATMENT IN CACO-2 CELLS AND PANC-1 CELLS IN THE PRESENCE AND ABSENCE OF CHRYSIN (10 μ M)	168

Abbreviations

°C: Degree Celsius

5-FU: 5-fluorouracil

ABC: ATP-binding cassette

ANOVA: Analysis-of-variance

ATP: Adenosine-5'-triphosphate

ATP7A: P-type ATPase 7A

ATP7B: P-type ATPase 7B

BBB: Blood brain barrier

BCRP: Breast cancer resistance protein

BSA: Bovine serum albumin

CDCFDA: 5(6)-carboxy-2',7'-dichlorofluorescein diacetate

CDCF: 5(6)-carboxy-2',7'-dichlorofluorescein

CTR1: Copper transporter 1

DACH: Diaminocyclohexane

DAPI: 4',6-diamino-2-phenylindole

DDI: Drug-drug interaction

DMEM: Dulbecco's modified eagle's medium

DMSO: Dimethyl sulfoxide

DNA: Deoxyribonucleic acid

EGFR: Epidermal growth factor receptor

FBS: Foetal bovine serum

g: Gram

GSH: Glutathione

h: Hour

HEK: Human embryonic kidney

HPLC: High performance liquid chromatography

ICP-MS: Inductively coupled plasma mass spectrometry

IC-50: Concentration at half-maximal inhibitory effect

kg: Kilo-gram

LTC4: Leukotriene C4

LV: Leucovorin

M: Molar concentration

μ M: Micromolar concentration

mM: Millimolar concentration

μ g: Micro-gram

mg: Milli-gram

μ l: Micro-litres

ml: Milli-litres

mol: Mole

MDCK: Madin-Darby canine kidney

MDR: Multidrug resistance

MEM: Minimal essential medium

min: Minutes

mRNA: Messenger RNA

MRP: Multidrug resistance-associated protein

MTT: 3-(4,5-dimethylthiazol-2-yl)-2,5-diphenyltetrazolium bromide

OCT: Organic cation transporter

OCTN: Organic cation/carnitine transporter

Ng: Nano-gram

nM: Nanomolar concentration

nmol: Nanomole

NBD: Nucleotide binding domain

pmol: Picomole

PBS: Phosphate-buffered saline

PCR: Polymerase chain reaction

Pen-strep: Penicillin-streptomycin

PFA: Paraformaldehyde

PFS: Progression-free survival

P-gp: P-glycoprotein

ppb: Parts-per-billion

Pt: Platinum

RNA: Ribonucleic acid

r^2 : Coefficient of determination

rpm: Revolutions per minute

RT-PCR: Reverse transcription polymerase chain reaction

qPCR: Quantitative polymerase chain reaction

SLC: Solute carrier

TMD: Transmembrane domain

V_{max} : Maximum velocity

Chapter 1 General Introduction

1.1. Overview of cancer and Gastrointestinal (GI) cancer

Cancer arises when cells undergo uncontrolled growth and fail to adhere to normal death mechanisms, leading to continuous expansion and invasion into adjacent tissues. Over 200 types of cancer can emerge from various cell types, like prostate, colorectal, breast, lung, and lymphoma (*Cancer Statistics 2015, 2018*). Each cancer type originates from a specific cell type, and depending on the cell location and genetic mutations, multiple cancer forms can develop from each type. These malignant cells typically form a mass of cancerous tissue known as a tumor, which invades the primary site and spreads throughout the body, resulting in metastatic cancer. Several factors, including tumor growth rate, invasiveness, differentiation degree, and metastatic potential, determine tumor malignancy.

Cancers are classified into five groups: leukemia (originating in blood-forming tissues like bone marrow), myeloma and lymphoma (beginning in the lymphatic system and lymph nodes), carcinoma (which begins in the skin, lungs, pancreas, or tissues covering internal organs), sarcoma (arising from mesodermal cells, such as those in blood vessels, bone, muscle, and connective tissue), and central nervous system cancer (which start in the tissues of the brain and spinal cord) (*Chemotherapy and You, 2018*).

Historically cancer has long been viewed as a disease of acquired mutations in DNA sequences within abnormal cells. Although around 10% of cancers stem from inherited genetic defects (Kinzler, 2002), environmental factors such as smoking, dietary habits, chemical and radiation exposure, obesity, diabetes, and other pollutants can cause DNA damage and elevate cancer risk (American Cancer Society, 2015). Typically, cancer arises from a combination of genetic predisposition and environmental factors. The causes of cancer are complex, diverse, and highly variable. Cancer can affect individuals of any age, but the risk increases with age. According to the American Cancer Society in 2018, the most common cancers in men are prostate, lung, and colon cancer, while in women, they are breast, lung, and GI cancer (Society, 2018).

Various methods are used to detect cancer, including early signs and symptoms, screening tests, medical imaging, and biopsies. Common cancer treatments include

surgery, chemotherapy, immunotherapy, radiation therapy, targeted therapy, hormone therapy, and stem cell transplants (*NIH- Cancer Treatment*, 2018).

1.1.1. Cancer incidence in the world

Cancer is a major public health problem globally, affecting both developed and developing countries. It is the second leading cause of death in the United States. According to GLOBOCAN 2022 estimates, approximately 20 million new cancer cases were reported, suggesting approximately one in five men or women develop cancer in a lifetime (Bray et al., 2024). Nearly 9.7 million cancer-related deaths were documented in the same year (Bray et al., 2024). In 2022, liver, stomach, bowel, oesophagus and pancreatic cancers accounted for around 33% of all cancer deaths worldwide.

The National Cancer Institute estimated that in 2018, there would be 1,735,350 new cancer diagnoses and approximately 609,640 cancer-related deaths in the United States (*Cancer Statistics*, 2018). According to the 2011-2015 SEER Cancer Statistics Review (*SEER Cancer Statistics Review (CSR) 1975-2015*, 2018), the incidence of new cancer cases was 439.2 per 100,000 people, while the cancer death rate was 163.5 per 100,000 people (Siegel et al., 2018). With the rising incidence of cancer globally, it is projected that by 2030, there will be 23.6 million new cancer cases annually (Bray et al., 2013; Ferlay et al., 2015). This alarming rate of cancer incidence and associated mortality underscores the urgent need for effective and affordable methods for early detection, diagnosis, and treatment. Despite advances in cancer treatments, including chemotherapy, immunotherapy, and surgery, cancer remains one of the most prevalent health issues worldwide.

In 2022, the most common cancers globally were lung, female breast, colorectal, prostate, stomach, pancreatic, liver cancers, leukemia, endometrial, non-Hodgkin lymphoma, melanoma, thyroid, bladder, kidney and renal pelvis. GI cancers including colorectal (9.3%), liver (7.8%), stomach (6.8%) and pancreatic (4.8%) cancers, are also leading causes of cancer death (Bray et al., 2024).

1.1.2. Cancer incidence in New Zealand

According to the New Zealand Cancer Registry, there is a trend of increased new registrations of primary cancer (e.g. 18,895 new cases in 2006 vs 24,086 new cases in

2016, an increase of 13.4%). There are no significant changes in the sex differences in the new registration of primary cancers, with males accounting for 52.0% and females 48.0% in 2006, in comparison with the data in 2016, males 51.9% and females 48.1%. While the total number of cancer patients has steadily increased, the registration rates declined by 0.2%. In 2006, 4128 males and 3966 females had cancer recorded as their direct cause of mortality (Ministry of Health, 2006). Evidence accumulated over the last decade showed that lung cancer caused the most cancer deaths (18.01% of all cancer deaths) in NZ, followed by colon and rectum cancer (15.66%) and then breast cancer (7.73%) and prostate cancer (7.17%). In 2015, the incidence of new cancers was estimated at 331.7 per 100,000, and according to the 2013 report, the cancer death rate was 122.8 per 100,000 population (Cancer research UK, 2015; Ministry of Health, 2014). Cancer predominantly affects the aged population, with 57% of new cases registered among individuals over 65 years old (Ministry of Health, 2014).

In New Zealand, the most frequently diagnosed cancer is prostate cancer (3129 cases), followed by colorectal cancer (3075), breast cancer (3046), melanoma (2366), and lung cancer (2037) (*Cancer: New registration and deaths 2013, 2017*). Prostate cancer affects 27.3% of males, while breast cancer affects 28.7% of females, making them the most common cancers in each gender. Colorectal cancer and melanoma are the next most commonly registered cancers. Lung cancer has the highest mortality rate and is the leading cause of cancer death in New Zealand. Colorectal cancer ranks as the second leading cause of cancer death, followed by breast cancer, prostate cancer, and pancreatic cancer (Ministry of Health, 2014). The incidence and mortality rates of stomach cancer are higher in men than in women in New Zealand. Thus, GI cancers—including stomach, colorectal, liver, and pancreatic cancers—are among the most frequently diagnosed cancers and leading causes of cancer deaths both globally and in New Zealand. This thesis primarily focuses on pancreatic and colorectal cancers.

Pancreatic cancer is regarded as a highly fatal cancer, with a five-year survival rate of only 25-30% following surgery (Ryu et al., 2010). Globally, it is the twelfth most common cancer and the seventh leading cause of cancer mortality, accounting for 330,391 deaths according to GLOBOCAN 2012 (Ferlay et al., 2015). In New Zealand, pancreatic cancer has an incidence rate of 10.9 per 100,000 population (486 cases annually) and is the fifth leading cause of cancer mortality, with a mortality rate of 10.7 per 100,000 population (476 deaths annually).

Colorectal or bowel cancer is the third most commonly diagnosed cancer worldwide, with 1,360,602 new cases (19.3 per 100,000 population) and 693,933 deaths (9.8 per 100,000 population) as reported by GLOBOCAN 2012. The Australia/New Zealand region has the highest rate of colorectal cancer globally. In New Zealand, colorectal cancer is the second most common cancer in males after prostate cancer and in females after breast cancer. In 2012, there were 3018 new cases (67.6 per 100,000) and 1321 deaths (29.6 per 100,000).

These statistics highlight that GI cancer is one of the main types of cancer with the highest incidence and mortality rates globally and in New Zealand. Therefore, it is crucial to study, explore, and improve current treatment approaches for GI cancer to achieve better outcomes for patients.

1.1.3. GI Cancer and Colorectal Cancer

1.1.3.1. Definitions and classifications of Gastrointestinal Cancer

Gastrointestinal (GI) cancer is defined for a group of cancers that affect the digestive system, including cancers of the oesophagus, stomach, gallbladder & biliary tract, liver, pancreas, bowel (large intestine or colon and rectum), and anus, as well as rare cancers like neuroendocrine tumours and gastrointestinal stromal tumours (Institute, 2023). It has been suggested that digestive system cancers are responsible for more cancer deaths than any other system in the body (Goran Bjelakovic et al., 2008). They are primarily divided into upper and lower digestive tract cancers. The upper digestive tract includes oesophageal, stomach, pancreatic, liver, and gallbladder cancers, while the lower digestive tract includes colorectal and anal cancers. In New Zealand, GI cancers (ICD codes C15-C26) are among the most common types of cancer and cause of cancer death, with 4,426 new cases and 2,747 deaths reported in 2013 alone. Oesophageal cancer, the sixth most common cancer worldwide, has a high incidence rate (Yang et al., 2012). The two main types are adenocarcinoma and squamous cell carcinoma (G. Bjelakovic et al., 2008). Stomach or gastric cancer is the fourth most common cancer type and the second leading cause of cancer death globally (Ferlay et al., 2015). The predominant type of gastric cancer is adenocarcinoma (O'Connor et al., 2013). Australia and New Zealand have lower stomach cancer risk (*Cancer Statistics*, 2018). Pancreatic cancer, known for its poor prognosis, has major risk factors including advanced age, chronic pancreatitis, diabetes, and smoking (G. Bjelakovic et al., 2008). The most common pancreatic cancer type is ductal adenocarcinoma. Hepatocellular carcinoma, or liver cancer, is usually linked to hepatitis B or C, cirrhosis, or aflatoxins (Yates & Kensler,

2007). Colorectal cancer ranks as the third most common cancer globally (Ferlay et al., 2015), with most cases being adenocarcinomas.

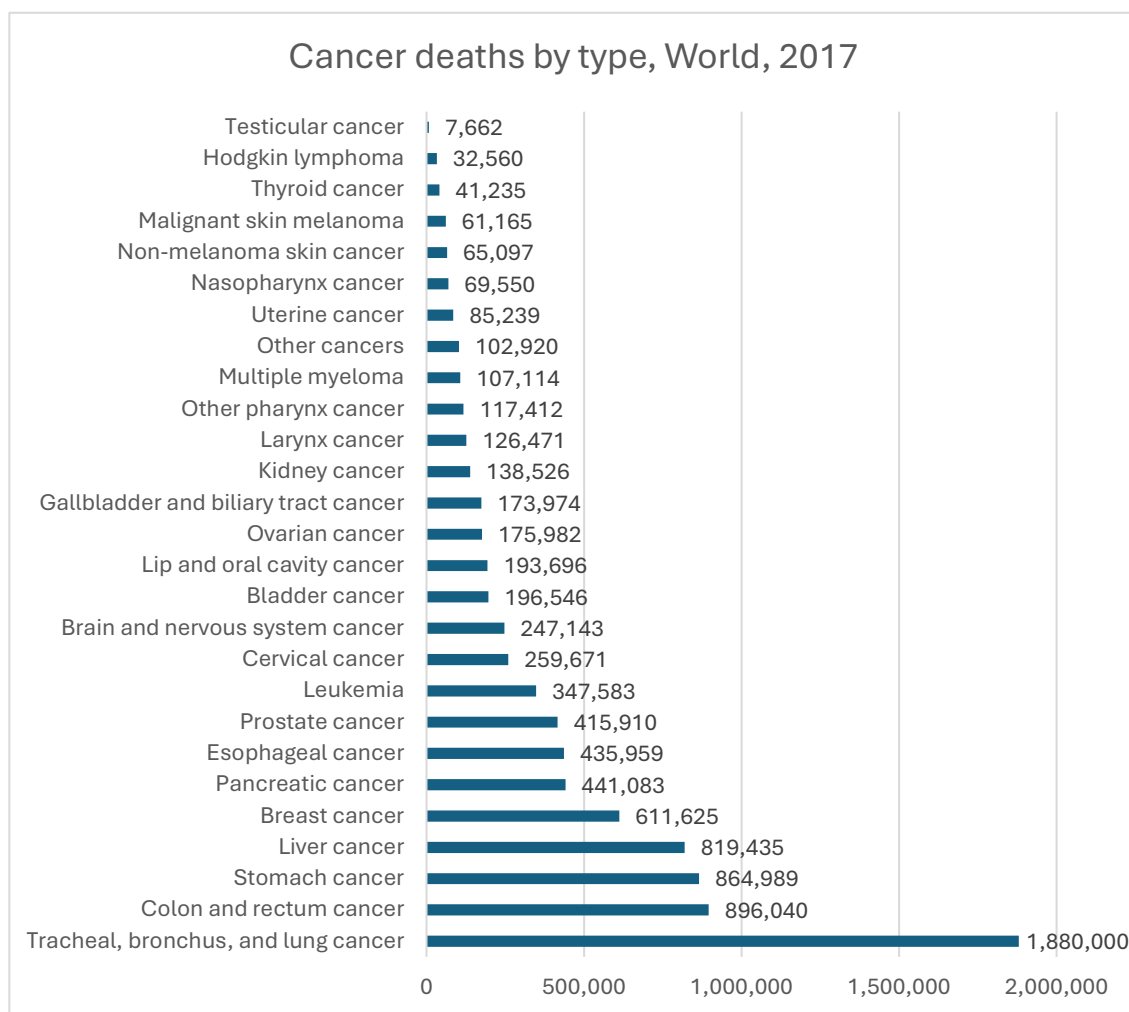


Figure 1- 1 Cancer deaths by type globally in 2017 (Source: IHME, Global Burden of Disease (GBD))

The total number of cancer-related deaths worldwide in 2017 includes all age groups and both genders, categorized by cancer type. Among these, GI cancers result in the highest mortality, with colon and rectum cancer (896,044 deaths), stomach cancer (864,989), liver cancer (819,435), pancreatic cancer (441,083), and oesophageal cancer (435,959). Altogether, this group accounts for 3,157,510 deaths, surpassing the number of fatalities caused by tracheal, bronchus, and lung cancer (1,880,000).

Compared with other more well-known cancers, such as prostate cancer, breast cancer and kidney cancer, the survival rate of GI cancer is relatively lower. The treatment depends on the location of the tumour, as well as the type of cancer cell and whether it has invaded other tissues or spread elsewhere. Last decade saw ongoing efforts to develop new targeted and immune therapies for GI cancer, and the implementation of a bowel cancer screening programme in NZ and world-wide.

1.1.3.2. Colorectal Cancer

Colorectal cancer (CRC), also known as a broad name of bowel cancer, is the tumour cells begins in the inner wall of the colons or rectum (Ozsahin et al., 2019). The Figure 1-1 and Figure 1-2 both show clearly that colorectal cancer is the most dangerous cancer in GI cancer group in NZ and even all over the world. CRC is ranked as the third most common cancer in men and second in females worldwide. The deaths are only lower than that from lung cancer.

Most common colorectal cancers are pathologically characterized as adenocarcinomas, suggesting they originate from cells that produce and secrete mucus and various intestinal fluids. Accumulating pathological studies suggest CRCs mostly route from small and benign clusters of cells named adenomatous polyps, which can be converted to cancerous tissues step by step under the driving force of overactive oncogenes. Colorectal cancers include colon cancer and rectal cancer have similar pathological features and therapeutic regimens. Many factors determine prognosis including the stage of CRC, genetic factors, the patient's comorbidities/underlying diseases and whether there are malignant residues after surgery. One study comparatively analysed some colon cancer treatment options which include radiation therapy, chemotherapy, surgery, immunotherapy and hormone therapy. This study suggests surgery is considered to be the best option for the treatment of CRC after taking into consideration of various factors including costs of treatment, survival rates and adverse events.

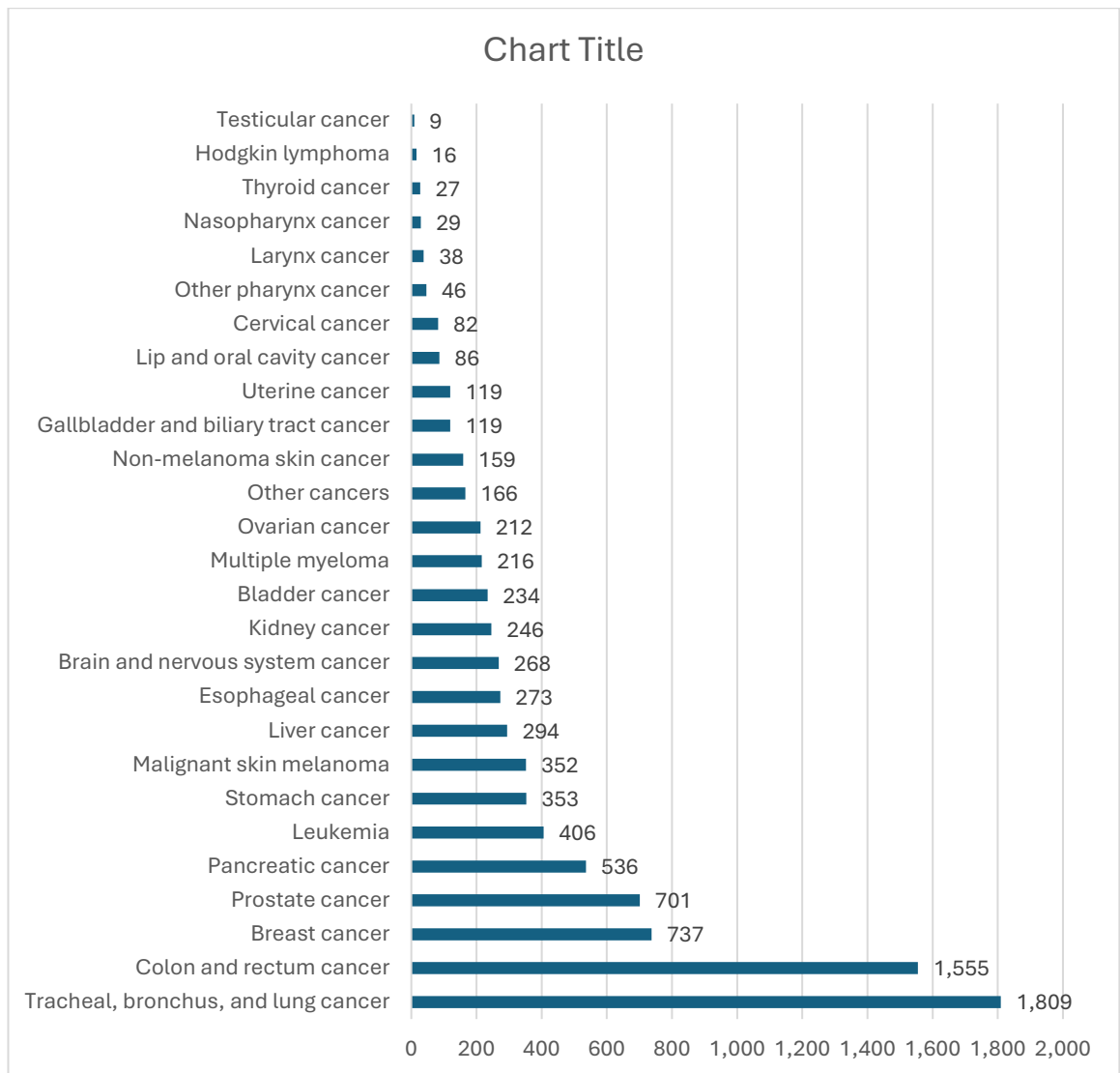


Figure 1- 2 Cancer deaths by type in NZ in 2017 (Source: IHME, Global Burden of Disease (GBD))

In New Zealand in 2017, cancer-related deaths across all age groups and genders were classified by cancer type. GI cancers had the highest mortality, with 1,555 deaths from colon and rectum cancer, 353 from stomach cancer, 294 from liver cancer, 536 from pancreatic cancer, and 273 from oesophageal cancer. Collectively, these cancers caused 3,011 deaths, exceeding the fatalities attributed to tracheal, bronchus, and lung cancer (1,809 deaths).

1.1.3.3. Causes and pathogenesis

Both environmental changes and genetic damage contribute to cancer pathogenesis. These affect the normal functions of the cell, including cell growth speed, apoptosis rate and DNA repair. As more damage accumulates, (Goran Bjelakovic et al., 2008) the risk of cancer increases. There are several lifestyle contributors to CRCs, such as lack of water, or fibre, or nutrients, smoking and so on. Genetic factors include a strong family history of CRC and/or polyps, a pathogenic variant in a mismatch repair (MMR) gene and early age at diagnosis of CRC. The signs of colon cancer patients may include

constipation, diarrhea, oddly shaped stool, difficult bowel movements, abdominal discomfort, blood in the stool, sudden weight loss, frequent bathroom trips, feeling gassy or bloated, feeling tired a lot, shortness of breath, frequent urinary tract infections, nausea or vomiting, enlarged liver, or swollen lymph nodes.

Not only do smokers have a higher risk of developing lung cancer, but they also increase the cancer incidence of all kinds of cancers including CRC, breast cancer and so on. Passive smoking (the inhalation of smoke from another's smoking) is a cause of cancers in non-smokers. A passive smoker can be classified as someone living or working with a smoker. Second-hand smoke has been suggested to be more dangerous than direct smoke (Schick & Glantz, 2005). This is because inhaled fresh side-stream cigarette smoke is approximately four times more toxic per gram of total particulate matter than mainstream cigarette smoke. Some research also suggests that second-hand smoke may increase the risk of breast cancer, nasal sinus cavity cancer, and nasopharyngeal cancer in adults (Courtney, 2015) and the risk of leukemia, lymphoma, and brain tumours in children ("Publication of Surgeon General's Report, The Health Consequences of Involuntary Exposure to Tobacco Smoke," 2006). Additional research is needed to determine whether a link exists between second-hand smoke exposure and these cancers.

1.1.3.4. Tumour invasion and metastasis

Tumour invasion and metastasis is one of the cancer hallmarks, which is characterised as the result of progress in tumour malignancy grade and the cumulative microenvironment changes that facilitate cell migration and invasion into healthy host tissue. Tumour invasion and metastasis is a multistep process involving tumour microenvironment changes, cell migration, and invasion into neighbouring and distant tissues and vasculature (Figure 1-3). The so-called invasion-metastasis cascades begin with local invasion, then penetration by cancer cells into nearby blood and lymphatic vessels, followed by escape of cancer cells from the vessels into the distant tissues, the formation of micro-metastases and macroscopic tumours (Friedl & Alexander, 2011). Before penetrating the blood vessel endothelium, cancer cells must invade local tissues by dissolving ECM and changing microenvironments and then, enter into the systemic circulation (Lu et al., 2011). Once in circulation, these cells can form metastatic colonies at secondary locations.

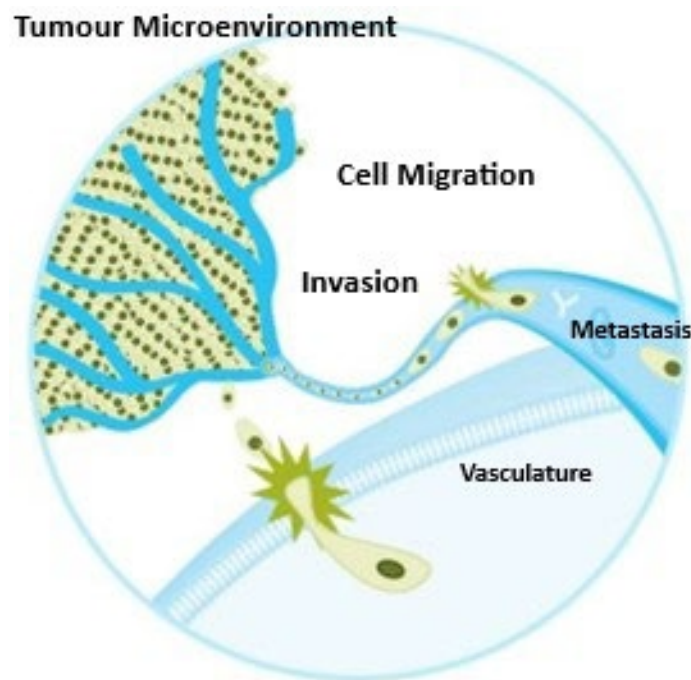


Figure 1- 3 Tumour invasion and metastatic

1.1.4. Gut microbiome and probiotics

It is reported that, honey contains oligosaccharides which can be converted to beneficial metabolites that promote the prebiotic effect (Mohan et al., 2017). As mentioned before, there are numerous studies on health-promoting effects and the antimicrobial components of honey, and lots of them have focused on the antibacterial activity of varieties like Manuka honey. However, the factors in honey for antibacterial activity effects still have a lot that remain unknown. The focus of this part of this study is to evaluate the effect of honey in improving the gut microbial balance and anti-cancer effects.

The human microbiome encompasses all microorganisms residing within various parts of the body, such as the skin, ears, nose, mouth, genital areas, as well as the gastrointestinal and respiratory systems, along with body fluids like breast milk, saliva, and urine. It is now regarded as a crucial and integral organ, playing a vital role in maintaining the host's health through its contributions to nutrition and immune regulation. (Thomas, 2022)

The gut microbiome plays a crucial role not only in digestive health but also in the overall functioning of the body. Microbiomes produce thousands of chemicals in our bodies. The extensive research over the past decade and a half has revealed its influence

on a wide range of conditions, from digestive disorders to systemic diseases such as cancer, diabetes, and mental health issues. Maintaining a balanced gut microbiome is therefore essential for preventing disease and promoting long-term health, underscoring its central importance in both immune regulation and overall well-being. (Clark et al., 2024) Recent research suggested that gut microbiomes could modulate immunity and anti-cancer responses through several different interactions (Eran Elinav et al., 2019; Khan et al., 2020). Gut microbiomes may interact with the host via several different mechanisms. Recently, more and more scientists have been working on the cancer microbiome, as microbiota could produce small metabolites and molecules that have both systemic and local effects on cancer therapy onset, progression and response. There is an interaction between three entities—the tumour, the immune system and the microbiota, which the effect of the gut microbiota on cancer are dependent on, but much remains unknown (E. Elinav et al., 2019; Xavier et al., 2020).

For example, FMT—faecal microbiome transplantation of stool samples from patients who have not responded to therapy into germ-free mice did not improve the effect of immune checkpoint inhibitor therapy in transplanted mice, but FMT from responding patients did (V et al., 2018). Other researchers also suggested that some integrating multi-omics with preclinical models to enable the identification of some commensal members contributing to the clinical effect (Vyara et al., 2018).

It is becoming more and more sophisticated in human-compatible preclinical models of cancer and will contribute to finding the role of the microbes in cancer. Recently, 3D cell culture is popular for anti-cancer drug research, which have a highly controlled environment for the cell lines, and is more close to the in-vivo situation. (d. V. M et al., 2024)

Probiotics are live bacteria and yeasts that, when consumed in the right amounts, can promote the health of the small intestine. While the body can naturally host these beneficial microorganisms, excessive intake may cause gastrointestinal issues. Recent studies have shown that probiotics can aid in modulating the metabolic activity and composition of the gut microbiome; however, they are not sufficient on their own to produce significant clinical outcomes. It is also reported that a four-strain probiotic influences gut microbiota composition and metabolic activity, and increases anti-inflammatory cytokines (IL-6) production in human and rat GI tract models (M. N. M et al., 2024; Moens et al., 2019). Both the mRNA and protein levels of MRP2 / ABCC2

levels were reported to be significantly downregulated by IL-6 in human hepatocytes (Diao et al., 2010). However, it remains unclear whether probiotics could modulate cytokine production and thus MRP2 expression and oxaliplatin sensitivity in GI cancer cells. Some proof-of-concept studies are proposed in this thesis.

1.2. Cancer chemotherapy regimens

Chemotherapy treats cancer by using anticancer drugs to kill or inhibit the proliferation of cancer cells. Unlike surgery and radiation therapy, which target cancer cells in specific areas, chemotherapy works throughout the entire body. It is typically administered orally or intravenously before surgery to shrink tumour size and/or after surgery to eliminate remaining cancer cells or treat those that have recurred or metastasized. In advanced cancer cases where tumours are difficult to remove surgically, chemotherapy serves as the primary treatment to reduce tumour size and alleviate symptoms. Chemotherapy is usually given in cycles, with a dose of one or more drugs administered at regular intervals, followed by a period of rest to allow normal cells to recover from drug side effects (American cancer society : Treatments and side effects).

1.2.1. Chemotherapy in colon cancer treatment

Oxaliplatin-based chemotherapy has been an efficient and preferred chemotherapy regimen for managing various gastrointestinal cancers including colorectal cancer (Stein, 2012). Oxaliplatin can increase the efficacy of 5-fluorouracil (5-FU), which was the first-choice chemotherapy drug for colorectal cancer for many years. Oxaliplatin has been used in combination with 5-fluorouracil and folinic acid (FOLFOX) or capecitabine (a prodrug that can be changed into 5-FU inside the tumour) (XELOX) as a front-line regimen for colorectal cancer. (WebMD, 2018) Oxaliplatin can also be used with other drugs such as irinotecan (Camptosar) to manage GI cancers in clinic.

The last decade has seen ongoing efforts to develop new targeted and immune therapies for GI cancers. Several new drugs also are approved for the management of metastatic colorectal cancer including afibercept (Zaltrap), bevacizumab (Avastin), cetumimab (Erbix), are co-administered along with FOLFOX or XELOX. (Andre et al., 2009; Cassidy, Taberero, Twelves, Brunet, Butts, Conroy, Debraud, Figer, Grossmann, Sawada, Schoffski, et al., 2004; de Gramont et al., 2000; Falcone, Ricci, Brunetti, Pfanner, Allegrini, Barbara, Crino, et al., 2007). Regorafenib (Stivarga) is a

novel drug that targets both tyrosine kinase and vascular endothelial growth factor receptor and was approved by FDA for the treatment of metastatic CRC. It is taken orally as a single agent and has been reported to improve overall survival in patients with heavily pre-treated metastatic colorectal cancer (*Chemotherapy for Colorectal Cancer*, 2024). However, such a target therapy is only effective in a small proportion of the patients due to the limited gene mutation ratio. Oxaliplatin-based chemotherapy has been world-widely recognized as standard regimens treating CRC, despite that tumour resistance is one of major limitations for many patients in clinical practice. It is evident that oxaliplatin, a platinum-based drug, is a common component in combination chemotherapy for the treatment of GI cancers, including colorectal and pancreatic cancer.

1.2.2. Chemotherapy in pancreatic cancer treatment

Gemcitabine, a fluorinated analogue of deoxycytidine, is the primary chemotherapeutic drug used as a first-line treatment for pancreatic cancer. Gemcitabine-based combinations have shown better response rates and longer progression-free survival (PFS) compared to gemcitabine alone, such as the combination of gemcitabine and capecitabine (Cunningham et al., 2009). Erlotinib, a tyrosine kinase inhibitor of EGFR, is also used in conjunction with gemcitabine (Bernhard et al., 2008; Moore et al., 2007). In clinical studies, the oxaliplatin-based combination chemotherapy FOLFIRINOX (5-fluorouracil, leucovorin, irinotecan, and oxaliplatin) has demonstrated good performance status. Another commonly used regimen, GEMOXEL (gemcitabine, oxaliplatin, and capecitabine), has improved survival rates for pancreatic cancer patients (Thierry Conroy et al., 2011; Conroy et al., 2013; Petrioli et al., 2015; Ryan et al., 2014). The overall survival of pancreatic cancer patients has been better when gemcitabine is combined with a platinum-based drug (Heinemann et al., 2008; Heinemann et al., 2006).

1.2.3. Platinum-based drugs

Various drugs are currently used to treat human malignancies such as lung, colon, rectum, breast, and ovarian cancers. Among these, platinum-based drugs are considered some of the most crucial chemotherapeutic agents (J. J. Liu et al., 2012). Since the late 1970s, several platinum-based drugs have been introduced globally for cancer treatment, including cisplatin, carboplatin, and oxaliplatin. Additionally, other platinum-based drugs like nedaplatin, lobaplatin, and heptaplatin have been developed for local use (Kelland, 2007; McKeage, 2001).

However, the mechanisms that confer resistance to platinum (Pt) drugs in cancer cells are complex and not fully understood (Szakacs et al., 2006). The clinical effectiveness of these drugs is often limited by tumour resistance. Cells acquire resistance to Pt drugs through various intracellular mechanisms, including: (a) increased detoxification of drugs by thiol groups; (b) enhanced tolerance to nuclear lesions, resulting in reduced apoptosis; and (c) decreased accumulation of cisplatin (Wang & Lippard, 2005), carboplatin (Shen et al., 2000), and oxaliplatin (Hector et al., 2001).

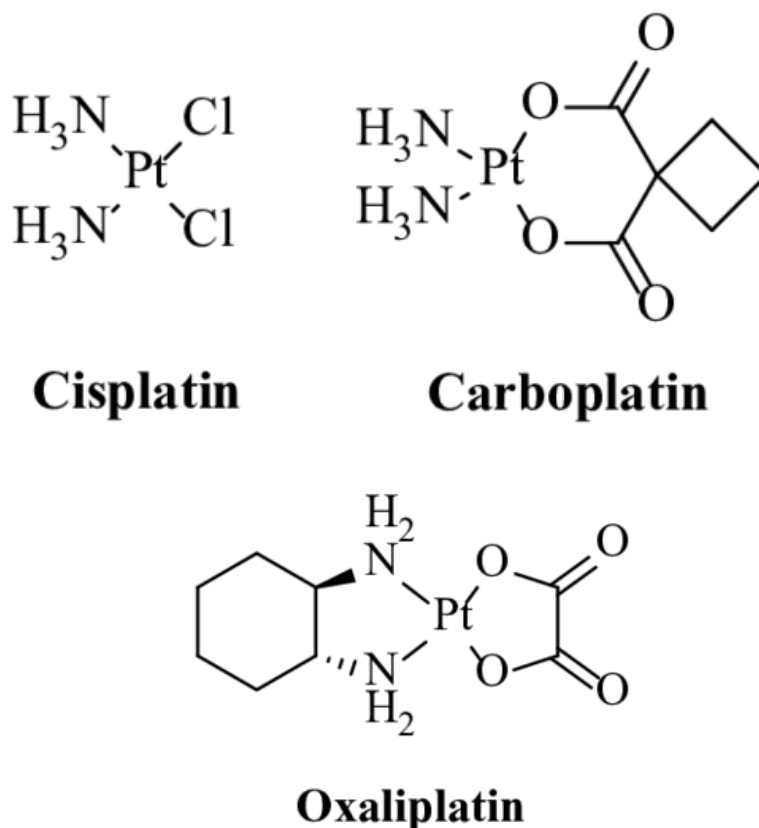


Figure 1- 4 Structures of the clinically important platinum drugs

The structures of various clinically significant platinum-based drugs are depicted in Figure 1-4. In colorectal cancer treatment, oxaliplatin demonstrates synergy with fluoropyrimidines (e.g., 5-FU), offering greater tolerability, reduced nephrotoxicity, and increased lipophilicity.

All platinum-based drugs primarily target DNA, forming intrastrand and interstrand cross-links. However, cisplatin and oxaliplatin differ in drug transport and mechanisms of action, leading to varied activity across different cell types (E. Raymond, S. Faivre, et al., 1998b). For example, the MMR complex plays a critical role in determining cell fate based on DNA damage. Oxaliplatin-DNA adducts are not recognized by the MMR complex, while MMR detects cytotoxic adducts induced by cisplatin (Fink, Nebel, Aebi, Zheng, Cenni, Nehme, et al., 1996; Raymond et al., 2002b; Siddik, 2003; Vaisman,

Varchenko, Umar, et al., 1998). Consequently, cancer cells lacking the MMR complex, such as colorectal cancer cells, resist cisplatin or carboplatin but remain sensitive to oxaliplatin. Thus, oxaliplatin is pivotal in treating cancers resistant to cisplatin and carboplatin (Fink, Nebel, Aebi, Zheng, Cenni, Nehme, et al., 1996; Raymond et al., 2002b; Siddik, 2003; Vaisman, Varchenko, Umar, et al., 1998).

1.2.3.1. Oxaliplatin

Oxaliplatin is a clinically important platinum-based drug for treating advanced cancer, but its clinical pharmacokinetics and biotransformation are not well understood. Oxaliplatin is a platinum (II) similar like carboplatin and cisplatin. This drug was invented by Yoshinori Kidani at Nagoya City University in 1976, and successively it was approved by FDA in 2002 to treat colorectal cancers and other GI adenocarcinoma.

Since 2012, oxaliplatin has been readily available within the New Zealand healthcare system as a fully subsidised generic medicine and PHARMAC designated “Pharmaceutical Cancer Treatment”. As such, District Health Boards are obligated to provide cancer specialists with unrestricted access to oxaliplatin to treat GI cancer patients in their hospitals and outpatient services. Initially, oxaliplatin was used exclusively for metastatic colorectal cancer but later found applications in adjuvant therapy combined with 5-FU and leucovorin to treat various carcinomas (Perego & Robert, 2016). Chemically known as trans-L-dach (1R, 2R-diaminocyclohexane) oxalatoplatinum (L-OHP), oxaliplatin distinguishes itself from cisplatin and carboplatin by having a large diaminocyclohexane (DACH) moiety and an oxalate “leaving group.” Despite advancements in targeted and immune therapies for GI cancers, and the implementation of the NZ bowel cancer screening programme, oxaliplatin-based chemotherapy seems likely to remain in common use as a preferred, standard, and cost-effective treatment for GI cancer for at least the next two decades. A better understanding of oxaliplatin combination therapy can generate novel strategies to further improve its efficacy.

1.2.3.2. Mechanism of oxaliplatin

Similar to cisplatin and carboplatin, oxaliplatin forms cytotoxic platinum-DNA adducts and induces cytotoxic effects in various cancer cells (E. Raymond, S. Faivre, et al., 1998a; Saris et al., 1996). Oxaliplatin-derived platinum binds mainly with guanines, forming intrastrand cross-links, and consequently blocking DNA synthesis, cell cycle

and cell proliferation (Saris et al., 1996). It was suggested that oxaliplatin-DNA adducts induced DNA damage are not recognized by mismatch repair (MMR) complex, leading to apoptosis and cell death rather than DNA repairing and cancer cell recovery (Fink, Nebel, Aebi, Zheng, Cenni, Nehmé, et al., 1996; Raymond et al., 2002a; Rixe et al., 1996; Vaisman, Varchenko, Chaney, et al., 1998; Zahid H, 2003). Colorectal cancer cells have no MMR and are substantially sensitive to oxaliplatin-induced cytotoxicity. Oxaliplatin is a third-generation platinum drug and is a standard therapy for CRC and other GI cancers, which is usually resistant to cisplatin and carboplatin (Fink, Nebel, Aebi, Zheng, Cenni, Nehmé, et al., 1996; Raymond et al., 2002a; Rixe et al., 1996; Vaisman, Varchenko, Chaney, et al., 1998; Zahid H, 2003). For example, compared with cisplatin, oxaliplatin triggers fewer amount of DNA lesions but has higher efficacy in terms of cytotoxicity in various cancer cells (Saris et al., 1996; Woynarowski et al., 1998). One possible explanation is that oxaliplatin-derived DACH-Pt-DNA adducts are larger and more lipophilic compared to cisplatin-derived cis-diamine-Pt-DNA adducts (Rixe et al., 1996; Saris et al., 1996; Woynarowski et al., 1998). Such a physiochemical characteristic could lead to less platinum-DNA binding velocity but more impact on DNA damage and cytotoxicity of oxaliplatin.

Given the importance of oxaliplatin, a large amount of GI cancer patients can be expected to present within the New Zealand healthcare system for treatment with oxaliplatin. Oxaliplatin resistance, however, is a major challenge in treating gastrointestinal cancers, including pancreatic and colorectal cancers, due to their genetic heterogeneity and drug-resistance mechanisms (Adamska et al., 2018). Understanding these mechanisms is crucial for improving the clinical efficacy of oxaliplatin, though the complexity of drug resistance makes it difficult.

Resistance to oxaliplatin was considered to be primarily pharmacodynamic, arising from adaptations within tumour cells. However, recent evidence suggests higher tumour platinum concentrations are associated with better clinical responses to oxaliplatin, indicating the importance of platinum accumulation (M. D. Hall et al., 2008). Reduced cellular uptake or increased efflux of oxaliplatin leads to lower drug accumulation and resistance (Arnould et al., 2003; Mishima et al., 2002; Mohn, Hacker, et al., 2013; C. Mohn, G. V. Kalayda, H. G. Hacker, et al., 2010; Raymond et al., 2002b; Stein & Arnold, 2012) (Khine, et al, 2019) (Biswas, et al, 2019). Other factors contributing to resistance include altered DNA repair systems, drug detoxification with glutathione, changes in membrane permeability, and modified apoptosis pathways (Dilruba & Kalayda, 2016; S et al., 2021).

Oxaliplatin resistance mechanisms can be categorized into pre-target (interfering with oxaliplatin transport), on-target (repairing Pt-DNA lesions), post-target (altered cellular events after Pt-DNA adducts), and off-target (changes in signalling pathways unrelated to oxaliplatin-induced apoptosis) (Martinez-Balibrea et al., 2015). Reduced uptake was considered to be a critical mechanism, with studies showing decreased oxaliplatin accumulation in OCT1-deficient cells and increased accumulation in cells overexpressing OCT1 and OCT2 (S. Li et al., 2011; Zhang et al., 2006). However, according to a clinical association study (Khine et al., 2019), only an efflux transporter MRP2 contributes to the clinical responses to oxaliplatin-based therapy in colorectal cancer patients, suggesting efflux transporters outweigh the importance of uptake transporters. Indeed, the transport of oxaliplatin by MRP2 has been confirmed by using an inside-out membrane vesicle assay (Myint et al., 2015), ATPase test and ABCC2 gene silencing techniques (R. Biswas et al., 2019).

Detoxification of oxaliplatin with glutathione is another significant resistance mechanism. Elevated levels of glutathione-S-transferase- π (GST- π) increase the formation of non-cytotoxic glutathione-oxaliplatin adducts, while higher cellular glutathione levels correlate with increased resistance (Mohn, Hacker, et al., 2013). These adducts are excreted by MRP2. Thioredoxin (Trx), which regulates the cellular redox environment, also contributes to resistance, with TrxR levels positively correlating with platinum resistance. Both cisplatin and oxaliplatin inhibit TrxR (Rabik & Dolan, 2007).

Altered DNA damage repair enhances cell survival and oxaliplatin resistance. Pt-DNA adducts are recognized by proteins like HMG1 and HMG2, which induce apoptosis, and their expression is linked to oxaliplatin cytotoxicity (Dilruba & Kalayda, 2016). Translesion DNA polymerases (POL β , POL η , POL ζ) facilitate DNA replication in the absence of repair, with their expression inversely related to oxaliplatin sensitivity (Albertella et al., 2005; Sharma et al., 2012; Yang et al., 2010). The nucleotide excision repair (NER) pathway, involving proteins like ERCC1 and ERCC2, is crucial for removing Pt-DNA adducts. ERCC1 and ERCC2 expressions are associated with resistance to cisplatin and oxaliplatin (Bohanes et al., 2011; P. Li et al., 2013; Perego & Robert, 2016). Single nucleotide polymorphisms (SNPs) in ERCC1 and ERCC2 genes affect clinical responses, with certain SNPs linked to poor outcomes (Yin et al., 2011).

Finally, altered apoptosis pathways contribute to oxaliplatin resistance. DNA platination

activates apoptosis-related signaling pathways, but inactivation of tumour suppressors like p53 and mutations in factors like NF- κ B can lead to resistance (Boyer et al., 2004; Bush & Li, 2002; Martinez-Cardus et al., 2009). Tumour microenvironment conditions, such as hypoxia, may also play a role (Roberts et al., 2009).

1.2.3.3. Pharmacokinetics of oxaliplatin

Cellular uptake of Pt drugs is often hindered by reduced drug accumulation, caused by the neutral intact drug. Many transporters regulating Pt drug accumulation do not necessarily transport intact drugs. Additionally, outside cells, the neutral drug avoids hydrolysis due to the high chloride level in the plasma (M. D. Hall et al., 2008). Thus, one or more biotransformation products of Pt drugs contribute to the pool of drugs entering cells. Administered intravenously to cancer patients, oxaliplatin has 100% bioavailability (Screnci et al., 2000). Post-administration, oxaliplatin and its intermediates are distributed in high concentrations to the kidneys, spleen, intestine, liver, and red blood cells within two hours (X. P. Liu et al., 2009; E. Raymond, S. G. Chaney, et al., 1998).

Oxaliplatin is generally recommended to be dosed as an intravenous infusion over 2 hours in clinical practice. In plasma oxaliplatin rapidly undergoes a non-enzymatic biotransformation into intermediates (Ehrsson et al., 2002; Stein & Arnold, 2012). Water, chloride, and sulphur-containing plasma proteins such as glutathione can quickly act on oxaliplatin by replacing the oxalate group in oxaliplatin to generate reactive intermediates such as Pt(DACH)(OH)₂, Pt(DACH)Cl₂, Pt(DACH)Cl(OH) and [Pt(DACH)]₂(glutathione) (Jerremalm et al., 2003; Jerremalm et al., 2009; Saris et al., 1996). The active oxaliplatin intermediates as well as the parent drug can enter into cells to induce DNA damage and cytotoxic effects (E Raymond et al., 1998). These intermediates can also be inactivated by metabolizing enzymes (David Cunningham et al., 2010; Graham et al., 2000).

Once inside the body, oxaliplatin mainly binds to albumin, erythrocytes and other plasma proteins. The distribution and elimination of oxaliplatin appear to be quick and the majority of a dose is “depleted” from the systemic circulation mainly by covalently binding to tissues and renal eliminations via urinary and faecal excretion. The mean volume of distribution of oxaliplatin-derived platinum ranged from 349 L to 812 L. Only about 15% of oxaliplatin remains in the body 2 hours after oxaliplatin administration (Synold et al., 2007). Approximately half of the dose of oxaliplatin is excreted via the

kidney with renal platinum clearance similar to or above the average human glomerular filtration rate. The systematic exposure to platinum increased with a decrease in renal function but did not correlate with hepatic dysfunction (Synold et al., 2007). In the presence of glutathione in the liver, oxaliplatin may be reduced to form oxaliplatin—glutathione complexes which can inactivate oxaliplatin. Several “glutathione transporters” (e.g. MRPs) are localized on the canalicular or basolateral side of hepatocytes, facilitating extrusion oxaliplatin—glutathione complex out of the cells through the membrane to eliminate oxaliplatin from the liver to the gut (Hagrman et al., 2004). It remains unclear if intestinal MRPs may also contribute to the clearance of oxaliplatin after IV dosing.

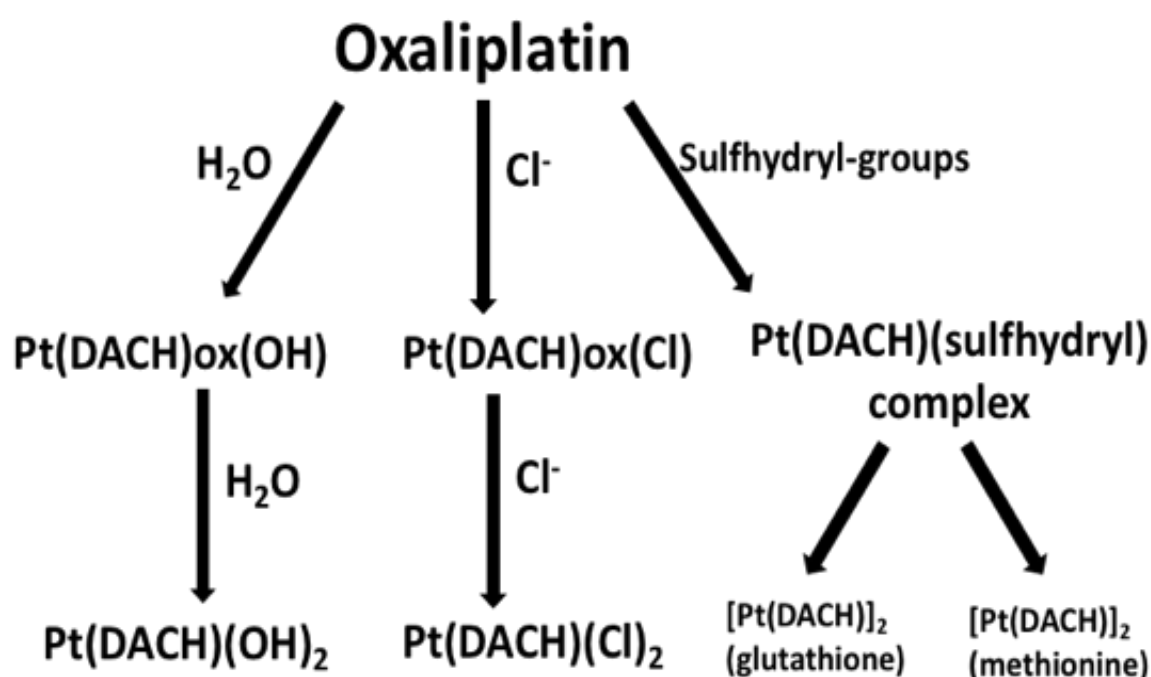


Figure 1- 5 Biotransformation of oxaliplatin

1.2.3.4. Cellular accumulation of oxaliplatin

Given the therapeutic target is within the cells, uptake of oxaliplatin into cancer cells appears to be a critical step to enable oxaliplatin to be effective. Indeed, the accumulation of platinum derived from oxaliplatin appear to be associated with oxaliplatin cytotoxicity in several GI cell lines (Khine et al., 2019). Oxaliplatin is present in the ionized form and unionized form at physiological pH. Historically it was postulated that passive diffusion plays a major role in cellular transport of oxaliplatin and other platinum drugs. Accordingly, the modulation of the lipophilicity and speciation of the platinum drugs was undertaken to improve the accumulation of drugs probably (Matthew D Hall et al., 2008). However, there are other factors influencing oxaliplatin transport across

the cellular membrane including different types of transporter, membrane stability, and surrounding temperature (Binks & Dobrota, 1990; Matthew D Hall et al., 2008; Mann et al., 1987). Several solute carrier (SLC) transporters are efficient in facilitating uptake of oxaliplatin. For example, organic cation transporters (OCTs) and copper influx transporters (CTR1) facilitate oxaliplatin uptake inside the cells and the protein level of these transporters appear to be key factors in determining oxaliplatin sensitivities in certain cancer cell lines (Larson et al., 2009; Song et al., 2004; Atsushi Yonezawa et al., 2006). In addition to drug uptake transporters, several other membrane transporters involved in drug export or efflux out of cells including copper efflux transporters (ATP7A and ATP7B) (Komatsu et al., 2000; Goli Samimi et al., 2004; Tadini-Buoninsegni et al., 2014) as well as multidrug resistance-associated proteins (MRPs). These efflux transporters may be rate-limiting factors in the cellular accumulation of oxaliplatin and thus its sensitivity. For example, using a CRC dataset stored in the Oncomine database, MRP2/ABCC2 has been found to be the only transporter whose expression is associated with oxaliplatin response in CRC patients treated with FOLFOX (Khine et al., 2019). Modulation of MRP2 by chemical inhibitor myricetin or ABCC2 siRNA significantly increased oxaliplatin accumulation and sensitivity in the human colorectal Caco-2 cancer cell line (R. Biswas et al., 2019). To translate the basic discovery into clinical application, further studies are required to find more potent MRP2 inhibitors or a better delivery system for siRNA.

1.2.3.5. Clinical trials

Oxaliplatin-based chemotherapy has become a cornerstone in treating colorectal cancer and other gastrointestinal malignancies, including liver, pancreatic, and gastric cancers. It is commonly used in combination with other anticancer drugs like 5-FU, folinic acid (leucovorin), or capecitabine as a first-line treatment for metastatic colorectal cancer (Andre, Boni, et al., 2004; Bukhari & Winquist, 2017). Additionally, oxaliplatin is frequently combined with 5-FU and irinotecan in advanced pancreatic cancer treatment regimens (Andre, Tournigand, et al., 2004).

Recent research has focused on adjuvant treatment combinations such as FOLFIRINOX (fluorouracil, irinotecan, oxaliplatin, and leucovorin) and gemcitabine. Studies have shown that these combinations enhance the immune response against pancreatic cancer (Ryan et al., 2014). Moreover, regimens like GEMOXEL (gemcitabine, oxaliplatin, and capecitabine) and FOLFIRINOX have demonstrated higher median overall survival rates in patients with metastatic pancreatic cancer compared to gemcitabine alone

(Conroy et al., 2013). Phase II trials reported an objective response rate (ORR) of about 20% with single-agent oxaliplatin, which increased to 50% when combined with fluoropyrimidines (5-FU) (Goldberg et al., 2004; Rothenberg et al., 2003).

Gemcitabine, a first-line drug for pancreatic cancer, shows modest activity when used alone compared to its combination with other chemotherapies (Thierry Conroy et al., 2011; Von Hoff et al., 2013). Two clinical trials confirmed this. The FOLFIRINOX regimen has recently shown significant effects in prolonging overall survival (OS) rates in metastatic pancreatic cancer patients (Ryan et al., 2014). Compared to gemcitabine, FOLFIRINOX improved median survival, quality of life, and health in metastatic patients. FOLFIRINOX, or its combination with gemcitabine and gemcitabine-nab-paclitaxel, is now considered a standard treatment, increasing the survival rate by up to 10% (Ryan et al., 2014). However, the molecular interactions between oxaliplatin, 5-FU, radiation, and gemcitabine remain unclear.

In clinical trials for colorectal cancer, oxaliplatin, unlike other platinum drugs such as cisplatin or carboplatin, has demonstrated significant antitumoral activity alone or in combination with 5-FU (E Raymond et al., 1998). Phase III trials in metastatic colorectal cancer by Giacchetti et al. and de Gramont et al. found that adding oxaliplatin to 5-FU and leucovorin significantly increased the ORR (16/22.3% vs. 53/50.7%) and progression-free survival (PFS) (6.1/6.2 vs. 8.7/9.0 months) (de Gramont et al., 2000; Giacchetti et al., 2000). These studies established FOLFOX4 (leucovorin, 5-FU, oxaliplatin) as a standard regimen for colorectal cancer (de Gramont et al., 2000). Another study showed that FOLFOX4 was more effective than FOLFIRI (leucovorin, 5-FU, irinotecan), with improved disease-free survival and OS (Stein & Arnold, 2012). The IROX regimen (irinotecan and oxaliplatin) showed similar ORR and better OS than FOLFIRI and irinotecan alone (Haller et al., 2008). FOLFOX4 also had significantly lower rates of toxicity, such as vomiting, diarrhea, neutropenia, and dehydration (Stein & Arnold, 2012). Combining oxaliplatin with FOLFIRI (FOLFOXIRI) improved ORR and OS compared to FOLFIRI alone (Falcone, Ricci, Brunetti, Pfanner, Allegrini, Barbara, Crino, et al., 2007; Souglakos et al., 2006). Subsequent clinical studies investigated the combination of oxaliplatin and capecitabine (XELOX) (Cassidy et al., 2008; Ducreux et al., 2011; Saltz et al., 2008), with several randomized Phase II and III trials showing similar PFS and OS for both XELOX and FOLFOX (Arkenau et al., 2008). Randomized data also indicated that combining FOLFOX with bevacizumab or anti-EGFR antibodies increased patient response rates (Stein & Arnold, 2012).

1.2.3.6. Cell toxicities to oxaliplatin

The clinical application of oxaliplatin-based chemotherapy is often hindered by its high toxicity profile, leading to severe adverse reactions early in treatment (Stein & Arnold, 2012). Common toxicities affecting hematopoietic, gastrointestinal, and peripheral systems include neutropenia, thrombocytopenia, anaemia, nausea, vomiting, acute neurotoxicity, and diarrhea. The adverse effects on hematopoietic and gastrointestinal systems are generally mild to moderate (Alcindor & Beauger, 2011; E Raymond et al., 1998; Screnci et al., 2000). Oxaliplatin has moderate myelotoxic effects on progenitor cells in the bone marrow and can cause anaemia and secondary immune thrombocytopenia with repeated infusions (Alcindor & Beauger, 2011; Stein & Arnold, 2012).

Neurotoxicity is the primary dose-limiting toxicity of oxaliplatin (E Raymond et al., 1998). It manifests in two distinct patterns: acute and chronic peripheral sensory neuropathy (Alcindor & Beauger, 2011; Stein & Arnold, 2012). Acute neuropathy results from effects on voltage-gated sodium channels involving calcium, while chronic neuropathy is linked to atrophy and mitochondrial dysfunction in dorsal root ganglion cells due to platinum accumulation (Alcindor & Beauger, 2011; Stein & Arnold, 2012). Studies have shown that despite higher platinum concentrations in peripheral nerves from cisplatin and carboplatin, oxaliplatin induces more severe neurotoxicity (Screnci et al., 2000). Acute neuropathy occurs during or shortly after infusion, presenting as paresthesia, dysesthesia, or allodynia affecting extremities, lips, and oropharyngolaryngeal areas. Chronic neuropathy, which progresses with ongoing treatment, affects approximately 40-50% of patients receiving oxaliplatin, with 15% experiencing severe neuropathy after cumulative doses of around 800 mg/m² (Grothey & Goldberg, 2004; Weickhardt et al., 2011). Symptoms include loss of vibration sensation, numbness, reduced proprioception, and sensory ataxia (Alcindor & Beauger, 2011). Unlike cisplatin and carboplatin, oxaliplatin does not significantly cause renal toxicity and ototoxicity (Alcindor & Beauger, 2011; E. Raymond, S. Faivre, et al., 1998b; Stein & Arnold, 2012).

1.3. Anti-cancer drug resistance and ABC transporters

Accumulating evidence suggests up-regulation of various ATP-binding cassette transporters (ABC transporters) leads to efficient extrusion of the drug from the cancer

cells, consequently insufficient accumulation of anti-cancer drugs and thus loss of anti-cancer efficacy. The human ABC transporter superfamily contains 48 members including several important drug transporters such as P-glycoprotein (P-gp, ABCB1), multidrug resistance-associated protein 1-9 (MRP 1-9, ABCC1-6 and ABCC10-12, respectively) and breast cancer resistance protein (BCRP, ABCG2) (Borst & Elferink, 2002a). ABC transporters transport some endogenous compounds such as amino acids, lipids, inorganic ions, peptides, saccharides, metals as well as structure-diverse drugs. Efflux of the substrates out of cells by ABC transporters is driven by the ATP hydrolysis to overcome concentration and chemical potential gradients in most cases that have been observed (Higgins, 1992). The expression of human ABC transporters on cell membranes are under tight transcriptional regulation by nuclear receptors (Borst & Elferink, 2002a). Nuclear receptors are generally activated by steroid hormones and other lipid-soluble chemicals derived from environmental and dietary contents. Thus, the functions of ABC transporters may be modulated by the phytochemical estrogens and other structure-similar compounds.

P-glycoprotein (P-gp) is the product of the multidrug resistance gene (MDR1/ABCB1). It is an efflux transporter expressed in many normal tissues such as the intestine, liver, kidney and brain, which limits the entry of its substrate into the major organs in the tissue distribution of and exposure to lipophilic and amphipathic drugs, carcinogens, toxins, cytokines and other xenobiotics (Drach et al., 1996; Litman et al., 2001). P-gp transports various anti-cancer drugs including vinca alkaloids (vinblastine, vinorelbine) (Tamai & Safa, 1991), DNA topoisomerase inhibitors (doxorubicin, topotecan) (Chen et al., 1997; Hendrik et al., 1996), microtubule stabilizers (paclitaxel, docetaxel), epipodophyllotoxins (etoposide) (Sikic et al., 1997). Overproduction of P-gp on many cancer cells plays a pivotal role in multidrug resistance, especially in cancer drug resistance. As the cell survival/proliferation appears independent of the function of P-gp, complete inhibition of P-gp mediated drug efflux by a non-toxic inhibitor or a group of inhibitors may represent a unique strategy to reverse multidrug resistance. The last three decades have seen the development of P-gp inhibitors such as verapamil, quinidine, erythromycin, tamoxifen, cyclosporine A, elacridar (GF120918), zosuquidar (LY335979) and tariquidar (XR9576) (Christopher A & Richard, 2007; Fox et al., 2015; Litman et al., 2001; Schwarz et al., 2000; Washington et al., 1998). However, there is no clinical success for P-gp inhibitors in the clinic because of the lack of patient selection or toxicity of inhibitors. Many natural compounds such as flavonoids (e.g. genistein, quercetin, morin, phloretin, silymarin, chrysin, hesperidin, naringenin), polyphenols, epicatechin gallate, alkaloids, and carotenoids have been shown to inhibit P-gp-mediated

efflux of its model substrates and/or reverse drug resistance (Castro & Altenberg, 1997; De Castro et al., 2007; Deli et al., 2001; Jodoin et al., 2002; Shuzhong & Marilyn E, 2003; Taur & Rodriguez-Proteau, 2008; Wang et al., 2002; Zhang & Morris, 2003).

There are also some P-gp modulators such as several polyoxyethylene ester surfactants Tween 40 which can diminish P-gp mediated drug extrusion from the cells. Since they are not P-gp inhibitors, the mechanism reversing the transporter proteins may be due to indirect induction of alteration of lipid fluidity in the plasma membrane (Dudeja et al., 1995). The C-C-N-C-C sequence plus the presence of a carboxylic acid or a quaternary ammonium group appears to be a basic structure-activity requirement for most of these P-gp reversal agents (Klopman et al., 1997). These P-gp modulators may be used a drug formulation excipient and increase drug absorption as P-gp also limits the intestinal absorption, bioavailability and brain distribution of its substrates. Several studies in experimental animals have indicated that co-administration of flavonoids increased the bioavailability of several P-gp substrates (Jun-Shik et al., 2004; Jun-Shik & Sang-Chul, 2005).

Multidrug resistance-associated protein (MRP, ABCC) was initially cloned from a multidrug-resistant lung cancer cell line without overexpressing P-gp (Cole et al., 1992). There are nine members (MRP1-9, ABCC1-6 and ABCC10-12, respectively) in this sub-family which pump out various endogenous compounds and anticancer drugs (Borst et al., 1999). MRP2, MRP3 and MRP6 were reported to be mainly detected in the liver, kidney and intestine, expression of MRP1, MRP4 and MRP5 proteins are detected in most major organs/tissues (Kool, De Haas, Borst, et al., 1997; Kool et al., 1999). MRP transport endogenous amphiphilic anions such as leukotriene C4, glutathione (GSH), glucuronic acid, sulphate conjugates, cyclic guanosine monophosphate (cGMP) and cyclic adenosine monophosphate (cAMP) (Chen et al., 2001; Jedlitschky et al., 2000; Kavallaris, 1997). MRP members transport many anticancer drugs such as antimetabolites, platinum compounds, arsenical and antimonial oxyanions, and peptide-based agents, causing increased efflux and decreased intracellular accumulation of anticancer drugs and thus multidrug resistance (Borst et al., 1999; Piet et al., 2000; Zhou et al., 2008). For example, MRP5 extrudes a nucleotide analogue gemcitabine efficiently and thus cancer cells overexpressing these MRP5 confer resistance to gemcitabine (Wijnholds et al., 2000).

MRPs play in concert with phase II conjugating or biosynthetic enzymes to confer

resistance to classical anti-cancer agents. Some phase II conjugates of GSH, glucuronate, or sulphate of anti-cancer drugs (e.g. cisplatin or arsenite) are high-affinity substrates of MRPs. Efflux leads to decreased cellular accumulation of anti-cancer drugs or their active or inactive metabolites and thus loss of cytotoxic effects in resistant cancer cells. MRP5 confers resistance to gemcitabine by effluxing its monophosphates, and MRP5 and 8 confer resistance to 5-FU by extrusion of 5-fluorodeoxyuridine monophosphate (Kruh et al., 2007; Pratt et al., 2005).

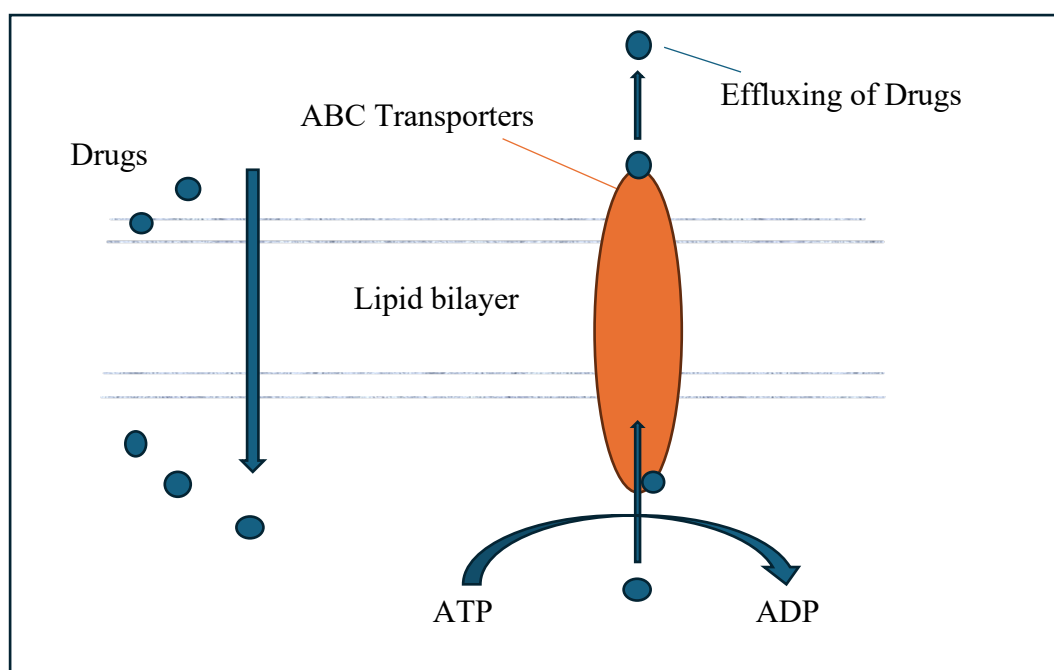


Figure 1- 6 Mechanism of anticancer drugs efflux by ABC transporters

Silencing MRP-mediated efflux by MRP inhibitors or modulators may represent a novel strategy in patients with overexpressed MRPs in their tumour tissues. Recent development of new generation liquid biopsy may help identify such patients in the clinic and eventually change an ineffective anti-cancer drug into an exceptional one. MRP transporter inhibitors can be identified using high-throughput methods such as fluorescent model substrate (e.g. BCPCF (2', 7'-bis-(3-carboxy-propyl)-5-(and-6)-carboxyfluorescein) for MRP1, CDCF for MRP2, BCECF for MRP5) accumulation assays. Some MRP1 inhibitors were derived from herb/plant/vegetable phytochemicals which include quercetin, myricetin, naringenin, genistein, biochanin A, apigenin, morin, silymarin, phloretin, chrysin and kaempferol, (Versantvoort et al., 1994; Versantvoort et al., 1996; Versantvoort et al., 1993). Myricetin is an MRP2 inhibitor, and it increases oxaliplatin sensitivity *in vivo* in HepG2 cell xenografted mice (Khine et al., 2019). Quercetin and silymarin have also been reported to be high-affinity inhibitors for MRP4- and 5 (Wu et al., 2005). However, the clinical implications of these MRP inhibitors

remain unknown but warrant further investigation.

1.3.1. ABC transporters

In recent decades, the significance of membrane transporters in drug disposition, response, therapeutic efficiency, and adverse drug reactions has become increasingly evident. These transporters, located in the plasma membrane, are crucial for the uptake and efflux of essential molecules such as cellular metabolites, organic ions, proteins, minerals, toxic substances, and xenobiotics. They facilitate the movement of these substances across cellular membranes via facilitated diffusion or active transport mechanisms that utilize various forms of energy (A et al., 2024; Busch & Saier, 2002; International Transporter et al., 2010; Kell et al., 2011). Membrane transporters are classified into several types, including electrochemical potential-driven transporters, primary active transporters, electron carriers, and channels or pores (Busch & Saier, 2002).

Transporter proteins are functionally categorized into influx and efflux transporters. Influx transporters are responsible for the uptake of molecules, including ions, minerals, nutrients, drugs, and xenobiotics, into cells such as enterocytes, hepatocytes, renal tubules, and endothelial cells of the blood-brain barrier and tumour cells. Efflux transporters mediate the export of these molecules out of cells (Chan et al., 2004; Huang et al., 2004; International Transporter et al., 2010).

The two major superfamilies of membrane transporters annotated in the human genome are ATP-binding cassette (ABC) and solute carrier (SLC) transporters (International Transporter et al., 2010). Extensive research indicates that these transporters significantly influence pharmacology by regulating drug entry and extrusion, disposition, efficacy, and adverse drug reactions. Clinically, transporter-based drug-drug interaction (DDI) studies suggest that these transporters often collaborate with drug-metabolizing enzymes in drug absorption and elimination processes (International Transporter et al., 2010). Consequently, membrane transporters are key determinants of drugs' pharmacokinetic properties, providing vital information on bioavailability, plasma concentration, exposure, clearance, and excretion (International Transporter et al., 2010; Oostendorp et al., 2009; Shitara et al., 2006).

Additionally, some membrane transporters are located in critical tissues such as the central nervous system (CNS), blood-brain barrier, placenta, and testis-blood barriers, where they limit drug disposition into these tissues, thereby preventing toxicity (International Transporter et al., 2010). In cancer pharmacology, understanding membrane transporters is crucial for determining the pharmacodynamics (PD) and pharmacokinetics (PK) of drugs in terms of drug disposition, efficacy, and sensitivity within cancer cells.

Membrane transporters are essential for the absorption and disposition of various drugs, xenobiotics, and endogenous compounds throughout the body. They also act as natural barriers, effluxing these molecules out of cells and contributing to multidrug resistance. Over time, research has shown that many pharmaceutical drugs are substrates, inhibitors, and inducers of multiple drug transporters, and some drugs serve both as substrates and inhibitors of membrane transporters (Keogh et al., 2016).

1.3.1.1. ABC Superfamily

In humans, the ABC (ATP-binding cassette) superfamily comprises seven families of transporter genes, labeled ABCA to ABCG, which encode 49 individual transporters involved in various physiological processes and diseases, including genetic disorders (Glavinas et al., 2004; Sarkadi et al., 2006). ABC transporters are primarily situated in the plasma membrane, where they facilitate the efflux of a diverse range of endogenous substrates, including drugs, conjugated bile salts, steroid hormones, and unconjugated bilirubin (Keogh et al., 2016). Consequently, alterations in the expression or function of these transporters can lead to specific diseases. For instance, mutations in the *ABCC2* gene (part of the ATP-binding cassette sub-family C) are linked to Dubin-Johnson Syndrome, characterized by intermittent jaundice due to impaired excretion of conjugated bilirubin (Gatti et al., 2011).

ABC transporters are extensively distributed throughout the human body, including in the liver, kidney, renal tubules, intestines, and blood-tissue barriers. They play a critical role in excreting waste products, toxins, and xenobiotics from the body via bile, urine, and feces. Additionally, they protect vital organs like the central nervous system (CNS) and brain from toxic substances by extruding these waste products into the bloodstream (Li et al., 2017; Oostendorp et al., 2009).

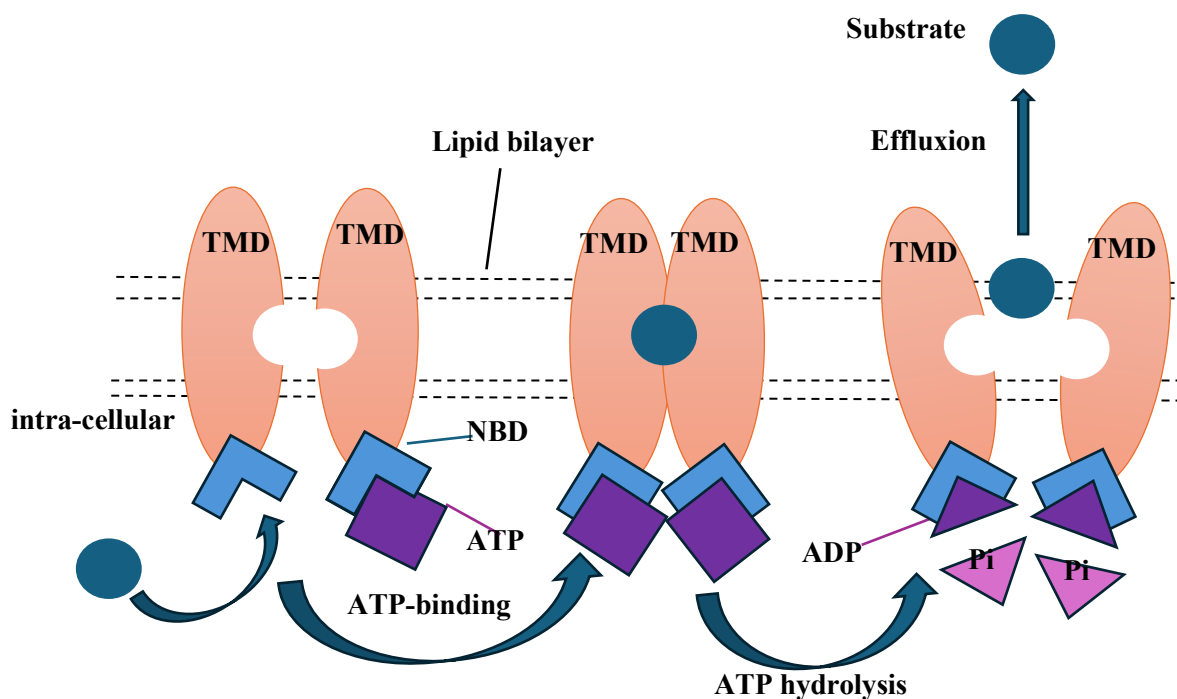


Figure 1- 8 Illustrates the function of ABC transporters.

In this figure, ABC stands for ATP-binding cassette, TMD represents the transmembrane domain, NBD refers to the nucleotide-binding domain, ATP is adenosine triphosphate, ADP is adenosine diphosphate, and Pi indicates phosphate.

The ABC drug transporters categorize into three classes. The first type, widely studied, is the ABCB family, which contains MDR1 (multidrug-resistant transporter 1; ABCB1) and ABCB11. The second type, the ABCC family, includes MRPs (ABCC1 to ABCC6). Multidrug resistance-associated proteins (MRPs) belong to the ATP-binding cassette (ABC) efflux transporter family, which effectively efflux various drugs and molecules to protect cells from toxins (Glavinas et al., 2004; Glavinas et al., 2008). The third, most well-known drug transporter family, the ABCG family, contains BCRP (ABCG2). Clinically, these ABC transporters are the most relevant and are discussed below.

ABCB1 (MDR1, P-gp)

Researchers first identified an ABC transporter from the ABCB family, MDR1 (multidrug-resistant transporter 1, ABCB1; also known as P-glycoprotein, P-gp), which the ABCB1 gene encodes (Huang & Sadee, 2006). P-gp localizes at the apical surface of epithelial cells of hepatocytes (Fromm, 2004; Leslie et al., 2005). P-gp mainly transports hydrophobic drugs with neutral or positive charges and anticancer drugs,

including taxanes (paclitaxel), vinca alkaloids (vincristine), an anthracycline (doxorubicin), imatinib, and irinotecan (Bugde et al., 2017). Several studies, including Mdr1a and Mdr1b knockout mice lacking Abcb1 proteins and clinical studies in humans using ABCB1 inhibitors such as cyclosporin A and elacridar, demonstrated that inhibiting the activity of the MDR1 transporter significantly increased the oral bioavailability of anticancer drugs like paclitaxel, etoposide, and topotecan (Bugde et al., 2017; Oostendorp et al., 2009). Expressed on the apical surface of the hepatocyte, P-gp transports substrates or drugs from portal circulation into bile, causing biliary excretion and hepatic clearance of anticancer drugs such as irinotecan, doxorubicin, and paclitaxel (Bugde et al., 2017; Chan et al., 2004). Administration of P-gp substrates, including digoxin and loperamide, inhibits the excretion of anticancer drugs, reducing their clearance and increasing their toxic effects (Keogh et al., 2016). Therefore, P-gp plays a role in DDI of anticancer drugs and is an important determinant of drug disposition, pharmacokinetics, clearance, and toxicity in cancer chemotherapy.

ABCCs (MRPs)

The multidrug resistance-associated protein (MRP) family, encoded by ABCC genes, represents the second most important ABC transporters; nine MRP proteins (MRP1 to MRP9) are encoded by ABCC1-6 and ABCC10-12, respectively (Huang & Sadee, 2006). All MRPs transport anionic compounds, glutathione, substrates conjugated with glutathione, and metabolites of substrates. Thus, MRPs play an important role in detoxifying chemotherapeutic drugs and their metabolites (Chan et al., 2004; Huang et al., 2004; Huang & Sadee, 2006).

N-linked glycosylation occurs on the fourth extracellular loop of multidrug resistance-associated protein 1-3 (MRP1, MRP2, MRP3). They also possess an additional N-terminal extension consisting of five putative transmembrane segments, resulting in a total of 17 transmembrane segments. MRP1 localizes mainly on the basolateral cell surface and is predominantly expressed in the lungs, kidney, peripheral blood cells, and liver (Flens et al., 1996). MRP1 translocates neutral or anionic compounds and complex hydrophobic substrates, including doxorubicin and methotrexate, conjugated with glutathione, glucuronic acid, or sulphate (Bugde et al., 2017; Huang & Sadee, 2006; Keppler, 2011). MRP1 translocates drugs into the blood, thereby protecting cells from drug toxicity. Therefore, MRP1 plays a crucial role in determining the PK and toxicity of several anticancer drugs. Overexpression of MRP1 in small cell lung cancer, non-small cell lung cancers, leukaemia, oesophageal carcinoma, prostate cancer, and breast

cancer correlates with resistance to several anticancer drugs (Fletcher et al., 2010; Huang & Sadee, 2006).

MRP1 and MRP2 transport mechanisms are similar and assist with transporting mostly anionic drugs and their metabolites (Flens et al., 1996). MRP2 transports drugs like anthracyclines, taxanes, vinca alkaloids, and platinum-based drugs such as cisplatin and their conjugates, including glutathione and sulphates. Physiologically, MRP2 expresses in tissue barrier sites such as the blood-brain barrier, blood-testis barrier, and placenta, as well as on the surface of the canalicular membrane of hepatocytes, the luminal surface of renal proximal tubules, and the small intestine, where it functions in the absorption, metabolism, and excretion of substrates and toxic substances. Thus, MRP2 plays a major role in the body's defense against drugs and toxins by controlling bioavailability and disposition of drugs and the excretion of toxic substances in bile and urine.

MRP3 is closely related to MRP1, expressing in the liver, intestines, adrenal gland, pancreas, and kidneys. MRP3 confers resistance to a variety of chemotherapeutic drugs such as etoposide and methotrexate (Bugde et al., 2017).

Researchers first reported MRP4 as an ABC transporter that translocates nucleoside monophosphates. It expresses in the lungs, kidneys, bladder, and prostate, as well as to some extent in the small intestine (Bugde et al., 2017). MRP4 mediates ATP-dependent accumulation of cyclic guanosine monophosphate (cGMP) and cyclic adenosine monophosphate (cAMP).

ABCG2 (BCRP)

The breast cancer resistance protein (BCRP or ABCG2), originally isolated from the P-gp inhibitor doxorubicin and verapamil (Bates et al., 2001), represents the last drug transporters group. BCRP is considered a half-transporter with six transmembrane segments and a single N-terminal NBD unit. Normally, the last extracellular loop is N-glycosylated (Schinkel & Jonker, 2003). Like P-gp and MRP2, BCRP transports a wide range of substrates like mitoxantrone, camptothecin, methotrexate, doxorubicin, and SN38 (a metabolite of irinotecan) (Fletcher et al., 2010). BCRP mainly expresses in the apical membrane of the intestine and effluxes anticancer drugs like doxorubicin, mitoxantrone, methotrexate, SN38, and flavopiridol (Oostendorp et al., 2009). Thus, it helps maintain the oral bioavailability, clearance, and toxicity of these drugs inside the

body. As BCRP expresses in the blood-brain barrier, along with P-gp, it prevents the penetration and efficacy of certain drugs such as imatinib in the CNS (Agarwal et al., 2010; Chen et al., 2009; Salphati et al., 2010). Researchers associate BCRP overexpression with chemoresistance in breast, colorectal, liver, gastric, and blood cancers (Fletcher et al., 2010).

1.3.1.2. SLC Superfamily

Classified into 52 different families based on amino acids, the SLC superfamily includes members responsible for transporting a broad spectrum of molecules such as amino acids, peptides, sugars, inorganic ions, organic anions and cations, electrolytes, metal ions, and neurotransmitters (Hagenbuch & Stieger, 2013; Keogh et al., 2016). Key members of this superfamily involved in drug transport are the SLCO, SLC22, and SLC47 families. The SLCO family includes pharmacologically significant members like OATP1B1 (SLCO1B1) and OATP1B3 (SLCO1B3), while the SLC22 family comprises OCT1 (SLC22A1), OCT2 (SLC22A2), OAT1 (SLC22A6), and OAT3 (SLC22A8). The SLC47 family includes MATE1 (SLC47A1) and MATE2-K (SLC47A2). Members of the SLCO and SLC22 families are primarily responsible for drug uptake, whereas members of the SLC47 family facilitate drug efflux. These transporters handle numerous essential chemotherapeutic agents and are vital for studying clinical transporter-mediated drug-drug interactions (DDI). The SLCO and SLC22 family members are characterized by 12 transmembrane domains TMDs (Binks & Dobrota, 1990). The next section will explore the role of the ABC and SLC superfamilies in oxaliplatin transport.

1.3.1.3. Ion pumps (ATPase) family

ATPases, or ion pumps, are a family of ATP-dependent active ion transporters that move ions such as Na⁺, K⁺, H⁺, Ca⁺, and Cu⁺ out of the cell (Hediger et al., 2004). These pumps are crucial for creating and maintaining electrochemical ion gradients across cellular membranes, which play a role in the disposition, accumulation, and sensitivity of cells to various drugs, including anticancer agents. Ion pumps work in conjunction with SLC transporters to facilitate the movement of nutrients, ions, and drugs (Huang & Sadee, 2006). Although ion pumps have not been extensively studied, it is believed that the effectiveness of several chemotherapeutic agents depends on their activity. Over the past few decades, research has focused on specific ATPase families, such as vacuolar-H⁺-ATPase and the copper export pumps ATP7A and ATP7B. The expression levels of ATP7A and ATP7B are strongly correlated with the cytotoxicity of platinum-based drugs in various cancer cell lines (Huang & Sadee, 2006). These findings suggest that

ATP7A and ATP7B expression could serve as predictive markers for chemoresistance to drugs like cisplatin and oxaliplatin (Dilruba & Kalayda, 2016; Kruh, 2003).

1.3.2. Oxaliplatin uptake and ABC transporters

The clinical efficacy of oxaliplatin is influenced by factors that regulate its cellular uptake and resistance, which are largely determined by the expression of various membrane transporters in tumour cells. Oxaliplatin can enter and exit cells through different membrane transporters, with members of the ABC, SLC, and ATPase superfamilies playing key roles in its chemosensitivity and chemoresistance.

1.3.2.1. *ATP7A and ATP7B*

The P-type ATPase family members, ATP7A and ATP7B, regulate copper efflux at the cellular level. While there is no direct evidence that these transporters efflux platinum drugs, their expression levels significantly influence oxaliplatin accumulation in cells (G. Samimi, K. Katano, et al., 2004). ATP7A is expressed in intestinal, endothelial, and aortic cells, whereas ATP7B is predominantly expressed in liver cells; both are also found in the brain, kidney, lung, placenta, and mammary gland cells (Lutsenko et al., 2007). Functional mutations in ATP7A and ATP7B lead to inherited neurodegenerative disorders such as Menkes disease and Wilson's disease, respectively, both characterized by abnormal copper metabolism (Lutsenko et al., 2007). In human fibroblast cell lines stably expressing ATP7A (MeMNK) and ATP7B (MeWND), increased levels of cellular platinum accumulation, DNA-platinum adducts, and sensitivity to oxaliplatin were observed compared to control cells. This suggests that ATP7A and ATP7B likely sequester oxaliplatin into cytoplasmic vesicles, preventing it from reaching DNA targets and inducing resistance to the drug (G. Samimi, K. Katano, et al., 2004; G. Samimi, R. Safaei, et al., 2004). In comparison to parental Me32a cells, platinum uptake and oxaliplatin-induced DNA adducts, and cytotoxicity were either increased or unchanged in MeWND (Rabik et al., 2009; G. Samimi, K. Katano, et al., 2004). Additionally, ATP7A presence has been shown to mitigate oxaliplatin-induced neurotoxicity in rat dorsal root ganglion tissues. Clinically, elevated ATP7B levels have been associated with poor outcomes in colorectal cancer patients undergoing oxaliplatin-based chemotherapy (Martinez-Cardus et al., 2009). This data suggests that both ATP7A and ATP7B are involved in the efflux of oxaliplatin.

1.3.2.2. *CTR1*

The copper influx transporter CTR1, encoded by the SLC31A1 gene and located in the plasma membrane, regulates cellular Cu⁺ homeostasis and is implicated in the accumulation of platinum-based compounds, including oxaliplatin. Studies have shown that overexpression of CTR1 in cancer cell lines enhances cellular uptake and cytotoxicity of oxaliplatin (J. J. Liu et al., 2012). One study using CTR1^{+/+} and CTR1^{-/-} mouse embryonic fibroblasts and xenografts demonstrated that CTR1 forms a pore through the plasma membrane to import Cu⁺, facilitating the cellular accumulation of cisplatin, carboplatin, and oxaliplatin (Perego & Robert, 2016). Another *in vivo* study reported increased cellular platinum accumulation and cytotoxic effects in rat Ctr1 overexpressing HEK293 cells compared to control cells (Hediger et al., 2004). Furthermore, elevated CTR1 expression has been linked to oxaliplatin-induced neurotoxicity in the neural cells of the dorsal root ganglia in rats (J. J. Liu et al., 2009). The role of the copper transporter CTR2 in the cellular transport of oxaliplatin has not been established.

1.3.2.3. *MATE1 and MATE2*

The multidrug and toxin extrusion transporters MATE1 (encoded by SLC47A1) and MATE2 (encoded by SLC47A2) are involved in the regulation of oxaliplatin transport (Yokoo et al., 2007; A. Yonezawa et al., 2006). MATE1 is localized in the canalicular membrane of liver cells and the luminal membrane of renal proximal tubules, while MATE2 is predominantly expressed in the luminal membrane of renal proximal tubules (Masuda et al., 2006; Otsuka et al., 2005). Research utilizing cell models with MATE1 overexpression has confirmed that oxaliplatin acts as a substrate for MATE1 (A. Yonezawa et al., 2006). Furthermore, oxaliplatin has been identified as a substrate for the MATE2 isoform, MATE2-K. The observed reduced neurotoxicity of oxaliplatin, in comparison to cisplatin, is hypothesized to be influenced by the tissue-specific expression of MATE2-K (Yokoo et al., 2007; A. Yonezawa et al., 2006). Presently, there is no clinical evidence directly linking MATE1 and MATE2 transporters to oxaliplatin pharmacokinetics or toxicity.

1.3.2.4. *OCTs*

Numerous studies indicate that organic cation transporters (OCTs) of the SLC superfamily are implicated in the uptake of platinum-based drugs, including oxaliplatin (Ciarimboli et al., 2010; Ciarimboli et al., 2005; A. Yonezawa et al., 2006; Zhang et al., 2006). OCTs are widely expressed across various human tissues, including intestinal,

hepatic, and renal epithelial cells, playing a crucial role in the pharmacokinetics of platinum drugs. However, conflicting preclinical data have led to an unclear understanding of the role of OCTs in oxaliplatin transport and pharmacokinetics. Evidence from studies using cell lines overexpressing OCT1 (SLC22A1 gene) and OCT2 (SLC22A2 gene) suggests that oxaliplatin is a substrate for both OCT1 and OCT2. The presence of an OCT inhibitor has been shown to reduce oxaliplatin accumulation (Zhang et al., 2006). Contrarily, other studies have reported that oxaliplatin is not a substrate for OCT1 (Yokoo et al., 2007; A. Yonezawa et al., 2006). The lack of pharmacokinetic changes in OCT1-deficient mice compared to wild-type mice suggests that multiple factors regulate platinum elimination (S. Li et al., 2011). Recently, it was demonstrated that in metastatic colorectal cancer patients treated with FOLFOX chemotherapy, OCT2 is involved in oxaliplatin accumulation, and both OCT2 and OAT2 are proposed to mediate cellular uptake of 5-FU (Tashiro et al., 2014). Some studies also indicate that oxaliplatin is a substrate for human OCT3 (SLC22A3 gene) (Yokoo et al., 2007; A. Yonezawa et al., 2006; Zhang et al., 2006). Moreover, it has been shown that organic cation/carnitine transporters OCTN1 (SLC22A4 gene) and OCTN2 (SLC22A5 gene), expressed in rat dorsal root ganglion tissues, contribute to oxaliplatin accumulation and cytotoxicity (Jong et al., 2011). This body of evidence suggests that OCT involvement may be a significant factor in oxaliplatin accumulation within tumours and drug distribution throughout the body.

1.3.2.5. MDR and MRPs

Efflux transporters of the ABC superfamily, particularly the MRP family, are known to play a role in the transport of platinum drugs (Sprowl et al., 2013). MRP transporters are extensively distributed throughout the human body, predominantly in excretory organs such as the liver, renal tubules, kidneys, and intestines, as well as in barrier sites like the blood-brain barrier and the blood-testis barrier (Borst & Elferink, 2002b; Jemnitz et al., 2010; Oostendorp et al., 2009; Uchida et al., 2011). Research indicates that elevated levels of MRP1 (ABCC1 gene) or MRP4 (ABCC4 gene) are linked to oxaliplatin resistance (Beretta et al., 2010). Additionally, inhibiting MRP1 and reducing cellular glutathione levels with verapamil has been shown to increase oxaliplatin sensitivity and decrease tumour growth in mice (Wang et al., 2013). MRP2 (encoded by ABCC2 gene) primarily effluxes drugs conjugated with glutathione (Gatti et al., 2009), and glutathione conjugation is a major pathway for platinum detoxification. This process leads to the formation of inactive metabolites, ultimately causing platinum resistance by the efflux of platinum-glutathione conjugates via MRP2 (Perego & Robert, 2016). Various studies have demonstrated that MRP expression levels are associated with cellular resistance to

oxaliplatin in different human oxaliplatin-resistant cancer cell lines (Beretta et al., 2010; Z. Liu et al., 2010; Mohn, Hacker, et al., 2013; C. Mohn, G. V. Kalayda, H. G. Hacker, et al., 2010). Another study highlighted that modulation of MRP-mediated drug transporters may explain the synergistic effect of FOLFOX combination chemotherapy, where the presence of 5-FU was found to increase MRP2 expression, resulting in increased sensitivity to oxaliplatin (Theile et al., 2009). Recently, it has been shown that MRP2 mediates oxaliplatin transport using ATP as an energy source in a membrane vesicle study (Myint et al., 2015). Collectively, these studies suggest that MRP2 is a crucial efflux transporter for oxaliplatin. The background knowledge of MRP2, its function, and its role in oxaliplatin resistance are discussed in the following section. Overall, the clinical impact of drug transporters on oxaliplatin accumulation and efflux is significant in determining the drug's pharmacokinetics, efficacy, and adverse reactions.

1.3.2.6. ABC transporters and multidrug resistance (MDR)

Multidrug resistance (MDR) is a major cause of treatment failure in various cancers. Research has shown that the expression levels of ABC transporters regulate the accumulation of various drugs, and overexpression of these transporters leads to MDR (Fletcher et al., 2010; Mohammad et al., 2018). Some ABC transporters are highly expressed in human cancers, including liver, pancreatic, colorectal, and breast cancers. This overexpression is associated with drug resistance in cancer patients, resulting in MDR. Several factors contribute to MDR in cancer patients, including activation of DNA repair mechanisms, alterations in apoptotic signaling pathways, activation of drug-metabolizing enzymes (cytochrome P450), reduced drug influx, and increased drug efflux activity (Cree & Charlton, 2017; Gottesman et al., 2002). A primary cause of MDR is the overexpression of several ABC transporters, leading to the efflux of various chemotherapeutic drugs from cells. The high expression of these transporters correlates with poor responses to anticancer drugs in certain cancers (Huang & Sadee, 2006). Numerous *in vitro* studies have shown that ABC transporters affect the sensitivity of anticancer drugs by decreasing their cellular accumulation. These findings highlight the critical role that ABC transporters play in cancer chemotherapy as important determinants of the pharmacokinetics and efficacy of certain chemotherapeutic drugs. At least 15 ABC transporters have been implicated in drug resistance, with major membrane transporters responsible for MDR belonging to the ABC superfamily, including P-gp, MRP1, MRP2, BCRP, and CFTR (cystic fibrosis transmembrane conductance regulator) (Mohammad et al., 2018; Robey et al., 2018a). Modulation of these transporters results in drug resistance and genetic diseases due to their inherent

substrate-pumping abilities. From the information discussed above, it can be concluded that the expression levels of ABC transporters and other membrane transporters can regulate the accumulation of oxaliplatin inside cells.

In some instances, cancer cells inherently express higher levels of ABC transporters even without the presence of chemotherapeutic agents. This phenomenon, referred to as intrinsic resistance, can be attributed to various factors such as genetic mutations, the specific characteristics of the tissue, and the tumor microenvironment (Szakacs et al., 2006). On the other hand, the overexpression of efflux transporters can also be induced by exposure to anticancer drugs. This induced overexpression, potentially resulting from mutations in the MDR gene, is known as acquired resistance. Furthermore, alterations in cellular detoxification processes, such as glutathione conjugation, can contribute to acquired resistance by enabling cells to expel chemotherapeutic drugs more rapidly, thereby diminishing their therapeutic efficacy (Mohammad et al., 2018).

Multiple *in vitro* and *in vivo* studies have demonstrated that the efflux activity of ABC transporters is a key mediator of MDR. The significance of ABC transporters in MDR is underscored by the identification of numerous anticancer drugs as substrates, including taxols, vinca alkaloids, anthracyclines, epipodophyllotoxins, and tyrosine kinase inhibitors (Robey et al., 2018a). Recently, it has been found that the MRP2 transporter is involved in the transport of oxaliplatin-associated platinum. This discovery has directed attention towards the inhibition of MRP2 activity, suggesting that modulating the MRP2 transporter could enhance the efficacy of oxaliplatin-based chemotherapy and improve patient outcomes through increased drug accumulation. Consequently, this thesis is centered on the modulation of MRP2 to overcome oxaliplatin chemoresistance in gastrointestinal (GI) cancer cells.

1.4. MRP2: Multidrug resistance-associated protein 2

Multidrug resistance-associated protein 2 (MRP2), also known as canalicular multiple specific organic anion transporter 1 (cMOAT) or ATP-binding cassette subfamily C member 2 (ABCC2), is a crucial membrane transporter protein encoded by the ABCC2 gene, a member of the ABC superfamily. Located on chromosome 10q24, the ABCC2 gene spans 69 kilobase pairs and consists of 32 exons (Taniguchi et al., 1996; Toh et al., 1999). Structurally, MRP2 comprises 17 transmembrane domains and 2 nucleotide-binding domains, amounting to 1545 amino acids with an additional 200 amino acids in

the amino-proximal domain (Tusnády et al., 1997).

MRP2 is a membrane protein of approximately 190 kDa, prominently expressed on the apical membranes of canalicular cells in the liver (Kool, de Haas, Scheffer, et al., 1997), small intestine, kidney renal proximal tubules, and gallbladder (Surowiak et al., 2006). Its primary role involves the excretion of small organic anions, particularly in biliary transport (Sekine et al., 2006).

1.4.1. MRP2 Transporter: A Key Player in Drug Metabolism, Detoxification, and Xenobiotic Defence

The MRP2 transporter protein is expressed across a range of tissues, indicating its vital physiological roles. In humans, MRP2 is localized at the apical sites of hepatocytes, renal proximal tubules, and the small intestine, as well as at physiological barriers like the blood-brain barrier, blood-tissue barrier, and placenta (Sandusky et al., 2002). This localization suggests MRP2's involvement in the absorption, metabolism, and excretion of drugs, xenobiotics, and toxins. MRP2's protective function is achieved through the elimination of toxins in the intestine or active excretion in the liver, kidney, or intestine. Thus, MRP2 is instrumental in both direct drug excretion and the limitation of xenobiotic uptake. A critical function of MRP2 is detoxification by transporting a variety of compounds and xenobiotics, notably through glutathione conjugation.

MRP2 is notably present on the apical membrane of polarized cells, governing crucial processes of drug absorption, distribution, and excretion, and is also expressed at physiological barriers such as the blood-brain barrier and placenta (Potschka et al., 2003; St-Pierre et al., 2000). MRP2's role includes the transport of a wide array of anionic compounds, both conjugated and unconjugated, into bile ducts, such as glutathione (GSH), glucuronides, 17 β -glucuronosyl estradiol (Jemnitz et al., 2010; Keppler, 2011; König et al., 1999; Naruhashi et al., 2002), and cysteinyl leukotriene (leukotriene C₄). MRP2 transports numerous organic anionic anticancer drugs, including anthracyclines, vincristine, methotrexate, and cisplatin (Schinkel & Jonker, 2003). Additionally, weakly basic drugs, such as vinblastine, are generally transported in conjunction with GSH by MRP2 (Evers et al., 2000).

Mutations in the MRP2 gene cause Dubin-Johnson syndrome (DJS), an autosomal

recessive disorder characterized by conjugated hyperbilirubinemia, resulting in jaundice (Toh et al., 1999). The importance of MRP2 is highlighted in studies using mutant rat strains like Groningen Yellow GY/TR--Wistar and Eisai hyperbilirubinemic rats (EHBR), which are *Mrp2*-deficient and exhibit hyperbilirubinemia (Kawabe et al., 1999; Paulusma et al., 1997), along with defective ATP-dependent transport of conjugated bilirubin across the canalicular membrane of hepatocytes (Sandusky et al., 2002). MRP2 expression is linked to the renal and liver toxicity of anticancer drugs like cisplatin and methotrexate.

Thus, MRP2 is crucial in the body's defence against drugs and xenobiotics by facilitating their excretion through bile or urine, influencing drug bioavailability and disposition.

1.4.2. MRP2 Expression in Human Cancers: Implications for Chemoresistance and Potential as a Biomarker

MRP2 protein expression is observed in various human cancers, including colorectal, ovarian, lung, and other gastrointestinal cancers (Gatti et al., 2011; Baohui Han et al., 2011; Noma et al., 2008). MRP2 has also been detected in clinical specimens of renal, gastric, colorectal, and hepatocellular cancers (Szakacs et al., 2006). Both *in vitro* and *in vivo* studies have demonstrated MRP2's role in effluxing a broad range of clinically used chemotherapeutics, including cisplatin, doxorubicin, docetaxel, etoposide, irinotecan, methotrexate, and vincristine (Jemnitz et al., 2010).

The functional activity of MRP2 is associated with the sensitivity of different anticancer drugs, including cisplatin, methotrexate, etoposide, and vinca alkaloids (Szakacs et al., 2006). MRP2 expression is notably higher in various platinum-based drug-resistant human cancer cells, such as those from bladder, prostate, colon, ovarian, adrenocortical, and melanoma origins (Kool, de Haas, Scheffer, et al., 1997; Minemura et al., 1999; Noma et al., 2008; Taniguchi et al., 1996). Increased MRP2 expression is linked to reduced cellular accumulation of cisplatin, consequently diminishing its toxicity in MRP2-overexpressing human cancer cell lines (Y. Cui, J. Konig, et al., 1999; Taniguchi et al., 1996). These findings underscore MRP2's significant role during chemotherapy in cancer cells.

One study highlighted that MRP2 mRNA is expressed in both human pancreatic cancer

and normal pancreatic tissues, with expression levels being 1.2 to 30-fold higher in pancreatic cancer tissues (Noma et al., 2008). Additionally, *in vitro* studies showed a 1.5-fold higher expression of MRP2 mRNA in CDDP (gemcitabine and cisplatin) drug-resistant pancreatic cell lines compared to parent cells. Therefore, MRP2 expression is vital in human pancreatic cancer. Higher MRP2 expression in human colorectal cancer tissues compared to non-cancerous tissues suggests that the MRP2 gene could serve as a potential biomarker for colorectal cancer (Andersen et al., 2015; Hinoshita et al., 2000). Elevated MRP2 expression is associated with reduced sensitivity to platinum-based therapy (Liedert et al., 2003; Materna et al., 2006; Taniguchi et al., 1996; Wen, Buckley, et al., 2014; Xie et al., 2008). Numerous studies have reported significantly upregulated ABCC2 mRNA levels in colorectal cancer tissues compared to non-cancerous regions from the same patients, with normal colorectal mucosa showing minimal or no ABCC2 mRNA expression (Arana et al., 2016). These results indicate that MRP2 is frequently upregulated in various tumour types, leading to increased drug efflux and resistance to chemotherapeutic agents (Chen et al., 2016).

1.4.3. Genetic Variants in the MRP2 Transporter (ABCC2): Implications for Dubin-Johnson Syndrome and Cancer Chemotherapy

In contrast to other ABC transporters like P-gp, fewer data are available on genetic variants in the MRP2 transporter gene (ABCC2). Dubin-Johnson syndrome (DJS), a disorder causing impaired hepatobiliary secretion of organic anions, conjugated hyperbilirubinemia, and liver pigmentation, results from a rare missense mutation (2302C>T) in the MRP2 gene, located in the first NBD C motif (Hoffmann & Kroemer, 2004; Szakacs et al., 2006).

Other causative missense, nonsense, splice site, and deletion mutations have also been linked to DJS (Hoffmann & Kroemer, 2004). Several single nucleotide polymorphisms (SNPs) or genetic variants have been identified in ABCC2. The three most commonly reported ABCC2 SNPs are C24T SNP (C to T substitution in the promoter region), G1249A SNP (G to A substitution at exon 10), and C3972T SNP (C to T substitution at exon 28, resulting in a silent mutation at codon 1324) (Suzuki & Sugiyama, 2002). These SNPs are associated with defects in MRP2 expression or functionality. One study reported that the frequently studied ABCC2 C24T SNP does not affect ABCC2 mRNA expression in human duodenal enterocytes (Moriya et al., 2002), but a significant

association was found between C24T SNP and lung cancer patients (B. Han et al., 2011). Another study indicated that C24T SNP correlates with reduced disease-free survival and overall survival (OS) in lung cancer patients undergoing platinum-based chemotherapy (Campa et al., 2012). The ABCC2 G1249A SNP is linked to poor response to FOLFOX4 chemotherapy and shorter survival in colorectal cancer patients (Mirakhorli et al., 2013). Moreover, this SNP is associated with poor response to platinum-based chemotherapy in ovarian cancer patients, although another study showed no correlation between G1249A SNP and progression-free survival (PFS) or OS in ovarian cancer patients receiving platinum-based chemotherapy (Tian et al., 2012). The ABCC2 C3972T SNP is linked to an increased risk of grade 3 or 4 thrombocytopenia toxicity in lung cancer patients treated with platinum-based chemotherapy (B. Han et al., 2011).

The impact of ABCC2 SNPs on MRP2 functional activity remains controversial due to conflicting findings and the complex nature of multiple SNPs. However, the available evidence suggests that ABCC2 SNPs significantly influence cancer treatment and could be utilized in personalized therapy for cancer patients receiving MRP2 substrate drugs.

1.4.4. The Role of MRP2 Transporters in Multidrug Resistance and Clinical Outcomes of Gastrointestinal Cancers: Implications for Platinum-Based Chemotherapy

The role of MRP2 transporters in multidrug resistance (MDR) and clinical outcomes in gastrointestinal cancer patients receiving platinum-based chemotherapy has been extensively studied. MRP2 expression is elevated in tumor tissues from patients with hepatocellular carcinoma, pancreatic cancer, and colorectal cancer (Hinoshita et al., 2000; Korita et al., 2010; Mirakhorli et al., 2013; Nies, König, et al., 2001; Noma et al., 2008). Platinum-based chemotherapy has shown significant effects in gastrointestinal cancer tumors, including pancreatic cancer with elevated MRP2 levels (Hinoshita et al., 2000; Noma et al., 2008).

Numerous *in vitro* studies have demonstrated the association of MRP2 with the cellular accumulation of cisplatin in human liver and ovarian cancer cells (Materna et al., 2006). *In vitro* studies also indicated that MRP2 contributes to cellular resistance to cisplatin in human liver cancer (Korita et al., 2010). Unlike other ABC transporters, high levels of MRP2 expression at both mRNA and protein levels have been observed in the platinum

drug-resistant melanoma cancer cell line MeWo CIS 1. Overexpressed MRP2 reduces the formation of platinum-induced intra-strand cross-links in nuclear DNA and decreases platinum DNA [Pt-d(GpG)] adducts in platinum-resistant melanoma cells (Liedert et al., 2003). These findings suggest that MRP2 is involved in the cellular transport of platinum-based drugs. In pancreatic cancer patients receiving gemcitabine and cisplatin therapy, the MRP2 G40A GG genetic variant is associated with low OS and poor chemotherapy response (Tanaka et al., 2011). Another study examined ABC transporter expression in oxaliplatin-resistant colon cancer cell lines SW620/L-OHP and LoVo/L-OHP, finding that only MRP2 expression was upregulated in resistant cell lines, with no significant changes in P-gp and MRP1 (Zhen Liu et al., 2010). Cellular accumulation of oxaliplatin increased nearly two-fold in the presence of the MRP1 and MRP2 inhibitor Gü83 in the HCT8 human ileocecal colorectal adenocarcinoma cell line and its oxaliplatin-resistant variant, HCT8 ox (C Mohn et al., 2010). This suggests that MRP2 contributes to oxaliplatin transport and cellular accumulation in cancer cells. Studies have shown increased MRP2 expression in colorectal cancer tissues compared to normal tissues, with high MRP2 expression linked to recurrence during FOLFOX4 chemotherapy (Mirakhorli et al., 2013). Preincubation with 5-FU in FOLFOX therapy increases MRP2 expression, enhancing oxaliplatin sensitivity and resistance to DACH, oxalate, and Pt (DACH)Cl₂ platinum adducts (Theile et al., 2009).

In conclusion, MRP2 transporters play a significant role in cellular resistance to oxaliplatin in human gastrointestinal (GI) cancer cells. There is a strong association between MRP2 expression levels and oxaliplatin resistance in human GI cancer, indicating the importance of determining cellular platinum accumulation and oxaliplatin sensitivity in GI cancer cells after modulating MRP2 transporters.

1.5. Phytochemical inhibitors of ABC transporters

Accumulating evidence has demonstrated that ABC transporters play a crucial role in drug efflux, leading to reduced intracellular drug levels and ultimately contributing to chemotherapy failure. To combat this, effective strategies to sensitize drug-resistant cancer cells to anticancer treatments involve inhibiting ABC transporter activity either by downregulating their expression or by coadministering inhibitors, such as synthetic inhibitors, alongside anticancer drugs. Previous studies by our team revealed that inhibiting the MRP2 transporter in GI cancer cells using ABCC2-siRNAs increased their sensitivity to oxaliplatin. However, delivering functional siRNAs specifically to certain cell types is challenging. The primary obstacle in siRNA-based clinical applications is

getting siRNAs across the cell plasma membrane, and most previously described methods fail due to non-specific delivery to cells (Lorenzer et al., 2015). To address this issue, this section explores a different strategy to overcome MDR in GI cancer cells, utilizing a small molecule to inhibit MRP2 transport activity.

The development of synthetic inhibitors initially focused on inhibiting P-gp activity. First-generation P-gp inhibitors, including cyclosporine A, erythromycin, tamoxifen, and verapamil, were found to have low efficacy and high toxicity at tolerable doses, requiring high dosages to reverse MDR (Tan et al., 2000; Thomas & Coley, 2003). Second-generation P-gp inhibitors improved efficacy and reduced side effects, with valsopodar (a cyclosporine A analogue) being 10 to 20 times more effective than cyclosporine A in reversing MDR in cell lines and animal models (Bugde et al., 2017; Krishna & Mayer, 2000). However, these inhibitors necessitated high concentrations of chemotherapeutic drugs, leading to increased drug metabolism, excretion, and a heightened risk of off-target toxicity (Bates et al., 2004). This led to the development of third-generation P-gp inhibitors like tariquidar and phenothiazines, which were more effective than earlier inhibitors (Abraham et al., 2009; Coley, 2010; Takacs et al., 2015).

In trials, tariquidar was combined with carboplatin (a non-P-gp substrate) to treat advanced lung cancer, though the results were inconclusive (Fox & Bates, 2007). The clinical application of most synthetic inhibitors targeting other ABC transporters has been limited to *in vitro* studies. MK571, a well-known third-generation inhibitor, effectively inhibits MRP activity, including MRP2, in various cancer cell lines (Abrahamse & Rechkemmer, 2001; P. Matsson et al., 2009; Yokooji et al., 2007). However, the use of synthetic inhibitors in *in vivo* systems has been scarcely studied, with concerns about toxicity, altered drug clearance, and limited knowledge of pharmacokinetic properties being the primary barriers (Choi & Yu, 2014; El-Awady et al., 2016; Kathawala et al., 2015). MK571 might not even be appropriate for *in vitro* studies on oxaliplatin-MRP2 interactions due to its potential to directly interact with oxaliplatin, forming Pt(DACH) sulfhydryl complexes that could obscure the effects of MRP2 modulation.

Several other small molecules have been developed to modulate ABC transporters, showing lower cytotoxicity than synthetic inhibitors. Natural compounds derived from plants, fruits, vegetables, herbs, and animals, or their chemically modified derivatives, can reverse MDR in ABC transporters or modulate efflux transporter activity with fewer

toxic effects than synthetic inhibitors (Li et al., 2016; Li et al., 2010). Well-known natural products that inhibit or modulate transporter activity include curcumin, fumitremorgin C (FTC), myricetin, saponin, and Sipholenol A (Ceballos et al., 2018; Hillgren et al., 2013; Li et al., 2010; P. Matsson et al., 2009). Indeed, coadministration of myricetin with oxaliplatin has been shown to enhance oxaliplatin efficacy in liver tumour xenografted mice without causing toxicity (Khine, et al, 2019).

Chrysin is a flavonoid derived from plants, primarily found in honey, propolis, and various medicinal plants and fruits (Stompor-Goracy et al., 2021). It exhibits a broad range of biological activities, including antioxidant, antidiabetic, and anti-inflammatory effects, as well as antibacterial, antihypertensive, anti-allergic, vasodilatory, anxiolytic, antiviral, anti-estrogenic, liver-protective, anti-aging, anti-seizure, and anticancer properties (Anand et al., 2012; Brown et al., 2007; Chen et al., 2012; Critchfield et al., 1996; Du et al., 2012; Duarte et al., 2001; Gresa-Arribas et al., 2010; Khoo et al., 2010; Machala et al., 2001; Medina et al., 1990; Pushpavalli et al., 2010; Salari et al., 2022; Torres-Piedra et al., 2010; Villar et al., 2002; J. Wang et al., 2011). Chrysin triggers apoptosis via the intrinsic mitochondrial pathway, causing disruption of mitochondrial membrane potential (MMP) and enhancing DNA fragmentation. It also induces proapoptotic proteins like Bax and Bak, and activates caspase-9 and caspase-3 across various cancer cell types (Pichichero et al., 2011; Xue et al., 2016). Moreover, chrysin inhibits tumour growth by activating P38 MAPK and inducing cell cycle arrest (Weng et al., 2005). Given its potent antitumor properties, chrysin, as a natural plant-derived compound, could be effective in combating chemotherapy resistance in cancer cells (Martins et al., 2015). Additionally, chrysin inhibits tumour development by targeting histone deacetylase 8 (HDAC8) (Xuan et al., 2016).

In an *in vitro* study utilizing the Caco-2 cell culture model, the presence of MK-571, a specific MRP2 inhibitor, reduced the apical efflux of both chrysin glucuronide and sulfate, indicating that these conjugates are MRP2 substrates (Walle et al., 1999). Another *in vitro* study with HEK293 cells demonstrated that MK-571 inhibited the efflux of chrysin-7-O-sulfate, leading to a significant increase in intracellular sulfate levels (Li et al., 2015). These studies provide some of the only direct evidence that MRP2 is involved in chrysin conjugate efflux, a finding further supported in this thesis through module fitting in Chapter 4. Additionally, chrysin-7-O-sulfate has been identified as an effective substrate for the MRP4 transporter. Supporting this conclusion, the knockout of MRP4 in HEK293 cells significantly reduced chrysin-7-O-sulfate secretion while significantly increasing its intracellular accumulation by 125–135% (Li

et al., 2015). MPR4 is expressed on the apical or basolateral surfaces of various organs. For example, in the kidney and blood-brain barrier (BBB), MPR4 is located on the apical side, where it pumps chrysin-sulfate into urine in the kidney or into the bloodstream in the brain. Conversely, in hepatocytes, MPR4 is found on the basolateral side, where it transports chrysin-sulfate back into the bloodstream (Giacomini et al., 2010). Additionally, MPR1 has been identified as a transporter that facilitates the efflux of chrysin-7-O-glucuronide in Hela cells (Quan et al., 2015).

1.6. Manuka Honey

Manuka honey is produced from the nectar of a New Zealand (NZ) native plant, Manuka tree, which is also known as *Leptospermum scoparium*. It is common to see Manuka flower between September and February. Manuka honey stands out for its potent medicinal properties, which far exceed those of regular honey. The composition of Manuka honey gives it a distinct therapeutic profile.

Manuka honey has been used in wound healing since ancient times in NZ. There have been so many studies showing that more flavonoid and phenolic antioxidants are found in Manuka honey rather than other honey in the world. Manuka honey is graded by its UMF (unique manuka factor) or MGO (methylglyoxal) which is an additional antibacterial compound in Manuka honey, a rating system that measures the antibacterial strength of Manuka honey. UMF levels range from 5+ to 20+ or higher, with higher UMF levels indicating greater therapeutic effectiveness.

Due to the conversion of DNA (dihydroxyacetone) present in the nectar of Manuka flower, the concentration of MGO in Manuka honey is much higher compared to other types of honey. This compound is largely responsible for Manuka honey's potent antibacterial properties, making it a popular ingredient in wound care and infection prevention (Adams et al., 2008).

In addition, more and more Manuka honey products are labelled by this indication. More and more researchers care about natural products with antitumor properties, as they may reduce side effects on humans. Recently our team and another Italian group have reported that NZ Manuka honey showed selective toxicity and induced apoptosis in colorectal cancer cell lines but not in normal human cells (Chan & Li, 2016; D et al.,

2024). Consistently other researchers also reported that early apoptosis in bone cancers in a dose-dependent manner and attenuates proliferation in Hela cell lines (Y. Wang et al., 2011). Honey can increase apoptosis in oral cancers as well.

Manuka honey is renowned for its remarkable antibacterial properties, supported by various studies that highlight its effectiveness. Research indicates that the higher the MGO (methylglyoxal) content in Manuka honey, the greater its ability to inhibit a broad spectrum of pathogens, including *Staphylococcus Aureus* and *Helicobacter Pylori* (Roberts et al., 2015). In addition to its antibacterial benefits, Manuka honey exhibits antiviral properties that make it useful in combating infections such as influenza and herpes simplex (Jenkins et al., 2011).

Historically, Manuka honey has been utilized for its wound-healing abilities. It creates a moist environment at the site of an injury, which promotes tissue regeneration and reduces the risk of infection. This property is especially significant in the context of antibiotic-resistant bacteria, such as methicillin-resistant *Staphylococcus aureus* (MRSA). Studies have demonstrated that Manuka honey is quite effective in addressing these resistant strains (Cooper et al., 2010). Furthermore, Manuka honey is commonly included in skincare products due to its anti-inflammatory and moisturizing properties, which are beneficial in wound care.

In addition to its wound-healing capabilities, Manuka honey has been noted for its anti-inflammatory and immune-modulating effects. It plays a therapeutic role in managing conditions like inflammatory bowel disease (IBD) and arthritis (Seraglio et al., 2021). Manuka honey helps alleviate symptoms of chronic inflammation by reducing the production of pro-inflammatory cytokines.

Recent research also points to the potential of Manuka honey in cancer prevention and treatment. It shows promising antitumor activity, particularly due to its ability to induce apoptosis, or programmed cell death, in cancer cells. The honey contains various flavonoids and phenolic compounds, such as myricetin, pinocembrin, and quercetin, which contribute to its antitumor effects (Gośliński et al., 2020). Studies have shown that Manuka honey can inhibit the growth of various cancer cells, including those associated with colorectal cancer, breast cancer, and melanoma (Nolan et al., 2020).

Moreover, Manuka honey is beneficial in managing gastrointestinal issues. It has proven effective against conditions like gastritis, peptic ulcers, and acid reflux. Its antibacterial properties are particularly useful in combating *Helicobacter pylori*, a bacterium often linked to gastric ulcers (Yupanqui Miele et al., 2022).

In contrast to regular sugars, Manuka honey does not contribute to tooth decay. In fact, it has been shown to reduce the buildup of plaque and gingivitis due to its antibacterial properties. Manuka honey can inhibit the growth of oral bacteria such as *Streptococcus mutans*, which are known to cause dental caries (Sell et al., 2012).

In summary, Manuka honey's multifaceted benefits extend beyond its traditional uses. Its potent antibacterial, antiviral, anti-inflammatory, and antitumor properties make it a valuable natural remedy for a range of health issues, from wound healing to cancer prevention and oral health.

Myricetin (Figure 1-10) is found in honey, fruits, tea, red wine, nuts, berries, and vegetables, which is a flavonoid of a polyphenolic compound. Recently, our team has reported that myricetin could inhibit MRP2 resulting in a significant increase in cellular accumulation of oxaliplatin. As an MRP2 inhibitor, myricetin increased oxaliplatin cytotoxicity in human GI cancer cell lines — Caco-2, HepG2, and PANC-1 cells, and cellular platinum accumulation (Riya Biswas et al., 2019; Khine et al., 2019).

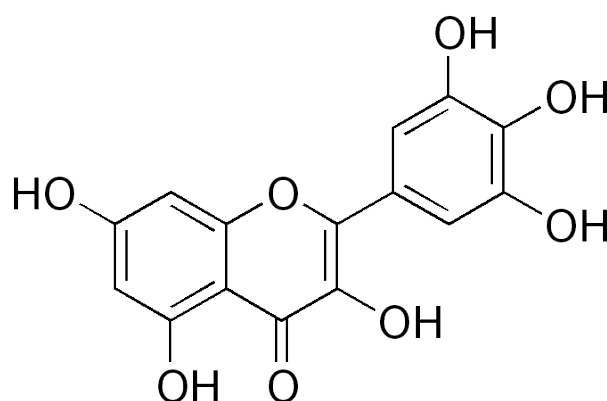


Figure 1- 9 Myricetin structure

There are many myricetin analogues found in honey: pinobanksin, chrysin, caffeic acid, galangin, and phenyl esters, apigenin, acacetin, pinocembrin, kaempferol, and quercetin. All of these phenolic compounds also have possible anti-cancer effects (Wahdan, 1998).

Given the structural similarity, these phenolic compounds could be good candidates as MRP2 inhibitors. However, whether these myricetin analogues are potent MRP2 inhibitors remains to be determined. The presence of multiple polyphenols in NZ Manuka honey may act synergistically to achieve anticancer and/or tumour resistance reversal effects.

1.7. Hypothesis and aim of the thesis

The platinum-based anticancer drug oxaliplatin, along with its combination therapies, plays a crucial role in the clinical treatment of colorectal cancer and other gastrointestinal (GI) malignancies (Stein & Arnold, 2012). However, the efficacy of oxaliplatin chemotherapy is limited in a subset of patients for reasons that remain unclear. A significant challenge in the treatment of GI cancer is the development of multidrug resistance (MDR) to chemotherapy. The primary mechanism underlying MDR involves the decreased cellular accumulation and increased efflux of anticancer drugs by ABC transporters. Various *in vitro* and *in vivo* studies have indicated that overexpression of different ABC transporters in many cancers correlates with poor treatment outcomes. Clinical studies have shown that high expression of MRP2 in GI cancers, including pancreatic, and colorectal cancers, is associated with reduced sensitivity to platinum-based chemotherapy (Cecchin et al., 2013; Mirakhorli et al., 2013). It is suggested that the main reason for poor efficacy is associated with the reduced cellular accumulation of oxaliplatin (J. J. Liu et al., 2012; Wersto et al., 2001). Factors regulating oxaliplatin accumulation, whether through their expression in GI cancer cells or through biological barriers affecting drug disposition, may play a role in its clinical activity. Studies have identified several membrane transporters, such as CTR1, OCTs, ATP7A, ATP7B, MATE1, and MATE2, that regulate oxaliplatin accumulation in cells (Jong et al., 2011; Liu et al., 2013; G. Samimi, K. Katano, et al., 2004; G. Samimi, R. Safaei, et al., 2004; Yokoo et al., 2007; A. Yonezawa et al., 2006). A recent study also suggests that MRP2 acts as an efflux transporter for oxaliplatin (Myint et al., 2015). Recently, our team has reported that MRP2 (a member of ABC transporter protein) confers oxaliplatin resistance and a phytochemical MRP2 inhibitor myricetin increased cellular platinum accumulation and oxaliplatin cytotoxicity in several human GI cancer cell lines (Riya Biswas et al., 2019; Khine et al., 2019). However, myricetin is not a potent MRP2 inhibitor, and it only marginally enhanced oxaliplatin sensitivity in tumour xenograft mouse model (Khine et al., 2019). Recently, our team discovered the anti-proliferation effects of NZ Manuka honey in several CRC cell lines but not in normal cells (Chan, 2016). However, the exact anti-cancer compound(s) remain unknown in NZ Manuka honey. Given the fact that NZ Manuka

honey contains abundant myricetin analogues and more than 90% ABC transporter inhibitors is derived from phytochemicals, we may identify novel and potent chemosensitizer (e.g. MRP2 inhibitors/modulators) from NZ Manuka honey, which contains several myricetin analogues.

This thesis involves the MRP2 gene (ABCC2) with high MRP2 expression, including MRP2 over-expressing and normal human embryonic kidney cells, and human pancreatic and colorectal cancer cell lines. For this research, we used HEK293, HEK-MRP2, PANC-1, and Caco-2 cells. Clinical studies indicate that MRP2 expression is higher in cancer tissues compared to non-cancer tissues (Andersen et al., 2015; Hinoshita et al., 2000). Previous studies have reported high MRP2 expression levels in PANC-1 and Caco-2 cells (Myint, 2015; Prime-Chapman et al., 2004). These cell lines were chosen to mimic clinical situations, making them suitable for our translational research. The phenolics and flavonoids were first separated by using LC-MS. The potential MRP2 inhibitors were then verified by model fitting. The MRP2-mediated transport of the substrate was verified using the MRP2-specific substrate 5(6)-carboxy-2',7'-dichlorofluorescein (CDCF) and chrysin as MRP2 inhibitor. Subsequently, oxaliplatin-derived platinum accumulation via MRP2-mediated transport in Caco-2 cells was measured by ICP-MS for platinum analysis method after exposure to oxaliplatin. The cellular sensitivity of MRP2 over expressing cells to oxaliplatin-induced cytotoxicity was also studied to determine the role of MRP2 in conferring cellular oxaliplatin resistance. The expression levels of MRP2 in MRP2 over expressing cells were assessed using a cell surface staining method. We determined the rate of oxaliplatin-induced apoptosis in GI cancer cell lines with varying concentrations of oxaliplatin after inhibiting MRP2 expression through pretreatment of varying concentrations of chrysin. The primary objective of this study is to identify the novel MRP2 inhibitors from NZ Manuka honey phenolic compounds and to evaluate the cellular platinum accumulation, and oxaliplatin-induced sensitivity and apoptosis rates.

Specific Aims of This Thesis:

- i. Develop and validate an LC-MS method to determine the phenolic compound fingerprint of NZ Manuka honey. (Chapter 3)
- ii. To find out the potential MRP2 inhibitor by using Model software to simulate the combination of phenolic compounds in Manuka honey extracts with MRP2. (Chapter 4)

- iii. Evaluate the modulation effects of Chrysin on MRP2 expression/activities by using an isogenic cell line (HEK293 and HEK-MRP2 cell panels) (Chapter 5)
- iv. Evaluate the anti-proliferation effects of Manuka honey extracts (Chrysin) in human colorectal Caco-2 cells: Using cell culture, cell proliferation (MTT assays), cell cycle (flow cytometric analysis), apoptotic cell death (CDCF accumulation). (Chapter 6)

Chapter 2 Materials and Methodology

2.1. Chemicals and equipment

The materials and reagents, including chemical compounds, buffers and solutions that were used in this research are listed in table 2-1.

Table 2- 1 List of chemicals used in this study with their sources

Chemicals	Suppliers
70% Nitric acid	Thermo Fisher Scientific (NZ)
Absolute Ethanol	Thermo Fisher Scientific (NZ)
Absolute Methanol	Thermo Fisher Scientific (NZ)
Anti-MRP2 antibody [M2 III-6] (catalogue # ab3376) (dilution: 1:400 ratio in 2% NZ milk powder)	Abcam (Melbourne, VIC, AU)
Alexa Fluor 488-labeled anti-mouse IgG Ab (catalogue # ab150120) (dilution: 1:1000 ratio in 2% BSA)	Abcam (Melbourne, VIC, AU)
Apoptosis Kit (catalogue # V13245)	Invitrogen (Carlsbad, CA, USA)
ABC Transporter Control membrane vesicles (catalogue # GM0003)	GenoMembrane (Life Technologies)
Bovine serum albumin (BSA)	Sigma-Aldrich (St Louis, MO, USA)
CDCFDA (5(6)-carboxy-2',7'-dichlorofluorescein diacetate) (catalogue # 21884- 100MG)	Sigma-Aldrich (St Louis, MO, USA)
Fatal bovine serum (FBS)	MediRay (NZ)
LC480 LightCycler Master Kit (catalogue # 04707516001)	Roche life science (NZ)
L-Glutamine (200 mM; 100 ml)	Life Technologies
Mouse IgG2a Isotype Control (catalogue # MA1-10419) (dilution: 1:1000 ratio in 2% NZ milk powder)	Invitrogen (Carlsbad, CA, USA)
MTT (3-(4, 5-Dimethylthiazol-2-yl)-2, 5-Diphenyltetrazolium Bromide) Formazan powder (catalogue # M5655-500MG)	Sigma-Aldrich (St Louis, MO, USA)
PrestoBlue™	Sigma-Aldrich (St Louis, MO, USA)
Myricetin (catalogue # M6760-25MG)	Sigma-Aldrich (St Louis, MO, USA)
Opti-MEM 1 (catalogue # 31985-070)	Life Technologies (Thermo Fisher Scientific, NZ)
Oxaliplatin solution	Actavis (Auckland, NZ)
Paraformaldehyde powder (catalogue # P6148- 500g)	Sigma-Aldrich (St Louis, MO, USA)
Penicillin-Streptomycin (10,000 U/mL; 100 mL)	Life Technologies (Thermo Fisher Scientific, NZ)

Platinum standard	Sigma-Aldrich (St Louis, MO, USA)
Roswell Park Memorial Institute (RPMI) 1640 Medium	Life Technologies (NZ)
DMEM Medium	Life Technologies (NZ)
Dimethyl sulfoxide (DMSO)	Sigma-Aldrich (St Louis, MO, USA)
Saponin (catalogue # 47036-50g)	Sigma-Aldrich (St Louis, MO, USA)
Stealth ABCC2-siRNAs (catalogue # 1299001)	Life Technologies (Thermo Fisher Scientific, NZ)
Stealth siRNA Negative control, Medium GC (catalogue # 12935-300)	Life Technologies (Thermo Fisher Scientific, NZ)
Synth-a-Freeze Medium	Life Technologies (Thermo Fisher Scientific, NZ)
Thallium standard	SPEX CertiPrep (NJ, USA)
Trypan Blue Stain (0.4%)	Life Technologies (NZ)
Myricetin powder	Sigma-Aldrich (St Louis, MO, USA)
Chrysin powder	Sigma-Aldrich (St Louis, MO, USA)
RIPA buffer (Radioimmunoprecipitation Assay buffer)	Abcam (Melbourne, VIC, AU)
4X Laemmli buffer	Abcam (Melbourne, VIC, AU)
10X Tris-Glycine / SDS buffer	Abcam (Melbourne, VIC, AU)
5X Semi-Dry Transfer buffer	Abcam (Melbourne, VIC, AU)
10X TBS buffer	Abcam (Melbourne, VIC, AU)
TBST buffer	Abcam (Melbourne, VIC, AU)
Blocking buffer (2% skim milk powder in TBST)	Anchor Skim milk powder (NZ)
Pierce™ ECL Western Blotting Substrate	Thermo Fisher Scientific (NZ)

Table 2- 2 List of equipment used in this study with their sources

Equipment	Suppliers
Inverted phase contrast microscope	Zeiss Primovert (Fisher scientific, NZ)
15 ml and 50 ml centrifuge tubes	<i>In vitro</i> Technologies (NZ)
25 ml and 75 ml vented cap tissue culture flasks	<i>In vitro</i> Technologies (NZ)
1 ml, 5 ml, 10 ml and 25 ml sterile disposable pipettes	<i>In vitro</i> Technologies (NZ)
Microtiter plate reader	Tecan Spark 10M (Mannedorf, Switzerland)
0.22 µM filter and a 10 ml syringe	Thermo Fisher Scientific (NZ)

Haemocytometer (Improved Neubauer)	Boeco (Germany)
6, 12 and 96-well plate	<i>In vitro</i> Technologies (NZ)
Centrifuge 5418 R	Eppendorf (North Ryde, NSW, AU)
Flow cytometer	Beckman Coulter MoFlo™ XDP (NZ)
Fluorescent microscope	Leica Microsystems (NZ)
LightCycler 480	Roche Life Science (NZ)
Agilent 1260 Infinity Quaternary LC System	Santa Clara, CA 95051 USA
Kinetex Evo C18 (2.1 X 150mm, 1.7µm) column for LC-MS/MS	Phenomenex (NZ)
Strata C18-E (55µm, 70A) 200mg / 3mL, Tubes	Phenomenex (NZ)
Assemble mini gel tank	BIO-RAD (NZ)
SDS-PAGE Gels	BIO-RAD (NZ)
PowerPac Basic Power Supply	BIO-RAD (NZ)
Trans-Blot Turbo instrument	BIO-RAD (NZ)
ImageQuant LAS 500	Thermo Fisher Scientific (NZ)
96 well plates reader	Thermo Fisher Scientific (NZ)

Twelve millimolar MTT (3-(4, 5-dimethylthiazil-2-yl)-2, 5-diphenyl tetrazolium bromide) stock solution was prepared by adding 1 ml of sterile PBS to 5 mg of MTT and stored at 4°C.

CDCFCFCD and myricetin stock solution was prepared at the concentration of 1000 times higher than working solution by dissolving in DMSO and these were stored at -20°C.

Oxaliplatin (Actavis, New Zealand) stock solution at 5 mg/ml was prepared by dissolving 100 mg powder into 20 ml MiliQ grade water followed by sonication and filtered with a 0.22 µm Millipore filter.

The stock solutions prepared above were immediately aliquot and stored at -20°C. The stock solutions were discarded one month after preparation.

Chrysin working solution at 60mM was prepared by dissolving 15.25mg powder into 1 ml DMSO and were prepared each time for fresh.

10X TBS stock solution was prepared by mixing 24g Tris-base, 88g NaCl, 900mL *Mili-Q* water, then adjust pH to 7.6 with HCl, add *mili-Q* water to 1L to make TBS buffer. Can be stored in fridge.

TBST working solution was prepared by diluting 10X TBS into 1X TBS and add Tween 20 (0.1%). Mix 10X TBS buffer 100mL, *Mili-Q* water 900mL and Tween 20 1mL.

Blocking buffer was prepared as 2% milk solution in TBST buffer and filtered before use.

2.2. Cell lines and cell culture

All cell culture procedures were conducted under sterile conditions using sterile solutions and equipment, adhering to sterile techniques within a Class II biological safety cabinet.

2.2.1. Human cell lines

The parental human embryonic kidney cell line (HEK293) and MRP2 overexpressing HEK293 (HEK-MRP2) cell lines, a panel of human gastrointestinal cancer cell lines, including PANC-1 and Caco-2 cell lines with a endogenous overexpression of MRP2 were employed for this project. HEK-MRP2 cell was obtained from the Netherland Cancer Research Institute (Borst group). The GI cell lines were purchased from the American Type Culture Collection (ATCC, Manassas, VA, USA). Once the cells were received from ATCC, they were stored in liquid nitrogen Dewar and maintained according to ATCC protocol. The general information about cell lines is listed in table 2-3.

Table 2- 3 Characteristics of human cell lines used in the experiment

Cell lines	General description	Culture properties	Morphology (Tissue)
PANC-1	Human pancreatic epithelioid carcinoma	Adherent	Epithelial (pancreas/duct)
Caco-2	Human colorectal adenocarcinoma	Adherent	Epithelial-like (Colon)

HEK293	HEK293 Human embryonic kidney parental	Adherent	Embryonic
HEK-MRP2	HEK293 Human embryonic kidney MRP2 over-	Adherent	Embryonic

2.2.2. Thawing cells

The frozen cell stocks in cryovials were swiftly thawed in a 37°C water bath after being removed from liquid nitrogen storage. The thawed cell suspension was then placed into a sterile 15 ml centrifuge tube that had been prefilled with prewarmed complete RPMI medium. After spinning at 500 × g for 5 minutes, the supernatant was carefully removed, and the cell pellets were resuspended in 1 ml of complete medium. This suspension was then added to T25 flasks (BD Falcon, Auckland, NZ) containing prewarmed complete RPMI medium, which was supplemented with 10% (v/v) fetal bovine serum (FBS), 2 mmol/L L-glutamine, 100 units/mL penicillin, and 100 units/mL streptomycin. The cells were cultured and allowed to grow in a humidified environment with 5% carbon dioxide at 37°C. (R. Biswas et al., 2019)

2.2.3. Cell maintenance and sub-culture

Cells were regularly monitored and sub-cultured when they reached 80% to 90% confluency, signalling the end of their exponential growth phase. To sub-culture, the cell flask was rinsed with prewarmed PBS, followed by the addition of TrypLE™ Express—approximately 1.5 ml for T-25 flasks and 2 ml for T-75 flasks—to detach the cells. The cells were incubated at 37°C for 5 to 10 minutes, depending on the cell line. For example, Caco-2 cells required a longer incubation time of 10 minutes, while PANC-1 and HEK293 cells needed about 5 minutes. To halt the trypsinization process, 3 to 4 ml of prewarmed complete RPMI medium—double the volume of the dissociation reagent—was added. The cell suspension was then transferred into 15 ml centrifuge tubes and centrifuged at 1200 RPM for 3 minutes. After removing the supernatant, the cell pellet was resuspended in 1 to 3 ml of complete RPMI medium. Cells were counted using a hemacytometer, and an appropriate volume was transferred into a new flask containing prewarmed complete medium, where they were cultured in a humidified incubator at 37°C with 5% CO₂.

For Caco-2 and PANC-1 cell lines, the cells were seeded at 250,000 cells in a T25 flask and 750,000 cells in the T75 flask. For HEK293 and HEK-MRP2 cell lines, seeding density for passaging and maintenance was kept at 100,000 cells in a T25 flask and 300,000 cells in a T75 flask. Cells with a passage number greater than 60 were discarded.

2.2.4. Cell counting

The quantity of viable cells was assessed using a hemacytometer. A 10 μ L aliquot of the cell suspension was combined with 20 μ L of 0.4% Trypan Blue stain, which selectively colours dead cells blue, leaving live cells unstained. Then, 10 μ L of the resulting cell-stain mixture was loaded into a hemacytometer counting chamber. The cells within four large quadrants were counted under an inverted microscope. The cell concentration was calculated using the following equation:

$$\text{Concentration (cells/ml)} = \text{Average cell count} \times \text{dilution factor} \times 10,000$$

Following the determination of cell density, the cells were seeded into a new culture flask. The cultures were maintained until they reached 80% to 90% confluence, after which they were either passaged or used for experimental procedures.

2.3. Cell viability Assay

Cell viability assays are extensively used in research and drug development to assess the potency or toxicity of drugs. In previous studies, it is well known that these assays are based on different cellular functions such as membrane permeability, enzymatic activity, cell adhesion, ATP production, or nucleotide uptake (Kamiloglu et al., 2020; Kocherova et al., 2020). Cell viability assays can be categorized based on their detection methods into several groups: dye exclusion tests (such as trypan blue, eosin, congo red, and erythrosine B), colourimetric assays (including MTT, MTS, XTT, WST-1, WST-8, LDH, SRB, NRU, and crystal violet), fluorometric assays (like resazurin and various fluorogenic esterase substrates including PrestoBlue, AlamarBlue, CellTiter-Blue), luminometric tests (including ATP and real-time viability assays), and flow cytometry assays, which can detect changes in cell membrane asymmetry, membrane integrity, or mitochondrial activity (Kamiloglu et al., 2020; Nozhat et al., 2022). The MTT assay (3-(4,5-Dimethylthiazol-2-yl)-2,5-Diphenyltetrazolium Bromide) and PrestoBlue™ assay were the primary methods used in this study to assess cell viability.

2.3.1. Sample preparation

Cells were seeded into 96-well plates at a density of 5,000-8,000 cells per well, allowing them to adhere to the well surface over 16 – 24-hour incubation in drug-free complete growth medium. After attachment, cells were exposed to oxaliplatin solutions with varying concentrations for 2 hours. Following drug exposure, the medium containing oxaliplatin was replaced with fresh, drug-free growth medium, and the cells were incubated for a total of 70 hours at 37 °C with 5% CO₂/ 95% air from the time of oxaliplatin addition to reach optimal density. Cell viability was then determined by different detection methods: MTT or PrestoBlue™. Each experiment was performed independently at least three times.

2.3.2. MTT assay

The MTT assay was mainly used to assess the sensitivity to oxaliplatin in gastrointestinal cell lines in the presence and absence of MRP2 inhibitors. MTT assay relies on the conversion of the water-soluble MTT tetrazolium salt into an insoluble purple formazan precipitate, which is mediated by mitochondrial succinate dehydrogenase enzymes in living cells, which generate reducing equivalents such as NADH and NADPH. The resulting formazan crystals were then dissolved in an organic solvent like DMSO, and the amount of formazan, directly proportional to the number of viable cells, was quantified by measuring absorbance or optical density (OD) at 540 nm using a plate reader, with a reference wavelength of 680 nm.

After sample preparation, all but 25 µL of medium was removed from each well. An aliquot of 150 µL of DMSO was added to each well, followed by thoroughly mixture using a plate shaker for 30 min. The plate was then incubated at 37°C for 10 minutes. After brief shaking, the absorbance was read at 540 nm (with a reference wavelength of 680 nm) by a microplate reader (Tecan Spark 10M, Mannedorf, Switzerland).

The percentage of cell viability was calculated by normalizing OD values at different oxaliplatin concentrations to those of untreated control cells, which were set at 100%. These viability percentages were used to plot a nonlinear dose-response curve (inhibition), and IC₅₀ values were determined using GraphPad Prism 6 software. The IC₅₀ values represent the concentration of oxaliplatin required to reduce cell viability

by 50% compared to untreated control cells, thereby indicating the sensitivity of the cell lines to oxaliplatin-induced cytotoxicity.

2.3.3. PrestoBlue™ Cell Viability

Monitoring changes in the cellular reducing environment or metabolic activity using resazurin-based reagents is a well-established and reliable method for assessing cell viability or death. Resazurin, the active component in the PrestoBlue™ Cell Viability reagent, is a non-toxic, cell-permeable compound that is blue and nearly non-fluorescent. Upon entering viable cells, resazurin is reduced by the cellular environment to resorufin, a red, highly fluorescent compound. This continuous conversion by living cells enhances the fluorescence and colour intensity of the surrounding media.

The PrestoBlue™ Cell Viability Reagent is an easy-to-use, non-toxic reagent that requires no cell lysis. Because lysis is not necessary, the diluted PrestoBlue™ solution can be removed and replaced with complete growth media, allowing further culturing of the cells and undertaking other functional assays.

After sample preparation, all cell culture medium was removed from each well and an aliquot of 100 µL of PrestoBlue™ reagent (1 in 10 dilutions in HBSS) was added. After incubation for 60 minutes at 37°C in a cell culture CO₂ incubator, with protection from direct light, fluorescence signals were recorded by using a fluorescence plate reader (Tecan Spark 10M, Mannedorf, Switzerland) with the wavelength of Excitation 560 nm/ Emission 590 nm.

2.4. LC-MS/MS

2.4.1. LC-MS/MS Method Development

2.4.1.1. *Choosing a column*

Choosing a HPLC column for unknown compounds represents a typical challenge. In this study, based on our pilot LC-MS/MS method development for myricetin, other phytochemical MRP2 inhibitor candidates were identified from Manuka honey. Compared to the methods other researchers used, the columns for LC-MS mainly used C18 columns (Table 2-4). Only one researcher was using 250 mm length column (Xiang et al., 2017). Although the longer column may warrant better separation, the

pressure of the column would be higher and the retention time would be longer. In general, 150 mm long column (Fang et al., 2002) would be enough for good separation, and can get results faster. The particles of ODS column or similar column (Kumar et al., 2018; Selby-Pham et al., 2018; Yilmaz et al., 2018) is too small which may lead higher pressure and easier to be contaminated, so it is quite hard to use and easily to be broken. From the columns listed below, particle size at least has 1.7 μm .

Table 2- 4 Methods comparison table

Columns (Methods)	Size of columns	Parti cles	Mobile phase	Flow rate	Injection volume
C18 (HPLC)	4.6mm X 250mm (Xiang et al., 2017)	5 μm	Water (0.1 phosphoric acid):ACN	0.8 ml/min	20 μl
Zorbax C18 (LC-MS-MS)	4.6mm X 150mm (Fang et al., 2002)	5 μm	Water(0.1 formic acid):Methnol	1 ml/min	20 μl
RP C18 ODS-4 (LC-MS)	2.1mm X 100mm (Yilmaz et al., 2018)	2 μm	Water(10mM ammonium formate and 0.1% formic acid):ACN	0.25 ml/min	4 μl
Waters HSS T3 (UPLC-MS)	2.1mm X 100mm (Kumar et al., 2018)	1.7 μm	Water (0.1% formic acid): ACN (0.1% formic acid)	0.3 ml/min	2 μl
C18 XDB (LC-MS)	2.1mm X 100mm (Selby-Pham et al., 2018)	1.8 μm	Water (0.1% formic acid):ACN (0.1% formic acid)	0.4 ml/min	1 μl

Most standard and preferred LC-MS/MS mobile phase additive is formic acid for (Fang et al., 2002; Yilmaz et al., 2018), but one of them also using phosphoric acid in mobile phase (Xiang et al., 2017) which was using HPLC methods not LC-MS. Compared with phosphoric acid, formic acid is preferred as an LC-MS/MS mobile phase additive due to its easier evaporation and less ion suppression effects. Phosphoric acid is non-volatile, and can cause contamination and build-up in the ion source and mass analyzer.

For conclusions, C18 (2.1mm X 150mm, 1.7 μm) column in a gradient mobile phase, ACN in water (0.1% formic acid, v/v) would be good choices. Phenomenex Kinetex Evo C18 (2.1mm X 150mm, 1.7 μm) column would be used for separation in LC system in this study.

2.4.1.2. MRM Method Optimisation

Sensitive, accurate and precise LC-MS/MS methods are essential for identification of the phytochemicals from Manuka honey and for quantitation of cellular accumulation of oxaliplatin. In studies to identify the phytochemicals from Manuka honey, a comprehensive LC-MS/MS method was optimized and validated for the quantification of myricetin standard using a C18 column from Waters (Cortecs, C18, 2.1X100mm, 2.7 μ m). Determination of the limit of quantification is critical for the next experiment design, guiding the preparation in cell culture for uptake study. To determine the concentration of phytochemicals in cell homogenates may need to use an internal standard such as kaempferol.

Mass spectrometry was performed on Agilent 6420 Triple Quadruple equipped with ESI source operated in negative mode. The parameters were as follows: gas temperature, 300 °C; Nebulizer 50 psi; Gas Flow, 6 L/min; Capillary voltage, -4000 V; Injection Volume, 3 μ L; Flow rate, 0.25 mL/min. Gradient mobile phase, MeCN in miliQ water (0.1% formic acid, V/V). Solvent composition was 90%A, 10%B; 5min, 10%A, 90%B; 7min, 10%A, 90% B; 8min, 90%A, 10%B. The retention time for myricetin is around 6.1min, and the recording time would be 23 mins to see if there still have components or if the pressure would be stable back to the beginning. Other analytical parameters for myricetin LC-MS/MS method validation studies are given in Table 2-5 below.

The qualitative analysis was done by Agilent MassHunter Qualitative Analysis B.07.00 software, and the quantification was done by Agilent MassHunter Quantitative Analysis (for QQQ) software. Linearity, accuracy (recovery), inter-day and intra-day precision (repeatability), limits of detection and quantification (LOD/LOQ) and relative tankard uncertainty (U% at 95% confidence level (k=2)) were carried out under the developed method mentioned above.

Table 2- 5 Optimized parameters for Myricetin

Cod Name ^a	Prec Ion (m/z) ^b	Prod Ion ^c	Dwell	Frag (V)	CE (V)	Cell Acc (V) ^d	Polarity ^e
Myricetin	317	179	200	140	10	7	Negative
Myricetin	317	151	200	140	14	7	Negative

^a Cod Name: Analytes.

^b *Prec Ion: Preceding ion (Mother ion / Molecular ions of the standard compounds).*

^c *Prod Ion: Product ion (Fragment ion).*

^d *Cell Acc(V): Collision cell accelerator voltage.*

^e *Polarity: Ion mode*

Duration of the transition

2.4.2. Method validation for myricetin quantification by LC-MS/MS

2.4.2.1. Linearity – Myricetin standard curve in the cell lysate

The standard calibration curve was linear with 6 concentration levels in triplicate over the concentration range of 50–800 nM. The differences between the theoretical and the actual concentration and the relative standard deviations were all less than 15% at any QC concentrations. The determination coefficient is shown in Figure 14, which is not less than 0.990 ($R^2 \geq 0.990$), and the equations for the standard calibration curve is also shown in Figure 14. Which means the method is well developed.

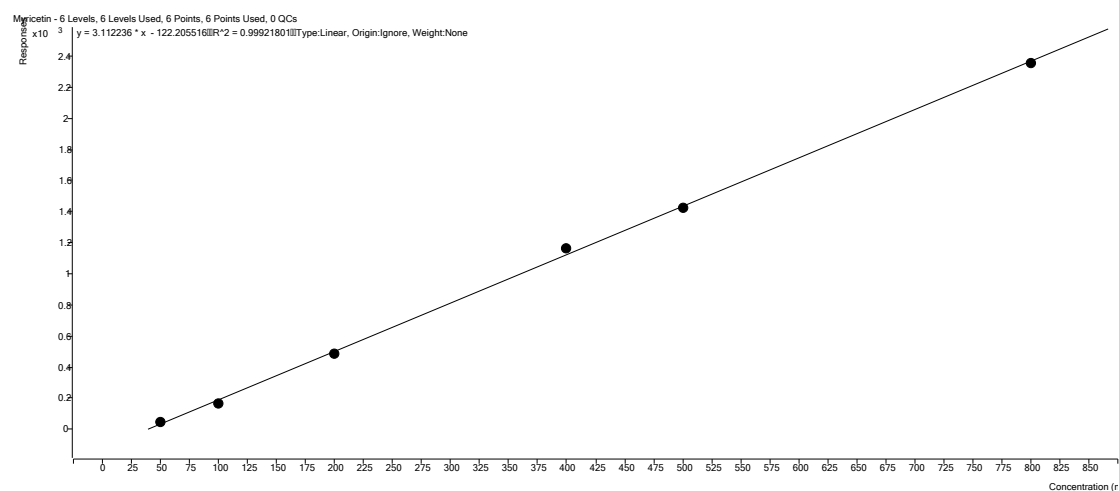


Figure 2- 1 Standard calibration curve

Myricetin was prepared in DMSO as stock solution. Use methanol to dilute myricetin to 800 nM, 500 nM, and then by using 800 nM solution make one in two dilution to 400 nM, 200 nM, 100 nM, 50 nM. Inject into columns for analysing. Linear curve-fitting and corresponding equations are shown in figure.

2.4.2.2. Accuracy and precision

The data collections are from both intra-day and inter-day analysis. The differences between the theoretical and the actual concentration and the relative standard deviation were less than 15% at medium and high QC concentrations.

The accuracy and precision are performed by myricetin standards, which are calculated from the recovery value and RSD percentage value. The equation of recovery calculation is:

$$\text{Recovery}\% = \frac{\text{Amount found} - \text{Original amount}}{\text{Amount spiked}} \times 100\%$$

2.4.2.3. Limits of detection and quantification (LOD/LOQ)

The LOD and LOQ values for the myricetin by using the LC-MS/MS, could be calculated by the equations below using mean value and standard deviation (SD) value. The standards were injected to the instrument at the lowest concentration to see the signal to noise value first, then run standards triplicate.

$$\text{LOD} = \text{Mean} + 3 \times \text{SD}$$

$$\text{LOQ} = 10 \sigma / S$$

Where:

σ = the standard deviation of the response

S = the slope of the calibration curve ([ICH Official web site : ICH](#))

A specific calibration curve should be studied using samples, containing an analyte in the range of QL. The residual standard deviation of a regression line or the standard deviation of y-intercepts of regression lines may be used as the standard deviation.

2.4.2.4. Relative standard uncertainty (U95)

Standard uncertainties of the analytes were determined by the accuracy and precision studies according to EURACHEM Guide (S. L. R. Ellison & A. Williams).

2.5. Western Blotting

“Western blotting is an important technique used in cell and molecular biology. By using a western blot, researchers are able to identify specific proteins from a complex mixture of proteins extracted from cells.” (Mahmood & Yang, 2012) Western Blotting is divided into three parts: (1) SDS-PAGE: separation proteins by size, (2) Transferring the protein from the gel to the membrane: transfer to a solid support, and (3) Antibody Staining: marking target protein using a proper primary and secondary antibody to visualize.

2.5.1. Cell lysate preparation

The cell culture medium was discarded, and the cells were washed twice with 5 mL of ice-cold PBS (phosphate-buffered saline) or TBS (Tris-buffered saline) to remove any residual medium. Prior to cell lysis, a microcentrifuge was precooled in the refrigerator. Following the wash, the PBS was discarded, and 0.5 mL to 1 mL of ice-cold lysis buffer was added, depending on the cell density (1 mL for 10^7 cells in a 100 mm dish or 150 cm² flask; 0.5 mL for 5×10^6 cells in a 60 mm dish or 75 cm² flask). To protect protein integrity, 10 μ L of Halt Protease Inhibitor Cocktail, EDTA-free, was directly added per milliliter of lysis buffer. The cells were then incubated on ice for 30 minutes, with occasional swirling to ensure even lysis.

The lysate was collected using a cell scraper, pooled to one side of the dish, and transferred into a microcentrifuge tube. The lysate was centrifuged at $14,000 \times g$ for 15 minutes in a precooled microcentrifuge set at 4°C to separate the cell debris. Depending on the cell type, the centrifugation force and time could be adjusted, with a standard guideline of 20 minutes at $12,000$ – $16,000 \times g$. To enhance yield, the pellet was sonicated for 30 seconds with a 50% pulse. After centrifugation, the tubes were gently removed from the centrifuge and placed on ice. The supernatant was carefully aspirated into a fresh tube kept on ice, while the cell debris pellet was discarded.

2.5.2. DC Protein Assay

To prepare the working reagent, 20 μ L of reagent S was added to each milliliter of reagent A. A series of protein standards were prepared, ranging from 0 to 3 mg/mL, by dissolving 0.003 g of Bovine Serum Albumin (BSA) in 1 mL of RIPA buffer, with the 0 mg/mL standard consisting solely of RIPA buffer. These standards were crucial for generating a standard curve, which was recreated with each assay to ensure accuracy. Subsequently, 5 μ L of the standards and samples were pipetted into a clean, dry microtiter plate. Following this, 25 μ L of the combined S + A reagent was added to each well, and the plate was vortexed to ensure proper mixing. Then, 200 μ L of reagent B was introduced into each well. If the microplate reader included a mixing function, the plate was mixed for 5 seconds, with any bubbles being carefully removed to prevent cross-contamination. After a 15-minute incubation with agitation, absorbance was measured at 750 nm to determine protein concentration.

2.5.3. Sample Preparation

A small volume of the lysate, approximately 20 µg (as determined by DC protein analysis), was taken for further processing. To prepare the samples for SDS-PAGE, 4X Laemmli sample buffer was added to the lysate in a 3:1 ratio (sample to buffer). The sample buffer consisted of 2.5% 2-mercaptoethanol (50 µL) mixed with 4X Laemmli sample buffer (450 µL). To ensure the reduction and denaturation of proteins, the lysates were boiled at 70°C for 10 minutes. This step is crucial as it facilitates the separation of proteins based on molecular weight and protects them from proteolytic degradation.

Following this, the lysates were centrifuged briefly at $14,000 \times g$ for 1 minute in a microcentrifuge. Although this step was temporarily omitted, typically, it helps to remove any remaining cell debris. The processed lysates were then aliquoted and stored at -20°C for future use, with care taken to minimize freeze-thaw cycles to avoid protein degradation.

2.5.4. SDS PAGE

Prepare Assemble Mini Gel Tank, adding running buffer (dilute 10X running buffer with *Mili-Q* water) to the mark line. Prepare gel cassette, and load samples into gel cassette wells. The amount of loading samples' proteins can be calculated by DC Protein assay. Connect the electrophoresis cells to the power supply, and turn power on, the samples will be separated by the electrophoresis because of the different size (molecular weight) between the proteins. Run 50V for 10mins first, then run 100V for about one hour till the blue dye reach the bottom line.

2.5.5. Transferring the protein from the gel to the membrane

Prepare a transfer kit which contains reservoir stacks (fibre pad), PVDF membrane, and transferring buffer. After proteins separation by electrophoresis, open Mini Gel Cassette, place the gel above the membrane like the figure showing below:

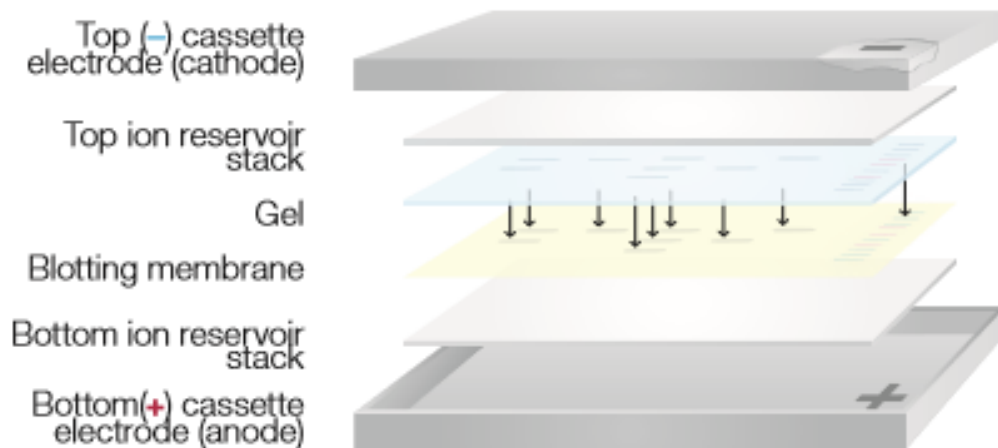


Figure 2- 2 Proper layering of the assembled transfer pack

The diagram illustrates the assembly of a transfer sandwich used in blotting techniques. The layers are arranged as follows: starting from the top, the negative (-) electrode (cathode), the top ion reservoir stack, the gel, the blotting membrane, the bottom ion reservoir stack, and finally, the positive (+) electrode (anode) at the bottom. During the process, electrons flow from the cathode (negative electrode) to the anode (positive electrode). This movement drives the transfer of proteins or other molecules from the gel onto the blotting membrane.

Place the sandwich in a transferring cassette and remove the bubbles in the stacks. Slide the cassette into the one of the Trans-Blot Turbo instrument bays, and chose the right transferring programme on the screen. About 5-10 mins, transferring would be finished.

2.5.6. Antibody Staining

Block the membrane for 1 hour after transferring at room temperature by blocking buffer (filtered 2% milk dissolved in TBST) in a plastic container with agitation. Then decant the solution. Wash membrane with TBST for 5 mins on a rotator, and incubate in primary antibody (Anti-MRP2 antibody [M2 III-6], 1:400 dilution in blocking buffer) overnight at 4 °C in fridge. Then decant the solution. Wash the membrane in three washes of TBST for 5 mins each time. Then incubate the membrane in secondary antibody (anti-Rat IgG2a Monoclonal, 1:1000 dilution in blocking buffer) at room temperature for 1 hour. Wash the membrane in three washed (1st with TBST, 2nd and 3rd with *Mili-Q* water) for 5 mins each time.

2.5.7. Western Blotting Imaging and Data Analysis

ImageQuant LAS 500 was used in this study for western blotting imaging and Image J was used for image analysing. Prepare Pierce™ ECL Western Blotting Substrate

working solution, which is used for enhanced chemiluminescence (ECL) that directly replaces costlier products without the need to re-optimize conditions, by mixing Reagents 1 and 2 at a 1:1 ratio. Incubate membrane after washes from section 2.5.6. in the working solution for about 5 mins. Then it is ready for Imaging.



Figure 2- 3 MRP2 western blotting image by ImageQuant LAS 500

The standard ladder shows different colour of the specific molecular weight, the blots showing in the figure is showing that MRP2 protein molecular weight is close to 250kD

2.6. Platinum cell accumulation by inductively coupled plasma spectrometry (ICP-MS)

Inductively coupled plasma mass spectrometry (ICP-MS) was employed to quantify the accumulation of oxaliplatin-derived platinum in transfected cells. Initially, cells were seeded at a density of 250,000 cells per well (with Caco2 and PANC-1 cells at 350,000 cells per well) in a 6-well plate, followed by transfection and cultivation in RPMI complete medium until reaching approximately 80% to 90% confluence. Subsequently, the cells were exposed to varying concentrations of oxaliplatin for 2 hours. After incubation, the reaction was halted by washing the cells three times with ice-cold PBS, followed by a 30-minute drying period.

2.6.1. Protein concentration determination

The air-dried cells were subjected to digestion using 300 μ L of 70% nitric acid at room temperature with continuous agitation for 2 hours. Simultaneously, BSA standard solutions were prepared to evaluate the protein concentration within the samples. The

concentration selected are respectively: 2800, 1400, 700, 350, 175 and 87.5 $\mu\text{g}/\text{mL}$. Following this, 300 μL of both the BSA standards and lysate samples were placed into a 96-well plate, where protein concentration was assessed by recording absorbance at 358 nm. These samples were then utilized for platinum analysis through ICP-MS.

2.6.2. Accumulation study of oxaliplatin

Cell samples were transferred to 5 mL screw-capped polypropylene vials and left to digest overnight at room temperature. The digestion process was further enhanced by heating the cell lysates at 95°C for 30 minutes. Following digestion, 200 μL of the samples were diluted with 1.8 mL of a 50 ppb thallium solution (used as an internal standard) in ICP-MS tubes. Platinum levels in the samples were measured using a Varian 820 ICP-MS (Agilent Technologies Inc., Santa Clara, CA, USA). The platinum concentration for each sample was determined by calculating the ratio of platinum to thallium counts, using a standard curve method. To ensure accuracy, platinum counts were normalized against thallium internal standard counts. A standard curve was created by preparing solutions with desired platinum concentrations in the same matrix as the cell samples, spiked with a known platinum stock concentration, and included in the same ICP-MS run as the samples.

2.6.3. ICP-MS method validation for platinum quantification

The validation of elements was determined according to the US FDA guidelines for bioanalytical method validation.

2.6.3.1. Linearity

The linearity of the method was determined by preparing different concentrations of the platinum standard from a platinum stock standard solution of 1,000,000 ppb in the cell lysate. The platinum stock solution was further diluted in a cell lysate to produce 200 μl of the desired concentration range. The final concentrations of 200 μl platinum standards were further diluted with 1750 μl of 50 ppb thallium internal standard (IS) and transferred to screw-capped 5ml PP vials for ICP-MS analysis. The serial dilutions of platinum standards are shown in table 2-6:

Table 2- 6 Preparation of platinum standard in cell lysate with Thallium Internal Standard

Final Pt concentration for ICPMS analysis (μM)	The volume of HNO3 and cell lysate (μL)	50 μl of [Stock Pt] to add (μM)	The volume of thallium spiked MiliQ water to add (μL)
1	200	40	1750
0.75	200	30	1750
0.5	200	20	1750
0.25	200	10	1750
0.1	200	4	1750
0.05	200	2	1750

The equation of the linearity was calculated using linear regression analysis. Slope, intercept and regression coefficient values were calculated using standard formulas or with the aid of Microsoft EXCEL.

Linear Regression (Coefficient of Determination)

$$r^2 = \left[\frac{\sum_i \{(x_i - x)(y_i - y)\}}{\{[\sum_i (x_i - x)^2][\sum_i (y_i - y)^2]\}^{1/2}} \right]^2$$

x_i = Expected Concentration

x = Expected mean value

y_i = Measured and calculated mean value in ratio (Pt/Thallium)

y = MV of y_i

2.6.3.2. Accuracy and precision

The method's accuracy and precision were confirmed by generating three replicates of quality control (QC) samples, labeled as lower QC, middle QC, and upper QC, spanning the standard curve range. Each replicate's actual concentration was computed in relation to the standard curve. The transformation was then calculated as outlined below:

$$Pt \text{ concentration found (in ppb)} = \frac{Y_i - b}{a}$$

Y_i = The response ratio of platinum to thallium (IS)

b = intercept point of the regression line

a = slope of the line

$$\% \text{ Recovery (Accuracy)} = \frac{\text{Concentration Pt found}}{\text{Theoretical Pt concentration}} \times 100\%$$

The precision of the method was measured with respect to the coefficient of variation (CV) of three replicates results of platinum across the concentration range.

$$CV\% = \frac{S}{MV_n} \times 100$$

$$S = \sqrt{\frac{1}{n-1} \times \sum_{i=1}^n (x_i - MV_n)^2}$$

Where:

N = No. of values

x_i = Value of single value in series

The ICP-MS analysis was deemed valid only when the standard curve demonstrated linearity, and the QC samples fell within an accuracy range of 85% to 115% across the standard curve. Based on various ICP-MS runs, the method's limit of detection (LOD) and lower limit of quantification (LLOQ) were determined to be 0.3 ppb and 1 ppb of platinum, respectively.

2.7. Effect of chrysin on oxaliplatin-induced apoptosis in Caco-2 and PANC-1 cells by using Flow cytometry

To evaluate the transport activity of MRP2 in cell lines, cells were treated with a fluorescent probe known as CDCF (5(6)-carboxy-2',7'-dichlorofluorescein). CDCF serves as an MRP2-specific substrate in this study, utilized to confirm MRP2-mediated membrane transport activity (Heredi-Szabo et al., 2008). The assay involved the use of CDCFDA (5(6)-carboxy-2',7'-dichlorofluorescein diacetate), a non-fluorescent, cell-permeable probe that, once inside the cell, undergoes de-esterification to form the fluorescent CDCF.

Apoptosis, a tightly controlled process of programmed cell death, is essential for the elimination of damaged cells and acts as a crucial mechanism in tumor suppression (Lincz, 1998). Apoptotic cells are marked by distinct morphological and biochemical features, such as cytoplasmic shrinkage, nuclear condensation and fragmentation, loss of membrane asymmetry, and the division of cellular components into apoptotic bodies (Allen et al., 1997). Apoptosis can be initiated through two primary pathways: the intrinsic and extrinsic mechanisms. The intrinsic pathway is triggered by internal signals, including DNA damage, nutrient deprivation, and oxidative stress, which lead to the release of mitochondrial proteins and subsequent activation of various caspase proenzymes, thereby inducing apoptosis. Conversely, the extrinsic pathway is activated by external death signals that engage cell surface receptors, leading to apoptosis through the activation of caspase proenzymes.

In this study, the Invitrogen Alexa Fluor® 488 annexin V kit was utilized to assess apoptosis induced by oxaliplatin in gastrointestinal cell lines. During apoptosis, phosphatidylserine (PS), which is normally situated on the inner leaflet of the cell membrane, is relocated to the outer membrane surface (van Engeland et al., 1998). Annexin V, a calcium-dependent phospholipid-binding protein with a high affinity for PS, is tagged with a fluorophore in this kit, allowing it to bind to PS and detect apoptotic cells (Koopman et al., 1994). The kit includes annexin V conjugated to the Alexa Fluor® 488 dye, along with red-fluorescent propidium iodide (PI), a nucleic acid binding dye that marks dead cells with red fluorescence. The Alexa Fluor® 488 annexin V kit facilitates the detection of apoptosis rates by flow cytometry, where annexin V identifies early apoptotic cells and PI detects late apoptotic cells. Using a 488 nm excitation laser, flow cytometry was employed to differentiate between treated and untreated cell populations exposed to varying concentrations of oxaliplatin in different cell lines.

2.7.1. Drug treatment

Caco-2 and PANC-1 cells were seeded in 6-well plates at a density of 500,000 cells per well. After 24 hours, the cells were pretreated with either 10 μ M chrysin or DMSO for 45 minutes, followed by a 2-hour treatment with 25 μ M oxaliplatin. To end the drug incubation, the cells were rinsed with 2 mL of ice-cold PBS, the medium was replaced with 2 mL of complete growth medium, and the cells were incubated for 48 hours at 37°C in a 5% CO₂ environment.

2.7.2. Sample preparation and flow cytometric analysis

The kit included a 5X annexin-binding buffer, which was diluted to 1X by mixing 1 mL of the 5X buffer with 4 mL of deionized water. A working solution of propidium iodide (PI) at 100 $\mu\text{g}/\text{mL}$ was prepared by adding 5 μL of a 1 mg/mL PI stock solution to 45 μL of the 1X annexin-binding buffer. Following the incubation period, the cells were harvested and washed with ice-cold PBS. After washing, the cells were trypsinized and centrifuged at 500 g for 5 minutes at 4°C. The resulting cell pellet was resuspended in 100 μL of 1X annexin-binding buffer. To assess oxaliplatin-induced apoptosis, 4 μL of Alexa Fluor 488 annexin V and 1 μL of the 100 $\mu\text{g}/\text{mL}$ PI working solution were added to each 100 μL of cell suspension. The cells were then incubated at room temperature for 15 minutes. To stop the reaction, the cells were placed on ice, and 400 μL of 1X annexin-binding buffer was added. The samples were mixed gently and kept on ice until flow cytometric analysis. The stained cells were analysed by flow cytometry, measuring fluorescence emissions at 530 nm and 575 nm using 488 nm excitation. Cells were gated based on forward and side scatter and acquired through the fluorescence signal. The fluorescence intensity was plotted as a histogram within the gate, and the mean fluorescence intensity was determined using Kaluza Flow Cytometry software (Beckman Coulter).

2.8. Cell immunostaining of MRP2-Surface staining

The surface expression of MRP2 in gastrointestinal (GI) cancer cell lines was analyzed using immunofluorescence staining followed by flow cytometry. To specifically detect MRP2 on the cell surface, an anti-MRP2 antibody targeting an internal epitope of the MRP2 protein was employed. Direct immunostaining involved the use of a secondary antibody, anti-mouse IgG H&L (Alexa Fluor 488), which is conjugated to a fluorophore and binds directly to the anti-MRP2 primary antibody, producing a fluorescence signal.

To minimize the risk of false positives due to non-specific binding of the primary and secondary antibodies, an IgG2a isotype control, matched to the host species, was used in the cell surface staining experiment. This control antibody, which targets an irrelevant antigen but shares the same isotype as the MRP2 primary antibody, plays a crucial role in assessing background signal caused by non-specific interactions with cellular proteins and in evaluating the non-specific binding of the secondary antibody. The fluorescence signal representing MRP2 expression in the GI cell lines was determined by subtracting the isotype control signal from the MRP2 fluorescence signal. Flow cytometry was then

utilized to quantify surface staining, as it offers a high degree of sensitivity and precision in detecting subtle changes in protein expression.

2.8.1. MRP2 surface expression in HEK cell lines

HEK293 and HEK-MRP2 cell lines were grown in T-75 flasks until it was 90% confluent, trypsinised, counted and resuspended in RPMI medium, according to the procedure mentioned in section 2.2.3 and 2.2.4. The cell density of 1×10^6 cells per ml were aliquoted into a 2 ml Eppendorf tube and kept on ice. Most of the experimental procedure was conducted on ice, unless otherwise stated. The cell samples were centrifuged at $400 \times g$ for 3 min at 4°C and cell pellets were washed with 1 ml of PBS and spun down again at $400 \times g$ for 3 min at 4°C . The cell pellets were then resuspended in freshly prepared 1% paraformaldehyde in PBS and incubated for 15 min on ice. After fixing the cells with paraformaldehyde, the cells were washed twice with PBS 0.2% Tween-20 as washing buffer and centrifuged at $400 \times g$ for 3 min. The cells were then permeabilised with a permeabilising agent by adding 100 μl of 0.1% saponin and incubating for 30 min at room temperature. After incubation, the cells were washed twice with washing buffer and centrifuged at $400 \times g$ for 3 min. The cells were blocked with 100 μl of 5% BSA in PBS for 15 min at room temperature to block non-specific binding sites. The cells were washed twice with washing buffer and centrifuged at $400 \times g$ for 3 min. The cell pellets were then resuspended in 2.5 $\mu\text{g/ml}$ of the primary anti-MRP2 antibody in 2% BSA in PBS and 2.5 $\mu\text{g/ml}$ of IgG2a isotype control in 2% BSA in PBS. The samples were incubated with primary and isotype control antibody for 60 min at room temperature in the dark. The cells were washed three times with washing buffer after incubation by centrifugation at $400 \times g$ for 3 min. Meanwhile, the Alexa Fluor 488-labeled secondary antibody was diluted in 1:1000 ratio in 2% BSA in PBS and the cells were resuspended in this solution. The cells were again incubated for 60 min at room temperature in the dark. After incubation, the cells were washed three times with washing buffer by centrifugation at $400 \times g$ for 3 min. The cell pellets were resuspended in 300 μl of ice-cold 1% paraformaldehyde in PBS and stored on ice in the dark until analysis. For the best results, the cell samples were analysed on flow cytometry as soon as possible.

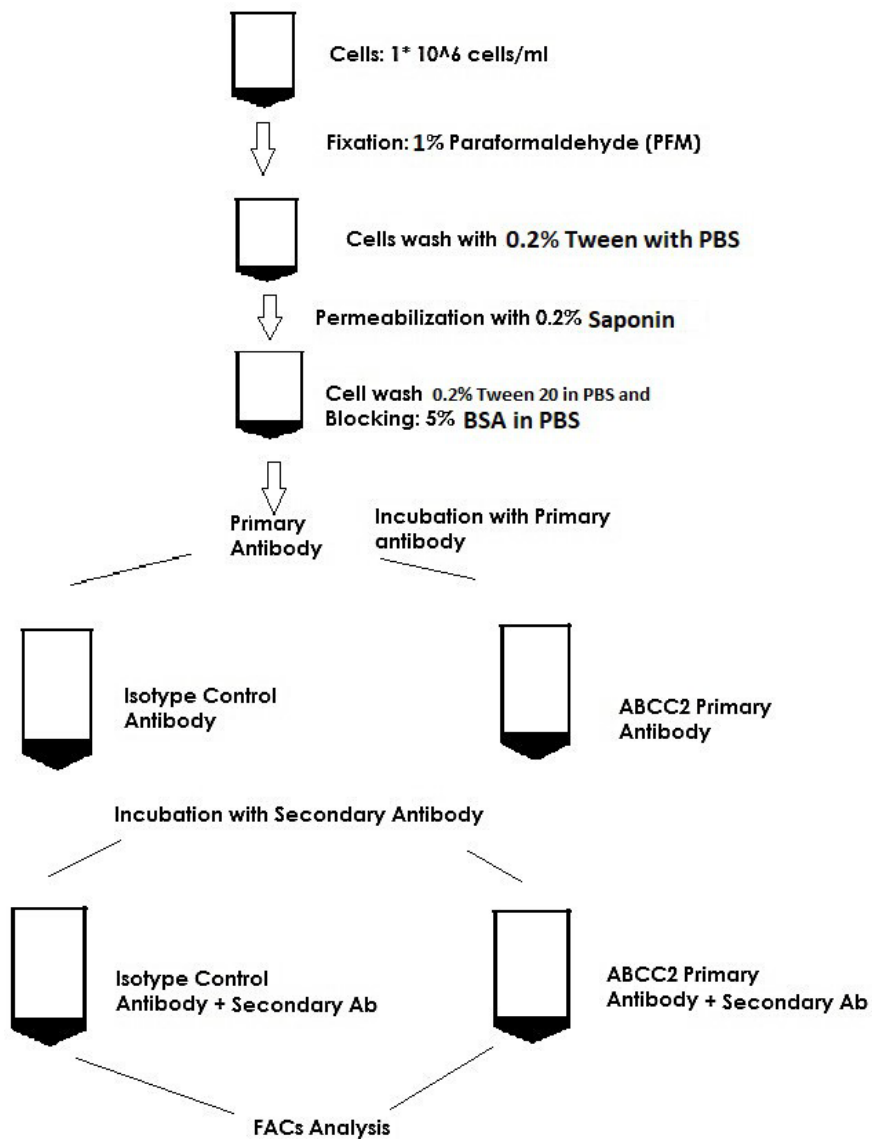


Figure 2- 4 Cell surface staining protocol

2.8.2. Flow cytometry data analysis

The MRP2 cell surface staining was determined using flow cytometer and data was analysed with Kaluza software. The cells were gated and forward and side scatter parameters were used to exclude cell doublets, cellular debris, dead and non-viable cells. Mean fluorescence intensity was measured with the blue laser channel using 488 nm excitation and 519 nm emission. The flow cytometry histogram was produced using Kaluza software.

2.9. Flow cytometry analysis-Beckman Coulter Kaluza software

For all the flow cytometry experiments, samples were analysed using Beckman Coulter Kaluza software. The flow cytometry experiments were analysed using gating strategies to exclude cell doublets, cellular debris and non-viable cells. The histograms were designed according to the respective experiments and based on forward and side scatter parameters. Forward scatter measures cell size and side scatter measures cell intracellular complexity or shape and increases with greater particle density within cells. The total cell population was plotted using forward and side scatters parameters. The non-viable or dead cells appear on the left or upper-left side of the cell population in the forward vs side scatter histogram (FSC vs SSC) due to their lower forward scatter and high side scatter. These populations were excluded from subsequent analysis by forming a gate “A” around the viable cells only.

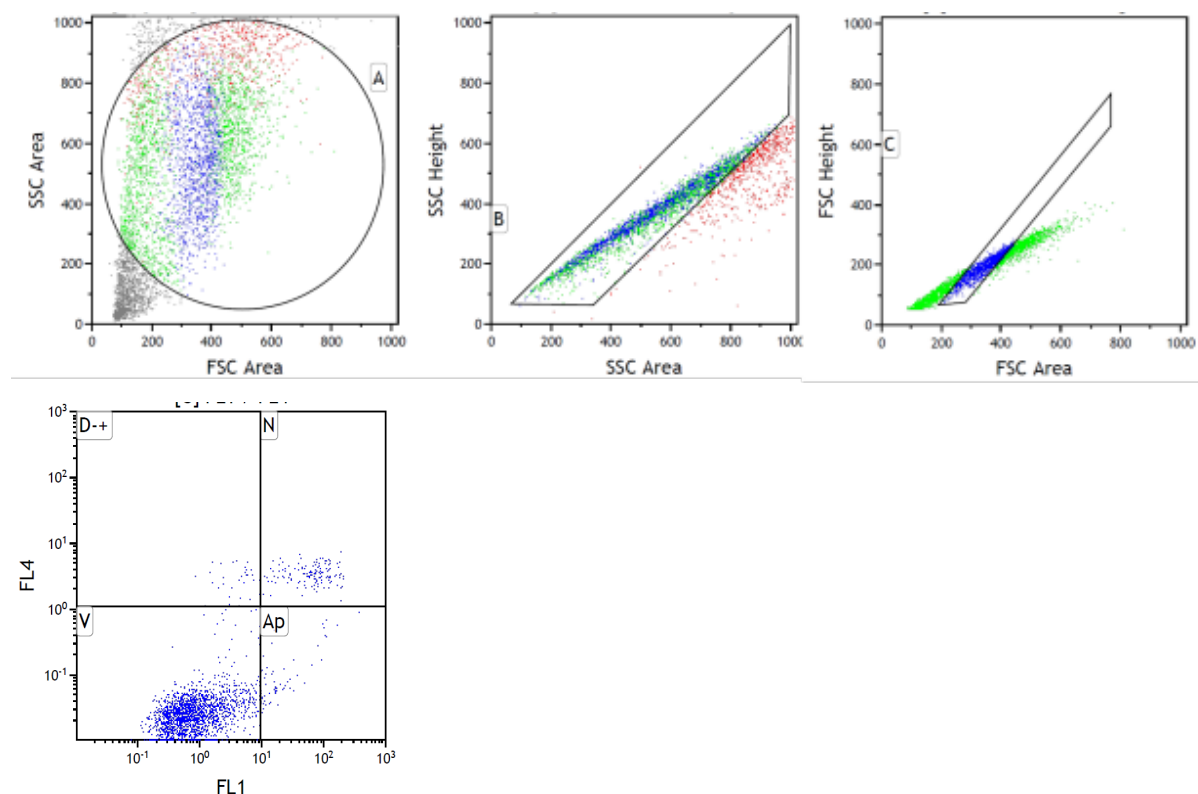


Figure 2- 5 A representative example of data acquisition using the XDP MoFlow.

A The dot plot of cells gated on signal pulse area of the forward scatter (FSC) and side scatter (SSC). A population of cells were selected so that only cells that were in the gating were analyzed. These cells were designated as population **A**; **B** population **A** was further analyzed as the signal pulse height versus area of the SSC. Events along the diagonal of the plot, which represent single cells, were selected and designated as population **B**; **C** the population **B** was plotted as the signal pulse height versus area of

the FSC, and the selected cells were designated as population C. The population C was used in the measurement of fluorescence level associated with single cells.

To measure the fluorescence intensity from single cells only, doublets were gated out using the doublet exclusion method (Wersto et al., 2001). For this method, we plotted a histogram of forward scatter area vs height signal (FSC-A vs FSC-H) and side scatter area vs height signal (SSC-A vs SSC-H). The area of the signal for the forward or side scatters increased proportionally to the height of the signal in single cells. From the viable population “A”, a SSC-A vs SSC-H plot was created and a gate “B” was designed in the cell population. From the population B, the same process is repeated using FSC-A vs FSC-H plot to create a “C” gate. Thus, the population under gate C was considered as a single cell and for all the samples, mean fluorescence was measured for the cell population under gate C.

2.10. Statistical analysis

All data were analyzed using Prism 6 software (GraphPad, San Diego, CA, USA) and presented as mean \pm standard error of the mean (S.E.M.). Results were derived from two to three independent experiments, unless otherwise specified. Statistical significance was assessed using analysis of variance (ANOVA) with post-hoc tests, where a p-value <0.05 was considered significant.

For transfected cells, statistical analysis was performed using one-way ANOVA. IC₅₀ values for oxaliplatin were calculated from normalized mean absorbance values obtained from three independent experiments, applying non-linear regression analysis in Prism software.

For the apoptosis assay and cell surface staining, samples were analyzed using Kaluza software. Subsequent multiple comparisons between control and treatment groups were conducted using one-way ANOVA with Dunnett’s post-hoc test.

Chapter 3 LC-MS/MS

3.1. Introduction

High-performance liquid chromatography-mass spectrometry (HPLC-MS, Fig 1) is now a routine technique to quantitate a wide range of drugs or bioactive molecules in biological matrix (e.g. plasma, urine). With HPLC, solubilized compounds (the mobile phase) are passed through a column packed with a stationary (solid) phase. This effectively separates the compounds based on their affinity for the mobile and stationary phases of the column. Once the sample is separated, the components would be identified and then quantified through the use of the mass spectrometer. Mass spectrometers convert the analyte molecules to a charged (ionized) state, with subsequent analysis of the ions and any fragment ions that are produced during the ionization process, on the basis of their mass to charge ratio (m/z). Depending on the ionization source and specific type of mass spectrometer, the main types of ionization are electron impact, chemical ionization, and electrospray ionization. The development of electrospray ionization (ESI) has provided a simple and robust interface. The use of tandem MS and stable isotope internal standards further allows highly sensitive and accurate assays to be developed.

3.1.1. Machine and column information

LC-MS analyses were conducted using an Agilent 1260 Infinity Quaternary LC System (Santa Clara, CA 95051 USA). The system consisted of the following components: 1260 quaternary pump (model number: G1311B), 1260 infinity ALS sampler (model number: G1329B), 1260 infinity TCC column component (model number: G1316A), 1260 infinity diode array detector (DAD) (model number: G4212B), connected to a 6420 triple quadrupole LC/MS system with electrospray ionisation (ESI) source (model number: G1948B).

Quadrupole made up of four parallel rods. The four rods are electrodes, with electric fields around them. (Figure 3-1) The first and third quadrupole works as mass filter, and the electrodes have both DC and AC (RF) voltages applied on them. The second quadrupole called Collision Cell, which is unlike the first and third quadrupole, does not have any DC voltages apply on it. It only has radio frequency (AC voltages), because in the Collision Cell, we want all the ions from second quadrupole to the third quadrupole.

Phenomenex Kinetex Evo C18 (2.1 x 150mm, 1.7 μ m) was used for this analysis. The

mobile phases were consisted of water containing 0.1%(v/v) formic acid (A) and acetonitrile containing 0.1% (v/v) formic acid (B). The flow rate was 0.30 mL/min and the column temperature was 40 °C. The initial gradient condition was 90:10 (A:B) and hold for 1 min. From 1 to 6 min the B was increased to 25% and from 6 to 9 min the B was increased to 40% held for 7 min, and from 16 to 20 min B was increased to 80% and hold for 3 min. From 23 to 24 min the B was increased to 10% and hold for 11 min. The total run time was 35 min and the injection volume was 2 μ L.

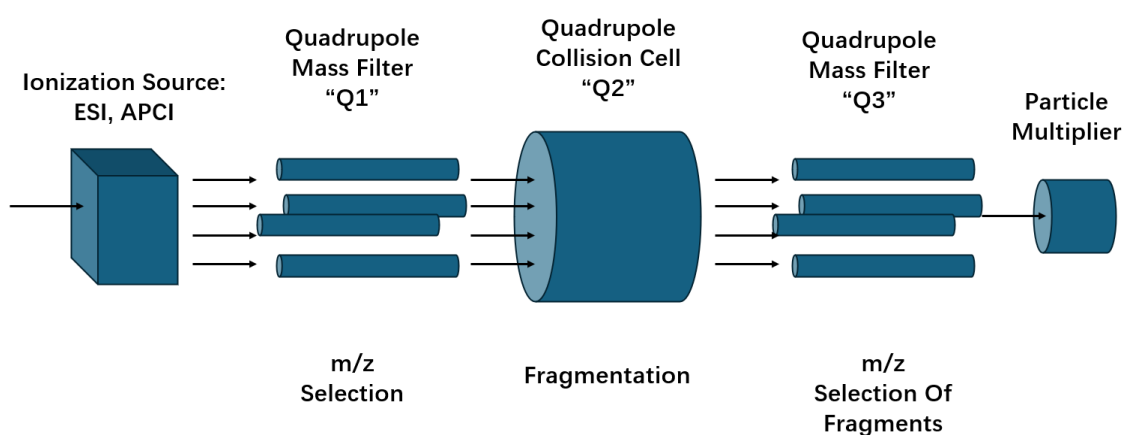


Figure 3- 1 Schematic of a triple quadrupole mass spectrometer

Triple quadrupole mass spectrometer construction drawing is shown in the figure. The arrow is showing the particle flow.

3.1.2. The function of phenolics compounds in Manuka Honey

There are lot of research showing that honey contains all kinds of flavonoids and phenolic acids which play an important role in antioxidant and anti-inflammatory properties on human health (Cianciosi et al., 2018; da Silva et al., 2022; Gašić et al., 2014; Shamsudin et al., 2022).

Since ancient times, honey has been valued not only as a food and sweetener but also as a medicine for promoting wound healing, tissue regeneration, and relieving gastrointestinal disorders, gingivitis, and various other ailments. The therapeutic properties of honey are attributed to its diverse antioxidant molecules, including phenolic compounds like flavonoids and phenolic acids (Al-Waili et al.).

Manuka honey is produced from the nectar of the Manuka tree, *Leptospermum scoparium*, a native of New Zealand. Manuka flowers are generally white in the wild and 10 to 12 mm across in diameter. Flowering takes place between September and February. The Manuka plant is often colonised by scale insects that feed off the phloem of the tree and excrete honeydew. This encourages black sooty mould to grow on the bark, giving it a dark colouring (White, 1978). There have been so many research showing that the content of Manuka honey contains more phenolic and flavonoid antioxidants than other honey worldwide. Since the antibacterial properties are well characterized, Manuka honey has an additional antibacterial component which is referred to as the “unique Manuka factor” (UMF), which is also known as “methylglyoxal” (MGO). More and more researchers care about natural products on inhibiting tumour cell growth and metastasis, as they may reduce side effects during chemotherapy in humans. It is also reported that early apoptosis in osteosarcomas in a relatively dose-dependent manner and attenuates proliferation in hela cell lines. Apoptosis is also enhanced in oral squamous cell carcinomas following exposure to honey (Y. Wang et al., 2011). With expanding interest in anti-oxidant- rich substances, honey has received more research consideration since it is rich in phenolic compounds and additional anti-oxidants, as well as amino acids, ascorbic acid, and proteins (Wahdan, 1998). Some simple and straightforward polyphenols were found in honey: chrysin (CR), quercetin (QU), caffeic acid (CA), caffeic acid and phenyl esters (CAPE), galangin (GA), Acacetin (AC), pinobanksin (PB), pinocembrin (PC), kaempferol (KP), and apigenin (AP). All of these phenolic compounds and anti-oxidants have advanced as promising pharmacologic reagents in terms of cancer treatment (Wahdan, 1998). Myricetin (Figure 3-2) is a member of the flavonoid class of polyphenolic compounds, with antioxidant properties. It is commonly derived from honey, vegetables, fruits, nuts, berries, tea, and is also found in red wine.

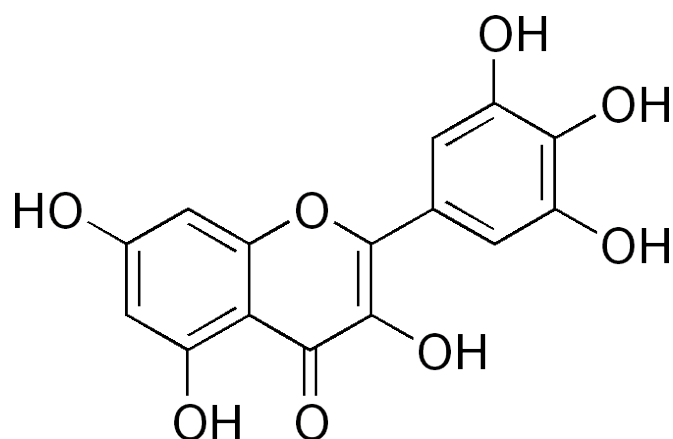


Figure 3- 2 Myricetin structure

The chemical structure of myricetin is shown in this figure. It is characterized by multiple hydroxyl groups that enhance its ability to scavenge free radicals, contributing to its potent antioxidant activities. The structure belongs to the flavanol subclass of flavonoids, commonly found in fruits, vegetables, and teas.

There are also more and more evidence showing that phenolics have significant cytotoxic effects on cancer cells. Abdelhakim et al. (2022) have found that phenolic compounds offer extensive prophylactic and therapeutic potential against diverse cancer types (Bouyahya et al., 2022). These compounds can be administered alone or alongside other anticancer drugs. Notably, phenolic compounds like gallic acid and quercetin are well-recognized for their mechanisms of action. These molecules primarily target multiple checkpoints within cancer cells, making them a valuable source of natural anticancer agents (Bouyahya et al., 2022).

Recently, our team has reported that myricetin could inhibit MRP2 impact in pumping out platinum drugs. As a MRP2 inhibitor it increased cellular platinum accumulation and oxaliplatin cytotoxicity in human HepG2 and PANC-1 cells (GI cancer cell lines) (Khine et al., 2019).

Although oxaliplatin-based chemotherapy has been widely adopted as the standard and preferred regimen for treating colorectal cancer (CRC), tumour resistance is one of major limitations for many patients in clinical practice. Recently, our team has reported that MRP2 (a member of ABC transporter protein) confers oxaliplatin resistance and a phytochemical MRP2 inhibitor

myricetin increased cellular platinum accumulation and oxaliplatin cytotoxicity in several human GI cancer cell lines (Riya Biswas et al., 2019; Khine et al., 2019). However, myricetin is not a potent MRP2 inhibitor and it only marginally enhanced oxaliplatin sensitivity in tumour xenograft mouse model (Khine et al., 2019). Recently, our team discovered the anti-proliferation effects of NZ Manuka honey in several CRC cell lines but not in normal cells (Chan & Li, 2016). However, the exact anti-cancer compound(s) remain unknown in NZ Manuka honey. Given the fact that more than 90% ABC transporter inhibitors are derived from phytochemicals, we may identify novel and potent MRP2 inhibitors from NZ Manuka honey, which contains several myricetin analogues. Manuka Honey is also known to be an effective prebiotic and a recent paper reported that probiotics increase the production of anti-inflammatory cytokines (IL-6) (Moens et al., 2019), which has been reported to downregulate MRP2 /ABCC2 levels significantly (Diao et al., 2010).

3.2. Materials and methods

3.2.1. Chemicals and Standards

The chemicals used in this chapter would be mobile phase and sample preparation, which are all LC-MS grade chemicals whose details are listed in table 3-1.

Phenolics standards are pure powder form (>99.8%) on-site in university for use. The details are listed in table 3-2.

Table 3- 1 List of chemicals used in this chapter

Chemicals	Suppliers
Formic acid	Thermo Fisher Scientific (NZ)
Acetonitrile	Thermo Fisher Scientific (NZ)
Methanol	Thermo Fisher Scientific (NZ)
Hydrochloric acid	Thermo Fisher Scientific (NZ)
Ethanol	Thermo Fisher Scientific (NZ)

Table 3- 2 List of phenolics standards would be used in this chapter

Chemicals	Supplier
-----------	----------

Gallic acid	Sigma-Aldrich
Caffeic acid	Sigma-Aldrich
Chlorogenic acid	phyproof [®] Reference Substance
p-coumaric acid	Sigma-Aldrich
Ferrulic acid	Sigma-Aldrich
Rutin	phyproof [®] Reference Substance
Kaemferol rutinoside	phyproof [®] Reference Substance
Kaempferol	phyproof [®] Reference Substance
Quinic acid	Sigma-Aldrich
Epigallocatechin gallate	Sigma-Aldrich
Procyanidin B1	phyproof [®] Reference Substance
Salicylic acid	Sigma-Aldrich
Ellagic acid	phyproof [®] Reference Substance
p-Hydroxybenzoic acid	Sigma-Aldrich
m-Hydroxybenzoic acid	Sigma-Aldrich
Abscisic acid	Sigma-Aldrich
Luteolin	phyproof [®] Reference Substance
Sakuranetin	phyproof [®] Reference Substance
Pinobanksin	Sigma-Aldrich
Pinocembrin	phyproof [®] Reference Substance
Chrysin	Sigma-Aldrich
Acacetin	phyproof [®] Reference Substance

3.2.2. Standard Solutions

The standard stock solutions (1 mg/mL) of the phenolic compounds were prepared using DMSO as a solvent and stored at $-20\text{ }^{\circ}\text{C}$. Aliquots of each stock solution were mixed in order to prepare standard mixtures at a concentration level of 50 $\mu\text{g/mL}$ and stored at $-20\text{ }^{\circ}\text{C}$. Mixed working solutions of phenolics were prepared freshly in methanol as a dilution series at an approximate concentration of 0.078, 0.15625, 0.3125, 0.625, 1.25, 2.5, 5, 10 and 20 $\mu\text{g/mL}$ or 25, 50, 75, 100, 200 $\mu\text{g/mL}$ for methyl syringate, DL-3-phenyllactic acid, 2-hydroxy-3-(4-methoxyphenyl)propanoic acid, Quercetin, isorhamnetin, kaempferol, myricetin, isorhamnetin rutinoside, kaempferol rutinoside, rutin, ellagic Acid, ferrulic acid, p-coumaric acid, epicatechin, chlorogenic acid, caffeic acid, catechin, gallic acid, chrysin.

3.2.3. Extraction Procedure

Honey Samples (1 g) were extracted with 10 mL ethanol or *Mili-Q* water for 60 mins at $30\text{ }^{\circ}\text{C}$ using an ultrasonic bath. The extract was then centrifuged at

10,000× g for 10 min at 4 °C and the extraction was repeated one more time. The clear supernatants were mixed, filtered through a membrane filter with a porosity of 0.45 μm, and prepared for SPE sample preparation (details are presented in section 3.3) or stored at –20 °C until analysis.

3.2.4. LC-MS Method development by using myricetin-known phenolic

Method development was carried out according to the details mentioned in section 2.11.

3.2.5. Method Validation

LC-MS data analysis was carried out according to the details mentioned in section 2.11.

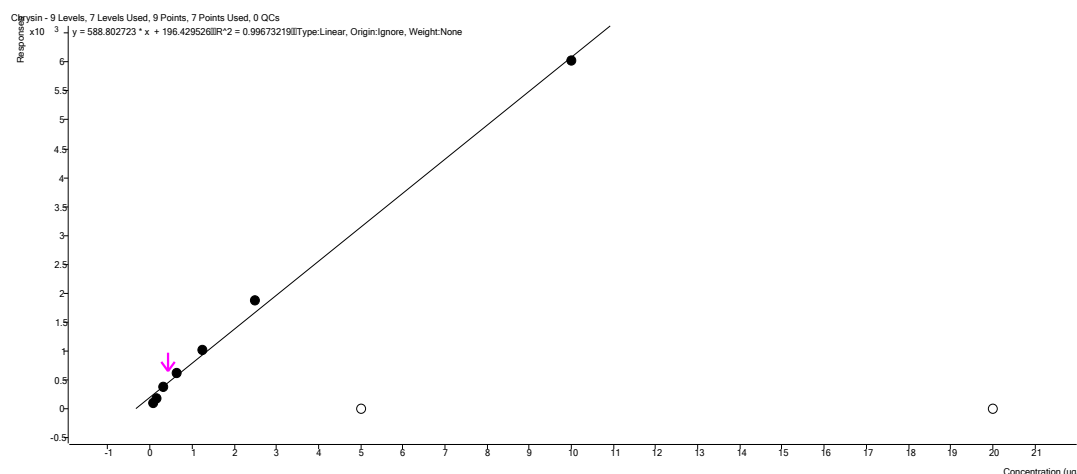


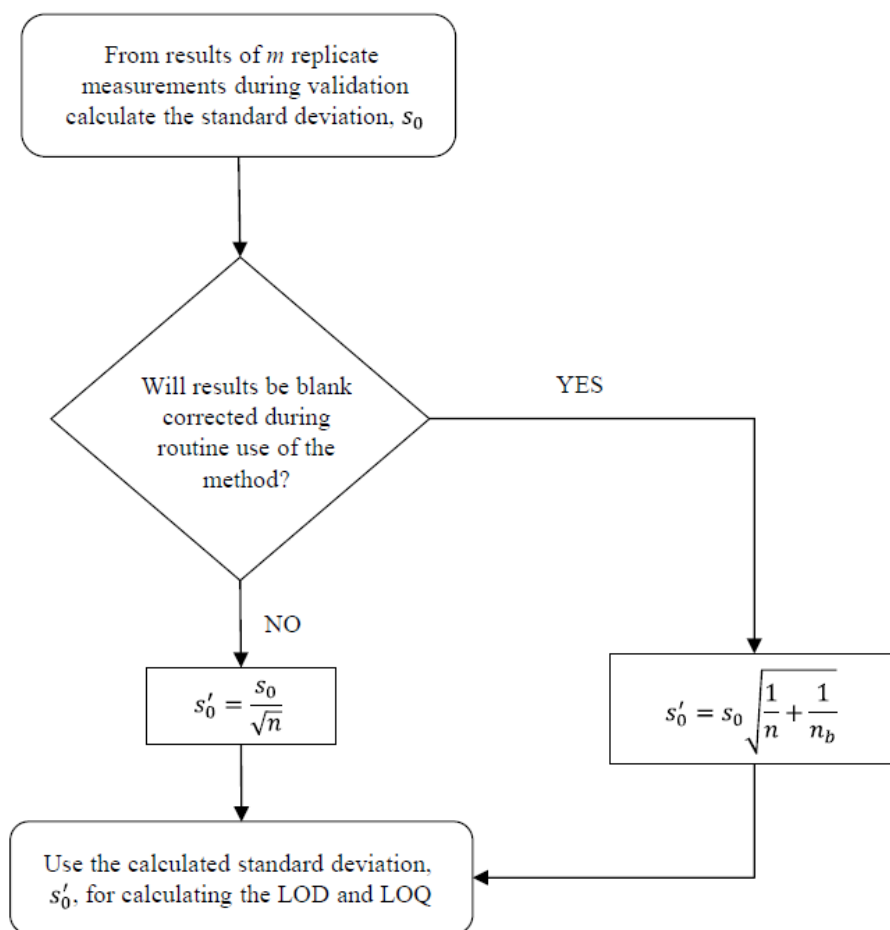
Figure 3- 3 Linear curve of Chrysin

Run 6 reagent blanks spiked with low concentration of analyte.

$$LOD = 3 \times S'_0$$

$$LOQ = 10 \times S'_0$$

Follow the flow chart to calculate S'_0 :



s_0 is the estimated standard deviation of m single results at or near zero concentration.

s'_0 is the standard deviation used for calculating LOD and LOQ.

n is the number of replicate observations averaged when reporting results where each replicate is obtained following the entire measurement procedure.

n_b is the number of blank observations averaged when calculating the blank correction according to the measurement procedure.

Figure 3- 4 Ref: **Eurachem Guide: The Fitness for Purpose of Analytical Methods – A Laboratory Guide to Method Validation and Related Topics, (2nd ed. 2014).** ISBN 978-91-87461-59-0. Available from www.eurachem.org.

From the chart above and the data tested by LC-MS, $S'_0=0.011354546$:

LOD= 0.034 ($\mu\text{g/ml}$)

LOQ= 0.114 ($\mu\text{g/ml}$)

3.2.6. LC-MS Analysis

The details of the Analysis will be carried out according to the details mentioned in section 3.3 in this chapter.

3.2.7. MS-DIAL

MS-DIAL was developed as a comprehensive software platform for untargeted metabolomics, supporting a range of instruments (GC/MS, GC/MS/MS, LC/MS, and LC/MS/MS) and accommodating various MS vendors, including Agilent, Bruker, LECO, Sciex, Shimadzu, Thermo, and Waters. The program also handles common data formats such as netCDF (AIA) and mzML. To facilitate user adoption, several MSP files containing both EI- and MS/MS spectra are provided as a 'start-up kit.' Additionally, MS-DIAL includes an integrated version of the Fiehn lab's GC/MS database (aligned with the FAME RI index) and an in silico retention time- and MS/MS database for LC/MS/MS-based lipidomics. Isotope-labeled tracking is also available for LC/MS projects.

Key features of MS-DIAL include:

- (1) Spectral deconvolution for both GC/MS and data-independent MS/MS,
- (2) Streamlined criteria for peak identification,
- (3) Comprehensive support for all data processing steps, from raw data import to statistical analysis,
- (4) A user-friendly graphical interface.

3.2.8. Data analysis

LC-MS/MS data analysis was carried out by Agilent MassHunter Qualitative Navigator B.08.00, and Agilent MassHunter Quantitative Analysis B.08.00.

3.3. LC-MS Analysis for Phenolics in Manuka Honey extract

3.2.1. Solid Phase Extraction (SPE) Sample Preparation

Solid phase extraction (SPE) is a widely utilized sample preparation technique in chromatography, primarily employed to eliminate interfering compounds

from samples. Additionally, SPE can be used to enrich and concentrate target analytes within the sample. This technique involves using a solid phase material, which selectively retains interfering substances, while solvents elute the analytes, allowing for their collection and subsequent analysis.

For the extraction and isolation of phenolics from honey, a modified version of the method described by Michalkiewicz, Biesaga, and Pyrzynska (Michalkiewicz et al., 2008) was used. Honey samples (1 g) were mixed with 10 mL of ultrapure water, adjusted to pH 2 using 0.1% HCl, and homogenized in an ultrasonic bath for 30 minutes at room temperature. The samples were then filtered through filter paper to remove solid particles. An SPE cartridge (Strata C18-E (55 μ m, 70A) 200mg / 3mL, Tubes) was conditioned by washing with 3 mL of acetonitrile followed by 9 mL of ultrapure water. Three filtrates were then passed through one cartridge, which was subsequently washed with 6 mL of acidified water to remove sugars and other polar constituents of honey. The retained compounds were eluted with 3 mL of acetonitrile. Then the extracts were filtered through a 0.45- μ m PTFE membrane filter and analyzed by UHPLC-HESI-MS/MS. (Gašić et al., 2014) In the end, samples were diluted in methanol with 1 in 10 ratio.

3.2.2. Phenolics LC-MS Total Ion Chromatogram (TIC) Scan in Manuka honey extract and MS-DIAL analysis

TIC of water extract from Manuka Honey in both negative and positive ionization modes are shown below followed by the UV chromatograms at wavelength of 254nm, 278nm and 300nm. By comparing the UV chromatogram with ESI scan, we can identify the polyphenol compounds using the molecular weights listed in the database of Phenol Explorer (Neveu et al., 2010; Rothwell et al., 2013; Rothwell et al., 2012). The tentative phenolic compounds are listed in Table 3-3.

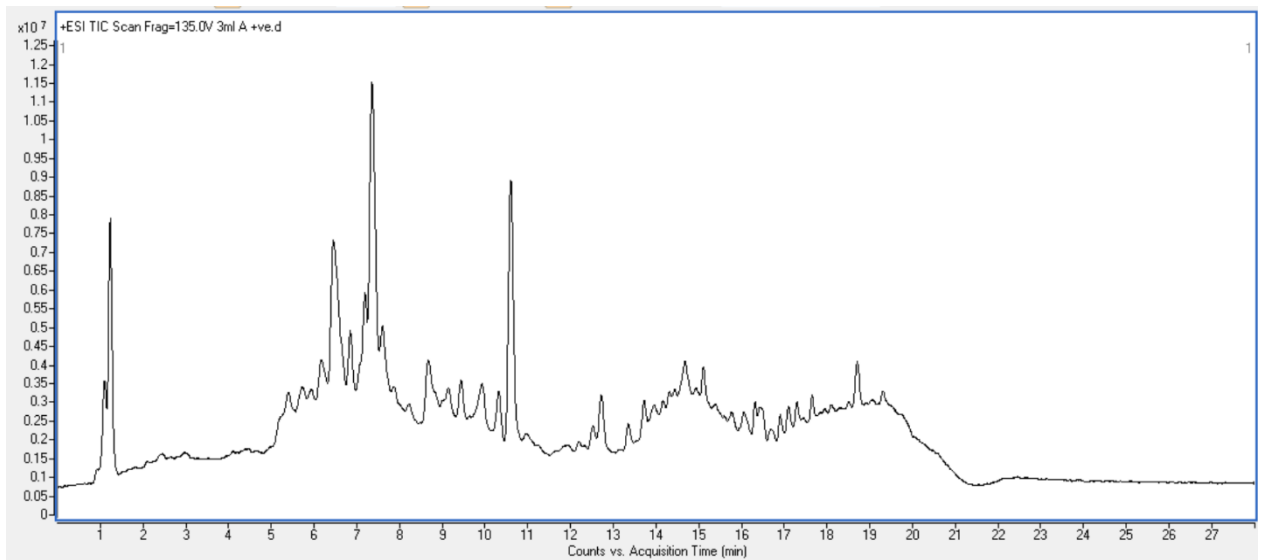


Figure 3- 5 Phenolics Positive TIC Scan in Manuka Honey

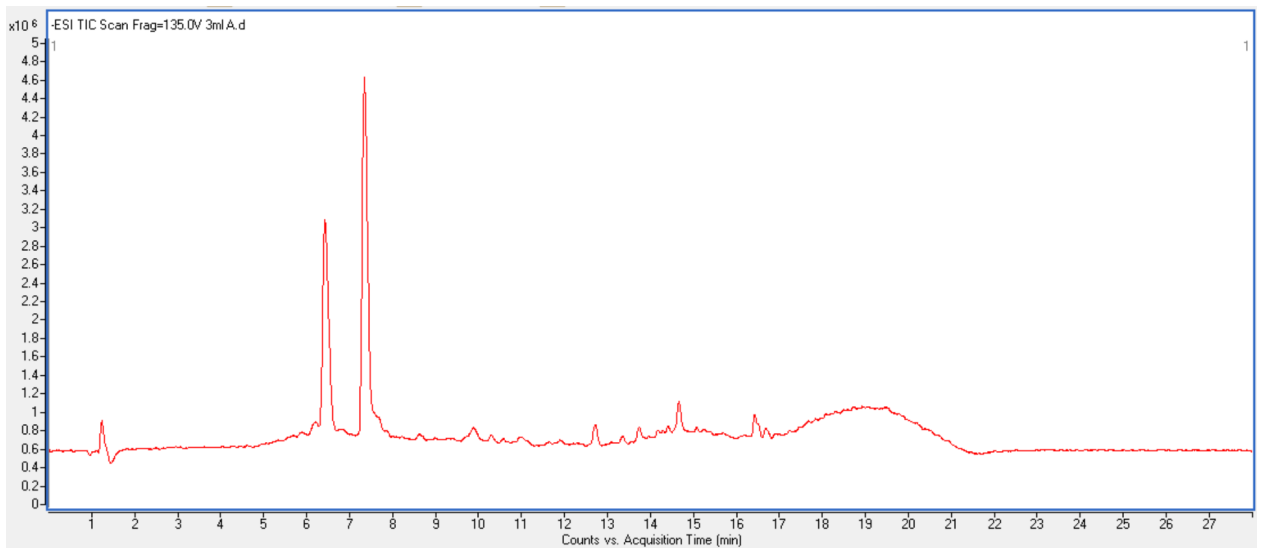


Figure 3- 6 Phenolics Negative TIC Scan in Manuka Honey

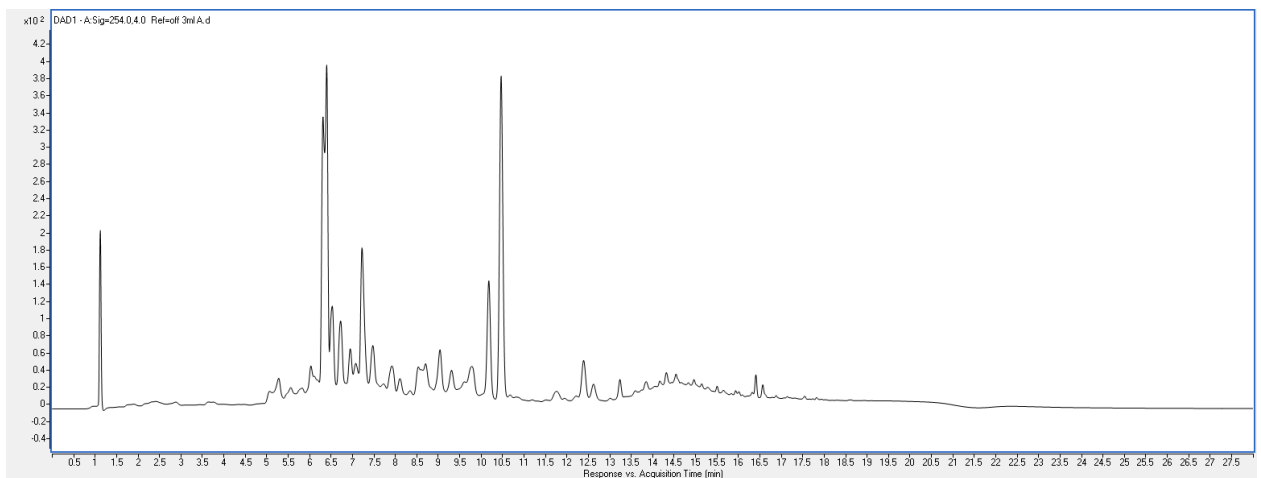


Figure 3- 7 UV chromatogram at the wavelength of 254nm

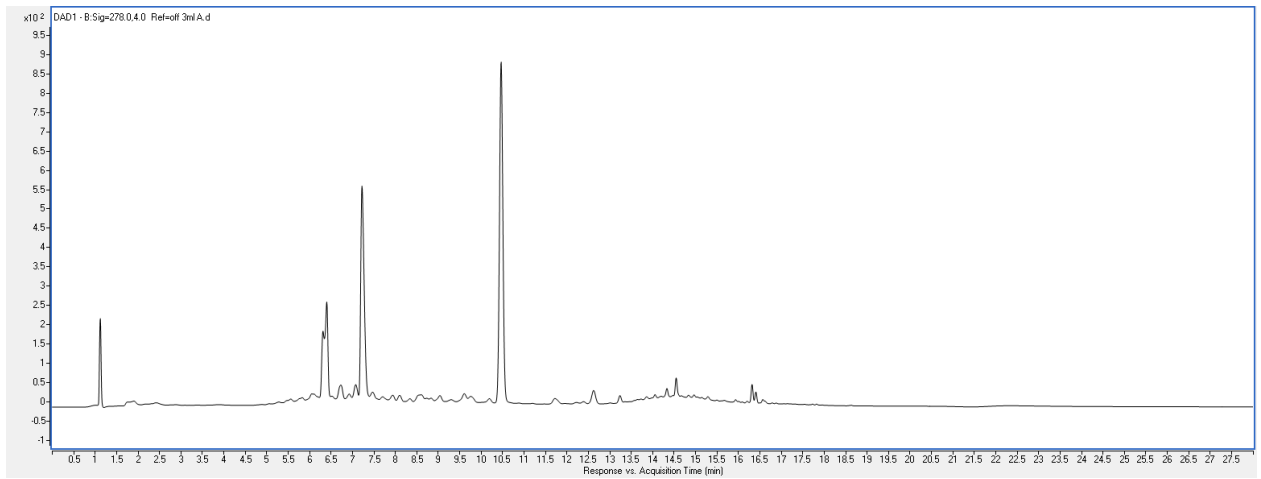


Figure 3- 8 UV chromatogram at the wavelength of 278nm

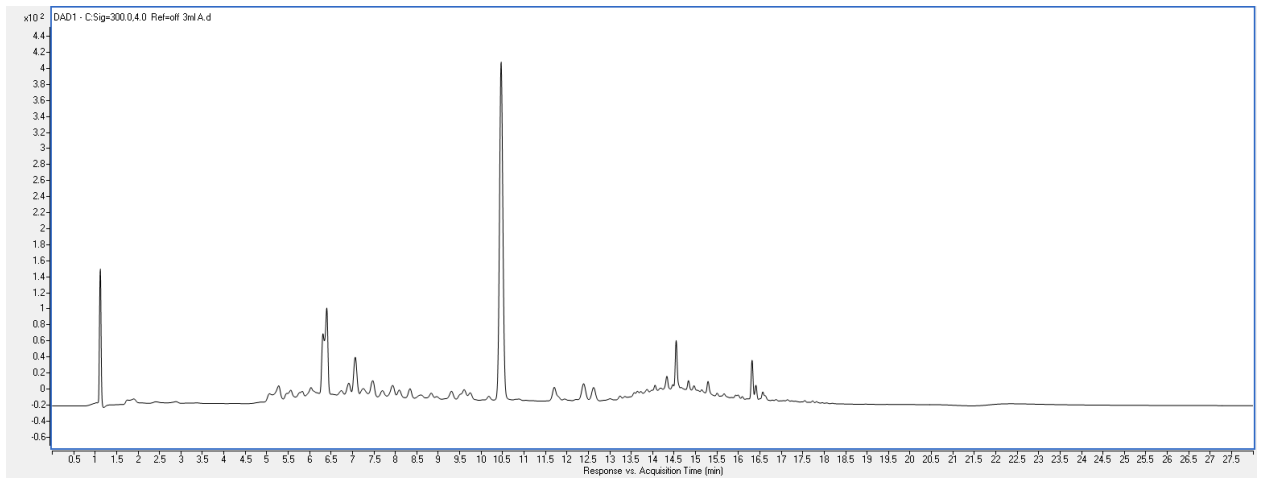


Figure 3- 9 UV chromatogram at the wavelength of 300nm

Table 3- 3 Major compound ID negative scan extract from MS-DIAL

RT	M/Z of Ve-	M/Z of Ve+	254nm	278nm	300nm	ID 1	ID 2	ID3	comments
6.41596	165	189	Y	Y	Y	Methoxyphenylacetic acid	Dihydro-p-coumaric		prominent
6.81885	357.1	N	Y	Y-	N	Gardenin B	Matairesinol	Pinoresinol	prominent
7.34111	195	N	Y	Y	N	Hydroxycaffeic acid	3,4-DHPEA-AC		prominent
7.60223	223	247	Y	Y	Y	Sinapic acid			
7.62461	285	Y	Y	Y	Y	Luteolin	Scutellarein		
7.70668	239	N	N	N	N				prominent
8.05735	181	183	Y	Y	Y	Syringaldehyde	Homovanillic acid		prominent
8.72881	279.1	303.1	Y&	Y-	Y-	p-Coumaroyl malic acid			prominent
9.86286	361.1	385.1	Y-	Y-	Y-	Caffeoyl tartaric acid			weak peak
10.2732	241	243	Y	Y-	Y-	4-Vinylsyringol			prominent
11.8549	263	N	Y-	Y-	Y-				NOT IN LIB
13.3172	347.1	371.1	Y-	Y-	N	5-Heptadecylresorcinol			
13.9439	391	415.1	Y-	N	N				NOT IN LIB
14.1528	285	309	N	N	N				prominent
14.2647	300.9	303	Y-	N	N	quercetin			prominent
14.4064	285	299	Y-	Y-	Y-	Luteolin	Scutellarein		prominent
14.6452 3	271	295	Y-	Y-	Y	Arbutin (271->109) (271->108,109 (35eV))	Butein (271->269,135,271)		prominent peak
15.3763	298.9	323	N	N	Y-	4-Hydroxybenzoic acid 4-O-	Hispidulin		
15.3838	327	N	N	N	Y-				NOT IN LIB
16.4283	254.9	258	N	Y	Y	Pinocembrin	Pterostilbene		prominent
16.5178	253	255	Y	Y	Y	7,4'-Dihydroxyflavone	Chrysin		prominent
16.6745 7	269	271	Y-	N	Y-	7,3',4'-Trihydroxyflavone 269->131,156(20eV)	Apigenin 269->117,151,149,107(30eV)		prominent peak

* RT: Retention Time

M/Z: Mass-to-Charge Ratio

254nm, 278nm, 300nm: If it is presented under those wave length of DAD detector.

ID1-ID3: Identify the compounds by using database will be discussed in section 3.5 in this chapter.

3.4. MRM validation for major phenolic compounds

The MS ionisation source conditions were as follows: capillary voltage of 4 kV, drying gas temperature of 300 °C, drying gas flow of 10 L/min, nebulizer pressure of 40 psi. Positive and negative scans with a scan range from 100-1000 Da were performed for unknown phenolic compound identification. The negative ionisation mode was performed with MRM for quantitative analysis. The MRM transitions are followed.

Table 3- 4 MRM transitions condition for main phenolics compounds confirmed by standard

Compound Name	Precursor Ion	Product Ion	Fragmentor	Collision Energy (eV)	Cell Accelerator Voltage	Polarity
Gallic Acid	169	79	100	24	7	Negative
Gallic Acid	169	125	100	10	7	Negative
Chlorogenic Acid	353	85	80	42	7	Negative
Chlorogenic Acid	353	191	80	13	7	Negative
Catechin	289	245	140	6	7	Negative
Catechin	289	203	140	12	7	Negative
Ferrulic Acid	193	178	80	8	7	Negative
Ferrulic Acid	193	134	80	12	7	Negative
Caffeic Acid	179	135	80	13	7	Negative
Caffeic Acid	179	134	80	34	7	Negative
Isorhamnetin rutinoside	623	300	240	46	7	Negative
Isorhamnetin rutinoside	623	315	240	28	7	Negative
Rutin	609	300	240	40	7	Negative
Rutin	609	271	240	64	7	Negative
Kaempferol rutinoside	593	285	220	30	7	Negative
Kaempferol rutinoside	593	255	220	44	7	Negative
Myricetin	317	179	140	10	7	Negative
Myricetin	317	151	140	14	7	Negative
Ellagic Acid	301	284	200	26	7	Negative
Ellagic Acid	301	145	200	36	7	Negative
Isorhamnetin	315	151	140	24	7	Negative
Isorhamnetin	315	300	140	14	7	Negative
Quercetin	301	179	140	10	7	Negative
Quercetin	301	151	140	16	7	Negative
Kaempferol	285	285	140	5	7	Negative
Kaempferol	285	185	140	23	7	Negative
Kaempferol	285	156	140	26	7	Negative
Chrysin	253	143*	160	24	7	Negative
Chrysin	253	119	160	32	7	Negative

Table 3- 5 Comparison of the standards in ethanol extract and water extract-1

Sample			Gallic Acid Results			Catechin Results			Caffeic Acid Results			Chlorogenic Acid Results			Epicatechin Results			p-coumaric acid Results			Ferrulic Acid Results			Ellagic Acid Results			Qua lifier (30 1.0 -> 145 .0) Results		
Name	Type	Level	Area	RT	Ratio	Area	RT	Ratio	Area	RT	Ratio	Area	RT	Ratio	Area	RT	Ratio	Area	RT	Ratio	Area	RT	Ratio	Area	RT	Ratio	Area	RT	Ratio
Blank1	Sample		1.868 5054 2	1.7 31 5	54. 528	0.166 25294 2	5.3 52	816 .71	1.809 26535 3	5.7 83 7	290 .89	2.254 03537 8	5.9 02 9		0.668 07150 9	6.1 15 1	225 .92	4.900 54978 8	7.1 15 1	37. 53	0.621 65703 4	8.0 13 4	82. 53	1.311 57808 1	9.6 75 3				
Quercetin_a	Cal	a	1.607 2275 2	1.7 17 9		0.811 83909	5.3 52		1.249 80793 8	6.1 39 8	81. 524	0.219 20045 5	5.9 90 1		0.515 05276 8	6.6 82	137 .63	1.412 59043 4	7.1 51 5	67. 73	0.858 23631 7	8.3 98 6	121 .22	4.196 92706 2	9.6 36 7				
Quercetin_b	Cal	b	5.038 0767 6	1.7 17 9	16. 87	0.649 64945 8	5.2 64 8	50. 959	0.694 49850 3	5.8 27 3		1.145 49111 8	5.9 17 4	43. 576	0.481 60048 6	6.5 29 3	95. 563	7.173 37167 6	7.1 15 1	6.1 5	0.283 92805 4	8.1 66		0.769 26367 5	9.7 78 3				
Quercetin_c	Cal	c	3.997 4439 2	1.7 04 3	18. 742	0.834 73891 1	5.1 92 1		0.732 33932 4	5.8 85 4	85. 108	1.491 14076 3	5.8 88 3	18. 763	1.180 75544 3	6.5 36 6	146 .38	2.936 48858 4	7.0 86 1	16. 98	0.175 09892 3	7.9 04 4	221 .85	0.652 13653 2	9.7 07 5				
Quercetin_d	Cal	d	1.951 9672 5	1.7 17 9	36. 314	0.652 55081 9	5.2 21 2		1.632 74920 1	5.9 21 8	11. 105	1.088 98008 8	5.8 95 6	100 .32	0.563 61905 4	6.7 25 6	98. 319	5.344 77475 9	7.2 16 9	7.1 06	0.290 01302 4	8.3 40 4	244 .3	0.592 9385 1	9.7 46 1				
Quercetin_e	Cal	e	2.233 5649 3	1.7 31 5	328 .69	1.007 12884 4	5.0 83 1		1.119 51560 9	6.1 18 5	61. 545	1.190 57544 9	5.8 66 5		3.521 40468 6	6.4 78 5	7.5 131	0.839 96083 5	7.2 45 9		0.341 58208 8	7.9 98 9	138 .65	3.394 34519 3	9.6 94 7				
Quercetin_f	Cal	f	1.065 2843 3	1.7 24 7		0.803 88751 8	5.3 73 8		1.349 38467 3	5.8 12 8		1.822 87407 9	5.9 10 1		0.773 58223 5	6.4 49 4		5.341 15867 7	7.1 00 6	34. 24	4.581 55923 5	7.9 40 7	50. 973	1.200 68211 6	9.7 13 9				
Quercetin_g	Cal	g	1.356 3746 3	1.7 24 7	39. 644	0.651 84944 5	5.2 93 8		1.699 08939 7	5.5 80 2		1.125 47252 9	6.0 77 3		0.661 92945 5	6.5 07 5		8.307 52223 4	7.2 89 5	9.8 33	0.541 32407 8	8.0 64 3	45. 265	2.285 82115 3	9.9 97 1	32. 158			
Blank2	Sample		0.685 3419 8	1.7 38 3		0.651 73954 4	5.1 63		1.118 81363 5	5.8 41 8	538 .53	0.609 46117 1	5.9 31 9	729 .31	1.370 82642 9	6.4 34 9		1.497 50872 3	7.1 51 5	42. 63	0.956 69638 1	7.7 80 8	55. 824	0.967 91052 2	9.6 81 8	23. 098			
Honey in ethano l1_1	Sample		97.86 4199 4	1.7 51 8	6.9 923	0	4.9 52 3		721.2 43642 1	5.7 40 1	6.7 999	53.64 34741 5	5.8 59 3	7.4 539	0	6.7 91		131.0 08308	7.0 64 2	10. 68	0	8.2 38 7		40.32 32424 7	9.5 85 2	86. 708			
Honey in ethano l1_2	Sample		119.8 9737 7	1.7 38 3	6.4 139	0	5.2 28 4		778.6 93848 2	5.7 25 5	7.7 97	66.19 24803 2	5.8 37 5	5.9 229	0	6.3 91 3		121.4 76907 4	7.0 35 2	7.8 09	0	7.9 84 3		46.88 44622 8	9.5 40 2	77. 063			

Honey in ethano l1_3	Sampl e	118.0 2240 7	1.7 51 8	5.7 048	0	5.1 48 5		716.7 94469 4	5.7 11	7.6 388	58.84 25707	5.8 81 1	11. 218	0	6.5 00 3		109.8 75552 2	6.9 84 3	15. 19	0	7.8 60 8		39.76 16423 4	9.5 14 5	82. 202
Honey in ethano l2_1	Sampl e	176.2 8525 2	1.7 45 1	3.9 78	0	5.1 99 4		1263. 60958 8	5.7 03 7	7.2 948	113.0 55470 9	5.8 73 8	12. 055	0	6.6 52 9		133.7 92703 5	6.9 91 6	13. 85	0	8.3 04 1		91.98 43583 6	9.5 27 3	81. 852
Honey in ethano l2_2	Sampl e	161.1 5796 1	1.7 51 8	7.9 784	0	5.4 02 9		1264. 00486 6	5.6 96 5	8.2 236	102.2 76252 7	5.8 81 1	12. 011	0	6.5 22 1		232.9 24665 5	6.9 77	4.4 89	0	8.2 02 4		82.05 73443 8	9.5 53 1	81. 586
Honey in ethano l2_3	Sampl e	160.9 8710 7	1.7 51 8	7.4 728	0	4.9 45		1174. 23550 5	5.7 25 5	8.1 349	102.7 32906 7	5.8 88 3	9.3 035	0.302 02135 7	6.4 93		229.5 86200 4	7.0 35 2	5.8 49	0	7.9 69 8		83.61 72436 8	9.5 33 8	71. 932
Honey in ethano l3_1	Sampl e	239.0 1009 5	1.7 51 8	9.0 24	0	5.0 97 6		2196. 67887 1	5.7 03 7	8.0 328	134.6 20224 6	5.8 66 5	12. 935	0	6.6 09 3		309.2 13605 5	6.9 98 8	10. 41	0	7.9 84 3		144.0 46240 2	9.5 33 8	87. 265
Honey in ethano l3_2	Sampl e	268.0 4678 6	1.7 51 8	5.1 545	0	5.3 08 4		2181. 74791 3	5.7 11	8.1 636	137.4 30228 6	5.8 73 8	7.4 803	0	6.2 96 8		314.4 17677	7.0 06 1	9.2 98	0	7.9 33 5		140.2 33654 7	9.5 46 6	87. 057
Honey in ethano l3_3	Sampl e	234.5 0996 2	1.7 51 8	3.7 913	0.442 19380 3	5.2 72	301 .86	2213. 47687 6	5.7 03 7	9.2 345	155.1 30409 5	5.8 73 8	9.0 793	0	6.8 41 9		313.9 96106 7	7.0 35 2	8.6 02	0	8.3 04 1		165.5 37583 3	9.5 27 3	82. 369
Honey in water4_1	Sampl e	391.3 9303 7	1.7 24 7	7.4 815	0	5.0 75 8		2330. 43635 7	5.7 25 6	8.3 32	349.4 33960 2	5.8 95 6	10. 02	0.401 12086 5	6.4 42 1	244 .91	185.2 67260 3	7.0 49 7	10. 07	0	8.0 13 4		115.5 03035 1	9.5 59 5	71. 213
Honey in water4_2	Sampl e	402.7 8522 1	1.7 24 7	8.0 482	0	5.4 46 5		2307. 73370 6	5.7 25 6	8.4 998	351.6 49968 5	5.8 88 3	10. 473	0	6.5 87 5		180.5 90779 8	7.0 64 3	10. 22	0	7.9 98 9		112.7 63901	9.5 66	82. 151
Honey in water4_3	Sampl e	378.3 6781 9	1.7 24 7	7.9 313	0	5.3 37 5		2247. 78505 6	5.7 18 3	9.2 294	388.5 64174 5	5.8 81 1	7.4 962	0	6.2 31 4		188.2 36594 9	7.0 64 2	9.4 97	0	8.0 20 7		140.9 19498 3	9.5 78 8	86. 03
Querc etin_d 2	Sampl e	7.467 0956 8	1.7 45 1	4.7 763	0.624 69658 7	5.1 63		0.913 59191 5	5.7 98 2		2.262 21295 3	6.1 42 7		1.512 16026 8	6.8 49 1	78. 974	2.238 76653 2	7.1 36 9	28. 54	0.823 70680 4	8.4 27 7	128 .99	2.269 41077 8	9.7 14	110 .9
Blank3	Sampl e	0.304 7656	1.6 97 5		0.622 30593 2	5.2 72	91. 787	1.626 56703 2	5.6 38 3		0.265 23370 2	5.9 10 1	338 .19	0.675 94966 9	6.5 36 6	300 .69	2.358 61187	7.1 00 6	11. 15	0.848 83197 8	8.2 46	37. 017	2.180 68803 9	9.7 26 8	54. 162
20210 507 2uL Tung	Sampl e	2784 4.909 2	1.6 97 5	7.7 267	31563 .4271 9	5.3 08 4	49. 134	19790 .9989 2	5.7 98 2	8.8 405	8388. 78958 6	5.9 82 8	8.8 991	34149 .9111 7	6.4 93	48. 654	5052. 54716 9	7.1 36 9	8.5 49	8342. 73922 7	8.1 29 7	32. 109	521.7 77698 6	9.4 69 4	82. 781

Honey in ethano I2_1	Sam ple		0	9.74 87		0	11.4 618		0	12.0 641		0	12.7 63		864.61 455	14.3 889	45.5 49	2619.8 41997	15.1 584	1.77	0.16 7	974.73 80171	15.3 021	13.5 7
Honey in ethano I2_2	Sam ple		0	9.70 37		0	11.5 776		0	12.1 606		0	12.6 15		889.77 255	14.3 812	44.9 44	2544.9 1506	15.1 429	1.72 6	0.21 4	944.93 88403	15.2 866	14.0 5
Honey in ethano I2_3	Sam ple		0	9.74 87		0	11.4 746		0	12.0 126		0	12.6 15		901.65 097	14.3 734	46.0 89	2684.7 49965	15.1 429	1.56 7	0.12 8	953.20 55518	15.2 944	14.0 4
Honey in ethano I3_1	Sam ple		0	9.76 16		0	11.4 682		0	12.1 092		0	12.8 531		2652.6 719	14.3 889	46.5 71	4639.1 93081	15.1 506	1.75 1	0.25	1695.5 97947	15.2 944	14.0 8
Honey in ethano I3_2	Sam ple		0	9.74 87		0	11.5 068		0	12.1 156		0	12.8 788		2597.3 959	14.3 734	46.4 03	4761.4 57096	15.1 429	1.77 7	0.27 8	1789.4 64955	15.2 866	13.4 1
Honey in ethano I3_3	Sam ple		0	9.71 65		0	11.4 296		0	12.0 062		0	12.5 763		2669.8 035	14.3 812	46.7 87	4978.5 71155	15.1 506	1.44 9	0.21 5	1893.8 11605	15.2 944	13.0 9
Honey in water4_1	Sam ple		0	9.77 45		15.417 00533	11.4 489	50.5 9	115.76 08999	12.1 22	27.8 28	0	12.4 541		765.48 853	14.3 657	46.3 76	1953.0 54171	15.1 429	1.53 8	0.26 9	760.56 02231	15.2 944	12.2 5
Honey in water4_2	Sam ple		0	9.78 73		17.492 81955	11.5 133	66.0 77	109.42 75967	12.1 542	29.8 95	0	12.7 951		715.53 434	14.3 889	44.8 12	2090.0 19312	15.1 584	1.58 2	0.24 7	822.82 62236	15.3 021	12.6 9
Honey in water4_3	Sam ple		0	9.74 23		22.365 67501	11.4 875	30.5 15	119.50 14537	12.1 349	28.2 2	0	12.5 892		686.67 98	14.3 812	43.9 07	2058.4 26379	15.1 506	1.45 7	0.16 3	784.98 21902	15.2 944	13.0 5
Quercetin_d_2	Sam ple		130.73 50422	9.77 44	65.8 96	1.5523 12698	11.4 939	10.9 32	2.0018 89481	12.1 284		1.4214 6641	12.5 377	38.1 22	21185. 012	14.3 812	45.1 95	3094.8 16958	15.1 584	1.70 1	0.29 6	1253.2 89715	15.3 021	13.6 3
Blank3	Sam ple		3.4016 40451	9.94 18	27.2 2	0.2143 97206	11.5 325	44.5 37	0.3262 08695	12.0 898	476. 67	0.8818 33206	12.8 402	43.3 06	7.6443 818	14.5 052		20.281 91388	15.1 274			11.516 80885	15.2 866	14.2 6
20210 507 2uL Tung Pheno lic std B	Sam ple		10330. 98282	9.76 8	67.0 37	11789. 14004	11.5 197	39.8 64	7870.2 54512	12.1 864	29.5 03	4748.2 84188	11.9 65	85.6 47	6488.8 81	14.3 269	46.3 4	61132. 64267	15.1 429	1.58 7	0.23 6	24241. 00619	15.3 099	13.6 3

Table 3- 7 Comparison of the two major compounds' content in Manuka Honey and Thyme Honey: 2-hydroxy-3-(4-methoxyphenyl)propanoic acid; and DL-3-phenyllactic acid, and chrysin quantitative analysis.

Sample				DL-3-phenyllactic acid Method	DL-3-phenyllactic acid Results	2-hydroxy-3-(4-methoxyphenyl)propanoic acid Method	2-hydroxy-3-(4-methoxyphenyl)propanoic acid Results	Chrysin Method	Chrysin Results
Name	Type	Level	Acq. Date-Time	Units	Calc. Conc.	Units	Calc. Conc.	Units	Calc. Conc.
Blank0	Sample		26/03/2024 20:16	µg/ml	0.00096451	µg/ml	0.00085695	µg/ml	0
Std A 20	Cal	A	26/03/2024 20:57	µg/ml	17.56131927	µg/ml	14.86788848	µg/ml	0
Std B 10	Cal	B	26/03/2024 21:38	µg/ml	9.772076404	µg/ml	8.534508193	µg/ml	9.898720489
Std C 5	Cal	C	26/03/2024 22:19	µg/ml	5.225160621	µg/ml	4.899851406	µg/ml	0
Std D 2.5	Cal	D	26/03/2024 23:00	µg/ml	2.799446313	µg/ml	2.578064019	µg/ml	2.838083516
Std E 1.25	Cal	E	26/03/2024 23:41	µg/ml	1.479447699	µg/ml	1.403195393	µg/ml	1.381772268
Std F 0.625	Cal	F	27/03/2024 0:22	µg/ml	0.755305998	µg/ml	0.742173818	µg/ml	0.718190783
Std G 0.3125	Cal	G	27/03/2024 1:02	µg/ml	0.396502579	µg/ml	0.409655286	µg/ml	0.293233077
Std H 0.15625	Cal	H	27/03/2024 1:43	µg/ml	0.20332162	µg/ml	0.20238912	µg/ml	0
Std I 0.078	Cal	I	27/03/2024 2:24	µg/ml	0.115954471	µg/ml	0.120112538	µg/ml	0
Blank	Sample		27/03/2024 3:05	µg/ml	0.000923196	µg/ml	0.000418982	µg/ml	0
M1 50x	Sample		27/03/2024 3:46	µg/ml	3.298113552	µg/ml	2.947186112	µg/ml	0
M2 50x	Sample		27/03/2024 4:27	µg/ml	3.227279669	µg/ml	2.932502336	µg/ml	0
M3 50x	Sample		27/03/2024 5:08	µg/ml	3.229734654	µg/ml	3.077672757	µg/ml	0
T1 50x	Sample		27/03/2024 5:49	µg/ml	0.00291274	µg/ml	0.002203918	µg/ml	0
T2 50x	Sample		27/03/2024 6:30	µg/ml	0.002089464	µg/ml	0.001364006	µg/ml	0
T3 50x	Sample		27/03/2024 7:11	µg/ml	0.00171385	µg/ml	0.001136348	µg/ml	0
M1	Sample		27/03/2024 7:52	µg/ml	98.10282924	µg/ml	62.22832962	µg/ml	0.279221303
M2	Sample		27/03/2024 8:33	µg/ml	96.09060973	µg/ml	63.39899583	µg/ml	0.344987117
M3	Sample		27/03/2024 9:14	µg/ml	92.66362291	µg/ml	64.09830112	µg/ml	0.428937348
T1	Sample		27/03/2024 9:55	µg/ml	1.004038405	µg/ml	0.224324891	µg/ml	0.29051242
T2	Sample		27/03/2024 10:36	µg/ml	0.921891918	µg/ml	0.225277228	µg/ml	0.299949789
T3	Sample		27/03/2024 11:16	µg/ml	0.935991148	µg/ml	0.203543348	µg/ml	0.250924439
Std E 1.25 B	Sample		27/03/2024 11:57	µg/ml	1.484005305	µg/ml	1.359058971	µg/ml	2.132048092

Table 3- 8 Comparison of the other major compound's content in Manuka Honey and Thyme Honey: Methyl Syringate

Sample				Methyl Syringate Method	Methyl Syringate Results		
Name	Data File	Type	Level	Units	RT	Area	Calc. Conc.
Blank0	Blank0.d	Sample		µg/ml	23.3667	0.3	0
Std A 20	Std A 20.d	Cal	A	µg/ml	23.88	161	17.8115263
Std B 10	Std B 10.d	Cal	B	µg/ml	22.78	90.7	10.00312096
Std C 5	Std C 5.d	Cal	C	µg/ml	24.6267	45	4.917616267
Std D 2.5	Std D 2.5.d	Cal	D	µg/ml	22.4133	24.7	2.646488755
Std E 1.25	Std E 1.25.d	Cal	E	µg/ml	22.2267	12.3	1.266937808
Std F 0.625	Std F 0.625.d	Cal	F	µg/ml	22.0533	6.78	0.652024473
Std G 0.3125	Std G 0.3125.d	Cal	G	µg/ml	23.5933	3.38	0.272806002
Std H 0.15625	Std H 0.15625.d	Cal	H	µg/ml	22.0667	1.69	0.084755738
Std I 0.078	Std I 0.078.d	Cal	I	µg/ml	21.8867	1.02	0.009982821
Blank	Blank.d	Sample		µg/ml	21.4733	9.77	0.985339884
M1 50x	M1 50x.d	Sample		µg/ml	21.8733	5.27	0.483338698
M2 50x	M2 50x.d	Sample		µg/ml	22.7867	5.27	0.483025681
M3 50x	M3 50x.d	Sample		µg/ml	21.66	5.2	0.475297259
T1 50x	T1 50x.d	Sample		µg/ml	22.9133	0.11	0
T2 50x	T2 50x.d	Sample		µg/ml	22.4267	0.21	0
T3 50x	T3 50x.d	Sample		µg/ml	23.0067	0.06	0
M1	M1.d	Sample		µg/ml	21.5733	264	29.35285505
M2	M2.d	Sample		µg/ml	21.6533	257	28.50128988
M3	M3.d	Sample		µg/ml	21.2867	276	30.66447187
T1	T1.d	Sample		µg/ml	21.2667	5.04	0.457850879
T2	T2.d	Sample		µg/ml	21.24	4.82	0.433367563
T3	T3.d	Sample		µg/ml	21.2467	5.09	0.463164693
Std E 1.25 B	Std E 1.25 B.d	Sample		µg/ml	21.4	15.3	1.599459196

From Table 3-8, it is evident that Methyl Syringate in Manuka honey (29.5 µg/mL) is approximately sixty-six times higher than in thyme honey (0.45 µg/mL). Similarly, Table 3-7 indicates that the concentration of DL-3-phenyllactic acid in Manuka honey (95.6 µg/mL) is about 100 times greater than in thyme honey (0.95 µg/mL). Additionally, 2-hydroxy-3-(4-methoxyphenyl) propanoic acid in Manuka honey (63.24 µg/mL) is roughly 286 times that in thyme honey (0.22 µg/mL). On the other hand, the amount of chrysin is similar in both types of honey, with Manuka honey containing 0.35 µg/mL and thyme honey 0.28 µg/mL.

In Manuka honey, DL-3-phenyllactic acid is about 1.5 times the amount of 2-hydroxy-3-(4-methoxyphenyl) propanoic acid, 3.2 times that of Methyl Syringate, and 283 times that of chrysin. In thyme honey, DL-3-phenyllactic acid is around 4.4 times of the amount of 2-hydroxy-3-(4-methoxyphenyl) propanoic acid, twice that of Methyl Syringate, and 3.4 times that of chrysin.

When the honey samples are diluted fifty times, Methyl Syringate becomes undetectable in thyme honey, while chrysin cannot be detected in either type of honey.

Tables 3-5 and 3-6 illustrate the presence of specific phenolic compounds in Manuka honey under both ethanol and water extracts, as confirmed by MRM. Additionally, Quercetin in Table 3-3 was confirmed incidentally. The area readings for each compound further confirm the differences between the different extraction methods.

3.5. Identification of Phenolic Compounds in Manuka Honey Extract

The three major peaks in TIC scan are identified as methyl syringate, DL-3-phenyllactic acid, and 2-hydroxy-3-(4-methoxyphenyl) propanoic acid. The calibration curves of these three compounds are shown below, followed by the calibration curves of quercetin and chrysin (other major phenolic compounds in Manuka honey) .

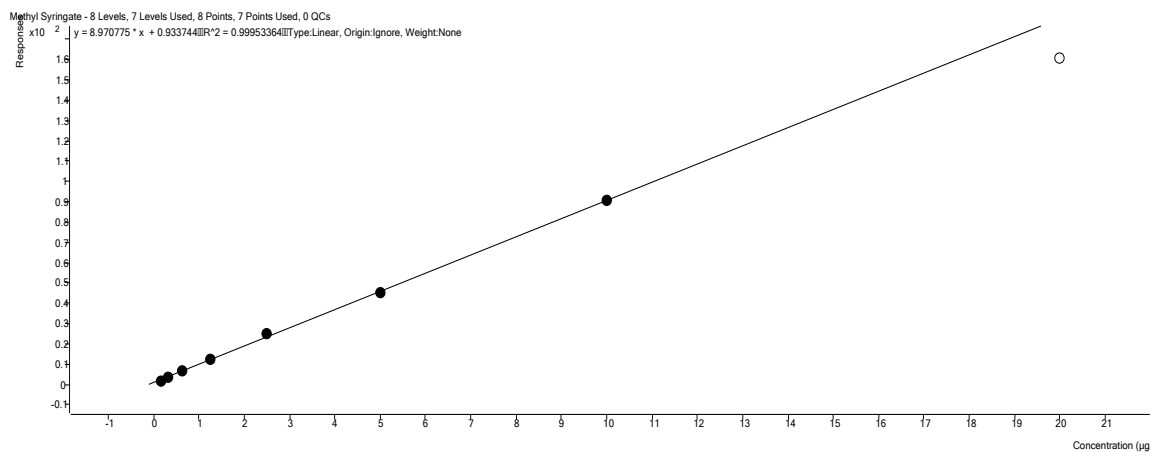


Figure 3- 10 LC-MS calibration curve of methyl syringate.

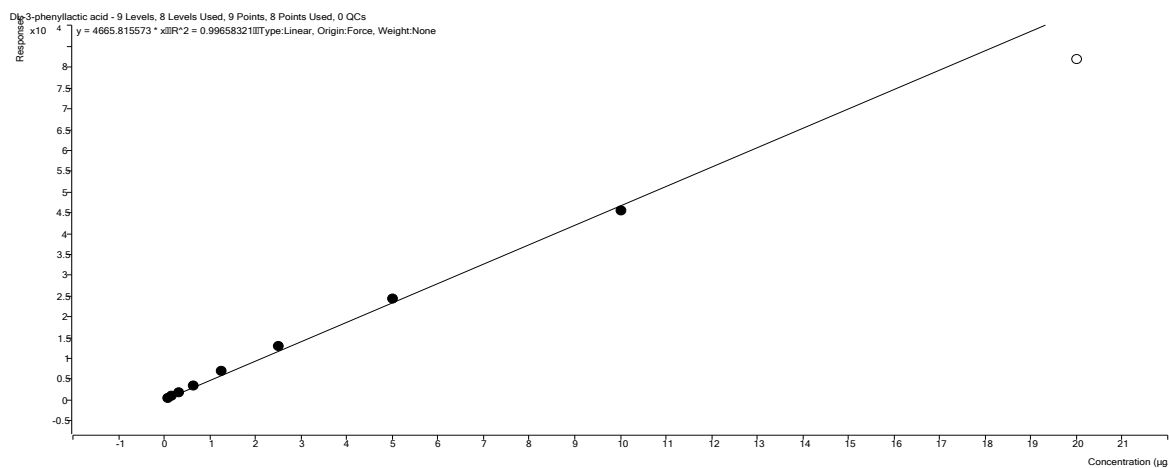


Figure 3- 11 LC-MS calibration curve of DL-3-phenyllactic acid.

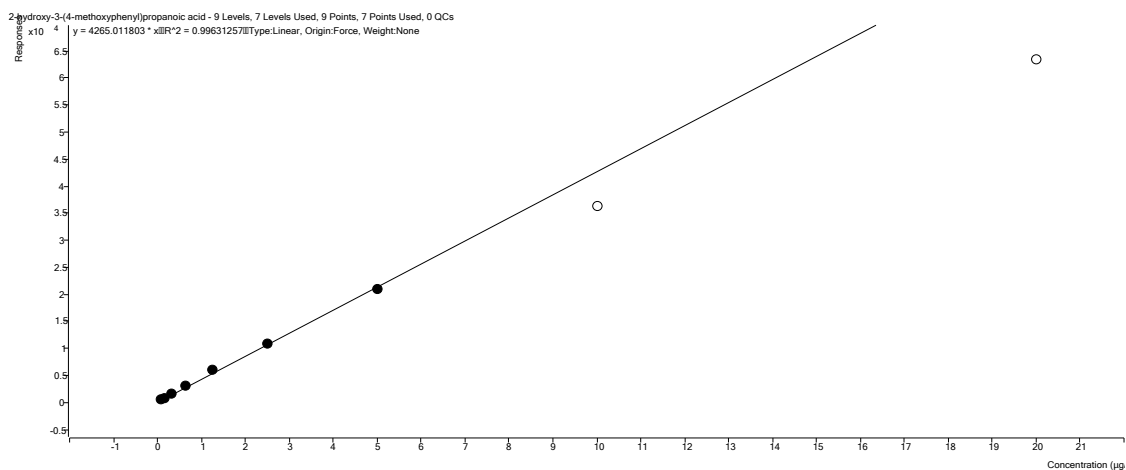


Figure 3- 12 LC-MS calibration curve of 2-hydroxy-3-(4-methoxyphenyl) propanoic acid.

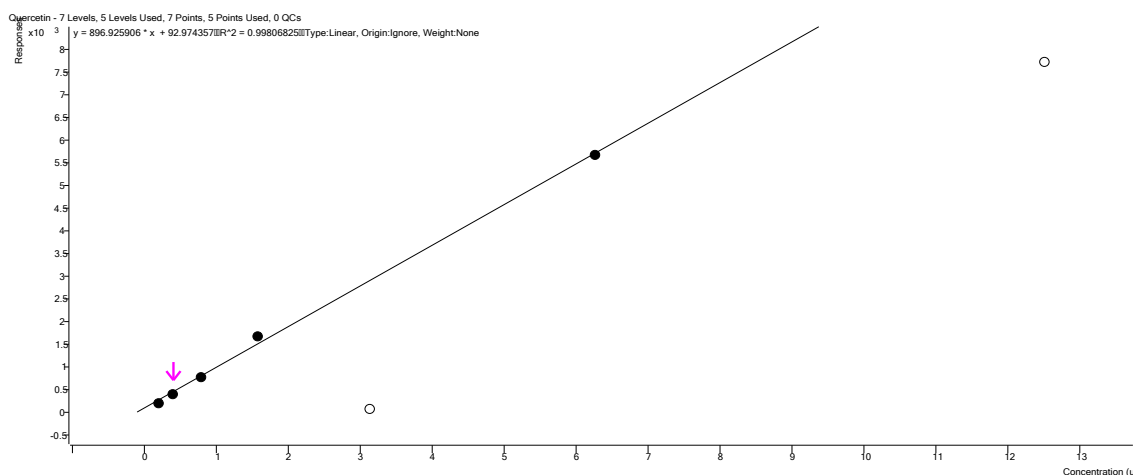


Figure 3- 13 LC-MS calibration curve of quercetin.

The tentative phenolic compounds listed in Table 3-5 would be tested in module fitting and will be presented in Chapter 4 for details, and chrysin is the only one compound can be combined with MRP-2 membrane protein. Linear curve of chrysin is shown below.

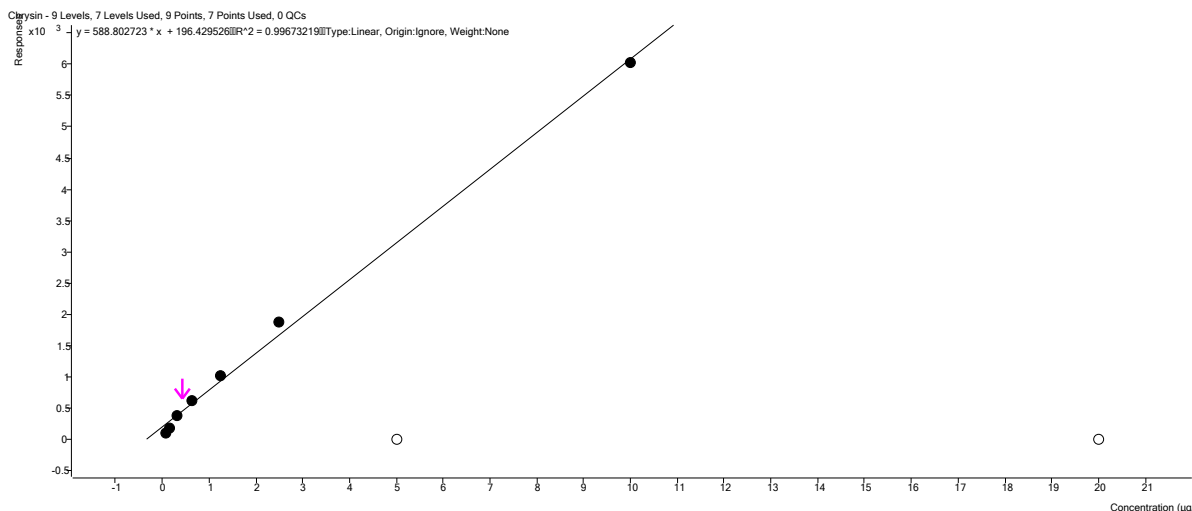


Figure 3- 14 LC-MS calibration curves of chrysin.

3.6. Summary

Honey is rich in phenolic compounds, flavonoids, and other antioxidants, which impart antibacterial, antioxidant, and anti-inflammatory benefits. These phenolic compounds are essential bioactive components that provide free radical scavenging and oxidation resistance properties (Velásquez et al.). The composition and concentration of these compounds differ among various honey types, depending on factors like botanical source, geographic region, and processing techniques. Research indicates that these variations significantly impact the bioactive properties of honey.

In comparing the ethanol and water extractions of honey, some phenolic compounds are present only in the water extract, while others are significantly more abundant in the ethanol extract, depending on the structure of the compounds. In this chapter, a comprehensive LC–MS/MS method has been developed and validated for the relative quantitation of 14 fingerprint phenolic compounds. NZ Manuka honey contains a significant amount of quercetin, methyl syringate, DL-3-phenyllactic acid, chlorogenic acid, chrysin, myrecitin, and 2-hydroxy-3-(4-methoxyphenyl) propanoic acid. Given the

diversity and complexity of phenolic compounds in Manuka honey, an in-silico screening approach may be used (Chapter 4) to perform a virtual screening and predict the molecular interactions with MRP2.

Chapter 4 In Silico Screening of MRP2 Inhibitors using AutoDock Vina

4.1. Introduction

Our recent studies suggest multi-drug resistance protein 2 (MRP2; ABCC2) is a targetable protein to confer multidrug resistance including the front-line drug oxaliplatin. MRP2 is one of the nine members of the MRP/ABCC sub-family, within a 48-member ABC transporter superfamily. MRP2 is predominantly expressed in the apical membranes of the epithelial cells and has been proved to extrude various substrates across cell membranes against the drug concentration gradient, which is consequently an “uphill” process that requires energy consumption using ATP hydrolysis (R. Biswas et al., 2019; Y. H. Cui et al., 1999; Myint et al., 2015). The MRP2 substrates include a structurally diverse range of compounds including phase II biotransformation products, non-modified drugs, as well as chemotherapeutic agents (Bugde et al., 2017; Robey et al., 2018b).

Accumulating evidence has proven endogenous overexpression of ABC transporters confers tumour resistance to anticancer drugs, and that tumour cells most likely develop multidrug resistance to majorly adopted drugs within a timeframe of only a few months of treatment (Fletcher et al., 2010; Robey et al., 2018b). MRP2-mediated tumour resistance is thus a critical factor that significantly reduces the efficacy of anticancer drugs and chemotherapeutic agents, and this is a major clinical limitation that needs to be overcome. Oxaliplatin, an anticancer drug for the treatment of metastatic colorectal cancer and other gastrointestinal malignancies, has been identified as an MRP2 substrate by using a membrane vesicle model (Myint et al., 2015). Endogenous overexpression of MRP2 decreases oxaliplatin accumulation in the gastrointestinal tumour cells and leads to resistance to oxaliplatin (R. Biswas et al., 2019; Myint et al., 2019).

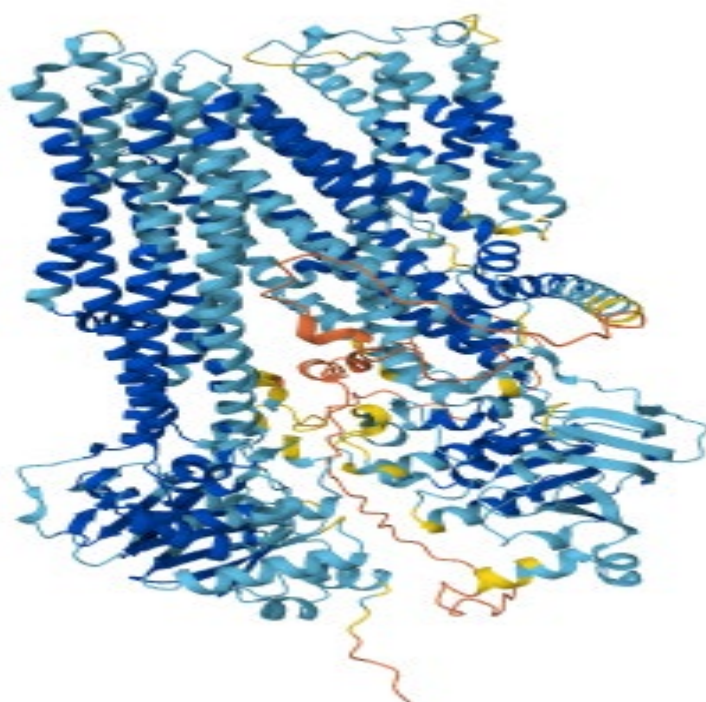


Figure 4- 1 The protein structure of MRP2 (ABCC2) is downloaded from AlphaFold and depicted in ribbon form.

Up to date, one of the major research areas have been to search for ABCC2 inhibitors/substrates that can reverse the effect of MRP2 on drugs. It has already been found that it may be possible to reverse multidrug resistance by inhibiting MRPs (Zhang et al., 2015). Myint et al. (2019) have discovered that the MRP2-mediated oxaliplatin transport out of tumour cells can be reversed when MRP2 is inhibited by myricetin or via siRNA knockdown. Biswas et al. (2019) were able to distinguish that oxaliplatin was a substrate of MRP2, therefore silencing MRP2 or inhibiting MRP2 at the binding sites may be able to successfully stop drugs from being pumped out of the cancer cells. Many inhibitors have been studied, such as derivatives of endogenous or natural products or miRNAs and other inhibitors also, but they have not yet been applied to clinical settings (Le et al., 2021; Zhang et al., 2015). Matsson et al. (2009) have also studied novel specific and general inhibitors of MRP2 and studied their specificities due to the limitation of intestinal absorption of drugs. Therefore, identification of potent inhibitors that can reverse this tumour resistance by blocking drug efflux function of MRP2 is critical in

enhancing the efficacy of chemotherapeutic agents and cancer therapy (Zhang et al., 2015).

Using computational approach such as *in silico* screening allows evaluation of the possible interactions between a transporter/receptor molecule and the binding affinity. Computational methods that dock ligands to proteins allow easier understanding of the binding mode and the orientation between the receptor and ligands that are preferred. Accumulating evidence has suggested this approach is both cost and time effective. The results can identify more stable complexes allowing prioritization and smaller range of molecules to concentrate on. Therefore, virtual screening could be the first step in identifying potent inhibitors. In this study, three-dimensional molecular docking of multiple ligands with MRP2 using an AutoDock Vina software was done to identify MRP2 inhibitors based on the binding affinity and hydrogen bond interactions.

4.2. Methods

This study was conducted *in silico*, using a free AutoDock Vina software that allows three-dimensional molecular docking. This software allows cost-effective prediction of ligand-protein binding affinity. Vina is known to produce more accurate results than AutoDock4 (AD4) regarding evaluation of ligand-binding affinity and thus, has been more popular than AD4 in recent years (Nguyen et al., 2020). The strong computing capabilities of Vina allow determination of binding affinities of small molecules to targets as well as binding pose prediction of larger substrates (Nguyen et al., 2020). Vina only requires the molecules structures and the search space specification such as the binding sites. It can significantly shorten the running time of the dockings by taking advantage of the CPU cores on the computer system. Trott and Olson (2010) explained that Vina can significantly enhance the binding mode prediction accuracies, in addition to achieving two orders of magnitude speed-up in comparison to AD4. Furthermore, Vina is able to calculate the grid maps automatically.

4.2.1. Protein preparation

The MRP2 protein structure (Primary Database Link: B2RMT8; UniProtKB: Q92887) was downloaded from ModBase in PDB format as used in a previous study by Biswas et al. (2021). Three structures were downloaded, each with different target regions, structure 1 with a target region between 636 and 865, structure 2 with target region between 967 and 1531, and structure 3 with a target region from 43 to 158. MGL tools were used to convert the PDB file to PDBQT format for protein preparation. For protein preparation prior to docking, the water molecules were deleted followed by repairing the missing residues and adding polar hydrogens. Kollman charges were added and checked for equal distribution. The prepared protein structures are shown in Figure 4-1.

4.2.2. Ligand preparation

Analogues of known MRP2 inhibitors were used in this study. Ligands used were ampelopsin; Butein; chrysin; dihydro-p-coumaric acid; hispidulin; homovanillic acid; matairesinol; pterostilbene; scutellarein; apigenin; biochanin A; curcumin; cyanidin; daidzein; EGCG; epicatechin; genistein; myricetin; naringenin; naringin; puerarin; quercetin; resveratrol; and silymarin. All the ligands were obtained from PubChem in SDF format which were converted to PDBQT format using MGL tools prior to docking study.

4.2.3. Docking runs

AutoDock Vina 1.1.2 was used to perform the docking of all the ligands with the receptor molecule. The grid box dimensions were -12.705, 49.079, and 19.303 for x, y, and z respectively and the sizes of x, y, and z were 40 x 40 x 40 with a spacing of 0.375 Å. The number of modes were set to 10 with an energy range of 4. Docking runs were launched

once the binding sites were defined and the receptor-ligand preparations were done, with the ligand and receptor interaction energy expressed as binding affinity (kcal/mol).

4.2.4. Data analysis

For the analysis of the Vina results, PyMOL and Proteins Plus was used to visualize the docked molecules and the interactions within the complex. The tool PoseView was used to generate two-dimensional diagrams of the protein-ligand complexes and to visualize the interactions between the ligand and the protein. The .out files generated from Vina runs were visualized using PyMOL, then the protein-ligand complexes were exported in PDB format. The PDB files created were then uploaded on Proteins Plus for further analysis.

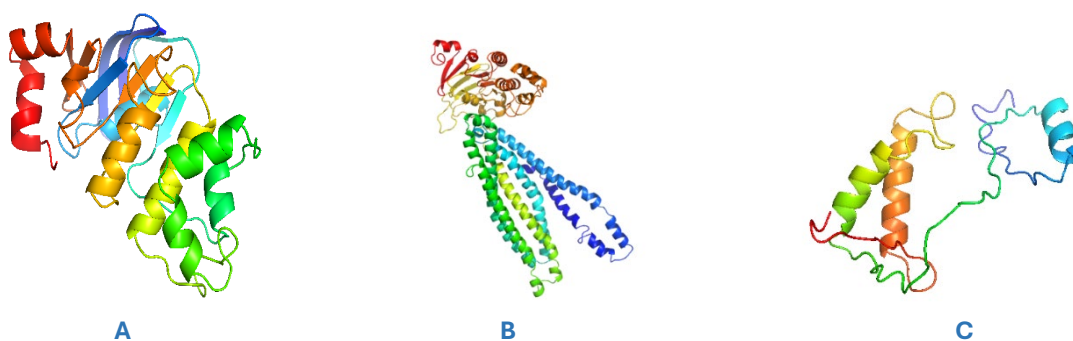


Figure 4- 2 Sub-structures of MRP2 molecule. A: Structure 1, target region 636-865; B: Structure 2, target region 967-1531; C: Structure 3, target region 43-158.

4.3. Results

4.3.1. Docking simulations

The binding affinities from the best binding modes for each ligand docked with structure 1, 2 and 3 are shown in Table 4-1. The binding affinities were shown to range from -6.0 kcal/mol to -9.2 kcal/mol. The ligands with the lowest binding affinities were chrysin, genistein, naringin, and silymarin as shown in Table 4-1. For structure 2, the docking runs

were repeated with the same ligands and consistent conditions. The binding affinities were overall lower than when docked with structure 1, with binding affinities for this set ranging from highest at -6.7 kcal/mol to lowest with a binding affinity of -10.6 kcal/mol. Ligands that produced lowest binding affinities were consistent to those with the lowest binding affinities when docked with structure 1 (Table 4-1).

Table 4- 1 Best Binding Modes of Ligands with MRP2 Structures 1, 2, and 3.

Ligand	Affinity (kcal/mol)		
	MRP2 structure 1	MRP2 structure 2	MRP2 structure 3
Ampelopsin	-7.9	-9.1	-8.9
Butein	-8.0	-9.9	-8.2
Chrysin	-8.7	-10.1	-9.1
Dihydro-p-coumaric acid	-6.3	-7.2	-6.1
Hispidulin	-8.3	-9.2	-9.2
Homovanillic acid	-6.0	-6.7	-6.1
Hydroxycaffeic acid	-6.8	-7.0	-6.8
Matairesinol	-7.6	-9.2	-9.0
Pterostilbene	-6.7	-9.6	-8.1
Scutellarein	-8.3	-9.1	-9.2
Apigenin	-8.2	-9.6	-9.4
Biochanin A	-8.2	-9.1	-8.9
Curcumin	-7.5	-9.0	-8.9
Cyanidin	-8.3	-9.6	-9.2
Daidzein	-8.4	-9.9	-8.9
EGCG	-8.5	-9.1	-9.3
Epicatechin	-8.3	-9.6	-9.2
Genistein	-8.7	-9.7	-8.9
Myricetin	-7.9	-9.1	-8.9
Naringenin	-8.2	-9.6	-9.4
Naringin	-9.2	-10.6	-9.0
Puerarin	-8.6	-9.3	-9.4
Quercetin	-8.2	-9.4	-9.4
Resveratrol	-7.4	-9.4	-8.3
Silymarin	-9.0	-9.9	-9.6

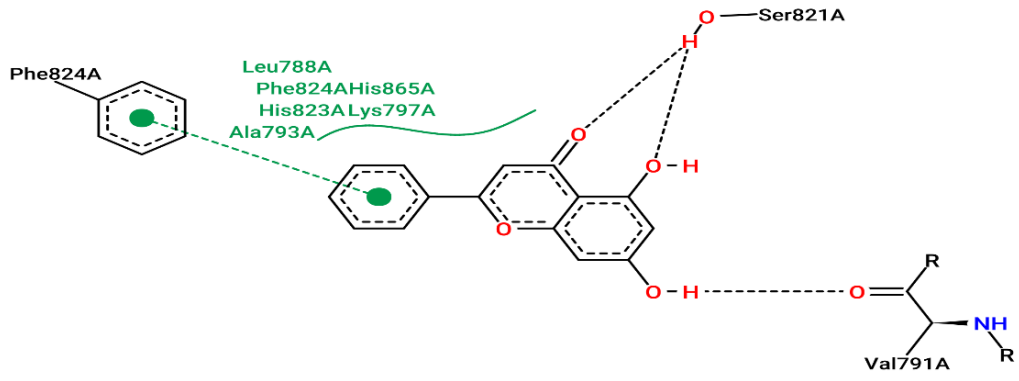
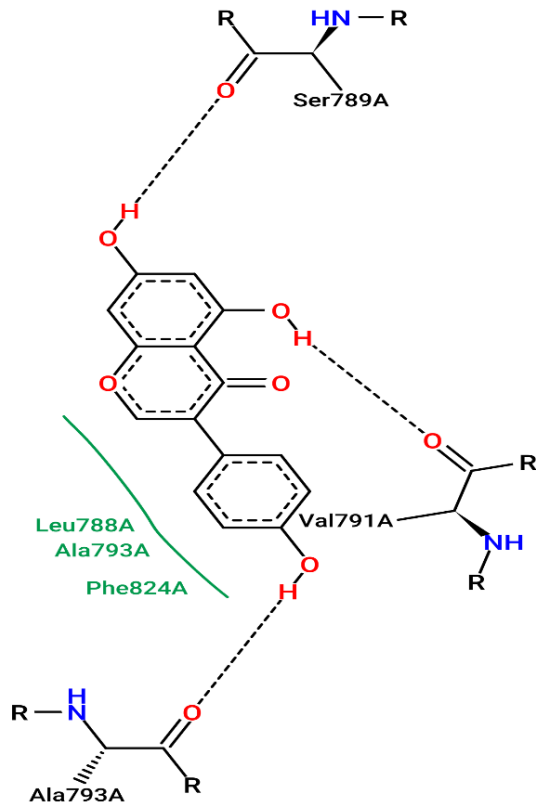
4.3.2. Interacting residues

As structures 1, 2, and 3 differed in that the target regions were different regions, it was expected to see different results specifically with the interacting residues and the type of interactions formed. PoseView analysis showed hydrogen bonds characterized by dashed

lines and spline segments were used for the representation of hydrophobic interactions between the ligand and protein. The ligand and receptor amino acids were shown as a structure diagram. The ligands with lower binding affinities compared to other ligands were chosen and analysed using Proteins Plus. Although the ligand-protein complexes with MRP2 structure 2 gave lower binding affinities, almost no hydrogen bonds were found to have interacted between the ligand and the protein. This was contrasting to the complexes created with structure 1, which had multiple hydrogen bonds within the complexes as shown in Table 4-2. In some of the complexes, π -stacking interactions were observed in addition to hydrogen bonding and hydrophobic bonding, as characterised in Figure 4-2.

Table 4- 2 Hydrogen Bond and Hydrophobic Bond of the Ligands with MRP2 Structures 1 and 2.

Ligand	MRP2 structure 1		MRP2 structure 2		MRP2 structure 3	
	Hydrogen bond	Hydrophobic interaction	Hydrogen bond	Hydrophobic interaction	Hydrogen bond	Hydrophobic interaction
	Amino acid		Amino acid		Amino acid	
Chrysin	SER821	LEU788	-	ILE1080	LEU49	LYS53
	SER821	PHE824		VAL1278	LEU49	ILE77
	VAL791	HIS865		PHE1084	GLY73	LEU49
		HIS823		ILE1064		LEU75
		LYS797				
	ALA793					
Daidzein			-	VAL1278	SER54	LYS53
				ILE1064	SER54	LEU49
				PHE1084	LEU75	LEU75
				LEU1060		LEU43
					PHE74	
Genistein	SER789	LEU788	-	VAL1278	LEU49	LEU49
	VAL791	ALA793		PHE1084	SER54	LYS53
	ALA793	PHE824		ILE1064		
				LEU1060		
Naringin	HIS865	PHE824	SER1098	VAL1142	TRP46	TRP123
	HIS820	HIS865	GLN1097	VAL1269	TRP46	
	SER821	LEU788	GLN1097		GLN47	
	SER821		GLN1138		LEU43	
	SER789		GLN1138		LEU75	
			VAL1142			
Silymarin	SER821	LEU788	VAL1142	ILE1262	ALA80	THR56
	SER789	PHE824	GLN1097	VAL1142	LEU78	LEU76
	ALA793	ALA793		TRP1102	LEU75	ARG55
		HIS865				

A**B**

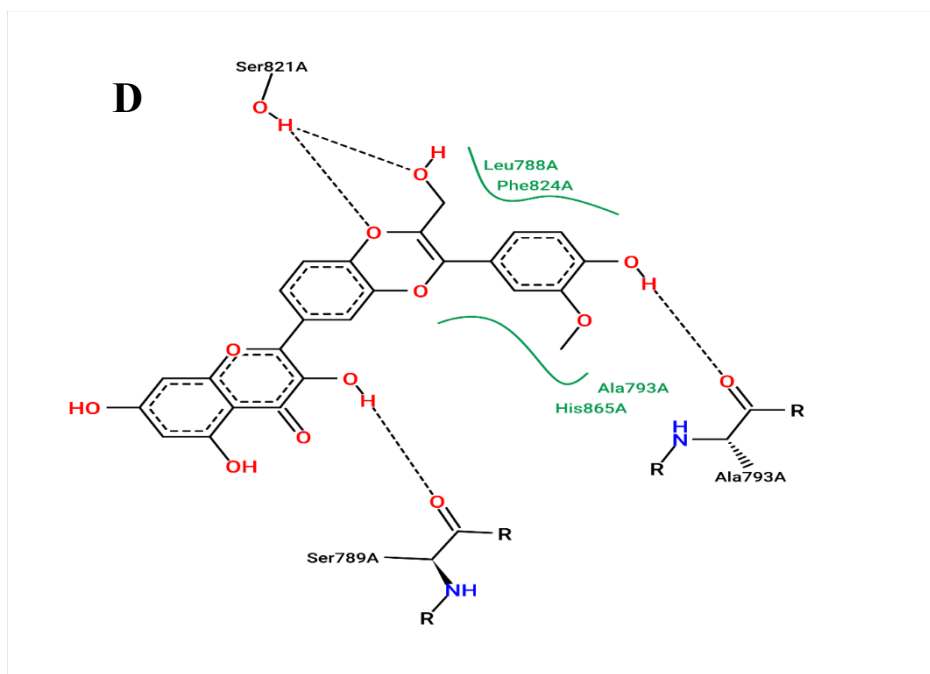
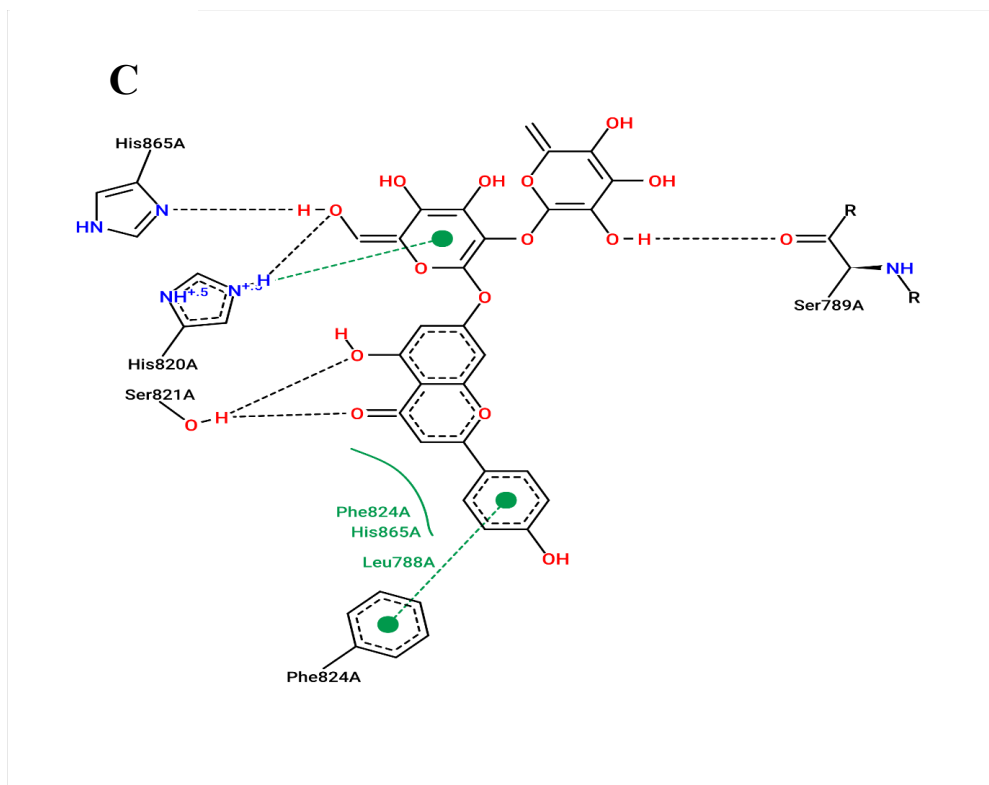
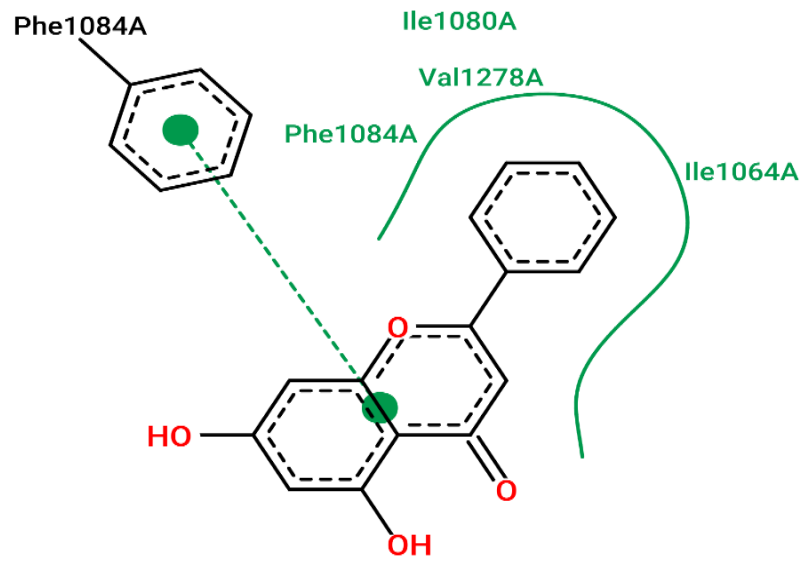
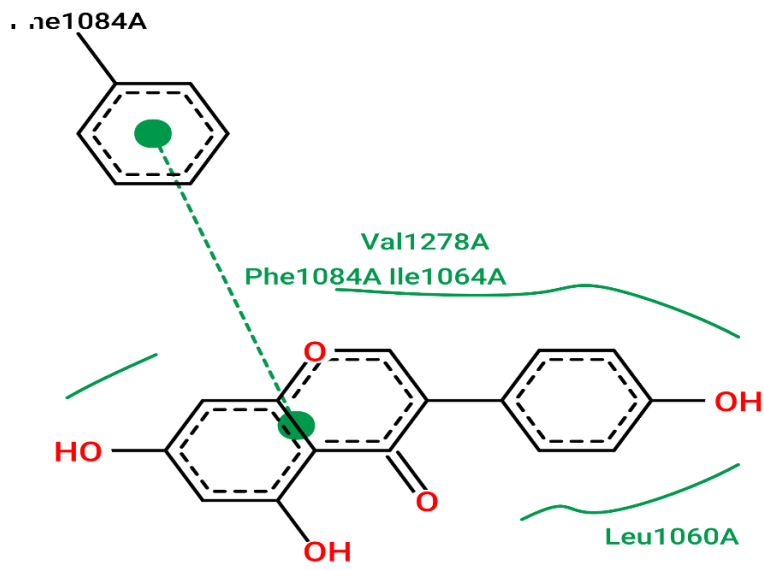


Figure 4- 3 Interactions within the MRP2 (substructure 1)-ligand (**A**, Chrysin; **B**, Genistein; **C**, Naringin; **D**, Silymarin) complex. Black dashed lines represent hydrogen bonds, green splines represent hydrophobic contacts, and green dashed lines represent π -stacking.

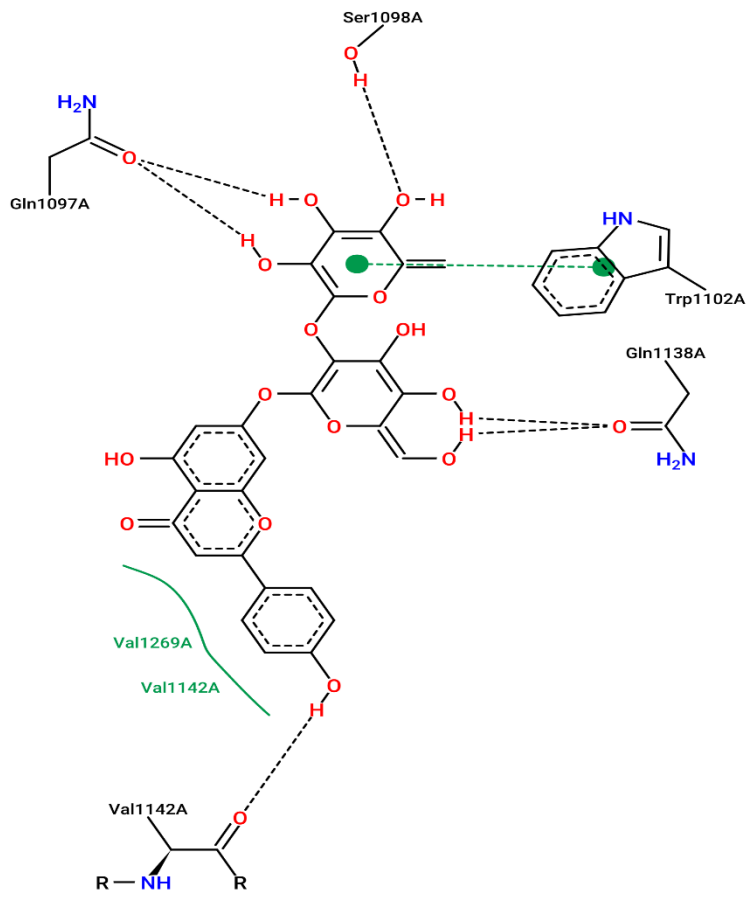
A



B



C



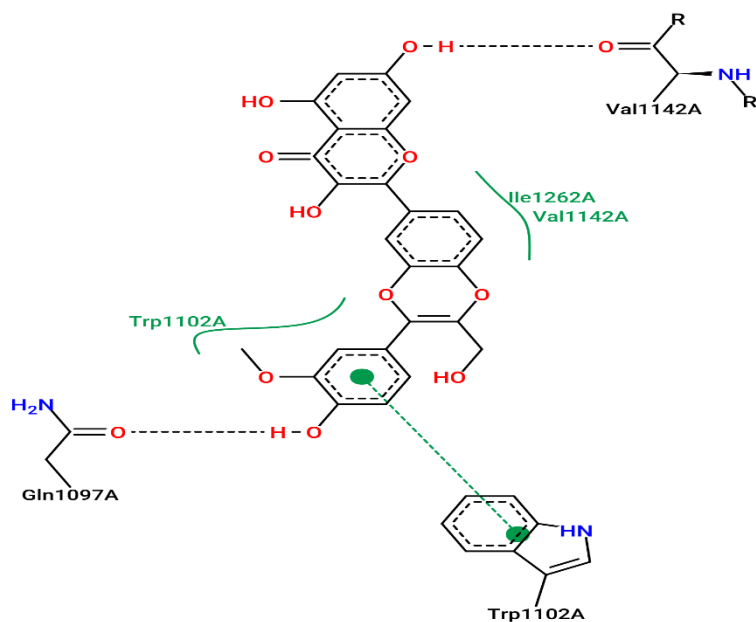
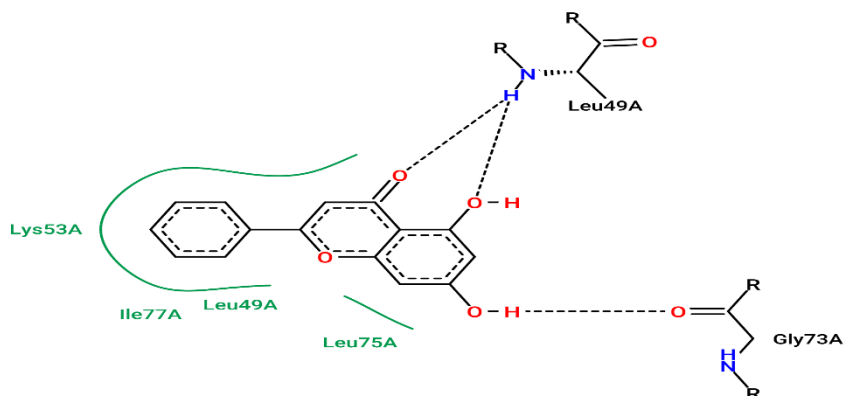
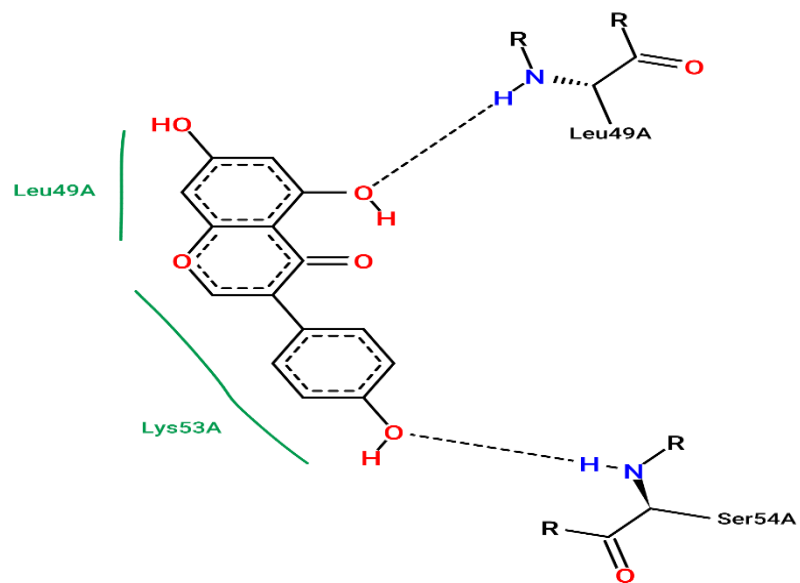
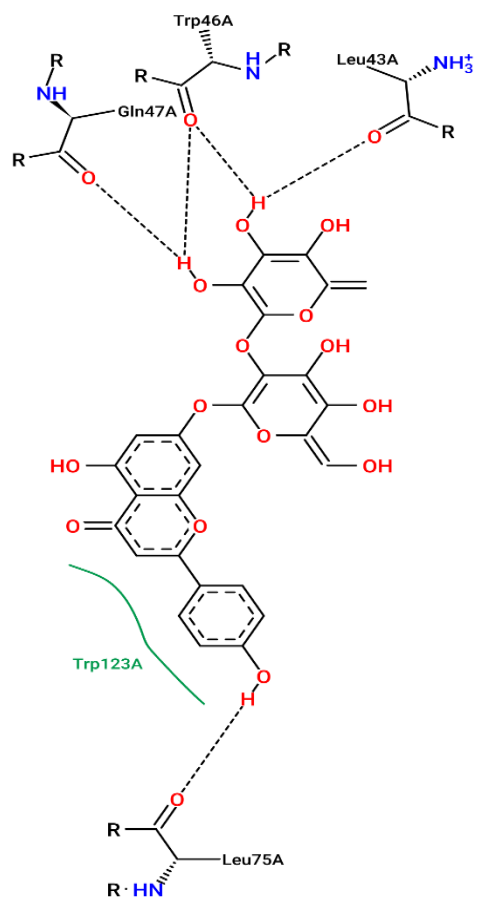
D

Figure 4- 4 Interactions within the MRP2 (substructure 2)-ligand (**A**, Chrysin; **B**, Genistein; **C**, Naringin; **D**, Silymarin) complex. Black dashed lines represent hydrogen bonds, green splines represent hydrophobic contacts, and green dashed lines represent π -stacking.

A

B**C**

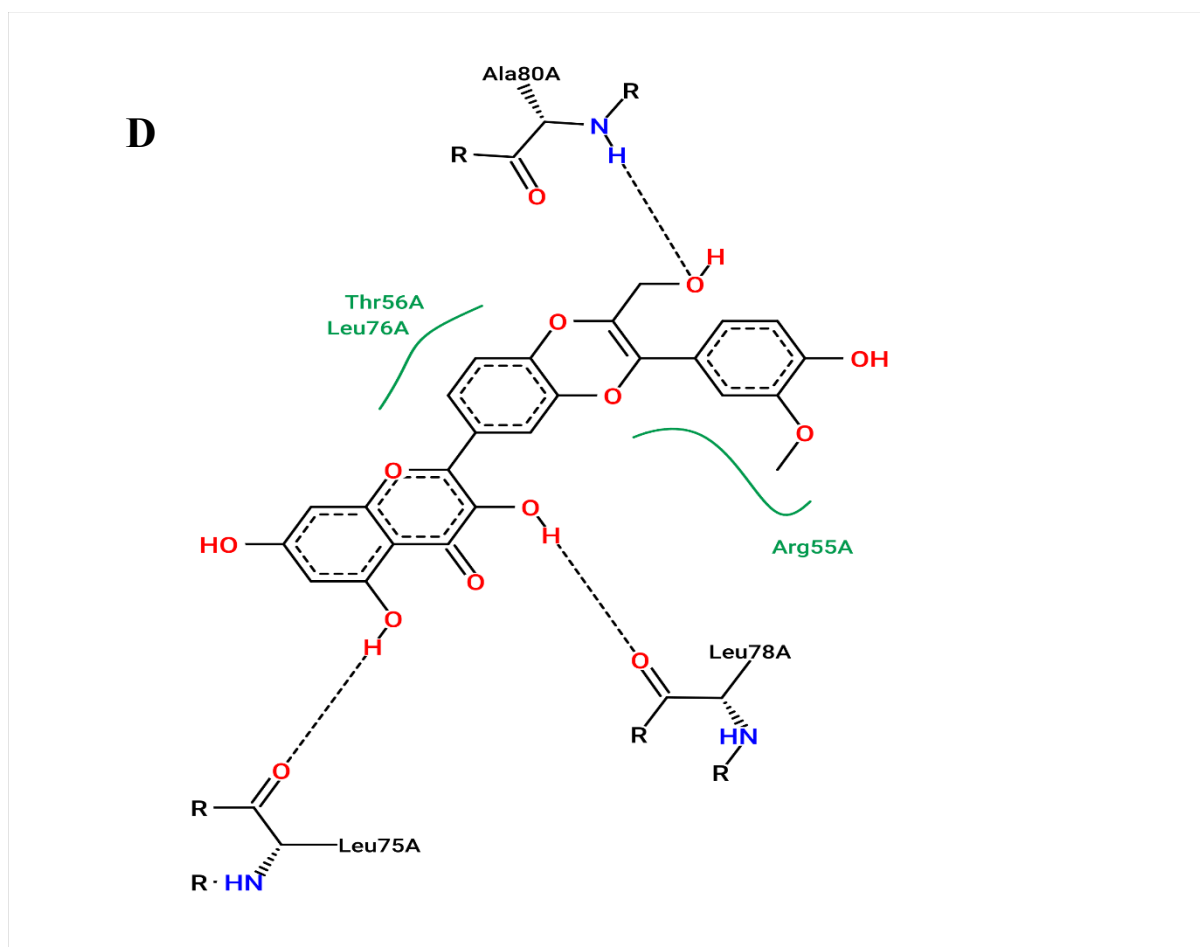


Figure 4- 5 Interactions within the MRP2 (substructure 3)-ligand (**A**, Chrysin; **B**, Genistein; **C**, Naringin; **D**, Silymarin) complex. Black dashed lines represent hydrogen bonds, green splines represent hydrophobic contacts, and green dashed lines represent π -stacking.

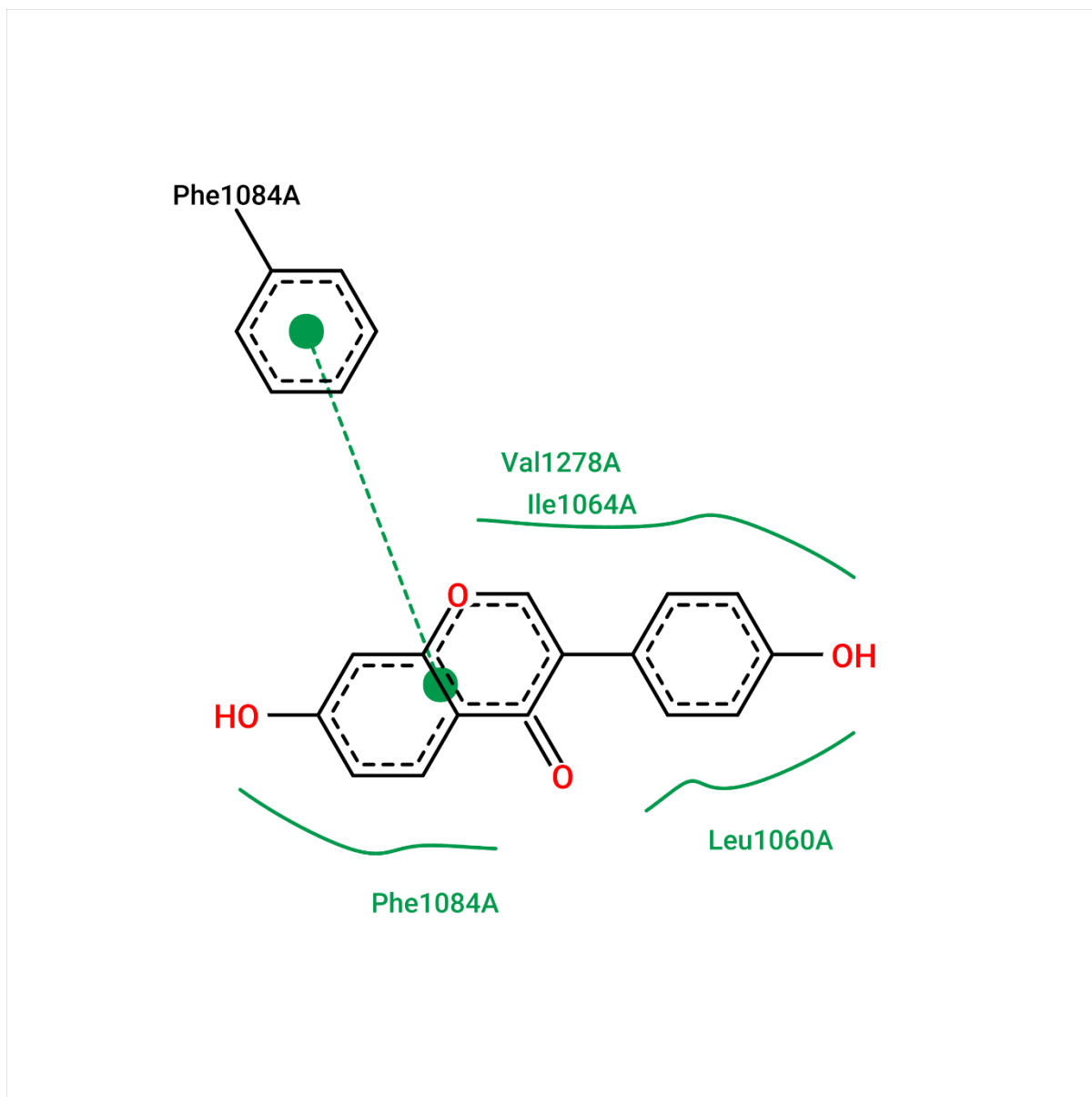


Figure 4- 6 Interactions within the MRP2 (substructure 1)-ligand (**Daidzein**) complex. Black dashed lines represent hydrogen bonds, green splines represent hydrophobic contacts, and green dashed lines represent π -stacking.

4.4. Discussion

4.4.1. Binding Affinity

Binding affinities represent how strong an interaction is, between molecules that are interacting. It is impacted by interactions that are non-covalent between two molecules such as between a ligand and a protein. Negative binding affinities are due to the free

energy of a favourable reaction, where energy is released because of the formation of the bond, or the interaction between the ligand and the protein. Therefore, the lower the binding affinity, the better the interaction is between the receptor-ligand complex. The docking results illustrated similar ligands to have lower binding affinities between complexes formed with MRP2 structure 1 and 2 as shown in Table 4-1. The ligands that showed lower binding affinities consistently between docking with the two structures in this study were chrysin, genistein, naringin, and silymarin. These ligands were observed to form potentially better interactions than myricetin with MRP2, which had a binding affinity of -7.9 kcal/mol. Myricetin is a well-known MRP2 inhibitor previously found to reduce the accumulation of oxaliplatin-derived platinum in membrane vesicles expressing MRP2 (Myint et al., 2015). A binding affinity of -7.9 kcal/mol was not the highest out of all the results, however it was an important finding that the four ligands mentioned previously produced much lower binding affinities. Furthermore, binding affinity cannot confirm whether a ligand is a potent inhibitor or not but requires further research and evaluations. Binding affinities is only one of the parameters that are important in the development of a potent inhibitor.

4.4.2. Non-Covalent Interactions

Non-covalent interactions are important factors in protein-ligand complexes and are always considered in the design process of ligands (Itoh et al., 2019). These interactions contribute to the binding affinity of a protein-ligand complex, and they can increase the binding energies with increased interactions (Shawon et al., 2021). Non-covalent interactions play a crucial role in stabilizing the protein-ligand complex by contributing to the stability of a ligand at the target site (Shawon et al., 2021). Hydrogen bonds have been known as facilitators of binding of protein-ligand complexes (Salentin et al., 2014). Hydrogen bonds have also been reported to enhance ligand binding affinity through displacement of water molecules that are protein-bound into the bulk solvent (Chen et al., 2016). Several hydrogen bonds have been observed in the selected complexes with

naringin showing the greatest number of hydrogen bond interactions formed in both structure 1 and 2 complexes. Chrysin, genistein, and silymarin also demonstrated hydrogen bonding primarily in structure 1 complex. Although the presence of hydrogen bonds along with hydrophobic interactions and π -stacking interactions do not result in determining a good binder, they are one of the parameters that determines binding affinities for the target site. The importance comes from that whether a ligand is stable in the protein-ligand complex or not is one of the important parameters in ligand development. The strength of hydrogen bonds is also important and can be altered with different environments. In a biological system, for good hydrogen bonding to be performed, the protein and the ligand need to be in the ionization state (Pantsar & Poso, 2018). Hydrophobic contacts were also observed along with π - π stacking interactions. These are also known to contribute to the binding affinities. Ferreira de Freitas and Schapira (2017) explained that small ligands with higher efficiency are more likely to be hydrophobic with the hydrophobic contacts being main contributors towards such efficiency. Small-molecule ligands being more optimized, polar bonds are more difficult to form, resulting in an increase of hydrophobic interactions (Ferreira de Freitas & Schapira, 2017). In this study, many hydrophobic bonds were observed in most protein-ligand complexes and along with hydrogen bonds, these are thought to play a crucial role in protein-ligand docking (Li et al., 2020).

4.4.3. Chrysin, Genistein, Naringin and Silymarin

In this study chrysin was among the ligands which showed lower binding affinities than other ligands. Chrysin has been studied for its anticancer effects in many different cancers including breast cancer, gastric cancer, and colorectal cancer in the past and previous animal studies showed MRP2 may potentially be involved in the disposition of chrysin and its conjugates (Walle et al., 2001; Ge et al., 2015, as cited in Mohos et al., 2020). Poor bioavailability is a major limitation of chrysin, and it has been found that it was due to efflux transporters including MRP2 (Gao et al., 2021). In an *in vitro* study done by Mohos

et al. (2020), chrysin and its conjugates in the sulfate and glucuronide form, has been observed for their activity against cytochrome P450 enzymes, organic anion transporting polypeptides (OATPs) and ATP binding cassette transporters. Chrysin's conjugates were found to have strong inhibitory effects on some OATPs and the breast cancer resistance protein (BCRP) and was found to be a weaker inhibitor of MRP2 than its conjugate chrysin-7-glucuronide. These results that chrysin's conjugates are transported by ABC transporters such as BCRP and MRP2, and the inhibitory effects it had on MRP2, the potential as an inhibitor lies consistent with the results from this study (Mohos et al., 2020).

Another ligand that showed potential as MRP2 inhibitor was genistein, with a binding affinity of -8.7 equal to chrysin and very similar residues involved in the non-covalent bond formations. In a study done by Schexnayder and Stratford (2016), where it was observed that in presence of genistein, MRP2-mediated 5 (and 6)-carboxy-2',7'-dichlorofluorescein (CDF) transport was increased. Genistein is also known to activate the pregnane-X-receptor which regulates ABC transporter expression (Rigalli et al., 2016). However, Rigalli et al. (2015) found MRP2 induction at translational and transcriptional phases in the presence of 1.0 and 10 μM genistein. However, *in vivo* studies have shown that genistein inhibits MRP2-mediated hepatobiliary secretion of anionic substrates suggesting the lower metabolic activity *in vitro* is the reason behind conflicting results (Schexnayder & Stratford, 2015). Naringin is already known to inhibit human organic cation transporting protein (OATP) 1A2 (Briguglio et al., 2018). In addition, naringin has been found to also inhibit P-glycoprotein mediated transport as well as cytochrome P450 3A4 mediated metabolism (Alvarez et al., 2010). Although naringin and its inhibitory effects on MRP2 are not clearly known, its aglycone naringenin has been found previously to be secreted by MRP2 (Nait Chabane et al., 2009). This suggested naringin could be a substrate of MRP2 also but is worth studying further as its inhibitory effects against OATP1A2 are known. Similarly, silymarin has been studied widely for its potential but limited due to low bioavailability caused MRP2-mediated transport of its

major active flavonolignan silybin (Xie et al., 2019). Again, this suggested silymarin may be a substrate of MRP2, hence the binding affinity as observed.

4.4.4. Limitations

The results from this study simply demonstrate whether the selected ligands can potentially bind stably in the target site or not. Further studies such as wet lab studies are required to identify potent inhibitors out of the docked ligands. Due to Covid-19, wet lab validations of the virtual screening results could not be done, thus only literature-based validations were possible. Literature review-based validations can only give suggestions, and proper validations are still required.

4.4.5. Recommendations for future studies

To further build on the current findings, wet lab validations may be the first step. Heterogeneous expression systems perhaps using human embryonic kidney 293 cells (HEK293) overexpressing MRP2 may be adapted to identify whether ligands that showed low binding affinities in this study can inhibit or reverse the MRP2-mediated transport of chemotherapeutic drugs.

4.5. Conclusion

The AutoDock Vina software was a cost-effective method that allowed screening of potential inhibitors of MRP2, producing valuable information about the possible ligand-protein complexes. Potential inhibitors were identified including chrysin and genistein, as well as opening new possible research directions for ligands that have not been studied in-depth regarding their interaction and activity with MRP2.

Chapter 5 Modulatory Effect of Chrysin on ABCC2 in Isogenic HEK293 Cells

5.1. Introduction

Cell-based models have been instrumental in previous *in vitro* studies examining the role of transporters in the pharmacology of anticancer drugs (An et al., 2024; Kim et al., 2024; J. J. Liu et al., 2012). Unlike membrane vesicle models, cell-based systems allow for the investigation of how drug transport mechanisms influence cellular sensitivity to anticancer agents. Researchers have utilized drug-resistant cancer cell lines as well as genetically engineered cell lines that overexpress specific membrane transporters (Giacomini et al., 2010). The use of genetically modified cell lines, particularly those that overexpress specific transporter genes, offers a controlled environment to study the function of the transporter of interest while minimizing the impact of other transport mechanisms. HEK293 cells, which have been genetically modified to overexpress a particular membrane transporter, are frequently employed in these studies due to their ease of manipulation, high transfection efficiency, and straightforward maintenance (Y. Cui, J. König, et al., 1999; Graham et al., 1977; Jong et al., 2011; Y. Li et al., 2011). MRP2 overexpressing cell lines have been used in several studies to explore the transport mechanisms and substrate specificities of MRP2 (F et al., 2020; Huisman et al., 2005; Pär Matsson et al., 2009; Zelcer et al., 2003).

In this study, we explored the role of MRP2 (ABCC2) in modulating the intracellular accumulation of platinum and the sensitivity of cells to oxaliplatin-induced cytotoxicity. We utilized a HEK293 cell line genetically engineered to overexpress MRP2 (HEK-ABCC2) and compared its behaviour to that of its unmodified parental counterpart (HEK293). Although numerous studies have connected MRP2 expression with decreased intracellular platinum accumulation and increased resistance to cisplatin across various models—including MRP2-overexpressing cell lines, human cancer cell lines, animal models, and clinical tumour samples (AD et al., 2006; F et al., 2020; Huang et al., 2024; K et al., 2002; K et al., 2023; T. Liu et al.,

2012; Mahapatra et al., 2022a, 2022b; Qu et al., 2020; W et al., 2016; Wen, Goedken, et al., 2014), similar data for oxaliplatin remain scarce and often inconsistent (Beretta et al., 2010; Z. Liu et al., 2010; Mirakhorli et al., 2013; Mirakhorli et al., 2012; Mohn, Häcker, et al., 2013; C. Mohn, G. V. Kalayda, H. G. Häcker, et al., 2010; Theile et al., 2009). Previous research has established a link between high MRP2 expression and resistance to drugs like vincristine, etoposide, and cisplatin. For example, cisplatin-resistant human cancer cell lines with elevated MRP2 expression have demonstrated reduced cisplatin accumulation (Fujii et al., 1994; Nakagawa et al., 1993; Taniguchi et al., 1996). Additionally, one study found that silencing the MRP2 gene in a human ovarian cancer cell line enhanced both cisplatin accumulation and sensitivity to the drug (Ma et al., 2009). In another study, Cui et al. demonstrated that resistance to etoposide, cisplatin, and doxorubicin was linked to MRP2 overexpression using MRP2-overexpressing cell lines such as HEK-MRP2 and MDCKII-MRP2 (Y. Cui, J. König, et al., 1999). Silencing MRP2 in human liver, ovarian, and nasopharyngeal cancer cell lines resulted in lower IC50 values for cisplatin, vincristine, and doxorubicin, indicating that MRP2 contributes to resistance against these drugs (Folmer et al., 2007; Kool, de Haas, Scheffer, et al., 1997; Ma et al., 2009; Xie et al., 2008). Several earlier studies have used 5(6)-carboxy-2,'7'-dichlorofluorescein (CDCF) as a model substrate to assess MRP2 transport activity (Colombo et al., 2012; Colombo et al., 2013; Heredi-Szabo et al., 2008; Siissalo et al., 2009; Zamek-Glisczynski et al., 2003). In many cases, 5(6)-carboxy-2,'7'-dichlorofluorescein diacetate (CDCFDA) is utilized because CDCFDA, a non-fluorescent precursor, can diffuse passively into cells and is subsequently metabolized into the fluorescent CDCF, which cannot permeate cell membranes and is only extruded by the MRP2 transporter.

The primary objective of this chapter was to assess how chrysin influences MRP2's role in the cellular accumulation of oxaliplatin-derived platinum and its effect on sensitivity to oxaliplatin-induced growth inhibition. This was carried out using a HEK293 cell line stably transfected to overexpress the *ABCC2* gene, encoding the MRP2 membrane transporter protein (HEK-ABCC2 cells). Given that this cell line had not been thoroughly characterized in prior studies, we first compared its phenotypic traits with those of its isogenic unmodified parental line (HEK293 cells). Following this, we examined the differences between HEK-ABCC2 and HEK293 cells regarding

platinum accumulation and sensitivity to oxaliplatin-induced growth inhibition, along with the inhibitory effects of chrysin on these processes. Additional exploratory studies were conducted to investigate the expression of other membrane transporter genes in both HEK-ABCC2 and HEK293 cells.

5.2. Materials and Methods

5.2.1. Chemicals and equipment

The sources of chemicals used in this study and the preparation details of the stock solutions were as mentioned in section 2.1.

5.2.2. Cell culture and cell surface ABCC2 immunostaining

HEK293 parental (HEK293) and MRP2 over-expressing HEK293 (HEK-ABCC2) cell lines were used in this study. The sources and cell culture conditions of these cell lines were described in section 2.2.

The cell surface expression of ABCC2 protein in isogenic HEK cell pairs was assessed by flow cytometry. Cells were harvested and counted at around 90% confluence. An aliquot of 100 μL of ice-cold PBS containing 1% paraformaldehyde (PFM; fixative) was used to resuspend cells (1×10^6). An incubation for 15 min at 4 $^{\circ}\text{C}$ is to fix the membrane proteins and prevent the modulation and internalization of surface antigens which could cause a loss of fluorescence intensity. After fixation, cells were washed twice with ice-cold PBS containing 0.1% saponin and 0.1% sodium azide and centrifuged at $400 \times g$ for 5 min. An aliquot of 100 μL ice-cold PBS containing 0.1% saponin was adopted to resuspend the cells and incubated for 15 min at 4 $^{\circ}\text{C}$ to resolve and remove cholesterol and increase membrane permeabilization. An aliquot of 200 μL of 5% BSA in PBS was then added to cells followed by incubation for 15 min at room temperature to prevent nonspecific binding of antibodies. After blocking, cells were washed twice with ice-cold PBS

containing 0.1% saponin and 0.1% sodium azide and centrifuged at $400 \times g$ for 5 min. 100 μL of MRP5 Monoclonal Antibody (M5I-1) in ice-cold diluted solution (2% BSA in PBS) was applied to cells. A mouse IgG2 α Isotype Control group was added to estimate the background staining, which could be caused by Fc receptors on target cells, nonspecific interactions with cellular proteins, carbohydrates, lipids and cell autofluorescence. After primary antibody incubation for 60 min at 4 °C in dark., cells were washed twice with ice-cold PBS containing 0.1% saponin and 0.1% sodium azide and centrifuged at $400 \times g$ for 5 min. Cells were then incubated with Goat Anti-mouse IgG H&L (DyLight® 488) in 100 μL ice-cold diluted solution for 60 min at 4 °C in dark. After secondary antibody incubation, cells were washed twice with ice-cold PBS containing 0.1% saponin and 0.1% sodium azide and centrifuged at $400 \times g$ for 5 min. Cells were ultimately resuspended with ice-cold PBS containing 1% PFM to a final volume of 200 μL in Beckman Coulter Blue Test Tubes. The flowcytometric analysis was immediately proceeded by using MoFlo™ XDP flow cytometer (Beckman Coulter, Inc., CA). The fluorescence intensity was determined with the fluorescence emission at 525 nm using 488 nm excitation. The geometric mean value of fluorescence intensity obtained from flow cytometry was analyzed by using Kaluza Analysis Software and the statistic analysis by PRISM® GraphPad 8.

5.2.3. Western blotting on HEK-ABCC2 and HEK293

Western blotting analysis of MRP2 protein on HEK293 and HEK-ABCC2 cell lines are conducted to verify differences in MRP2 expression level between these two cell lines. To conduct this experiment, cells were seeded in T-75 till they were fully confluent. The western blotting method details were described in section 2.5.

5.2.4. Cell viability assays

5.2.4.1. *Drug treatment*

For the assessment of effects on cell growth of drugs of interest, HEK293 cells were exposed to drugs for designated times, followed by replacement of the drug-containing medium with the

normal growth medium until 72 h after the initial exposure to the drugs. Varying concentrations of drugs and incubation periods were used for different experimental designs as summarized below in Table 5-1.

Table 5- 1 Drug treatments and incubation time used in cell viability assays

Experiment design	Drug Name	Drug concentration	Incubation periods
Cellular sensitivity to oxaliplatin	Oxaliplatin	0-200 μ M	72 hours
Cytotoxic effects of chrysin alone	Chrysin	0-60 μ M	72 hours
Cytotoxic effects of chrysin and oxaliplatin combination	Chrysin	0, 5, 10, 60 μ M	45 mins preincubation and 2 hours coincubation
	Oxaliplatin	0-200 μ M	2 hours coincubation

5.2.4.2. Cell Viability Assay (MTT assay/ Presto-Blue) with Chrysin

Presto-Blue assay was used to measure the number of viable cells in these experiments, and the details of the assay was mentioned in section 2.3. Prior to the growth inhibition experiments, seeding density experiments for each cell line were undertaken to determine the optimal seeding density for further experiments and to check the optical density values detected over the seeding density changes. To verify the assay accuracy, seeding eight increasing concentration HEK-ABCC2 cells (0-30000 cells/well) in 96 well plates with triplicate data set, standard curve was produced as Figure 5-1. Drug concentrations and incubation times were varied depending on the studies as shown in Table 5-1.

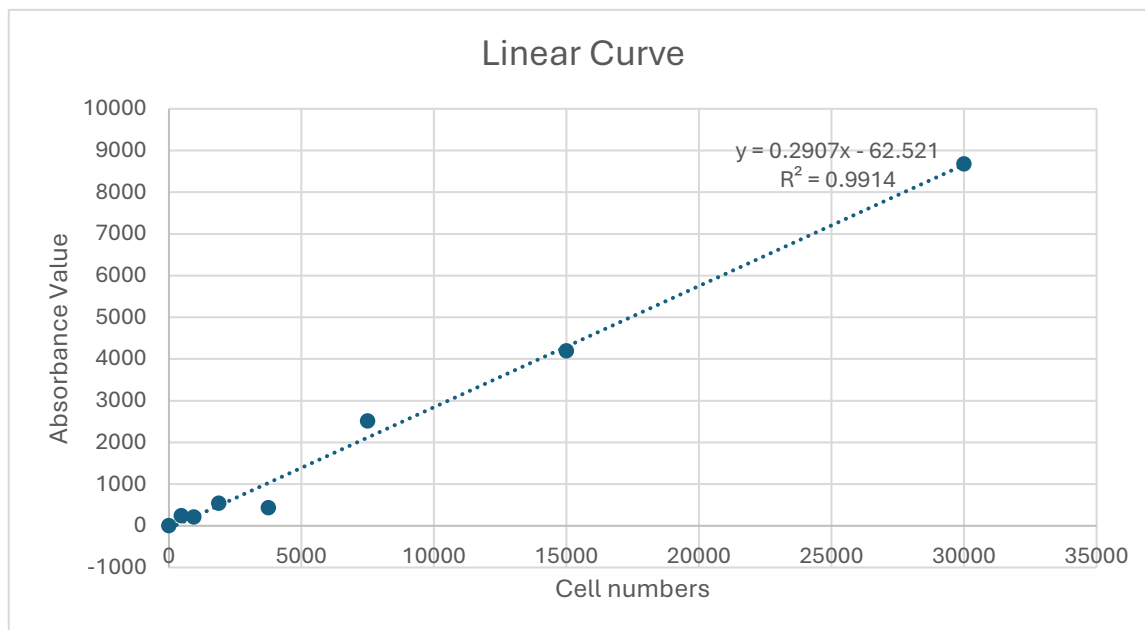


Figure 5- 1 Presto-Blue cell viability assay standard curve

In the Presto-Blue cell viability assay, HEK-ABCC2 cells were seeded in 96 well plates with eight increasing concentrations (0, 468.75, 937.5, 1875, 3750, 7500, 15000, and 30000 cells/well) allowing them to adhere to the well surface over 16 – 24-hour incubation in normal drug-free complete growth medium. After sample preparation, remove all of cell culture medium in each well and add 100 μ L of PrestoBlue™ reagent (1 in 10 dilutions in HBSS). Incubate for 60 minutes at 37°C in a cell culture incubator, protected from direct light. After incubation, record results using a fluorescence plate reader with the values of Excitation 560 nm/ Emission 590 nm. Linear curve-fitting and corresponding equations are shown.

5.2.5. CDCF [5(6)-carboxy-2,'7'-dichlorofluorescein] accumulation and efflux assays

CDCF was employed as a substrate to assess MRP2 transporter activity in HEK-ABCC2 and HEK293 cell lines. The non-fluorescent and cell-permeable precursor, CDCFDA [5(6)-carboxy-2,'7'-dichlorofluorescein diacetate], was utilized in these assays. Detailed procedures for this assay were mentioned in Section 2.8.1.

5.2.6. Statistical analysis

Data analysis was mentioned in section 2.10.

5.3. Results

5.3.1. Characterisation of HEK-ABCC2 cells

A HEK293 cell line stably transfected with the gene encoding human MRP2 (ABCC2), referred to as HEK-ABCC2 cells, alongside un-transfected parental HEK293 cells, was employed to investigate the role of MRP2 in the cellular transport of oxaliplatin and screen potential MRP2 inhibitors. Since the HEK-ABCC2 cell line had not been thoroughly characterized prior to this study, its functional expression of MRP2 was assessed in comparison to HEK293 cells. To detect MRP2 protein expression, cells were cultured on T-75 flasks and then incubated with a primary anti-MRP2 antibody, followed by a fluorescently secondary antibody. Flow cytometric analysis was used to measure the immunostaining, revealing the expression of MRP2 protein in HEK-ABCC2 cells is around 2.5-fold higher than in HEK293 cells (Figure 5-2). These findings were further confirmed through Western blot analysis, verifying the specific expression of MRP2 in the HEK-MRP2 cell line (Figure 5-3).

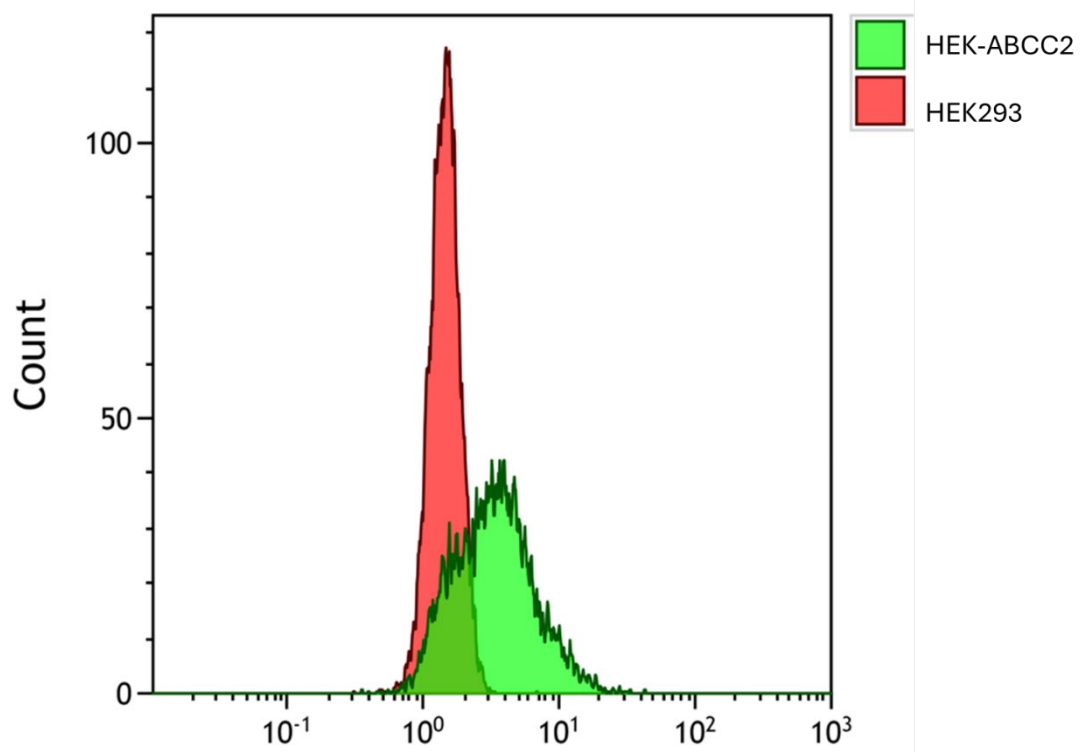


Figure 5- 2 Immunostaining of MRP2 protein was detected in the cytoplasmic and membrane regions of HEK-ABCC2 cells, but not in HEK293 cells.

HEK293 and HEK-MRP2 cells were cultured on T-75 flasks and then incubated with a primary anti-MRP2 antibody, followed by a fluorescently secondary antibody. Cells were ultimately resuspended with ice-cold PBS containing 1% PFM to a final volume of 200 μ L in Beckman Coulter Blue Test Tubes. The flow cytometric analysis was immediately proceeded by using MoFlo™ XDP flow cytometer (Beckman Coulter, Inc., CA). The fluorescence intensity was determined with the fluorescence emission at 525 nm using 488 nm excitation. The geometric mean values of fluorescence intensity were analyzed by using Kaluza Analysis Software and the statistic analysis by PRISM® GraphPad 6.

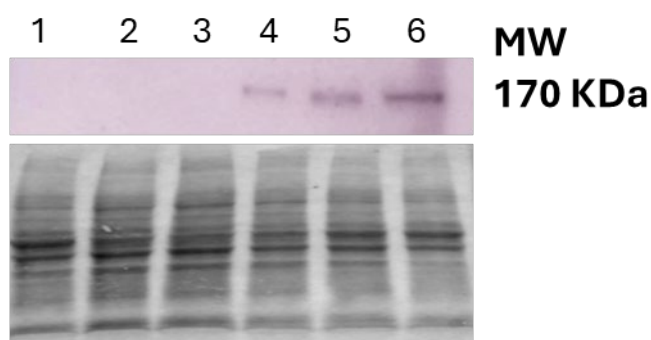


Figure 5- 3 Western blot image of MRP2 in HEK293 and HEK-ABCC2 cell lines

Standard ladder and HEK293 or HEK-ABCC2 cell samples were loaded into gel cassette wells as shown in the figure. After SDS-PAGE and proteins transferring from gel to membrane, the total protein stain (as shown in the bottom panel) was obtained as a loading control. The destained membrane was then incubated with antibodies (with 1:400 anti-MRP2 antibody (primary antibody), and 1:1000 anti-Rat IgG2a-HRP Monoclonal (secondary antibody)). The membrane was soaked in Prepare Pierce™ ECL Western Blotting Substrate working solution for 10 mins. ImageQuant LAS 500 was used for chemiluminescent western blotting imaging.

5.3.2. The effect of chrysin on inhibition of MRP2 transporter

5.3.2.1. The effect of chrysin on cell cytotoxicity

HEK-ABCC2 and HEK293 cells were pretreated with chrysin (0, 5, 10, 60 μ M) for 45 mins, followed by coincubation with different concentrations of oxaliplatin (0-200 μ M) for 2 hours. After coincubation, cells were incubated in drug free complete medium for 72 hours, and then was

assessed for cell viability by using Presto-Blue assay. The results demonstrated that chrysin enhanced oxaliplatin-induced growth inhibition in HEK-ABCC2 cells, while it had no significant effect on HEK293 cells (Figure 5-4 and 5-5). The IC-50 values for oxaliplatin in HEK-ABCC2 cells decreased by around 10% in the presence of chrysin. In contrast, HEK293 cells exhibited lower IC-50 values for oxaliplatin compared to HEK-ABCC2 cells, but these values remained unchanged with 10 μ M chrysin treatment, and even slightly increase IC-50 values for treatment with low concentration of chrysin (5 μ M) (Figure 5-6).

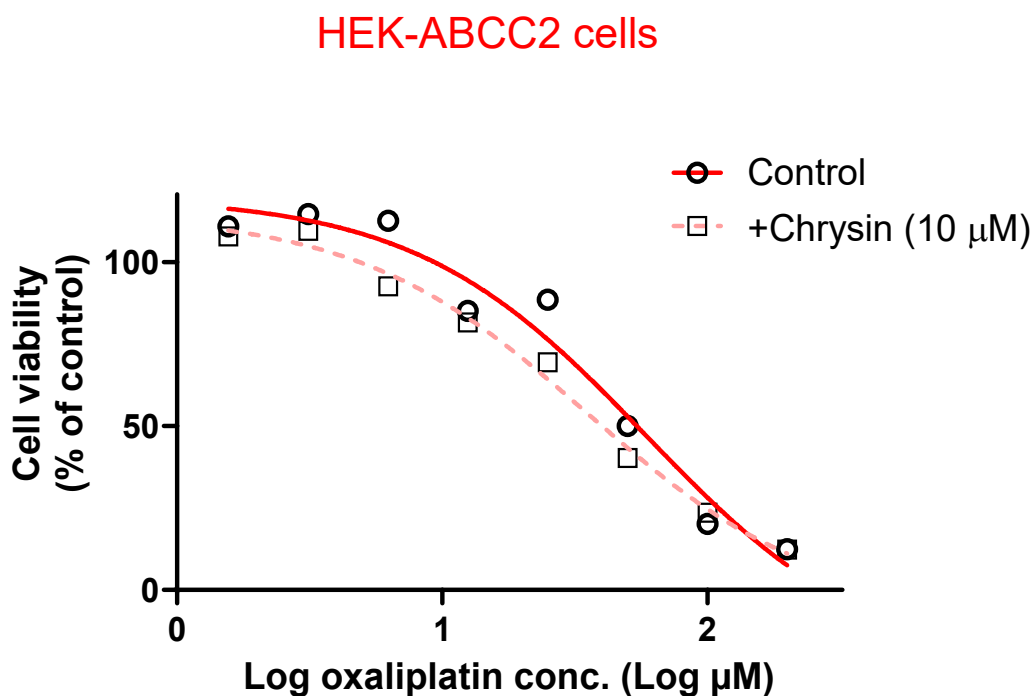


Figure 5- 4 Cell viability value of oxaliplatin or chrysin and oxaliplatin combination on HEK-ABCC2 cell lines

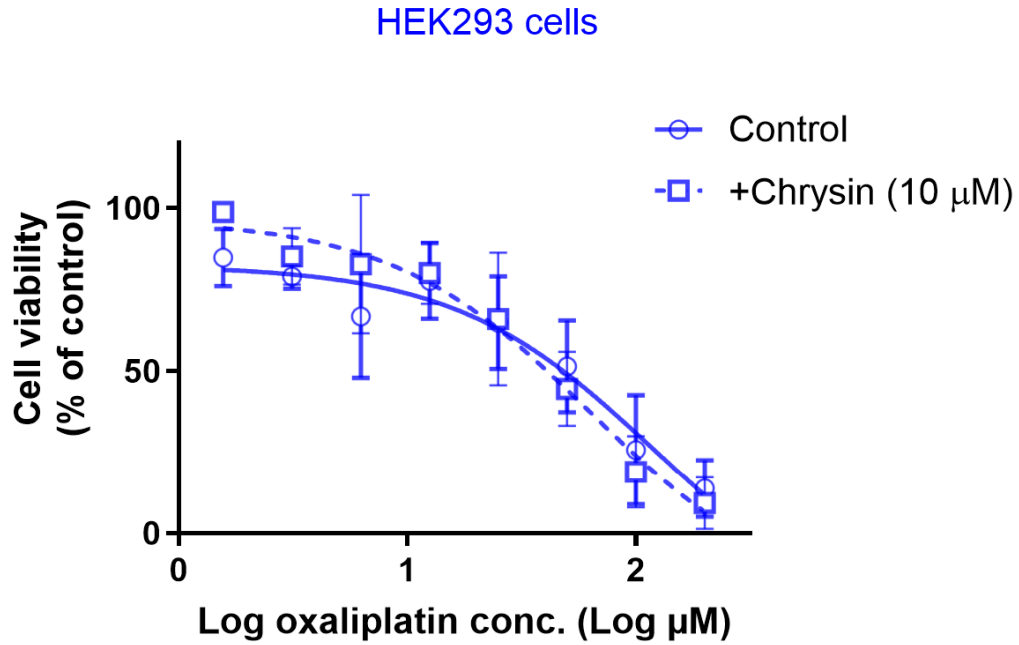


Figure 5- 5 Cell viability value of oxaliplatin or chrysin and oxaliplatin combination on HEK293 cell lines

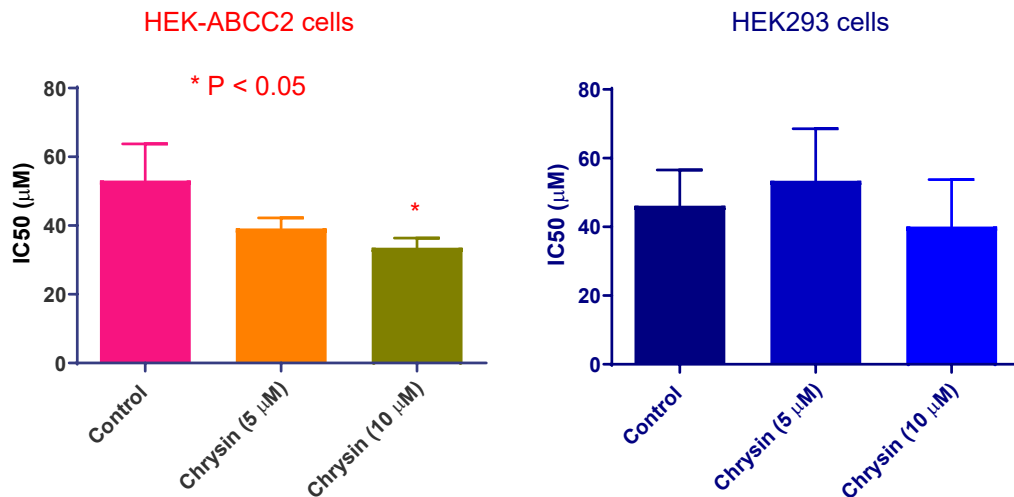


Figure 5- 6 IC₅₀ value of oxaliplatin or chrysin and oxaliplatin combination on HEK-ABCC2 and HEK293 cell lines

HEK-ABCC2 and HEK293 cells were pretreated with chrysin (0, 5 and 10 μM) for 45 mins, followed by coincubation with different concentrations of oxaliplatin (0-200 μM) for 2 hours. After coincubation, cells were incubated in drug free complete medium for 72 hours, and then was assessed for cell viability by using Presto-Blue assay. The results demonstrated that chrysin enhanced oxaliplatin-induced growth inhibition in HEK-ABCC2 cells, while it had no significant

effect on HEK293 cells. Data are presented as the mean and SEM of IC₅₀ of oxaliplatin in cells from two independent experiments. Asterisks is P values (*, P<0.05) from Dunnett's post hoc test that followed one-way ANOVA for comparisons of HEK-MRP2 and HEK293 cell lines samples to negative control sample.

From figures above, it is obviously showing that, chrysin significantly increased the sensitivity to an MRP2 substrate drug oxaliplatin in HEK-ABCC2 but not in HEK293 cells. The low chrysin concentration which is only 10 μ M is much more effective than the concentration used of myricetin which is 60 μ M in previous study from our team. This found is showing that chrysin is a better MRP2 inhibitor. To verify this hypothesis, further experiments were planned to be done.

5.3.2.2. The effect of Chrysin on CDCF accumulation and efflux

To investigate the role of MRP2 in the cellular accumulation of platinum derived from oxaliplatin, HEK293 and HEK-MRP2 cells were pretreated with chrysin (0, 10, 60 μ M) for 45 mins, and then were co-incubated with oxaliplatin (200 μ M) for 2 hours. Cells were then incubated in drug free complete medium for another 72 hours. The accumulation of CDCF [5(6)-carboxy-2,'7'-dichlorofluorescein] was performed by incubating the 0.25 ml of cells with addition of an aliquot of 0.5 μ l of 2.5 mM of CDCFDA [5(6)-carboxy-2,'7'-dichlorofluorescein diacetate] for 30 minutes. After incubation, 3 ml of ice-cold PBS was immediately added to stop the accumulation, and the cells were centrifuged at 250 g for 3 minutes. The supernatant was removed, and a second wash was performed. For further processing, the cell pellets were resuspended in 200 μ l of 0.5% Tween 20, mixed thoroughly by pipetting, and incubated for 15 minutes at room temperature, protected from light by aluminum foil. The resulting cell lysates were transferred to a black 96-well plate, and fluorescence intensity was measured using a fluorimeter at a wavelength of 495/520 nm. Additionally, the protein levels of the samples were assessed using a DC protein assay, with each sample run in duplicate.

CDCF accumulation One-way ANOVA

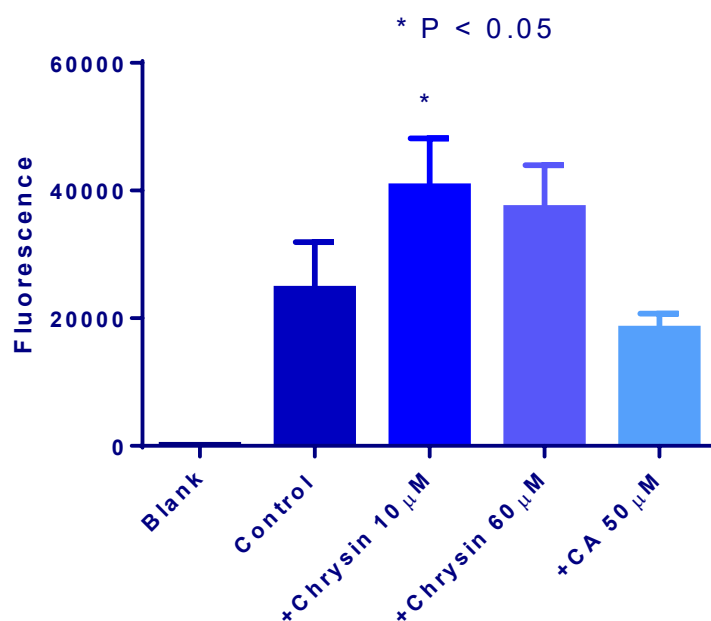


Figure 5- 7 A pilot study of CDCF accumulation in HEK-ABCC2 cells in the presence and absence of chrysin (10 and 60 μ M) and CA (50 μ M)

Accumulation of CDCF in HEK-ABCC2 cells was measured as fluorescence after 30 min incubation of the 80%-90% confluent cells with 2.5 μ M CDCFDA in the presence and absence of chrysin (10 and 60 μ M) and CA (50 μ M). Fluorescence was recorded by a plate reader (SPARK®, German) Data are presented as the mean (bar) and standard deviation (error bar) of individual values (circles) from two independent experiments. P-values shown as * ($P < 0.0001$) from one-way ANOVA.

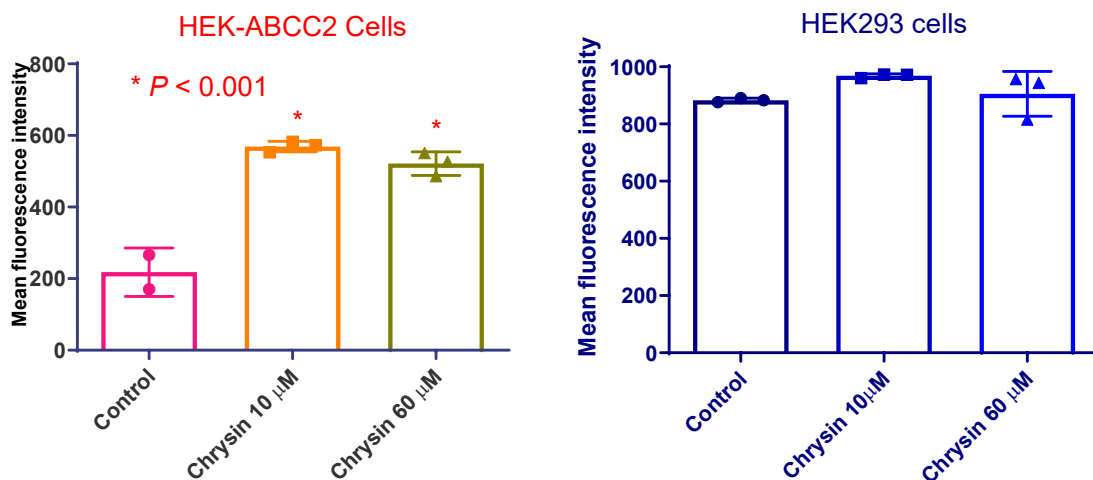


Figure 5- 8 Cellular accumulation of CDCF in HEK-ABCC2 and HEK293 cell lines

Accumulation of CDCF in HEK293 and HEK-ABCC2 cells was measured after 30 min incubation of the cells with 2.5 μM CDCFDA in the presence and absence of chrysin (10 and 60 μM) Geometric mean fluorescence was recorded by MDX flow cytometer (Beckman Coulter, German). Data are presented as the mean (bar) and standard deviation (error bar) of individual values (circles) from three independent experiments. P-values shown as * (P<0.0001) from one-way ANOVA.

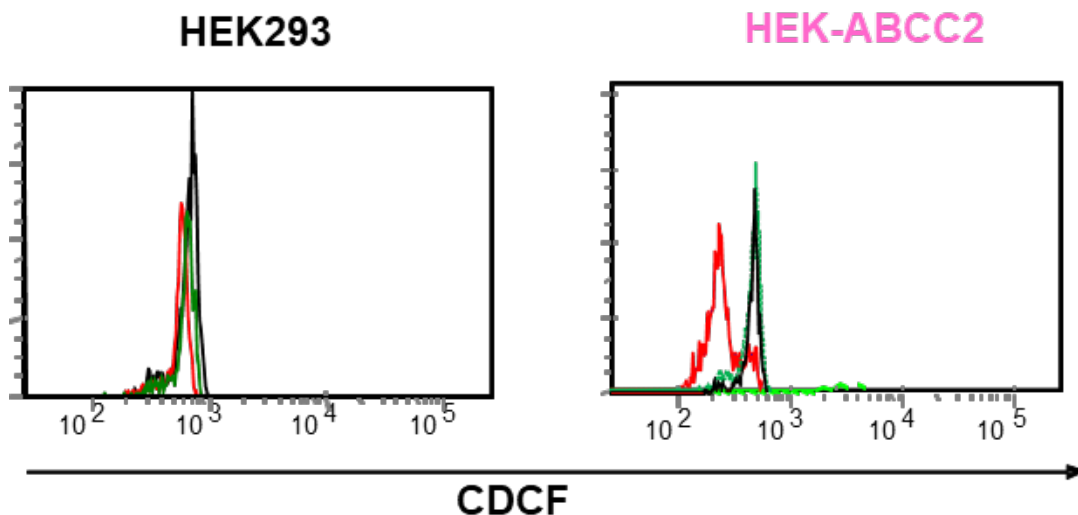


Figure 5- 9 Representative flow cytometric histogram of CDCF accumulation in HEK293 and HEK-ABCC2 cell lines, with red line showing control panel (CDCF only), green and black lines showing CDCF in the presence of 10 and 60 chrysin, respectively.

From Figure 5-7 to 5-9, results indicated that platinum accumulation increased by chrysin treatment in both HEK-ABCC2 and HEK293 cells. However, HEK-ABCC2 cells exhibited significantly lower platinum accumulation. Oxaliplatin with 10 μ M chrysin significantly increased the cellular accumulation of a model MRP2 substrate CDCF in HEK-ABCC2 cells to compare with control panel which was only use oxaliplatin. Even increase the concentration of chrysin to 60 μ M, the cellular accumulation of CDCF is slightly decreased. It is proved that chrysin significantly increased the cellular accumulation of a model MRP2 substrate CDCF in HEK-ABCC2 cells but not in HEK293 cells. Which also verify the results from cell viability assay. CDCF accumulation was determined by both fluorescence microscope and flow cytometric analysis.

5.4. Discussion

The findings presented in this chapter started with characterizing the phenotypic traits of a cell line stably transfected to overexpress the ABCC2 gene, which encodes the MRP2 membrane transporter protein, and comparing it to a non-transfected parental cell line. Ideally, a HEK293 cell line with ABCC2 gene knockout would have been utilized for comparative analysis against the HEK-ABCC2 overexpressing cell line. However, this knockout model was unavailable for the study. The HEK-ABCC2 cells exhibited significantly higher expression levels of MRP2 protein compared to HEK293 cells. Additionally, the efflux of CDCF was more pronounced in HEK-ABCC2 cells, resulting in a reduced accumulation of CDCF. Furthermore, the sensitivity of HEK-ABCC2 cells to the cytotoxic effects of MRP2 substrates, oxaliplatin, was found to be lower compared to that of the HEK293 cells.

build upon prior research that has investigated the role of MRP2 in drug resistance, particularly in relation to platinum-based chemotherapeutic agents like cisplatin and oxaliplatin. The use of the HEK293 cell line, genetically engineered to overexpress MRP2 (HEK-MRP2), provided a robust *in vitro* model to explore the transporter's involvement in oxaliplatin resistance.

Previous studies showed that MRP2 plays a crucial role in mediating resistance to oxaliplatin by reducing its intracellular accumulation, thereby decreasing its cytotoxic effects. Chrysin, a potential MRP2 inhibitor, like Myricetin (a known MRP2 inhibitor) both significantly enhanced oxaliplatin-induced growth inhibition in HEK-MRP2 cells but not in the parental HEK293 cells further supports the specificity of MRP2's involvement in oxaliplatin resistance.

In our study, it was also demonstrated that chrysin increased the accumulation of CDCF, a model substrate of MRP2, in HEK-MRP2 cells, but not in HEK293 cells. This increase in CDCF accumulation correlates with the observed increase in oxaliplatin sensitivity, reinforcing the hypothesis that MRP2 actively exports oxaliplatin out of cells, thereby reducing its cytotoxic efficacy. Interestingly, the effect of chrysin was more pronounced at a lower concentration (10 μ M) compared to previous studies using higher concentrations of other MRP2 inhibitors like myricetin. This suggests that chrysin may be a more potent and effective MRP2 inhibitor, which could have implications for its potential use in overcoming drug resistance in cancer therapy.

The results of this study align with earlier findings that link high MRP2 expression with decreased intracellular drug accumulation and increased resistance to chemotherapeutic agents. However, this study extends these findings specifically to oxaliplatin, a drug for which the role of MRP2 has been less well-characterized compared to other platinum-based drugs like cisplatin. The use of genetically modified cell lines in this study has provided clearer insights into the mechanistic role of MRP2 in oxaliplatin resistance, addressing some of the inconsistencies reported in the literature.

Overall, these findings suggest that MRP2 is a key player in mediating oxaliplatin resistance in cells, and that inhibition of MRP2 could be a viable strategy to enhance the effectiveness of oxaliplatin in cancer treatment. Future studies could further explore the clinical relevance of these findings, particularly in the context of gastrointestinal cancers where MRP2 expression has been linked to poor outcomes.

5.5 Conclusion

This chapter has provided significant evidence that the MRP2 transporter plays a pivotal role in reducing intracellular oxaliplatin accumulation, thereby contributing to drug resistance. With HEK-MRP2 cells, it was demonstrated that chrysin, an MRP2 inhibitor, can effectively enhance oxaliplatin-induced cytotoxicity by increasing the drug's intracellular accumulation. These findings highlight the potential of MRP2 inhibitors as adjuvant therapies to overcome resistance in oxaliplatin-based treatments, particularly in cancers where MRP2 is overexpressed.

The study underscores the importance of further research into MRP2's role in chemotherapy resistance, with the aim of developing targeted strategies to inhibit this transporter and improve the efficacy of platinum-based chemotherapeutics.

Chapter 6 Human gastrointestinal cancer cell line studies

6.1. Introduction

The previous chapter detailed studies on HEK-MRP2 and HEK293 cell lines, demonstrating MRP2's involvement in modulating oxaliplatin accumulation, as evidenced by CDCF (a model MRP2 substrate) accumulation through flow cytometry, and influencing sensitivity to oxaliplatin-induced growth inhibition. Further validation of MRP2's role was provided through inhibitor studies using chrysin, which effectively reversed the MRP2-mediated reduction in cellular CDCF accumulation and heightened sensitivity to oxaliplatin. In the current chapter, human gastrointestinal cancer cell lines are utilized to further investigate MRP2's role in cellular CDCF accumulation and their sensitivity to oxaliplatin.

Oxaliplatin-based combination chemotherapy is widely used for treating gastrointestinal cancers, including gastric, colorectal, hepatocellular, and pancreatic cancers. It serves as a first-line treatment for metastatic colorectal cancer in combination with other drugs, such as in FOLFOX (oxaliplatin, 5-fluorouracil, and folinic acid), XELOX (oxaliplatin and capecitabine), and FOLFOXIRI (oxaliplatin, 5-fluorouracil, folinic acid, and irinotecan) regimens (Cassidy, Tabernero, Twelves, Brunet, Butts, Conroy, Debraud, Figer, Grossmann, Sawada, Schöffski, et al., 2004; de Gramont et al., 2023; Falcone, Ricci, Brunetti, Pfanner, Allegrini, Barbara, Crinò, et al., 2007). It is also used as adjuvant therapy after surgery for advanced colorectal cancer (André et al., 2004; Diao et al., 2008), and for other gastrointestinal cancers, including pancreatic, gastric, and hepatocellular cancers (Conroy et al., 2013; D. Cunningham et al., 2010; Louafi et al., 2007; Petrioli et al., 2015; Zaanani et al., 2013; Zhong et al., 2015). Regimens like FOLFIRINOX and GEMOXEL have shown effectiveness in metastatic pancreatic cancer (T. Conroy et al., 2011; Conroy et al., 2013), and oxaliplatin with capecitabine or S-1 has been proven effective for advanced gastric cancer (D. Cunningham et al., 2010; Zaniboni & Meriggi, 2005; Zhong et al., 2015). Additionally, GEMOX, FOLFOX4, and XELOX are used in hepatocellular carcinoma

treatment (Boige et al., 2007; Coriat et al., 2012; Louafi et al., 2007).

Several studies have examined the relationship between MRP2 expression and tumour resistance or clinical outcomes in gastrointestinal cancer patients receiving platinum-based chemotherapy (El Khoury et al., 2016; Hinoshita et al., 2000; Mirakhorli et al., 2012; Namisaki et al., 2014; Noma et al., 2008). Elevated MRP2 expression was observed in tumours from patients with hepatocellular carcinoma (Korita et al., 2010; Nies, König, et al., 2001), colorectal carcinoma (Hinoshita et al., 2000; Mirakhorli et al., 2012), and pancreatic cancer (Noma et al., 2008). High MRP2 expression in colorectal tumours was associated with recurrence during FOLFOX-4 treatment, and although these patients had shorter survival, the difference was not statistically significant (Mirakhorli et al., 2012). Polymorphisms in the ABCC2 gene (MRP2) have been linked to better survival in colorectal cancer patients treated with oxaliplatin (Mirakhorli et al., 2013). In hepatocellular carcinoma, MRP2 overexpression was associated with lower tumour necrosis in patients receiving cisplatin (Korita et al., 2010). Additionally, in pancreatic cancer, the MRP2 G40A GG genotype was linked to lower survival rates and poor tumour response to chemoradiotherapy (Tanaka et al., 2011). These studies suggest MRP2 may contribute to chemotherapy resistance and outcomes in gastrointestinal cancer patients, but its role remains unclear. Further investigation into MRP2's involvement in cellular resistance to oxaliplatin is warranted.

In vitro studies have shown MRP2's involvement in cellular resistance to drugs like cisplatin in liver cancer (Yoshitomi et al., 2001), doxorubicin, vincristine in HepG2 cells (Folmer et al., 2007), and cisplatin in ovarian cancer (A2780) (Ma et al., 2009; Materna et al., 2006). However, limited studies on oxaliplatin resistance in gastrointestinal cancer cell lines have yielded conflicting results (Beretta et al., 2010; Z. Liu et al., 2010; Shen et al., 2012). Shen et al. found increased MRP2 expression in an oxaliplatin-resistant colorectal cancer cell line (HCT-116/LOHP) and that silencing ABCC2 enhanced oxaliplatin sensitivity and platinum accumulation (Shen et al., 2012). Liu et al. reported upregulated MRP2 expression in oxaliplatin-resistant colon cancer cell lines,

with no changes in P-gp or MRP1 levels (Zhen Liu et al., 2010). In contrast, Beretta and colleagues found no detectable MRP2 or MRP3 in oxaliplatin-resistant ovarian cancer cells (Beretta et al., 2010). These findings suggest a possible role for MRP2 in oxaliplatin transport and resistance in gastrointestinal cancers, but further clarification is needed.

Given this background, the experiments in this chapter aim to identify how chrysin influences MRP2's role in the cellular accumulation of oxaliplatin-derived platinum and its effect on sensitivity to oxaliplatin-induced growth inhibition. This was carried out using gastrointestinal cancer cell lines, including PANC-1 and Caco-2 cell lines, which have been identified as MRP2 overexpressing gastrointestinal cancer cell lines.

6.2. Materials and Methods

6.2.1. Chemicals and equipment

The sources of chemicals used in this study and the preparation details of the stock solutions were as mentioned in section 2.1.

6.2.2. Cell culture

A panel of human gastrointestinal cancer cell lines including pancreatic cancer cell line (PANC-1) and colorectal cell line (Caco-2) were used in this study. The sources and cell culture conditions of these cell lines were described in section 2.2.

6.2.3. Cell Viability Assay (MTT assay/ Presto-Blue) with Manuka honey or Chrysin

6.2.3.1. Drug treatment

For the assessment of effects on cell growth of drugs of interest, Caco-2 and PANC-1 cells were exposed to drugs for designated times, followed by replacement of the drug-containing medium with the normal growth medium until 72 h after the initial exposure to the drugs. Varying concentrations of drugs and incubation periods were used for different experimental designs as summarized below in Table 6-1.

Table 6- 1 Drug treatments and incubation time used in cell viability assays

Experiment design	Drug Name	Drug concentration	Incubation periods
Cellular sensitivity to oxaliplatin	Oxaliplatin	0-400 μ M	72 hours
Cytotoxic effects of manuka honey and oxaliplatin combination	Manuka honey	1%, 2.5%	30 mins preincubation and 2 hours coincubation
	Oxaliplatin	0-400 μ M	2 hours coincubation
Cytotoxic effects of chrysin alone	Chrysin	0-60 μ M	72 hours
Cytotoxic effects of chrysin and oxaliplatin combination	Chrysin	0, 5, 10, 60 μ M	45 mins preincubation and 2 hours coincubation
	Oxaliplatin	0-200 μ M	2 hours coincubation

6.2.3.2. Cell Viability Assay (MTT assay/ Presto-Blue) with Manuka honey or Chrysin

The MTT (3-(4,5-Dimethylthiazol-2-yl)-2,5-Diphenyltetrazolium Bromide) assay was used to

measure the number of viable cells in these experiments, and the details of the assay was mentioned in section 2.3. Prior to the growth inhibition experiments, seeding density experiments for each cell line were undertaken to determine the optimal seeding density for further experiments and to check the optical density values detected over the seeding density changes. Drug concentrations and incubation times were varied depending on the studies as shown in Table 6-1.

6.2.4. Chrysin effects on cellular accumulation of CDCF in GI cancer cell lines

Human Caco-2 or PANC-1 cells were seeded at a density of 1×10^4 cells per well in 200 μ L of complete RPMI medium in 96-well plates and allowed to incubate for 72 to 96 hours to ensure adequate adhesion and growth. Following incubation, the cells were washed once with warm phosphate-buffered saline (PBS) and subsequently treated in triplicate with 100 μ L of phenol red-free RPMI medium containing chrysin at increasing concentrations; control wells received only phenol red-free RPMI medium. After a 30-minute incubation period, 100 μ L of 5 μ M CDCFDA solution was added to each well, and the plates were incubated for an additional 30 minutes while protected from light to prevent photobleaching. The cells were then placed on ice and washed twice with 200 μ L of ice-cold PBS to remove excess dye and inhibitors, followed by fixation with 100 μ L of 1% paraformaldehyde (PFM) added to each well. Fluorescence intensity was measured using a SPARK® Microplate Spectrofluorometer (Molecular Devices, Life Technologies) at excitation and emission wavelengths of 467 nm and 539 nm, respectively. Additionally, fluorescent images were captured utilizing a Leica fluorescence microscope equipped with a GFP filter and a SPOT RT digital camera to visually assess intracellular fluorescence distribution.

To calibrate the chrysin effects on cellular accumulation of CDCF in Caco-2 cells, we used DC protein assay to evaluate the protein concentrations in samples. The details of procedures for this assay were mentioned in Section 2.5.2. To verify the accuracy of this assay, seeding six increasing concentrations of BSA standards (0-1.5 mg/ml) in 96 well plates with triplicate data set, linear

curve was produced as Figure 6-1.

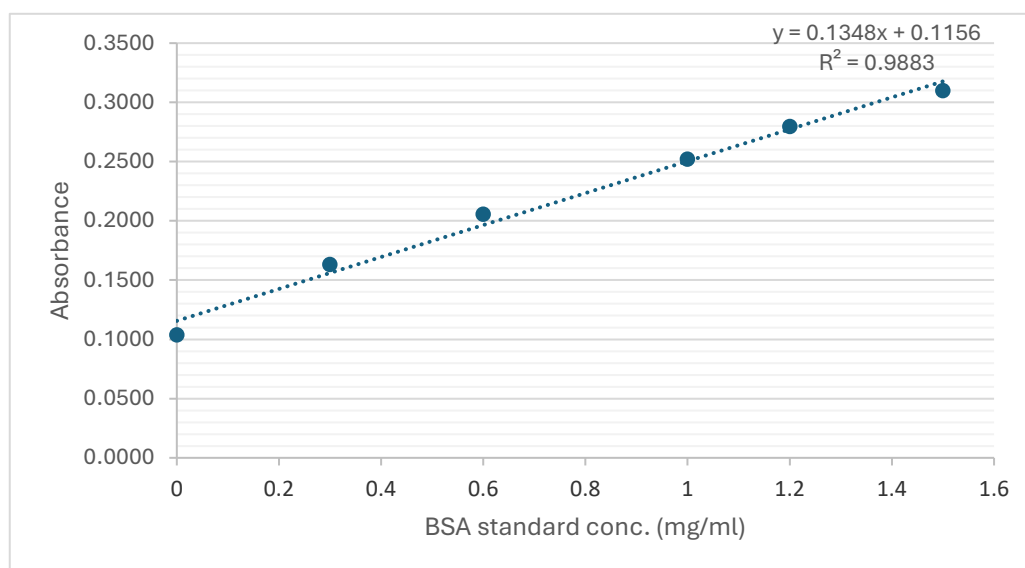


Figure 6- 1 DC protein assay linear curve.

A series of protein standards were prepared, ranging from 0 to 3 mg/mL (0, 0.3, 0.6, 1, 1.2, 1.5 mg/mL), by dissolving Bovine Serum Albumin (BSA) in RIPA buffer. Subsequently, 5 μ L of the standards were pipetted into a clean, dry microtiter plate. Following this, 25 μ L of the combined S + A reagent (20 μ L of reagent S was added to each millilitre of reagent A) was added to each well, and the plate was vortexed to ensure proper mixing. Then, 200 μ L of reagent B was introduced into each well. The plate was mixed for 5 seconds in plate reader, with any bubbles being carefully removed to prevent cross-contamination. After a 15-minute incubation with agitation, absorbance was measured at 750 nm to determine protein concentration. Linear curve-fitting and corresponding equations are shown.

6.2.5. Effect of chrysin on oxaliplatin-induced apoptosis in Caco-2 and PANC-1 cells

CDCF was employed as a substrate to assess MRP2 transporter activity in Caco-2 and PANC-1 cell lines. The non-fluorescent and cell-permeable precursor, CDCFDA [5(6)-carboxy-2,'7'-dichlorofluorescein diacetate], was utilized in these assays. Detailed procedures for this assay were mentioned in Section 2.7.

6.2.6. Statistical analysis

Data analysis was mentioned in section 2.10.

6.3. Results

6.3.1. The effect of Manuka honey on inhibition of MRP2 transporter

Caco-2 cells were pretreated with Manuka honey (0, 1%, 2.5%, w/w) for 30 mins, followed by coincubation with different concentrations of oxaliplatin (0-400 μM) for 2 hours. After coincubation, cells were incubated in drug free complete medium for 72 hours, and then was assessed for cell viability by using MTT assay. The results demonstrated that Manuka honey in 2.5% concentration significantly enhanced oxaliplatin-induced growth inhibition in Caco-2 cancer cell lines (Figure 6-2).

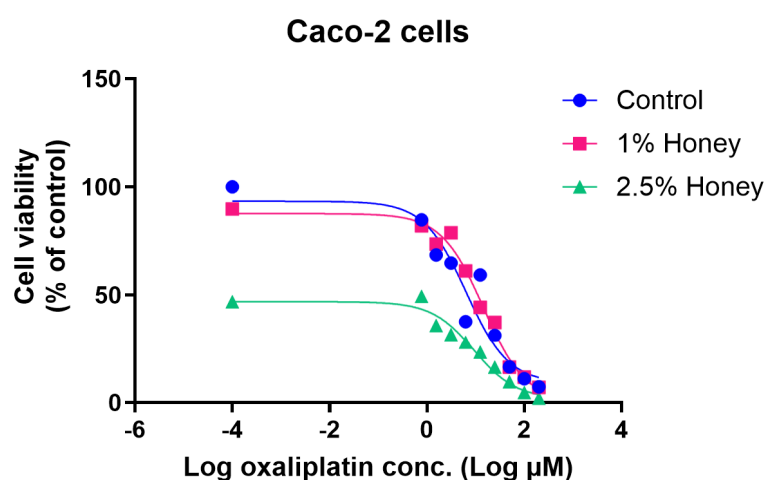


Figure 6- 2 Cell viability value of oxaliplatin or Manuka honey and oxaliplatin combination on Caco-2 cell lines

Caco-2 cells were pretreated with Manuka honey (0, 1%, 2.5%, w/w) for 30 mins, followed by coincubation with different concentrations of oxaliplatin (0-400 μM) for 2 hours. After coincubation, cells were incubated in drug free complete medium for 72 hours, and then was assessed for cell viability by using MTT assay. The results demonstrated that Manuka honey in 2.5% concentration significantly enhanced oxaliplatin-induced growth inhibition in Caco-2 cancer cell lines.

From the results above, and previous studies, we hypothesize that there would be any phenolic compounds which can inhibit MRP2 expression in cancer cell lines in Manuka honey. The further study was conducted by LC-MS (Chapter 3), module fitting (Chapter 4), and cell viability study in HEK-MRP2 cell lines (Chapter 5).

6.3.2. The effect of chrysin on inhibition of MRP2 transporter in Caco-2 and PANC-1 cancer cell lines

Caco-2 (seeding density with 5,000 cells/well) or PANC-1 (seeding density with 8,000 cells/well) cells were pretreated with chrysin (0, 5, 10, 60 μM) for 45 mins, followed by coincubation with different concentrations of oxaliplatin (0-200 μM) for 2 hours. After coincubation, cells were incubated in drug free complete medium for 72 hours, and then was assessed for cell viability by using MTT assay. The results demonstrated that chrysin significantly enhanced oxaliplatin-induced growth inhibition in PANC-1 cancer cell lines but not in Caco-2 cell lines (Figure 6-3 and 6-4). The IC-50 values for oxaliplatin in PANC-1 cancer cell lines decreased by around 18% in the presence of chrysin. In contrast, Caco-2 cancer cell lines exhibited lower IC-50 values for oxaliplatin compared to PANC-1 cancer cell lines, but these values remained unchanged with 5 μM chrysin treatment, and no significant changes with 10 μM chrysin (Figure 6-5).

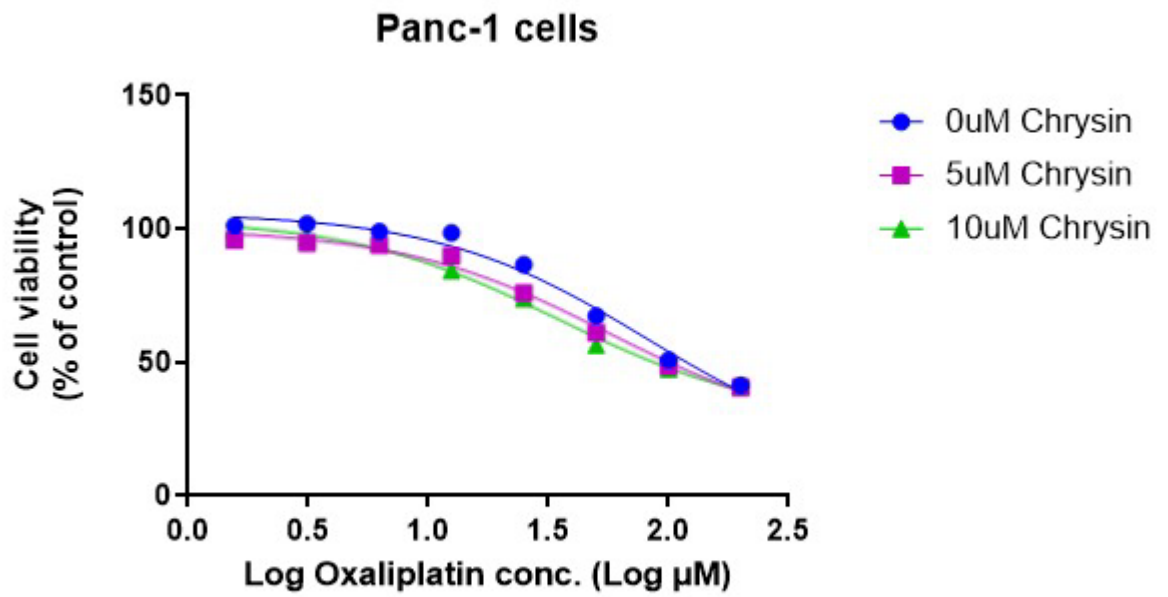


Figure 6- 3 Cell viability value of oxaliplatin or chrysin and oxaliplatin combination on PANC-1 cancer cell lines

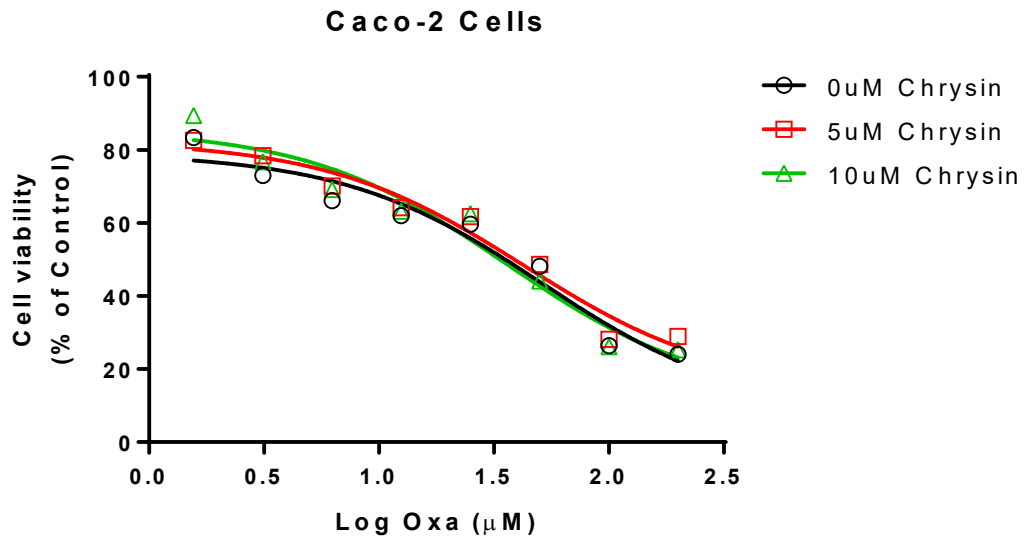


Figure 6- 4 Cell viability value of oxaliplatin or chrysin and oxaliplatin combination on Caco-2 cancer cell lines

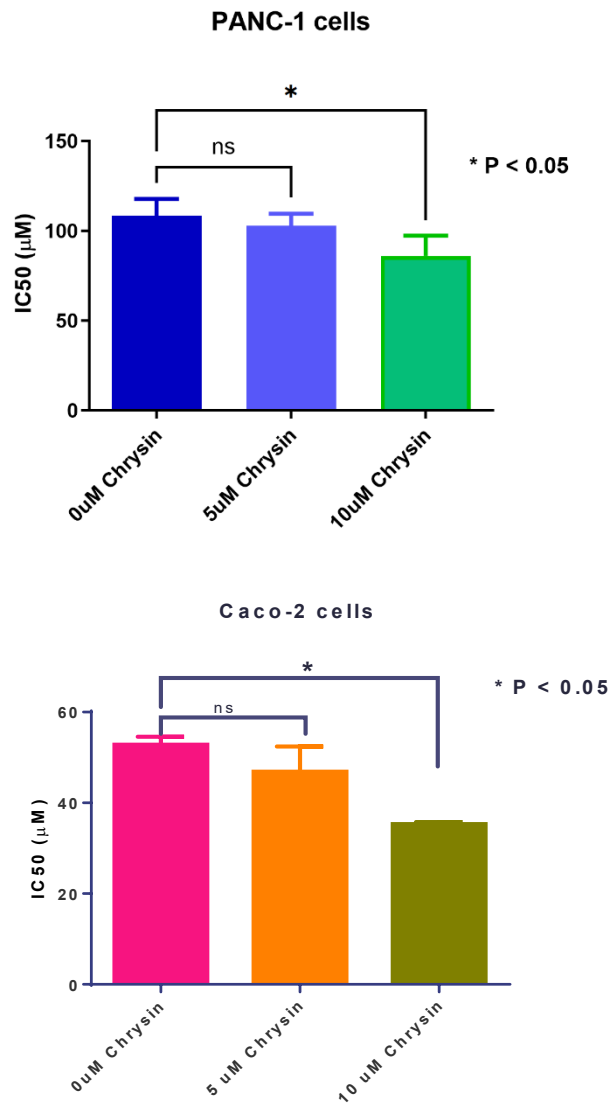


Figure 6- 5 IC50 value of oxaliplatin or chrysin and oxaliplatin combination on PANC-1 and Caco-2 cell lines

PANC-1 and Caco-2 cells were pretreated with chrysin (0, 5, 10, 60 μM) for 45 mins, followed by coincubation with different concentrations of oxaliplatin (0-200 μM) for 2 hours. After coincubation, cells were incubated in drug free complete medium for 72 hours, and then was assessed for cell viability by using MTT assay. The results demonstrated that chrysin significantly enhanced oxaliplatin-induced growth inhibition in PANC-1 and Caco-2 cancer cell lines, Data are presented as the mean and SEM of IC50 of oxaliplatin in cells from two independent experiments. Asterisks is P values (*, P<0.05) from Dunnett's post hoc test that followed one-way ANOVA for comparisons of each groups (oxaliplatin combined with 5 μM chrysin or 10 μM chrysin group) to control sample (oxaliplatin only).

6.3.3. Chrysin effects on oxaliplatin cellular accumulation of CDCF in GI cancer cells

The cellular accumulation of MRP2 substrate, CDCF, was observed to investigate the MRP2 functional activity in Caco-2 and PANC-1 cells. Chrysin was used as an inhibitor of MRP2. The efflux activity of MRP2 was determined in the presence of chrysin at different concentration using CDCF.

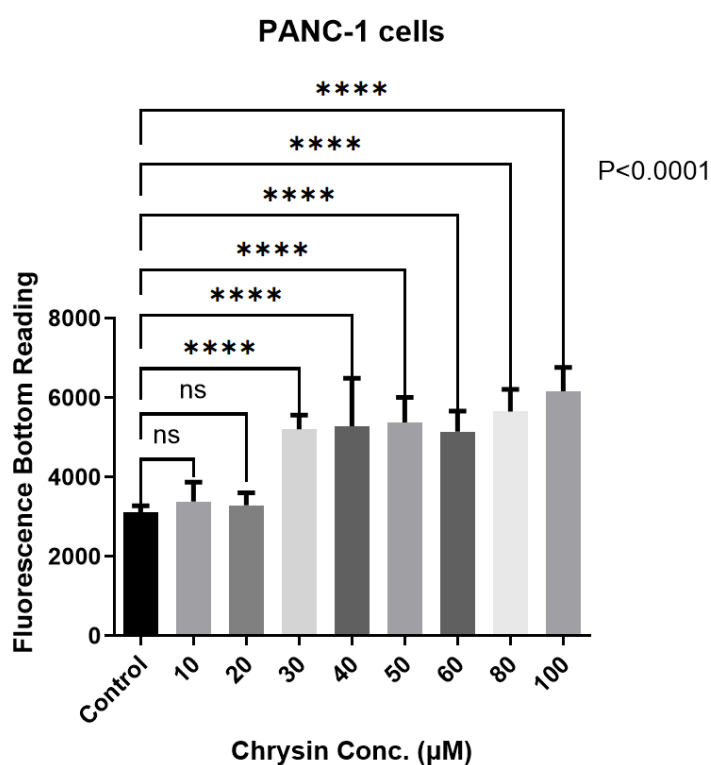


Figure 6- 6 Fluorescence intensity of CDCF in PANC-1 cancer cell lines for increasing concentration of chrysin.

PANC-1 cells were seeded at a density of 1×10^4 cells per well in 200 μL of complete RPMI medium in 96-well plates and allowed to incubate for 72 to 96 hours to ensure adequate adhesion and growth. Following incubation, the cells were washed once with warm phosphate-buffered saline (PBS) and subsequently treated in triplicate with 100 μL of phenol red-free RPMI medium containing chrysin at increasing concentrations; control wells received only phenol red-free RPMI medium. After a 30-minute incubation period, 100 μL of 5 μM CDCFDA solution was added to each well, and the plates were incubated for an additional 30 minutes while protected from light to prevent photobleaching. The cells were then placed on ice and washed twice with 200 μL of ice-cold PBS to remove excess dye and inhibitors, followed by fixation with 100 μL of

1% paraformaldehyde (PFM) added to each well. Fluorescence intensity was measured at excitation and emission wavelengths of 467 nm and 539 nm, respectively. Symbols are the mean (bar), standard deviation (error bar) and individual values (open circles) pooled from three independent experiments. P values are from one-way ANOVA and those shown as **** (P < 0.0001).

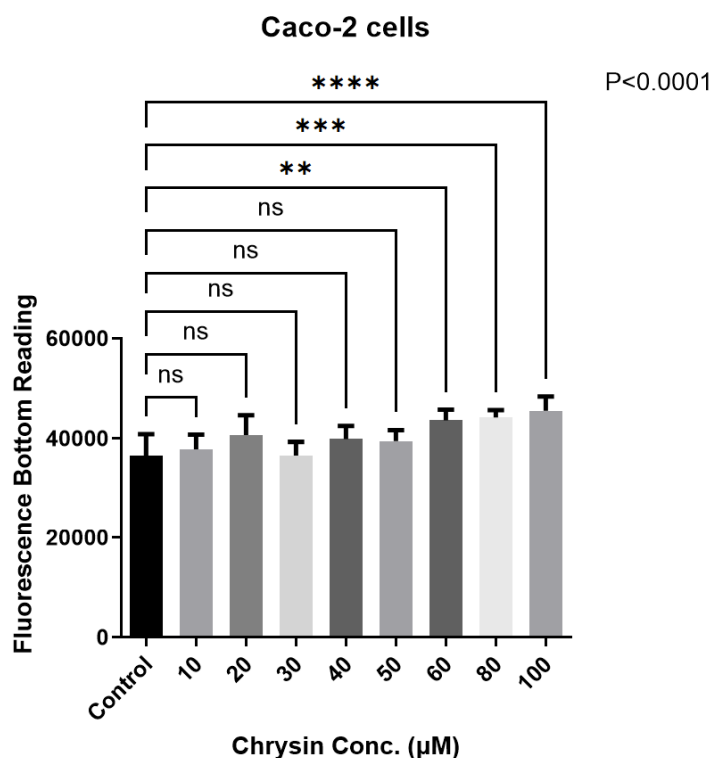


Figure 6- 7 Fluorescence intensity of CDCF in Caco-2 cancer cell lines for increasing concentration of chrysin.

Caco-2 cells were seeded at a density of 1×10^4 cells per well in 200 µL of complete RPMI medium in 96-well plates and allowed to incubate for 72 to 96 hours to ensure adequate adhesion and growth. Following incubation, the cells were washed once with warm phosphate-buffered saline (PBS) and subsequently treated in triplicate with 100 µL of phenol red-free RPMI medium containing chrysin at increasing concentrations; control wells received only phenol red-free RPMI medium. After a 30-minute incubation period, 100 µL of 5 µM CDCFDA solution was added to each well, and the plates were incubated for an additional 30 minutes while protected from light to prevent photobleaching. The cells were then placed on ice and washed twice with 200 µL of ice-cold PBS to remove excess dye and inhibitors, followed by fixation with 100 µL of 1% paraformaldehyde (PFM) added to each well. Fluorescence intensity was measured at excitation and emission wavelengths of 467 nm and 539 nm, respectively. Symbols are the mean (bar), standard deviation (error bar) and individual values (open circles) pooled from three independent experiments. P values are from one-way ANOVA and those shown as ** (P < 0.01), *** (P < 0.001) and **** (P < 0.0001).

From the figures above, the fluorescence intensity increased significantly when chrysin concentration reached 30 μM in PANC-1 cancer cell lines. To compare with Caco-2 cell lines, The fluorescence intensity increased significantly when chrysin concentration reached 60 μM . This result shows that chrysin enhance CDCF accumulation and was able to inhibit the functional activity of MRP2 in GI cancer cells. We could hypothesize that chrysin has the inhibition effect on MRP2 expression, while the condition of chrysin would be different in different cell lines.

To verify the fluorescence plate reading results above. Treated cells with 10 μM chrysin for 30 mins before adding oxaliplatin of different concentrations (0, 25, 100 μM), after coincubation 2 hours, cells were incubated with drug free complete medium for 24 hours. Fluorescent images (Figure 6-8) were captured utilizing a Leica fluorescence microscope equipped with a GFP filter and a SPOT RT digital camera to visually assess intracellular fluorescence distribution after treatment. The details of the procedures were mentioned in Section 6.2.4.

The figure above shows that the combination of 10 μM chrysin with 25 μM oxaliplatin exhibits a similar fluorescent intensity when compared to the combination of 10 μM chrysin with 100 μM oxaliplatin. It proved that, the combination increased the cell accumulation of oxaliplatin in Caco-2 cells. Notably, the fluorescent intensity observed in these drug treatment groups was significantly elevated compared to the control panels, indicating a marked increase in response to the combined treatments.

6.3.4. Effect of chrysin on oxaliplatin-induced apoptosis in Caco-2 and PANC-1 cells

The sensitization mechanism induced by oxaliplatin in Caco-2 and PANC-1 cells treated with chrysin was investigated through an apoptosis assay. The drug combinations used for this assay

included 10 μM chrysin plus 25 μM oxaliplatin and 10 μM chrysin plus 100 μM oxaliplatin. Cells were treated with the chrysin and oxaliplatin combination, as described above, for 2 hours and then analysed using flow cytometry.

In Caco-2 cells, the percentage of early apoptotic cells after exposure to 100 μM oxaliplatin alone was 8.77%. Following exposure to 10 μM chrysin, the early apoptotic cell percentage increased to 23.62%. The combination treatment resulted in a 1.7-fold increase in apoptosis, indicating a significant enhancement of cytotoxicity in Caco-2 cells. In contrast, the percentage of early apoptotic cells was 5.95% after exposure to 25 μM oxaliplatin alone, and 6.25% when combined with 10 μM chrysin. Thus, in the 25 μM oxaliplatin group, the addition of chrysin did not significantly enhance the cytotoxic effect. Similarly, the percentage of viable cells after treatment with 25 μM oxaliplatin alone was 89.17%, compared to 83.24% with the combination of 10 μM chrysin and 25 μM oxaliplatin. Statistical analysis revealed that combination treatments reduced the percentage of viable cells more than oxaliplatin treatment alone, while the early apoptosis rates increased.

In PANC-1 cells, the percentage of early apoptotic cells after treatment with 100 μM oxaliplatin alone was 12.36%. Following exposure to 10 μM chrysin, this percentage slightly increased to 12.49%. The percentage of viable cells decreased from 77.59% to 74.68%. When treated with 25 μM oxaliplatin alone, the early apoptotic cell percentage was 15.64%, and it slightly decreased to 14.61% when combined with 10 μM chrysin. Similarly, the percentage of viable cells was reduced from 76.11% to 74.72%. Statistical analysis indicated that the combination treatments did not significantly alter the percentage of viable cells or early apoptotic rates in PANC-1 cells.

These findings indicate that while chrysin has a modest cytotoxic effect on Caco-2 cells, enhancing early apoptosis when combined with oxaliplatin, it does not have a significant impact on PANC-1 cells. In Caco-2 cells, oxaliplatin-induced apoptosis was increased in a dose-dependent manner when combined with chrysin, highlighting the synergistic effect. However, in

PANC-1 cells, chrysin did not produce a comparable enhancement of oxaliplatin's effects.

Table 6- 2 Data analysis of apoptosis assay with oxaliplatin treatment in Caco-2 cells and PANC-1 cells in the presence and absence of chrysin (10 μ M)

Cell lines	Treatment	Viable Cells (mean %)	Early Apoptosis (%) (Mean \pm SD, n =3)
Caco-2	Oxa (25 μ M)	89.17	5.95 \pm 0.54
	Chrysin (10 μ M) and Oxa (25 μ M)	83.24	6.25 \pm 0.61
	Oxa (100 μ M)	83.19	14.7 \pm 5.15
	Chrysin (10 μ M) and Oxa (100 μ M)	70.78	24.3 \pm 2.51 ^a
PANC-1	Oxa (25 μ M)	76.11	15.64 \pm 2.68
	Chrysin (10 μ M) and Oxa (25 μ M)	74.72	14.61 \pm 2.97
	Oxa (100 μ M)	77.59	12.36 \pm 1.32
	Chrysin (10 μ M) and Oxa (100 μ M)	74.68	12.49 \pm 1.73

^a $P < 0.05$, Caco-2 cells treated with oxaliplatin (100 μ M) vs with a combination of oxaliplatin (100 μ M) and chrysin (10 μ M)

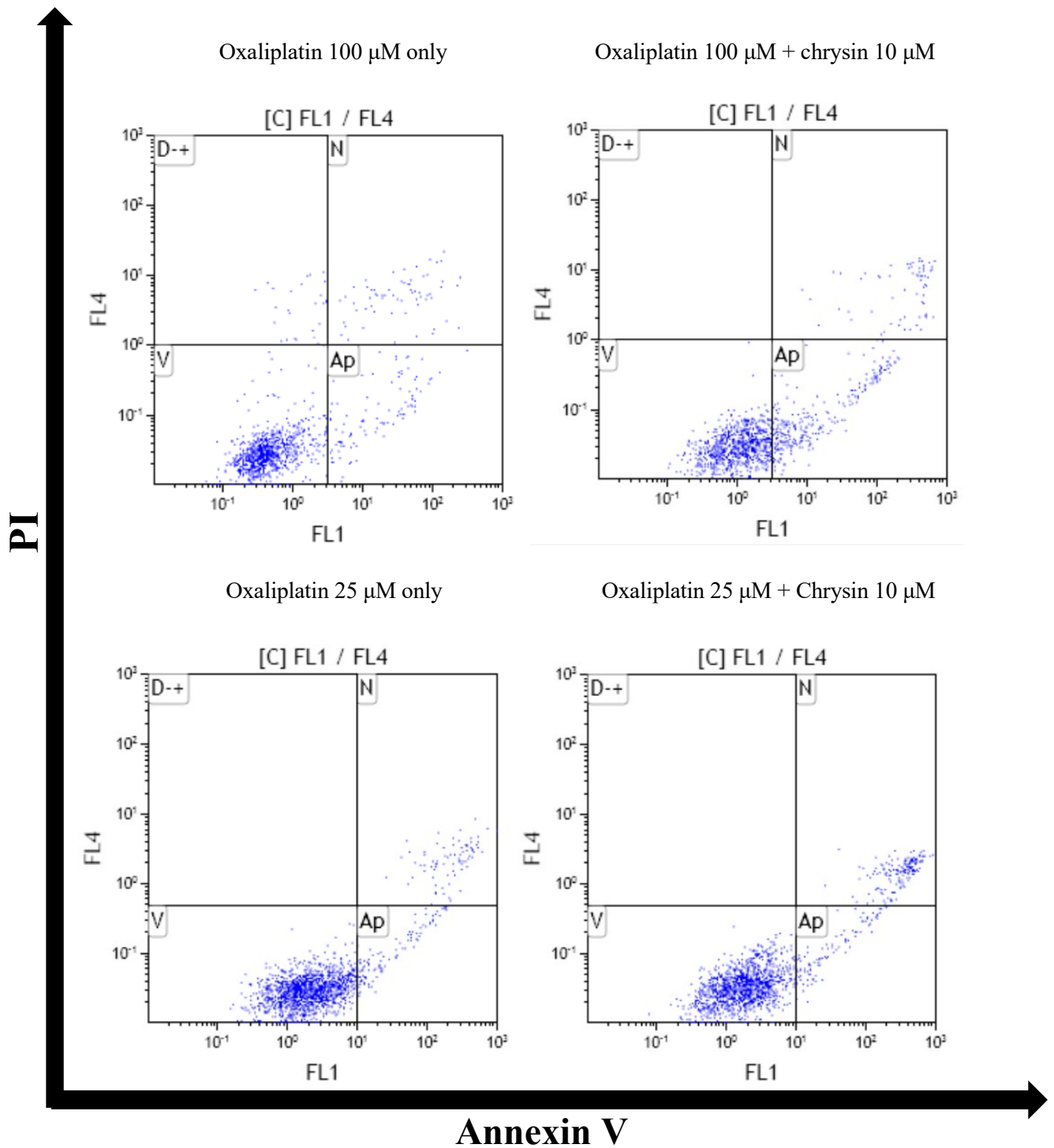


Figure 6- 8 Apoptotic changes in Caco-2 cancer cell lines and their treatment with chrysin and oxaliplatin.

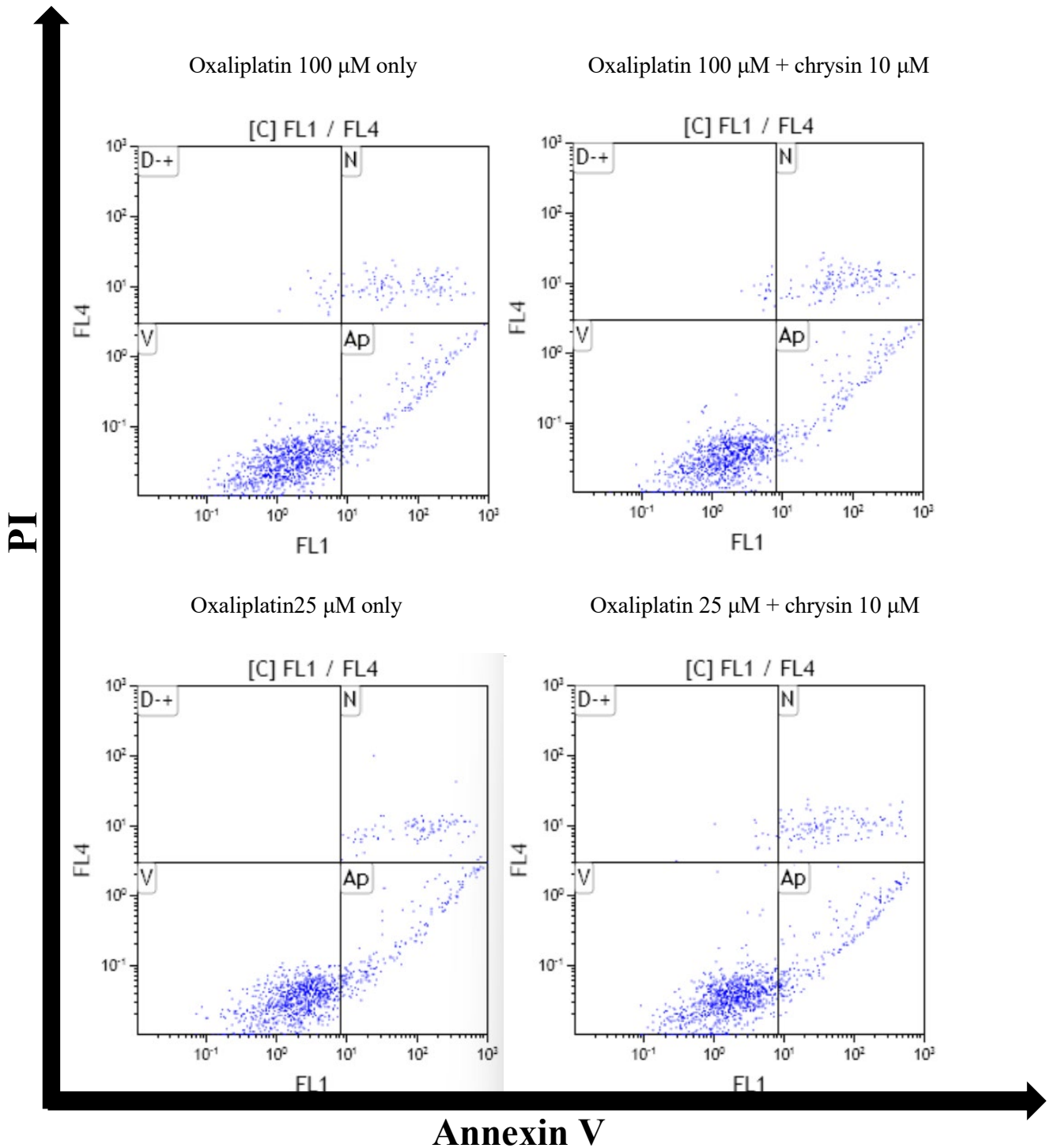


Figure 6- 9 Apoptotic changes in PANC-1 cancer cell lines and their treatment with chrysin and oxaliplatin.

Apoptosis was assessed using concurrent staining with Annexin-V and propidium iodide (PI). Caco-2 cells were either left untreated or treated with varying concentrations of chrysin and oxaliplatin. Following treatment, the cells were stained with Annexin-V and PI, and fluorescence was detected via flow cytometry. Viable cells (V) were identified as those negative for both Annexin-V and PI. Cells in the early stage of apoptosis (Ap) bound exclusively to Annexin-V, while those in the late stage of

apoptosis (N) were positive for both Annexin-V FITC and PI, indicating compromised membrane integrity. The final quadrant (D+) represents debris or dead cells, characterized by their staining with PI only. This method allowed for precise differentiation between viable, early apoptotic, late apoptotic, and dead cells.

6.4. Discussion

The results presented in this chapter underscore the role of MRP2 in mediating resistance to oxaliplatin in gastrointestinal cancer cells, as well as the modulatory effects of chrysin on this resistance. The data suggest that chrysin can inhibit MRP2 activity, thereby enhancing oxaliplatin-induced cytotoxicity in PANC-1 and, to a lesser extent, Caco-2 cancer cell lines.

Chrysin, a known MRP2 inhibitor, demonstrated a significant impact on oxaliplatin accumulation in PANC-1 cells, as evidenced by increased fluorescence intensity of the MRP2 substrate CDCF, which indicates reduced efflux activity of MRP2. In contrast, Caco-2 cells required higher concentrations of chrysin to achieve a comparable inhibitory effect. This differential response suggests that MRP2-mediated drug resistance might be more prominent in PANC-1 cells than in Caco-2 cells, and that the expression or functionality of MRP2 may vary between these cell lines. These findings align with previous studies, which have reported that MRP2 plays a significant role in drug resistance in gastrointestinal cancers but with variability depending on the cell type.

The apoptosis assay further supports the notion that chrysin enhances oxaliplatin-induced cell death, particularly in Caco-2 cells. The combination of 10 μ M chrysin with 100 μ M oxaliplatin led to a notable increase in early apoptotic cells compared to oxaliplatin treatment alone, indicating a synergistic effect. However, this synergy was not observed as strongly in PANC-1 cells, where chrysin only modestly enhanced apoptosis. These results may reflect differences in the underlying biology of these cell lines, including variations in MRP2 expression levels or the involvement of additional drug resistance mechanisms beyond MRP2.

Interestingly, while Caco-2 cells exhibited a higher baseline sensitivity to oxaliplatin compared to PANC-1 cells, the enhancement of oxaliplatin's cytotoxic effects by chrysin was more pronounced in PANC-1 cells at lower drug concentrations. This suggests that the modulation of MRP2 by chrysin may be particularly effective in overcoming resistance in PANC-1 cells, where MRP2 activity appears to play a critical role in oxaliplatin efflux and resistance. However, there was no apparent effect of chrysin on oxaliplatin-induced apoptosis, indicating other molecular mechanisms on cell death may be involved in. This warrant further investigation.

Overall, these findings contribute to a growing body of evidence indicating that inhibition of MRP2 could be a viable strategy for improving the efficacy of oxaliplatin in treating gastrointestinal cancers, particularly in patients or tumors that exhibit high levels of MRP2 expression. Moreover, the use of natural compounds like chrysin as adjunct therapies could offer a promising approach to overcoming drug resistance while minimizing toxicity.

6.5. Conclusion

This study demonstrates the potential of chrysin to enhance the cytotoxic effects of oxaliplatin by inhibiting MRP2-mediated drug efflux in gastrointestinal cancer cell lines. The results indicate that chrysin significantly improves oxaliplatin-induced growth inhibition and apoptosis in PANC-1 cells, with more modest effects observed in Caco-2 cells. The differential response between the two cell lines highlights the complexity of MRP2's role in drug resistance and underscores the need for further investigation into the specific mechanisms that govern MRP2 activity in different cancer types.

Chrysin's ability to inhibit MRP2 and sensitize cancer cells to oxaliplatin suggests that it could be used as part of a combination therapy to overcome resistance in patients with gastrointestinal cancers, particularly those exhibiting high MRP2 expression. Future studies should focus on confirming these findings in *in vivo* models and exploring the clinical relevance of MRP2

inhibitors such as chrysin in enhancing the efficacy of platinum-based chemotherapy.

In conclusion, this research provides valuable insights into the role of MRP2 in oxaliplatin resistance and offers a potential therapeutic strategy for improving treatment outcomes in gastrointestinal cancer patients.

Chapter 7 General Discussion

7.1. Introduction

Gastrointestinal (GI) cancer is defined for a group of cancers that affect the digestive system, including cancers of the oesophagus, stomach, gallbladder & biliary tract, liver, pancreas, bowel (large intestine or colon and rectum), and anus, as well as rare cancers like neuroendocrine tumours and gastrointestinal stromal tumours (Institute, 2023). It presents significant treatment challenges due to the development of chemoresistance, particularly against platinum-based chemotherapy such as oxaliplatin (Hector et al., 2001; Shen et al., 2000; Wang & Lippard, 2005). The role of efflux transporters, notably the multidrug resistance-associated protein 2 (MRP2/ABCC2), has been increasingly recognized in mediating this resistance (Potschka et al., 2003; Sandusky et al., 2002). This thesis explores the potential inhibitor of targeting MRP2 to overcome chemoresistance in GI cancers, especially in colorectal and pancreatic cancer. Through a series of *in vitro* experiments using phytochemicals like chrysin, manuka honey, and myricetin, the study evaluates the inhibition of MRP2 and its impact on enhancing oxaliplatin sensitivity in human GI cancer cell lines. This chapter synthesizes these findings, providing an overview of the results, and discusses the future direction of this research, its clinical implications, and final conclusions.

7.2. Summary of the findings

This thesis investigates the role of MRP2 transporters in mediating drug resistance in gastrointestinal (GI) cancers, focusing particularly on oxaliplatin resistance. Recently, our team has reported that MRP2 (a member of ABC transporter protein) confers oxaliplatin resistance and a phytochemical MRP2 inhibitor myricetin increased cellular platinum accumulation and oxaliplatin cytotoxicity in several human GI cancer cell lines (Biswas et al., 2019; Khine et al., 2019). At the meantime, our team and another Italian group have reported that NZ Manuka honey showed selective toxicity and induced apoptosis in colorectal cancer cell lines but not in normal human cells (Chan & Li, 2016; D et al., 2024). A series of experiments were performed using

various cell lines, including HEK293 embryonic kidney MRP2 over-expressing cell line (HEK-MRP2), HEK293 embryonic kidney parental cell line (HEK293), colorectal cancer cell line (Caco-2), and pancreatic cancer cell line (PANC-1), to assess the impact of chrysin, a phytochemical found in Manuka honey, on MRP2-mediated efflux and its potential to enhance oxaliplatin's cytotoxicity. The key findings revealed that chrysin significantly inhibited MRP2 function, increasing intracellular oxaliplatin accumulation and promoting apoptosis in cancer cells, particularly in Caco-2 and PANC-1 cell lines. These results support the hypothesis that MRP2 inhibition can reverse oxaliplatin resistance and may serve as a therapeutic strategy for improving chemotherapy outcomes in GI cancers.

7.2.1. MRP2 (multidrug resistance-associated protein 2) in gastrointestinal (GI) cancer resistance

The central focus of this research was to evaluate MRP2's role in oxaliplatin resistance in GI cancers. MRP2 functions by extruding chemotherapy drugs from cancer cells, thus reducing intracellular drug accumulation and decreasing cytotoxicity. Using the Caco-2 and PANC-1 cell lines, this study demonstrated that MRP2 overexpression leads to diminished oxaliplatin efficacy. The results align with previous findings that associate high MRP2 expression with poor clinical outcomes in GI cancer patients undergoing platinum-based chemotherapy.

Several studies have examined the relationship between MRP2 expression and tumour resistance or clinical outcomes in gastrointestinal cancer patients receiving platinum-based chemotherapy (El Khoury et al., 2016; Hinoshita et al., 2000; Mirakhorli et al., 2012; Namisaki et al., 2014; Noma et al., 2008). Elevated MRP2 expression was observed in tumours from patients with hepatocellular carcinoma (Korita et al., 2010; Nies, König, et al., 2001), colorectal carcinoma (Hinoshita et al., 2000; Mirakhorli et al., 2012), and pancreatic cancer (Noma et al., 2008). High MRP2 expression in colorectal tumours was associated with recurrence during FOLFOX-4 treatment, and although these patients had shorter survival, the difference was not statistically

significant (Mirakhorli et al., 2012). Polymorphisms in the ABCC2 gene (MRP2) have been linked to better survival in colorectal cancer patients treated with oxaliplatin (Mirakhorli et al., 2013). In hepatocellular carcinoma, MRP2 overexpression was associated with lower tumour necrosis in patients receiving cisplatin (Korita et al., 2010). Additionally, in pancreatic cancer, the MRP2 G40A GG genotype was linked to lower survival rates and poor tumour response to chemoradiotherapy (Tanaka et al., 2011). These studies suggest MRP2 may contribute to chemotherapy resistance and outcomes in gastrointestinal cancer patients, but its role remains unclear.

7.2.2. Phytochemicals as MRP2 Inhibitors

The thesis explored the effects of natural phytochemicals, particularly chrysin on inhibiting MRP2 function. Previous studies showed that MRP2 plays a crucial role in mediating resistance to oxaliplatin by reducing its intracellular accumulation, thereby decreasing its cytotoxic effects. Myricetin exhibited MRP2-inhibitory properties, enhancing oxaliplatin accumulation. This inhibition was particularly evident when myricetin was used in combination with honey, which further modulated the cellular oxidative environment, potentially sensitizing cells to oxaliplatin-induced apoptosis.

In an *in vitro* study utilizing the Caco-2 cell culture model, the presence of MK-571, a specific MRP2 inhibitor, reduced the apical efflux of both chrysin glucuronide and sulphate, indicating that these conjugates are MRP2 substrates (Walle et al., 1999). Another *in vitro* study with HEK293 cells demonstrated that MK-571 inhibited the efflux of chrysin-7-O-sulfate, leading to a significant increase in intracellular sulphate levels (Li et al., 2015). These studies provide some of the only direct evidence that MRP2 is involved in chrysin conjugate efflux, a finding further supported in this thesis through module fitting in Chapter 4. Additionally, chrysin-7-O-sulfate has been identified as an effective substrate for the MRP4 transporter. Supporting this conclusion, the knockout of MRP4 in HEK293 cells significantly reduced chrysin-7-O-sulfate secretion while significantly increasing its intracellular accumulation by 125–135% (Li et al., 2015). Chrysin, a

potential MRP2 inhibitor, like Myricetin (a known MRP2 inhibitor) both significantly enhanced oxaliplatin-induced growth inhibition in HEK-MRP2 cells but not in the parental HEK293 cells further supports the specificity of MRP2's involvement in oxaliplatin resistance.

7.2.3 Oxaliplatin-Induced Apoptosis

One of the primary goals of the study was to evaluate whether inhibiting MRP2 would enhance oxaliplatin-induced apoptosis in cancer cells. Flow cytometric analysis confirmed that chrysin-treated cells had significantly higher rates of apoptosis compared to untreated controls. This was correlated with higher intracellular oxaliplatin accumulation, reduced drug efflux, and increased DNA damage, ultimately leading to enhanced cell death in MRP2-expressing GI cancer cells. These results suggest that targeting MRP2 could be an effective strategy to reverse oxaliplatin resistance.

7.2.4. Clinical Relevance

The platinum-based anticancer drug oxaliplatin, along with its combination therapies, plays a crucial role in the clinical treatment of colorectal cancer and other gastrointestinal (GI) malignancies (Stein & Arnold, 2012). However, the efficacy of oxaliplatin chemotherapy is limited in a subset of patients for reasons that remain unclear. Various *in vitro* and *in vivo* studies have indicated that overexpression of different ABC transporters in many cancers correlates with poor treatment outcomes. Clinical studies have shown that high expression of MRP2 in GI cancers, including pancreatic, and colorectal cancers, is associated with reduced sensitivity to platinum-based chemotherapy (Cecchin et al., 2013; Mirakhorli et al., 2013). It is suggested that the main reason for poor efficacy is associated with the reduced cellular accumulation of oxaliplatin (J. J. Liu et al., 2012; Wersto et al., 2001). Factors regulating oxaliplatin accumulation, whether through their expression in GI cancer cells or through biological barriers affecting drug disposition, may play a role in its clinical activity. Clinical studies indicate that MRP2 expression is higher in cancer tissues compared to non-cancer tissues (Andersen et al., 2015; Hinoshita et al.,

2000). Previous studies have reported high MRP2 expression levels in PANC-1 and Caco-2 cells (Myint, 2015; Prime-Chapman et al., 2004). These cell lines were chosen to mimic clinical situations, making them suitable for our translational research. Chrysin, as a supplement or drug adjuvant, could be easily integrated into current clinical regimens. Further clinical studies are required to be done.

7.3. Future studies

7.3.1. Animal (*in vivo*) study

Further *in vivo* studies are essential to validate the findings from this research. While the *in vitro* data indicate promising results regarding chrysin's inhibition of MRP2, the efficacy and safety of this combination in live organisms need to be confirmed. Animal models of GI cancers can provide crucial insights into pharmacokinetics, drug toxicity, and the overall therapeutic potential of chrysin in reversing oxaliplatin resistance.

In drug metabolism between humans and animals, off-target effects of chrysin, and the need for precise pharmacokinetic measurements to correlate chrysin dosage and oxaliplatin accumulation are required more discussion.

For chrysin to be integrated into clinical regimens, it must undergo regulatory approval as a supplement or drug adjuvant, requiring clinical trials to prove its efficacy, safety, and therapeutic value. The ethical considerations and the importance of using appropriate models that minimize suffering while maximizing the relevance to human disease.

7.3.2. Inhibition of other signalling pathways

MRP2 is one of many factors involved in drug resistance. Future studies should explore other

signalling pathways contributing to oxaliplatin resistance, such as the PI3K/AKT, the Nrf2 activation (Yang et al., 2015), the nuclear factor- κ B (NF- κ B) (Ke et al., 2013) and the MAPK pathways (Kim et al., 2019; Li et al., 2023), which are often upregulated in chemo-resistant cancer cells. Targeting these pathways in conjunction with MRP2 inhibition may enhance the therapeutic efficacy of oxaliplatin and improve patient outcomes.

Nuclear factor-erythroid 2 p45-related factor 2 (Nrf2) is a transcription factor that binds to antioxidant response element (ARE) sequences in promoter regions, driving gene transcription. The MAPK and PI3K/Akt pathways have been shown to transmit signals via Smad, STAT3, NF- κ B, or β -catenin to activate the transcription of Snail1 and Twist1, two transcription factors involved in promoting metastasis (Cheng et al., 2008; Šošić et al., 2003). In addition to regulating transcription, these pathways also influence the post-translational modification of Snail1 and Twist1. Specifically, MAPK phosphorylates Twist1 at Ser68, leading to its stabilization (Hong et al., 2011). Chrysin may reduce MRP2 surface expression by inhibiting the PI3K/AKT pathway, a known regulator of the MRP2 transporter (Kang et al., 2010; Wu et al., 2016). However, the involvement of other signalling pathways in oxaliplatin resistance in GI cancers remains unclear. Additionally, chrysin is known to inhibit NF- κ B activity, which is a downstream effector of PI3K/AKT signalling (Cho et al., 2016). However, it has not been conclusively shown that chrysin directly inhibits NF- κ B, which in turn modulates PI3K/AKT signalling. Investigating whether chrysin inhibits the PI3K/AKT pathway and how this relates to MRP2 surface and total protein downregulation would be valuable, as the PI3K/AKT pathway is implicated in regulating MRP2 expression.

7.3.3. Inhibition of other efflux transporters

In addition to MRP2, other efflux transporters such as P-glycoprotein (P-gp) and BCRP (ABCG2) are also implicated in multidrug resistance. Investigating the potential of chrysin and other phytochemicals to inhibit these transporters could broaden the scope of therapeutic strategies against drug-resistant GI cancers. Combination therapies that inhibit multiple transporters may

offer a more comprehensive approach to overcoming drug resistance.

Platinum-based drugs such as oxaliplatin are vital in the clinical management of gastrointestinal (GI) cancers, particularly colorectal and pancreatic cancers. Several transporters responsible for oxaliplatin transport contribute to its response and sensitivity in GI tumours. Research has established clinical correlations between the expression of oxaliplatin transporters and patient responses to the drug. For instance, the MRP2 transporter shows differential expression among colorectal cancer patients who responded to FOLFOX chemotherapy (Tsuji et al., 2012). Numerous candidate genes encoding oxaliplatin transporters, including proteins from the ABC transporter family, SLC transporters, and the ATPase membrane protein superfamily, have demonstrated oxaliplatin transport activity *in vitro* (Hector et al., 2001). It is possible that the expression of other transporter genes interferes with the efficacy of oxaliplatin or oxaliplatin-based chemotherapy. However, it remains unclear which transporter plays the most critical role in determining clinical responses to oxaliplatin in GI cancer. Current studies strongly support the role of ATP7A and ATP7B in mediating platinum drug resistance, suggesting they could serve as biomarkers for predicting the sensitivity to oxaliplatin-based chemotherapy in GI cancers (Li et al., 2018). ATP7A and ATP7B may contribute to platinum resistance through mechanisms such as drug sequestration, efflux, or modulation of intracellular copper levels in platinum-resistant cells (Li et al., 2018). Nevertheless, the precise mechanisms remain uncertain, and further research is required to clarify the roles of ATP7A and ATP7B. Additionally, exploring other efflux transporters in the human genome as potential biomarkers could be valuable for identifying differential expression in GI cancer patients undergoing oxaliplatin-based chemotherapy.

7.3.4. Nanotechnology-based drug delivery

Nanotechnology-based drug delivery systems could enhance the specificity and efficacy of oxaliplatin and other chemotherapeutics in GI cancers. Future research should focus on developing nanoparticle formulations that co-deliver oxaliplatin and MRP2 inhibitors like chrysin. This approach could potentially reduce systemic toxicity, improve drug bioavailability, and ensure

more targeted delivery to cancer cells, thereby overcoming resistance mechanisms more effectively.

The delivery of oxaliplatin in combination with MRP2 gene-specific siRNA or inhibitors presents significant challenges, primarily due to the high risk of siRNA degradation owing to its small size. However, utilizing drug delivery systems such as nanoparticles or nano-liposomal formulations has proven effective. Encapsulating both siRNA or MRP2-specific inhibitors and the anticancer drug, and targeting these formulations to tumor sites, offers several advantages over traditional drug solutions. This approach enhances drug accumulation in tumor tissues due to the enhanced permeability and retention (EPR) effect. Moreover, it reduces off-target side effects such as myelosuppression, neurotoxicity, or nephrotoxicity, which may result from ABC transporter inhibition in non-target tissues like bone marrow, the blood-brain barrier (BBB), or kidneys (Ahmad et al., 2016).

Nano-formulation delivery systems are particularly effective in targeting both anticancer drugs and efflux-pump inhibitors to tumor tissues, while simultaneously minimizing toxic effects on healthy tissues (Kapse-Mistry et al., 2014). The EPR effect is primarily driven by the inter-endothelial gaps within tumor vasculature, which result in leaky blood vessels that allow the passage of nano-scale particles to tumor sites, but not to healthy tissues. This makes passive targeting of nanoliposomes feasible. Utilizing nanoparticles loaded with drugs and siRNA or inhibitors addresses common issues such as toxicity, low specificity, and challenges in intracellular delivery (Z. Li et al., 2013; Ogawara et al., 2009). In addition to tumor targeting, nanoparticles can modulate the pharmacokinetics of the encapsulated drug, extending its plasma half-life and limiting drug distribution to healthy tissues. Nanoparticle-based drugs like Doxil and DaunoXome, which have received FDA approval, have demonstrated significant antitumor activity in colon cancer models in mice (Graudens et al., 2006). Therefore, future *in vitro* and *in vivo* studies should consider nanoliposome formulations combining oxaliplatin and MRP2 modulators. It would be particularly insightful to assess oxaliplatin's efficacy against GI tumors

and its toxicity to healthy cells when delivered through these advanced nano-liposomal systems.

7.3.5. Development of Experimental Model for Analysing Oxaliplatin Resistance in GI Cancer

It is becoming more and more sophisticated in human-compatible preclinical models of cancer, and will contribute to finding the role of the microbes in cancer. Recently, 3D cell culture is popular for anti-cancer drug research, which have a highly controlled environment for the cell lines, and is more close to the *in-vivo* situation (d. V. M et al., 2024).

Colon is one of the GI tracts in human body, and has a lot of microorganism *in vivo* environment. Microbiomes produce thousands of chemicals in our bodies. So, it is important to consider the real environment in human body. The design of *in vitro* experiment by Caco-2 cell and probiotics or/and chrysin co-culture is novel and important methodology.

Probiotics are live bacteria and yeasts that, when consumed in the right amounts, can promote the health of the small intestine. While the body can naturally host these beneficial microorganisms, excessive intake may cause gastrointestinal issues. Recent studies have shown that probiotics can aid in modulating the metabolic activity and composition of the gut microbiome; however, they are not sufficient on their own to produce significant clinical outcomes. It is also reported that a four-strain probiotic influences gut microbiota composition and metabolic activity, and increases anti-inflammatory cytokines (IL-6) production in human and rat GI tract models (M. N. M et al., 2024; Moens et al., 2019). Both the mRNA and protein levels of MRP2 / ABCC2 levels were reported to be significantly downregulated by IL-6 in human hepatocytes (Diao et al., 2010). However, it remains unclear whether probiotics could modulate cytokine production and thus MRP2 expression and oxaliplatin sensitivity in GI cancer cells.

The co-culture with Caco-2 cell lines and probiotics/chrysin was performed like others done before (Daguet, Pinheiro, Verhelst, Possemiers, & Marzorati, 2016; Moens et al., 2019), but makes some changes to suit my project. Seed the Caco-2 cells in 24-well semi-permeable inserts, which is 0.4 μm pore size, at a density of 1×10^5 cells per insert, then culture the cells for fourteen days, change completed medium 3 times every week, till obtaining a functional monolayer with a transepithelial electrical resistance (TEER) of more than $300 \Omega \text{ cm}^2$ (measured with a Millicell ERS-2 epithelial volt-ohm meter, Millipore). Completed medium preparation is the same as cell culture, 10% (v/v) FBS, 1% (v/v) P/S, and 1% (v/v) L-glutamine.

After the Caco-2 functional monolayer obtained. Place the Caco-2 bearing inserts on the top of the 24-well plates. The apical side contained Caco-2 cells, and colonic SHIME media (diluted in Caco-2 completed medium, 1:5 (v/v)), which was sterile-filtered (0.22 μm). Cells were treated apically with probiotics or/and chrysin. The basolateral compartment was filled with Caco-2 in complete medium containing anti-cancer drugs. Treat the cells for 24 hours, 48 hours, and 72 hours respectively, and then measure the TEER. The supernatant from basolateral part was then discarded or to be waiting for testing metabolites. All measurements were performed in triplicate and cells were incubated at 37 °C with 5% CO₂/95% air.

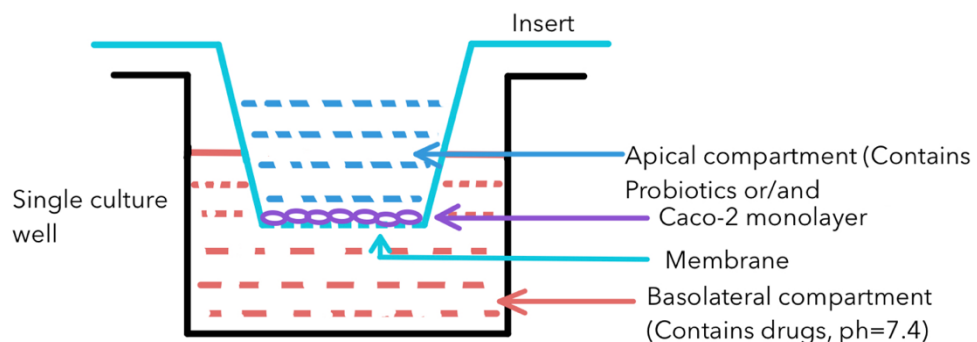


Figure 7- 1 Caco-2 cell and probiotics or/and chrysin co-culture

24-well semi-permeable inserts are designed to be used in this co-culture experiment, which is 0.4 μm pore size, at a density of 1×10^5 cells per insert, after seeding cells in the inserts, cells are cultured for fourteen days, change completed medium 3 times every week, till obtaining a functional monolayer with a transepithelial electrical resistance (TEER) of more than $300 \Omega \text{ cm}^2$

(measured with a Millicell ERS-2 epithelial volt-ohm meter, Millipore). Completed medium preparation is the same as cell culture, 10% (v/v) FBS, 1% (v/v) P/S, and 1% (v/v) L-glutamine. The apical side contained Caco-2 cells, and colonic SHIME media (diluted in Caco-2 completed medium, 1:5 (v/v)), which was sterile-filtered (0.22 μm). Cells were treated apically with probiotics or/and chrysin. The basolateral compartment was filled with Caco-2 in complete medium containing anti-cancer drugs.

7.4. Final conclusions

In conclusion, this thesis has shown that MRP2 plays a critical role in mediating resistance to oxaliplatin in GI cancers. The inhibition of MRP2 with chrysin significantly improves oxaliplatin accumulation and cytotoxicity in cancer cells, providing a potential avenue for overcoming chemoresistance. Future studies should focus on validating these findings *in vivo*, exploring the inhibition of other efflux transporters and signalling pathways, and developing advanced drug delivery systems. The results of this research have promising implications for improving chemotherapy outcomes in patients with GI cancers, particularly those who develop resistance to oxaliplatin.

References

- A, G., KLR, B., D, T., K, Y., N, S., L, A., X, C., R, E., MJ, H., Y, L., P, M., A, R., H, S., A, S., MVS, V., J, Y., X, Y., SW, Y., MJ, Z.-G.,...KM, G. (2024). *Membrane transporters in drug development and as determinants of precision medicine* (Vol. 23).
- Abraham, J., Edgerly, M., Wilson, R., Chen, C., Rutt, A., Bakke, S., Robey, R., Dwyer, A., Goldspiel, B., Balis, F., Van Tellingen, O., Bates, S. E., & Fojo, T. (2009). A phase I study of the P-glycoprotein antagonist tariquidar in combination with vinorelbine. *Clin Cancer Res*, 15(10), 3574-3582. <https://doi.org/10.1158/1078-0432.CCR-08-0938>
- Abrahamse, S. L., & Rechkemmer, G. (2001). Identification of an organic anion transport system in the human colon carcinoma cell line HT29 clone 19A. *Pflugers Arch*, 441(4), 529-537. <https://www.ncbi.nlm.nih.gov/pubmed/11212217>
- AD, G., RL, B., YE, C., LR, W., M, T., GC, F., PR, H., & A, D. (2006). *MRP2 (ABCC2) and cisplatin sensitivity in hepatocytes and human ovarian carcinoma* (Vol. 100).
- Adams, C. J., Boulton, C. H., Deadman, B. J., Farr, J. M., Grainger, M. N. C., Manley-Harris, M., & Snow, M. J. (2008). Isolation by HPLC and characterisation of the bioactive fraction of New Zealand manuka (*Leptospermum scoparium*) honey. *Carbohydrate Research*, 343(4), 651-659. <https://doi.org/https://doi.org/10.1016/j.carres.2007.12.011>
- Adamska, A., Elaskalani, O., Emmanouilidi, A., Kim, M., Abdol Razak, N. B., Metharom, P., & Falasca, M. (2018). Molecular and cellular mechanisms of chemoresistance in pancreatic cancer. *Adv Biol Regul*, 68, 77-87. <https://doi.org/10.1016/j.jbior.2017.11.007>
- Agarwal, S., Sane, R., Gallardo, J. L., Ohlfest, J. R., & Elmquist, W. F. (2010). Distribution of gefitinib to the brain is limited by P-glycoprotein (ABCB1) and breast cancer resistance protein (ABCG2)-mediated active efflux. *J Pharmacol Exp Ther*, 334(1), 147-155. <https://doi.org/10.1124/jpet.110.167601>
- Ahmad, J., Akhter, S., Greig, N. H., Kamal, M. A., Midoux, P., & Pichon, C. (2016). Engineered Nanoparticles Against MDR in Cancer: The State of the Art and its Prospective. *Curr Pharm Des*, 22(28), 4360-4373. <https://www.ncbi.nlm.nih.gov/pubmed/27319945>
- Al-Waili, N. S., Salom, K. Y., Al-Waili, F. S., Akmal, M., Ali, A., & Al Ghamdi, A. A. *Effects of natural honey on polymicrobial culture of various human pathogens* (Vol. 10). Termedia Publishing House Ltd.
- Albertella, M. R., Green, C. M., Lehmann, A. R., & O'Connor, M. J. (2005). A role for polymerase eta in the cellular tolerance to cisplatin-induced damage. *Cancer Res*, 65(21), 9799-9806. <https://doi.org/10.1158/0008-5472.CAN-05-1095>
- Alcindor, T., & Beauger, N. (2011). Oxaliplatin: a review in the era of molecularly targeted therapy. *Curr Oncol*, 18(1), 18-25. <https://www.ncbi.nlm.nih.gov/pubmed/21331278>
- Allen, R. T., Hunter, W. J., 3rd, & Agrawal, D. K. (1997). Morphological and biochemical characterization and analysis of apoptosis. *J Pharmacol Toxicol Methods*, 37(4), 215-228. <https://www.ncbi.nlm.nih.gov/pubmed/9279777>

- American Cancer Society. (2015). *What Causes Cancer?* Retrieved 25 May from <http://www.cancer.org/cancer/cancercauses/index>
- American cancer society : *Treatments and side effects.* <https://www.cancer.org/treatment/treatments-and-side-effects/treatment-types/chemotherapy.html>
- An, Q., Zhou, Z., Xu, C., & Xiao, Q. (2024). *Exosomes derived from mir-337-3p over-expressing tendon stem cells protect against apoptosis of tenocytes via targeting caspase3* (Vol. 25).
- Anand, K. V., Mohamed Jaabir, M. S., Thomas, P. A., & Geraldine, P. (2012). Protective role of chrysin against oxidative stress in d-galactose-induced aging in an experimental rat model. *Geriatr Gerontol Int*, 12(4), 741-750. <https://doi.org/10.1111/j.1447-0594.2012.00843.x>
- Andersen, V., Vogel, L. K., Kopp, T. I., Saebo, M., Nonboe, A. W., Hamfjord, J., Kure, E. H., & Vogel, U. (2015). High ABCC2 and low ABCG2 gene expression are early events in the colorectal adenoma-carcinoma sequence. *PLoS One*, 10(3), e0119255. <https://doi.org/10.1371/journal.pone.0119255>
- André, T., Boni, C., Mounedji-Boudiaf, L., Navarro, M., Tabernero, J., Hickish, T., Topham, C., Zaninelli, M., Clingan, P., Bridgewater, J., Tabah-Fisch, I., & de Gramont, A. (2004). Oxaliplatin, fluorouracil, and leucovorin as adjuvant treatment for colon cancer. *N Engl J Med*, 350(23), 2343-2351. <https://doi.org/10.1056/NEJMoa032709>
- Andre, T., Boni, C., Mounedji-Boudiaf, L., Navarro, M., Tabernero, J., Hickish, T., Topham, C., Zaninelli, M., Clingan, P., Bridgewater, J., Tabah-Fisch, I., de Gramont, A., & Multicenter International Study of Oxaliplatin/5-Fluorouracil/Leucovorin in the Adjuvant Treatment of Colon Cancer, I. (2004). Oxaliplatin, fluorouracil, and leucovorin as adjuvant treatment for colon cancer. *N Engl J Med*, 350(23), 2343-2351. <https://doi.org/10.1056/NEJMoa032709>
- Andre, T., Boni, C., Navarro, M., Tabernero, J., Hickish, T., Topham, C., Bonetti, A., Clingan, P., Bridgewater, J., Rivera, F., & de Gramont, A. (2009). Improved overall survival with oxaliplatin, fluorouracil, and leucovorin as adjuvant treatment in stage II or III colon cancer in the MOSAIC trial. *J Clin Oncol*, 27(19), 3109-3116. <https://doi.org/10.1200/JCO.2008.20.6771>
- Andre, T., Tournigand, C., Rosmorduc, O., Provent, S., Maindrault-Goebel, F., Avenin, D., Selle, F., Paye, F., Hannoun, L., Houry, S., Gayet, B., Lotz, J. P., de Gramont, A., Louvet, C., & Group, G. (2004). Gemcitabine combined with oxaliplatin (GEMOX) in advanced biliary tract adenocarcinoma: a GERCOR study. *Ann Oncol*, 15(9), 1339-1343. <https://doi.org/10.1093/annonc/mdh351>
- Arana, M. R., Tocchetti, G. N., Rigalli, J. P., Mottino, A. D., & Villanueva, S. S. (2016). Physiological and pathophysiological factors affecting the expression and activity of the drug transporter MRP2 in intestine. Impact on its function as membrane barrier. *Pharmacol Res*, 109, 32-44. <https://doi.org/10.1016/j.phrs.2016.04.014>
- Arkenau, H. T., Arnold, D., Cassidy, J., Diaz-Rubio, E., Douillard, J. Y., Hochster, H., Martoni, A., Grothey, A., Hinke, A., Schmiegel, W., Schmoll, H. J., & Porschen, R. (2008). Efficacy of

- oxaliplatin plus capecitabine or infusional fluorouracil/leucovorin in patients with metastatic colorectal cancer: a pooled analysis of randomized trials. *J Clin Oncol*, 26(36), 5910-5917. <https://doi.org/10.1200/JCO.2008.16.7759>
- Arnould, S., Hennebelle, I., Canal, P., Bugat, R., & Guichard, S. (2003). Cellular determinants of oxaliplatin sensitivity in colon cancer cell lines. *Eur J Cancer*, 39(1), 112-119. <https://www.ncbi.nlm.nih.gov/pubmed/12504667>
- Bates, S. E., Bakke, S., Kang, M., Robey, R. W., Zhai, S., Thambi, P., Chen, C. C., Patil, S., Smith, T., Steinberg, S. M., Merino, M., Goldspiel, B., Meadows, B., Stein, W. D., Choyke, P., Balis, F., Figg, W. D., & Fojo, T. (2004). A phase I/II study of infusional vinblastine with the P-glycoprotein antagonist valspodar (PSC 833) in renal cell carcinoma. *Clin Cancer Res*, 10(14), 4724-4733. <https://doi.org/10.1158/1078-0432.CCR-0829-03>
- Bates, S. E., Robey, R., Miyake, K., Rao, K., Ross, D. D., & Litman, T. (2001). The role of half-transporters in multidrug resistance. *Journal of bioenergetics and biomembranes*, 33(6), 503-511.
- Beretta, G. L., Benedetti, V., Cossa, G., Assaraf, Y. G., Bram, E., Gatti, L., Corna, E., Carenini, N., Colangelo, D., Howell, S. B., Zunino, F., & Perego, P. (2010). Increased levels and defective glycosylation of MRPs in ovarian carcinoma cells resistant to oxaliplatin. *Biochem Pharmacol*, 79(8), 1108-1117. <https://doi.org/10.1016/j.bcp.2009.12.002>
- Bernhard, J., Dietrich, D., Scheithauer, W., Gerber, D., Bodoky, G., Ruhstaller, T., Glimelius, B., Bajetta, E., Schuller, J., Saletti, P., Bauer, J., Figer, A., Pestalozzi, B. C., Kohne, C. H., Mingrone, W., Stemmer, S. M., Tamas, K., Kornek, G. V., Koeberle, D.,...Central European Cooperative Oncology, G. (2008). Clinical benefit and quality of life in patients with advanced pancreatic cancer receiving gemcitabine plus capecitabine versus gemcitabine alone: a randomized multicenter phase III clinical trial--SAKK 44/00-CECOG/PAN.1.3.001. *J Clin Oncol*, 26(22), 3695-3701. <https://doi.org/10.1200/JCO.2007.15.6240>
- Binks, S. P., & Dobrota, M. (1990). Kinetics and mechanism of uptake of platinum-based pharmaceuticals by the rat small intestine. *Biochemical Pharmacology*, 40(6), 1329-1336.
- Biswas, R., Bugde, P., He, J., Merien, F., Lu, J., Liu, D.-X., Myint, K., Liu, J., McKeage, M., & Li, Y. (2019). Transport-Mediated Oxaliplatin Resistance Associated with Endogenous Overexpression of MRP2 in Caco-2 and PANC-1 Cells. In (Vol. 11).
- Biswas, R., Bugde, P., He, J., Merien, F., Lu, J., Liu, D. X., Myint, K., Liu, J., McKeage, M. J., & Li, Y. (2019). Transport-mediated oxaliplatin resistance associated with endogenous overexpression of MRP2 in Caco-2 and PANC-1 cells. *Cancers (Basel)*, 11(9), 1330. <https://doi.org/10.3390/cancers11091330>
- Bjelakovic, G., Nikolova, D., Simonetti, R. G., & Glud, C. (2008). Antioxidant supplements for preventing gastrointestinal cancers. *Cochrane Database Syst Rev*(3), CD004183. <https://doi.org/10.1002/14651858.CD004183.pub3>
- Bjelakovic, G., Nikolova, D., Simonetti, R. G., & Glud, C. (2008). Antioxidant supplements for preventing gastrointestinal cancers. *The Cochrane Database Of Systematic Reviews*(3), CD004183. <https://doi.org/10.1002/14651858.CD004183.pub3>

- Bohanes, P., Labonte, M. J., & Lenz, H. J. (2011). A review of excision repair cross-complementation group 1 in colorectal cancer. *Clin Colorectal Cancer*, 10(3), 157-164. <https://doi.org/10.1016/j.clcc.2011.03.024>
- Boige, V., Raoul, J. L., Pignon, J. P., Bouché, O., Blanc, J. F., Dahan, L., Jouve, J. L., Dupouy, N., & Ducreux, M. (2007). Multicentre phase II trial of capecitabine plus oxaliplatin (XELOX) in patients with advanced hepatocellular carcinoma: FFCD 03-03 trial. *Br J Cancer*, 97(7), 862-867. <https://doi.org/10.1038/sj.bjc.6603956>
- Borst, P., & Elferink, R. O. (2002a). Mammalian ABC transporters in health and disease. In (Vol. 71, pp. 537-592).
- Borst, P., & Elferink, R. O. (2002b). Mammalian ABC transporters in health and disease. *Annu Rev Biochem*, 71, 537-592. <https://doi.org/10.1146/annurev.biochem.71.102301.093055>
- Borst, P., Evers, R., Kool, M., & Wijnholds, J. (1999). The multidrug resistance protein family. *Biochimica et Biophysica Acta (BBA) - Biomembranes*, 1461(2), 347-357. [https://doi.org/https://doi.org/10.1016/S0005-2736\(99\)00167-4](https://doi.org/https://doi.org/10.1016/S0005-2736(99)00167-4)
- Bouyahya, A., El Omari, N., Bakrim, S., El Hachlafi, N., Balahbib, A., Wilairatana, P., & Mubarak, M. S. (2022). *Advances in Dietary Phenolic Compounds to Improve Chemosensitivity of Anticancer Drugs* (Vol. 14).
- Boyer, J., McLean, E. G., Aroori, S., Wilson, P., McCulla, A., Carey, P. D., Longley, D. B., & Johnston, P. G. (2004). Characterization of p53 wild-type and null isogenic colorectal cancer cell lines resistant to 5-fluorouracil, oxaliplatin, and irinotecan. *Clin Cancer Res*, 10(6), 2158-2167. <https://www.ncbi.nlm.nih.gov/pubmed/15041737>
- Bray, F., Laversanne, M., Sung, H., Ferlay, J., Siegel, R. L., Soerjomataram, I., & Jemal, A. (2024). *Global cancer statistics 2022: GLOBOCAN estimates of incidence and mortality worldwide for 36 cancers in 185 countries*.
- Bray, F., Ren, J. S., Masuyer, E., & Ferlay, J. (2013). Global estimates of cancer prevalence for 27 sites in the adult population in 2008. *International Journal of Cancer*, 132(5), 1133-1145.
- Brown, E., Hurd, N. S., McCall, S., & Ceremuga, T. E. (2007). Evaluation of the anxiolytic effects of chrysin, a *Passiflora incarnata* extract, in the laboratory rat. *Aana j*, 75(5), 333-337.
- Bugde, P., Biswas, R., Merien, F., Lu, J., Liu, D. X., Chen, M., Zhou, S., & Li, Y. (2017). The therapeutic potential of targeting ABC transporters to combat multi-drug resistance. *Expert Opin Ther Targets*, 21(5), 511-530. <https://doi.org/10.1080/14728222.2017.1310841>
- Bukhari, N., & Winqvist, E. (2017). Chronic Oxaliplatin-Based Chemotherapy in a Primary Ampullary Adenocarcinoma Patient without Significant Peripheral Neuropathy: Case Report and Literature Review. *Case Rep Oncol*, 10(2), 577-581. <https://doi.org/10.1159/000477841>
- Busch, W., & Saier, M. H., Jr. (2002). The transporter classification (TC) system, 2002. *Crit Rev Biochem Mol Biol*, 37(5), 287-337. <https://doi.org/10.1080/10409230290771528>

- Bush, J. A., & Li, G. (2002). Cancer chemoresistance: the relationship between p53 and multidrug transporters. *Int J Cancer*, 98(3), 323-330. <https://www.ncbi.nlm.nih.gov/pubmed/11920581>
- Campa, D., Muller, P., Edler, L., Knoefel, L., Barale, R., Heussel, C. P., Thomas, M., Canzian, F., & Risch, A. (2012). A comprehensive study of polymorphisms in ABCB1, ABCC2 and ABCG2 and lung cancer chemotherapy response and prognosis. *Int J Cancer*, 131(12), 2920-2928. <https://doi.org/10.1002/ijc.27567>
- Cancer research UK. (2015, 25 May). *Cancer Worldwide*. <http://www.cancerresearchuk.org/cancer-info/cancerstats/world/>
- Cancer Statistics*. (2018). <https://www.cancer.gov/about-cancer/understanding/statistics>
- Cancer Statistics 2015*. (2018). <http://www.cancerresearchuk.org/health-professional/cancer-statistics-for-the-uk>
- Cancer: New registration and deaths 2013*. (2017). <https://www.health.govt.nz/publication/cancer-new-registrations-and-deaths-2013>
- Cassidy, J., Clarke, S., Diaz-Rubio, E., Scheithauer, W., Figer, A., Wong, R., Koski, S., Lichinitser, M., Yang, T. S., Rivera, F., Couture, F., Sirzen, F., & Saltz, L. (2008). Randomized phase III study of capecitabine plus oxaliplatin compared with fluorouracil/folinic acid plus oxaliplatin as first-line therapy for metastatic colorectal cancer. *J Clin Oncol*, 26(12), 2006-2012. <https://doi.org/10.1200/JCO.2007.14.9898>
- Cassidy, J., Tabernero, J., Twelves, C., Brunet, R., Butts, C., Conroy, T., Debraud, F., Figer, A., Grossmann, J., Sawada, N., Schoffski, P., Sobrero, A., Van Cutsem, E., & Diaz-Rubio, E. (2004). XELOX (capecitabine plus oxaliplatin): active first-line therapy for patients with metastatic colorectal cancer. *J Clin Oncol*, 22(11), 2084-2091. <https://doi.org/10.1200/JCO.2004.11.069>
- Cassidy, J., Tabernero, J., Twelves, C., Brunet, R., Butts, C., Conroy, T., Debraud, F., Figer, A., Grossmann, J., Sawada, N., Schöffski, P., Sobrero, A., Van Cutsem, E., & Díaz-Rubio, E. (2004). XELOX (capecitabine plus oxaliplatin): active first-line therapy for patients with metastatic colorectal cancer. *J Clin Oncol*, 22(11), 2084-2091. <https://doi.org/10.1200/jco.2004.11.069>
- Castro, A. F., & Altenberg, G. A. (1997). Inhibition of drug transport by genistein in multidrug-resistant cells expressing P-glycoprotein [Article]. *Biochemical Pharmacology*, 53(1), 89-93. [https://doi.org/10.1016/S0006-2952\(96\)00657-0](https://doi.org/10.1016/S0006-2952(96)00657-0)
- Ceballos, M. P., Rigalli, J. P., Cere, L. I., Semeniuk, M., Catania, V. A., & Ruiz, M. L. (2018). ABC transporters: Regulation and association with multidrug resistance in hepatocellular carcinoma and colorectal carcinoma. *Curr Med Chem*. <https://doi.org/10.2174/0929867325666180105103637>
- Cecchin, E., D'Andrea, M., Lonardi, S., Zanusso, C., Pella, N., Errante, D., De Mattia, E., Polesel, J., Innocenti, F., & Toffoli, G. (2013). A prospective validation pharmacogenomic study in the adjuvant setting of colorectal cancer patients treated with the 5-

- fluorouracil/leucovorin/oxaliplatin (FOLFOX4) regimen. *Pharmacogenomics J*, 13(5), 403-409. <https://doi.org/10.1038/tpj.2012.31>
- Chan, C. Y., & Li, Y. (2016). *Anti-proliferative effects induced by New Zealand honey in colorectal cancer: a thesis submitted to the Faculty of Health and Environmental Sciences of Auckland University of Technology in fulfilment of the requirements for the degree of Master of Philosophy (MPhil), 2016* [Electronic document]. <https://ezproxy.aut.ac.nz/login?url=https://search.ebscohost.com/login.aspx?direct=true&db=cab05020a&AN=aut.b27848875&site=eds-live>; <http://hdl.handle.net/10292/9990>
- Chan, L. M., Lowes, S., & Hirst, B. H. (2004). The ABCs of drug transport in intestine and liver: efflux proteins limiting drug absorption and bioavailability. *Eur J Pharm Sci*, 21(1), 25-51. <https://www.ncbi.nlm.nih.gov/pubmed/14706810>
- Chemotherapy and You*. (2018). NIH. <https://www.cancer.gov/publications/patient-education/chemotherapy-and-you.pdf>
- Chemotherapy for Colorectal Cancer*. (2024). WebMD. <https://www.webmd.com/colorectal-cancer/chemotherapy#2>
- Chen, G., Durán, G. E., Steger, K. A., Lacayo, N. J., Jaffrézou, J. P., Dumontet, C., & Sikic, B. I. (1997). Multidrug-resistant human sarcoma cells with a mutant P-glycoprotein, altered phenotype, and resistance to cyclosporins. *The Journal Of Biological Chemistry*, 272(9), 5974-5982. <http://ezproxy.aut.ac.nz/login?url=http://search.ebscohost.com/login.aspx?direct=true&db=cmedm&AN=9038218&site=eds-live>
- Chen, Y.-H., Yang, Z.-S., Chang, Y.-S., Wang, B.-C., Hsiao, C.-A., Shih, T.-L., & Wen, C.-C. (2012). *Evaluation of the structure-activity relationship of flavonoids as antioxidants and toxicants of zebrafish larvae* (Vol. 134).
- Chen, Y., Agarwal, S., Shaik, N. M., Chen, C., Yang, Z., & Elmquist, W. F. (2009). P-glycoprotein and breast cancer resistance protein influence brain distribution of dasatinib. *J Pharmacol Exp Ther*, 330(3), 956-963. <https://doi.org/10.1124/jpet.109.154781>
- Chen, Z., Shi, T., Zhang, L., Zhu, P., Deng, M., Huang, C., Hu, T., Jiang, L., & Li, J. (2016). Mammalian drug efflux transporters of the ATP binding cassette (ABC) family in multidrug resistance: A review of the past decade. *Cancer Lett*, 370(1), 153-164. <https://doi.org/10.1016/j.canlet.2015.10.010>
- Chen, Z. S., Lee, K., & Kruh, G. D. (2001). Transport of cyclic nucleotides and estradiol 17-beta-D-glucuronide by multidrug resistance protein 4. Resistance to 6-mercaptopurine and 6-thioguanine. *The Journal Of Biological Chemistry*, 276(36), 33747-33754. <http://ezproxy.aut.ac.nz/login?url=http://search.ebscohost.com/login.aspx?direct=true&db=cmedm&AN=11447229&site=eds-live>
- Cheng, G. Z., Zhang, W., Sun, M., Wang, Q., Coppola, D., Mansour, M., Xu, L., Costanzo, C., Cheng, J. Q., & Wang, L.-H. (2008). Twist Is Transcriptionally Induced by Activation of STAT3 and

- Mediates STAT3 Oncogenic Function. *Journal of Biological Chemistry*, 283(21), 14665-14673. <https://doi.org/10.1074/jbc.m707429200>
- Cho, B. O., Yin, H. H., Park, S. H., Byun, E. B., Ha, H. Y., & Jang, S. I. (2016). Anti-inflammatory activity of myricetin from *Diospyros lotus* through suppression of NF-kappaB and STAT1 activation and Nrf2-mediated HO-1 induction in lipopolysaccharide-stimulated RAW264.7 macrophages. *Biosci Biotechnol Biochem*, 80(8), 1520-1530. <https://doi.org/10.1080/09168451.2016.1171697>
- Choi, Y. H., & Yu, A. M. (2014). ABC transporters in multidrug resistance and pharmacokinetics, and strategies for drug development. *Curr Pharm Des*, 20(5), 793-807. <https://www.ncbi.nlm.nih.gov/pubmed/23688078>
- Christopher A, M., & Richard, C. (2007). How can we best use structural information on P-glycoprotein to design inhibitors? *Pharmacology & Therapeutics*(2), 429. <https://doi.org/10.1016/j.pharmthera.2006.10.003>
- Cianciosi, D., Forbes-Hernández, T. Y., Afrin, S., Gasparri, M., Reboredo-Rodríguez, P., Manna, P. P., Zhang, J., Lamas, L. B., Flórez, S. M., Toyos, P. A., Quiles, J. L., Giampieri, F., & Battino, M. (2018). *Phenolic Compounds in Honey and Their Associated Health Benefits: A Review* (Vol. 23).
- Ciarimboli, G., Deuster, D., Knief, A., Sperling, M., Holtkamp, M., Edemir, B., Pavenstadt, H., Lanvers-Kaminsky, C., am Zehnhoff-Dinnesen, A., Schinkel, A. H., Koepsell, H., Jurgens, H., & Schlatter, E. (2010). Organic cation transporter 2 mediates cisplatin-induced ototoxicity and nephrotoxicity and is a target for protective interventions. *Am J Pathol*, 176(3), 1169-1180. <https://doi.org/10.2353/ajpath.2010.090610>
- Ciarimboli, G., Ludwig, T., Lang, D., Pavenstadt, H., Koepsell, H., Piechota, H. J., Haier, J., Jaehde, U., Zisowsky, J., & Schlatter, E. (2005). Cisplatin nephrotoxicity is critically mediated via the human organic cation transporter 2. *Am J Pathol*, 167(6), 1477-1484. [https://doi.org/10.1016/S0002-9440\(10\)61234-5](https://doi.org/10.1016/S0002-9440(10)61234-5)
- Clark, T. A., Butler, K., & Wilson, D. R. (2024). *Gut microbiome and health: Learn about the connections to improve care* (Vol. 19).
- Cole, S. P. C., Bhardwaj, G., Gerlach, J. H., Mackie, J. E., Grant, C. E., Almquist, K. C., Stewart, A. J., Kurz, E. U., Duncan, A. M. V., & Deeley, R. G. (1992). Overexpression of a Transporter Gene in a Multidrug-Resistant Human Lung Cancer Cell Line [research-article]. *Science*, 258(5088), 1650. <http://ezproxy.aut.ac.nz/login?url=http://search.ebscohost.com/login.aspx?direct=true&db=edsjrs&AN=edsjrs.2882074&site=eds-live>
- Coley, H. M. (2010). Overcoming multidrug resistance in cancer: clinical studies of p-glycoprotein inhibitors. *Methods Mol Biol*, 596, 341-358. https://doi.org/10.1007/978-1-60761-416-6_15
- Colombo, F., Armstrong, C., Duan, J., & Rioux, N. (2012). A high throughput in vitro mrp2 assay to predict in vivo biliary excretion. *Xenobiotica*, 42(2), 157-163. <https://doi.org/10.3109/00498254.2011.614021>

- Colombo, F., Poirier, H., Rioux, N., Montecillo, M. A., Duan, J., & Ribadeneira, M. D. (2013). A membrane vesicle-based assay to enable prediction of human biliary excretion. *Xenobiotica*, 43(10), 915-919. <https://doi.org/10.3109/00498254.2013.769649>
- Conroy, T., Desseigne, F., Ychou, M., Bouché, O., Guimbaud, R., Bécouarn, Y., Adenis, A., Raoul, J.-L., Gourgou-Bourgade, S., & de la Fouchardière, C. (2011). FOLFIRINOX versus gemcitabine for metastatic pancreatic cancer. *New England Journal of Medicine*, 364(19), 1817-1825.
- Conroy, T., Desseigne, F., Ychou, M., Bouché, O., Guimbaud, R., Bécouarn, Y., Adenis, A., Raoul, J. L., Gourgou-Bourgade, S., de la Fouchardière, C., Bennouna, J., Bachet, J. B., Khemissa-Akouz, F., Péré-Vergé, D., Delbaldo, C., Assenat, E., Chauffert, B., Michel, P., Montoto-Grillot, C., & Ducreux, M. (2011). FOLFIRINOX versus gemcitabine for metastatic pancreatic cancer. *N Engl J Med*, 364(19), 1817-1825. <https://doi.org/10.1056/NEJMoa1011923>
- Conroy, T., Gavaille, C., Samalin, E., Ychou, M., & Ducreux, M. (2013). The role of the FOLFIRINOX regimen for advanced pancreatic cancer. *Curr Oncol Rep*, 15(2), 182-189. <https://doi.org/10.1007/s11912-012-0290-4>
- Cooper, R. A., Jenkins, L., Henriques, A. F. M., Duggan, R. S., & Burton, N. F. (2010). *Absence of bacterial resistance to medical-grade manuka honey* (Vol. 29).
- Coriat, R., Mir, O., Cessot, A., Brezault, C., Ropert, S., Durand, J. P., Cacheux, W., Chaussade, S., & Goldwasser, F. (2012). Feasibility of oxaliplatin, 5-fluorouracil and leucovorin (FOLFOX-4) in cirrhotic or liver transplant patients: experience in a cohort of advanced hepatocellular carcinoma patients. *Invest New Drugs*, 30(1), 376-381. <https://doi.org/10.1007/s10637-010-9525-0>
- Courtney, R. (2015). The Health Consequences of Smoking-50 Years of Progress: A Report of the Surgeon General, 2014. *Drug & Alcohol Review*, 34(6), 694-695. <http://ezproxy.aut.ac.nz/login?url=http://search.ebscohost.com/login.aspx?direct=true&db=s3h&AN=110482745&site=eds-live>
- Cree, I. A., & Charlton, P. (2017). Molecular chess? Hallmarks of anti-cancer drug resistance. *BMC Cancer*, 17(1), 10. <https://doi.org/10.1186/s12885-016-2999-1>
- Critchfield, J. W., Butera, S. T., & Folks, T. M. (1996). Inhibition of HIV activation in latently infected cells by flavonoid compounds. *AIDS Res Hum Retroviruses*, 12(1), 39-46. <https://doi.org/10.1089/aid.1996.12.39>
- Cui, Y., König, J., Buchholz, J. K., Spring, H., Leier, I., & Keppler, D. (1999). Drug resistance and ATP-dependent conjugate transport mediated by the apical multidrug resistance protein, MRP2, permanently expressed in human and canine cells. *Mol Pharmacol*, 55(5), 929-937. <https://www.ncbi.nlm.nih.gov/pubmed/10220572>
- Cui, Y., König, J., Buchholz, J. K., Spring, H., Leier, I., & Keppler, D. (1999). Drug resistance and ATP-dependent conjugate transport mediated by the apical multidrug resistance protein, MRP2, permanently expressed in human and canine cells. *Mol Pharmacol*, 55(5), 929-937.

- Cui, Y. H., Konig, J., Buchholz, U., Spring, H., Leier, I., & Keppler, D. (1999). Drug resistance and ATP-dependent conjugate transport mediated by the apical multidrug resistance protein, MRP2, permanently expressed in human and canine cells. *Molecular Pharmacology*, 55(5), 929-937. <Go to ISI>://WOS:000080070200017
- Cunningham, D., Chau, I., Stocken, D. D., Valle, J. W., Smith, D., Steward, W., Harper, P. G., Dunn, J., Tudur-Smith, C., West, J., Falk, S., Crellin, A., Adab, F., Thompson, J., Leonard, P., Ostrowski, J., Eatock, M., Scheithauer, W., Herrmann, R., & Neoptolemos, J. P. (2009). Phase III randomized comparison of gemcitabine versus gemcitabine plus capecitabine in patients with advanced pancreatic cancer. *J Clin Oncol*, 27(33), 5513-5518. <https://doi.org/10.1200/JCO.2009.24.2446>
- Cunningham, D., Okines, A. F., & Ashley, S. (2010). Capecitabine and oxaliplatin for advanced esophagogastric cancer. *N Engl J Med*, 362(9), 858-859. <https://doi.org/10.1056/NEJMc0911925>
- Cunningham, D., Okines, A. F., & Ashley, S. (2010). Capecitabine and oxaliplatin for advanced esophagogastric cancer. *New England Journal of Medicine*, 362(9), 858-859.
- D, C., T, F.-H., Y, A. D., M, E.-Z., JL, Q., M, B., & F, G. (2024). *Manuka honey's anti-metastatic impact on colon cancer stem-like cells: unveiling its effects on epithelial-mesenchymal transition, angiogenesis and telomere length* (Vol. 15).
- da Silva, B., Caon, T., Mohr, E. T. B., Biluca, F. C., Gonzaga, L. V., Fett, R., Dalmarco, E. M., & Costa, A. C. O. (2022). *Phenolic profile and in vitro anti-inflammatory activity of Mimosa scabrella Bentham honeydew honey in RAW 264.7 murine macrophages* (Vol. 46).
- De Castro, W. V., Mertens-Talcott, S., Derendorf, H., & Butterweck, V. (2007). Grapefruit juice-drug interactions: Grapefruit juice and its components inhibit p-glycoprotein (ABCB1) mediated transport of talinolol in caco-2 cells. In (Vol. 96, pp. 2808-2817).
- de Gramont, A., Figuer, A., Seymour, M., Homerin, M., Hmissi, A., Cassidy, J., Boni, C., Cortes-Funes, H., Cervantes, A., Freyer, G., Papamichael, D., Le Bail, N., Louvet, C., Hendler, D., de Braud, F., Wilson, C., Morvan, F., & Bonetti, A. (2000). Leucovorin and fluorouracil with or without oxaliplatin as first-line treatment in advanced colorectal cancer. *J Clin Oncol*, 18(16), 2938-2947. <https://doi.org/10.1200/JCO.2000.18.16.2938>
- de Gramont, A., Figuer, A., Seymour, M., Homerin, M., Hmissi, A., Cassidy, J., Boni, C., Cortes-Funes, H., Cervantes, A., Freyer, G., Papamichael, D., Le Bail, N., Louvet, C., Hendler, D., de Braud, F., Wilson, C., Morvan, F., & Bonetti, A. (2023). Leucovorin and Fluorouracil With or Without Oxaliplatin as First-Line Treatment in Advanced Colorectal Cancer. *J Clin Oncol*, 41(33), 5080-5089. <https://doi.org/10.1200/jco.22.02773>
- Deli, J., Molnar, P., Matus, Z., & Toth, G. (2001). Carotenoid composition in the fruits of red paprika (*Capsicum annuum* var. *lycopersiforme rubrum*) during ripening; Biosynthesis of carotenoids in red paprika. In (Vol. 49, pp. 1517-1523).
- Diao, C., Cheng, R. C., Zhang, J. M., Wei, X. P., Su, Y. J., Liu, Q. Y., & Xu, J. B. (2008). [Clinical observation of XELOX (Capecitabine plus Oxaliplatin): an adjuvant chemotherapy regimen used in stage III colorectal cancer]. *Zhonghua Zhong Liu Za Zhi*, 30(2), 147-150.

- Diao, L., Li, N., Brayman, T. G., Hotz, K. J., & Lai, Y. (2010). Regulation of MRP2/ABCC2 and BSEP/ABCB11 expression in sandwich cultured human and rat hepatocytes exposed to inflammatory cytokines TNF- α , IL-6, and IL-1 β . *J Biol Chem*, 285(41), 31185-31192. <https://doi.org/10.1074/jbc.M110.107805>
- Dilruba, S., & Kalayda, G. V. (2016). Platinum-based drugs: past, present and future. *Cancer Chemother Pharmacol*, 77(6), 1103-1124. <https://doi.org/10.1007/s00280-016-2976-z>
- Drach, J., Gsur, A., Hamilton, G., Zhao, S., Angerler, J., Fiegl, M., Zojer, N., Raderer, M., Haberl, I., Andreeff, M., & Huber, H. (1996). Involvement of P-glycoprotein in the transmembrane transport of interleukin-2 (IL-2), IL-4, and interferon- γ in normal human T lymphocytes [Article]. *Blood*, 88(5), 1747-1754. <http://ezproxy.aut.ac.nz/login?url=http://search.ebscohost.com/login.aspx?direct=true&db=edselc&AN=edselc.2-52.0-9544240355&site=eds-live>
- Du, Q., Gu, X., Cai, J., Huang, M., & Su, M. (2012). Chrysin attenuates allergic airway inflammation by modulating the transcription factors T-bet and GATA-3 in mice. *Mol Med Rep*, 6(1), 100-104. <https://doi.org/10.3892/mmr.2012.893>
- Duarte, J., Jiménez, R., Villar, I. C., Jiménez, J., Pérez-Vizcaíno, F., & Tamargo, J. (2001). *Vasorelaxant effects of the bioflavonoid chrysin in isolated rat aorta* (Vol. 67).
- Ducreux, M., Bennouna, J., Hebbar, M., Ychou, M., Lledo, G., Conroy, T., Adenis, A., Faroux, R., Rebischung, C., Bergougnoux, L., Kockler, L., Douillard, J. Y., & Centers, G. I. G. o. t. F. A.-C. (2011). Capecitabine plus oxaliplatin (XELOX) versus 5-fluorouracil/leucovorin plus oxaliplatin (FOLFOX-6) as first-line treatment for metastatic colorectal cancer. *Int J Cancer*, 128(3), 682-690. <https://doi.org/10.1002/ijc.25369>
- Dudeja, P. K., Anderson, K. M., Harris, J. S., Buckingham, L., & Coon, J. S. (1995). Reversal of multidrug-resistance phenotype by surfactants: Relationship to membrane lipid fluidity [Article]. *Archives of Biochemistry and Biophysics*, 319(1), 309-315. <https://doi.org/10.1006/abbi.1995.1298>
- Ehrsson, H., Wallin, I., & Yachnin, J. (2002). Pharmacokinetics of oxaliplatin in humans. *Medical Oncology*, 19(4), 261-265.
- El-Awady, R., Saleh, E., Hashim, A., Soliman, N., Dallah, A., Elrasheed, A., & Elakraa, G. (2016). The Role of Eukaryotic and Prokaryotic ABC Transporter Family in Failure of Chemotherapy. *Front Pharmacol*, 7, 535. <https://doi.org/10.3389/fphar.2016.00535>
- El Khoury, F., Corcos, L., Durand, S., Simon, B., & Le Jossic-Corcos, C. (2016). Acquisition of anticancer drug resistance is partially associated with cancer stemness in human colon cancer cells. *Int J Oncol*, 49(6), 2558-2568. <https://doi.org/10.3892/ijo.2016.3725>
- Elinav, E., Garrett, W. S., Trinchieri, G., & Wargo, J. (2019). The cancer microbiome. *Nature Reviews Cancer*, 19(7), 371-376. <https://doi.org/10.1038/s41568-019-0155-3>
- Elinav, E., Garrett, W. S., Trinchieri, G., & Wargo, J. (2019). The cancer microbiome. *Nat Rev Cancer*, 19(7), 371-376. <https://doi.org/10.1038/s41568-019-0155-3>
- Evers, R., De Haas, M., Sparidans, R., Beijnen, J., Wielinga, P., Lankelma, J., & Borst, P. (2000).

Vinblastine and sulfinpyrazone export by the multidrug resistance protein MRP2 is associated with glutathione export. *British Journal of Cancer*, 83(3), 375.

F, V. S., A, P., F, M., & K, J. (2020). *Glucosamine reverses drug resistance in MRP2 overexpressing ovarian cancer cells* (Vol. 868).

Falcone, A., Ricci, S., Brunetti, I., Pfanner, E., Allegrini, G., Barbara, C., Crinò, L., Benedetti, G., Evangelista, W., Fanchini, L., Cortesi, E., Picone, V., Vitello, S., Chiara, S., Granetto, C., Porcile, G., Fioretto, L., Orlandini, C., Andreuccetti, M., & Masi, G. (2007). Phase III trial of infusional fluorouracil, leucovorin, oxaliplatin, and irinotecan (FOLFOXIRI) compared with infusional fluorouracil, leucovorin, and irinotecan (FOLFIRI) as first-line treatment for metastatic colorectal cancer: the Gruppo Oncologico Nord Ovest. *J Clin Oncol*, 25(13), 1670-1676. <https://doi.org/10.1200/jco.2006.09.0928>

Falcone, A., Ricci, S., Brunetti, I., Pfanner, E., Allegrini, G., Barbara, C., Crino, L., Benedetti, G., Evangelista, W., Fanchini, L., Cortesi, E., Picone, V., Vitello, S., Chiara, S., Granetto, C., Porcile, G., Fioretto, L., Orlandini, C., Andreuccetti, M.,...Gruppo Oncologico Nord, O. (2007). Phase III trial of infusional fluorouracil, leucovorin, oxaliplatin, and irinotecan (FOLFOXIRI) compared with infusional fluorouracil, leucovorin, and irinotecan (FOLFIRI) as first-line treatment for metastatic colorectal cancer: the Gruppo Oncologico Nord Ovest. *J Clin Oncol*, 25(13), 1670-1676. <https://doi.org/10.1200/JCO.2006.09.0928>

Fang, N. B., Yu, S. G., & Prior, R. L. (2002). LC/MS/MS characterization of phenolic constituents in dried plums. In (Vol. 50, pp. 3579-3585).

Ferlay, J., Soerjomataram, I., Dikshit, R., Eser, S., Mathers, C., Rebelo, M., Parkin, D. M., Forman, D., & Bray, F. (2015). Cancer incidence and mortality worldwide: sources, methods and major patterns in GLOBOCAN 2012. *Int J Cancer*, 136(5), E359-386. <https://doi.org/10.1002/ijc.29210>

Fink, D., Nebel, S., Aebi, S., Zheng, H., Cenni, B., Nehme, A., Christen, R. D., & Howell, S. B. (1996). The role of DNA mismatch repair in platinum drug resistance. *Cancer Res*, 56(21), 4881-4886. <https://www.ncbi.nlm.nih.gov/pubmed/8895738>

Fink, D., Nebel, S., Aebi, S., Zheng, H., Cenni, B., Nehmé, A., Christen, R. D., & Howell, S. B. (1996). The role of DNA mismatch repair in platinum drug resistance. *Cancer Research*, 56(21), 4881-4886. <http://ezproxy.aut.ac.nz/login?url=http://search.ebscohost.com/login.aspx?direct=true&db=cmedm&AN=8895738&site=eds-live>

Flens, M. J., Zaman, G., Van der Valk, P., Izquierdo, M. A., Schroeijers, A. B., Scheffer, G. L., Van der Groep, P., de Haas, M., Meijer, C., & Scheper, R. J. (1996). Tissue distribution of the multidrug resistance protein. *The American journal of pathology*, 148(4), 1237.

Fletcher, J. I., Haber, M., Henderson, M. J., & Norris, M. D. (2010). ABC transporters in cancer: more than just drug efflux pumps. *Nat Rev Cancer*, 10(2), 147-156. <https://doi.org/10.1038/nrc2789>

Folmer, Y., Schneider, M., Blum, H. E., & Hafkemeyer, P. (2007). Reversal of drug resistance of hepatocellular carcinoma cells by adenoviral delivery of anti-ABCC2 antisense

- constructs. *Cancer Gene Ther*, 14(11), 875-884. <https://doi.org/10.1038/sj.cgt.7701082>
- Fox, E., & Bates, S. E. (2007). Tariquidar (XR9576): a P-glycoprotein drug efflux pump inhibitor. *Expert Rev Anticancer Ther*, 7(4), 447-459. <https://doi.org/10.1586/14737140.7.4.447>
- Fox, E., Widemann, B. C., Pastakia, D., Chen, C. C., Yang, S. X., Cole, D., & Balis, F. M. (2015). Pharmacokinetic and pharmacodynamic study of tariquidar (XR9576), a P-glycoprotein inhibitor, in combination with doxorubicin, vinorelbine, or docetaxel in children and adolescents with refractory solid tumors. In (Vol. 76, pp. 1273-1283).
- Friedl, P., & Alexander, S. (2011). Cancer invasion and the microenvironment: Plasticity and reciprocity [Review]. *Cell*, 147(5), 992-1009. <https://doi.org/10.1016/j.cell.2011.11.016>
- Fromm, M. F. (2004). Importance of P-glycoprotein at blood-tissue barriers. *Trends in Pharmacological Sciences*, 25(8), 423-429.
- Fujii, R., Mutoh, M., Niwa, K., Yamada, K., Aikou, T., Nakagawa, M., Kuwano, M., & Akiyama, S. (1994). Active efflux system for cisplatin in cisplatin-resistant human KB cells. *Jpn J Cancer Res*, 85(4), 426-433. <https://doi.org/10.1111/j.1349-7006.1994.tb02376.x>
- Gašić, U., Trifković, J., Milojković-Opsenica, D., Natić, M., Tešić, Z., Kečkeš, S., & Dabić, D. (2014). *Phenolic profile and antioxidant activity of Serbian polyfloral honeys* (Vol. 145).
- Gatti, L., Beretta, G. L., Cossa, G., Zunino, F., & Perego, P. (2009). ABC transporters as potential targets for modulation of drug resistance. *Mini Rev Med Chem*, 9(9), 1102-1112. <https://www.ncbi.nlm.nih.gov/pubmed/19689406>
- Gatti, L., Cossa, G., Beretta, G. L., Zaffaroni, N., & Perego, P. (2011). Novel insights into targeting ATP-binding cassette transporters for antitumor therapy. *Curr Med Chem*, 18(27), 4237-4249. <https://www.ncbi.nlm.nih.gov/pubmed/21838682>
- Giacchetti, S., Perpoint, B., Zidani, R., Le Bail, N., Faggiuolo, R., Focan, C., Chollet, P., Llory, J. F., Letourneau, Y., Coudert, B., Bertheaut-Cvitkovic, F., Larregain-Fournier, D., Le Rol, A., Walter, S., Adam, R., Missel, J. L., & Levi, F. (2000). Phase III multicenter randomized trial of oxaliplatin added to chronomodulated fluorouracil-leucovorin as first-line treatment of metastatic colorectal cancer. *J Clin Oncol*, 18(1), 136-147. <https://doi.org/10.1200/JCO.2000.18.1.136>
- Giacomini, K. M., Huang, S. M., Tweedie, D. J., Benet, L. Z., Brouwer, K. L., Chu, X., Dahlin, A., Evers, R., Fischer, V., Hillgren, K. M., Hoffmaster, K. A., Ishikawa, T., Keppler, D., Kim, R. B., Lee, C. A., Niemi, M., Polli, J. W., Sugiyama, Y., Swaan, P. W.,...Zhang, L. (2010). Membrane transporters in drug development. *Nat Rev Drug Discov*, 9(3), 215-236. <https://doi.org/10.1038/nrd3028>
- Glavinas, H., Krajcsi, P., Cserepes, J., & Sarkadi, B. (2004). The role of ABC transporters in drug resistance, metabolism and toxicity. *Current drug delivery*, 1(1), 27-42.
- Glavinas, H., Mehn, D., Jani, M., Oosterhuis, B., Heredi-Szabo, K., & Krajcsi, P. (2008). Utilization of membrane vesicle preparations to study drug-ABC transporter interactions. *Expert Opin Drug Metab Toxicol*, 4(6), 721-732. <https://doi.org/10.1517/17425255.4.6.721>

- Goldberg, R. M., Sargent, D. J., Morton, R. F., Fuchs, C. S., Ramanathan, R. K., Williamson, S. K., Findlay, B. P., Pitot, H. C., & Alberts, S. R. (2004). A randomized controlled trial of fluorouracil plus leucovorin, irinotecan, and oxaliplatin combinations in patients with previously untreated metastatic colorectal cancer. *J Clin Oncol*, 22(1), 23-30. <https://doi.org/10.1200/JCO.2004.09.046>
- Gośliński, M., Nowak, D., & Kłębukowska, L. (2020). Antioxidant properties and antimicrobial activity of manuka honey versus Polish honeys. *J Food Sci Technol*, 57(4), 1269-1277. <https://doi.org/10.1007/s13197-019-04159-w>
- Gottesman, M. M., Fojo, T., & Bates, S. E. (2002). Multidrug resistance in cancer: role of ATP-dependent transporters. *Nat Rev Cancer*, 2(1), 48-58. <https://doi.org/10.1038/nrc706>
- Graham, F. L., Smiley, J., Russell, W. C., & Nairn, R. (1977). Characteristics of a human cell line transformed by DNA from human adenovirus type 5. *J Gen Virol*, 36(1), 59-74. <https://doi.org/10.1099/0022-1317-36-1-59>
- Graham, M. A., Lockwood, G. F., Greenslade, D., Brienza, S., Bayssas, M., & Gamelin, E. (2000). Clinical pharmacokinetics of oxaliplatin: a critical review. *Clin Cancer Res*, 6(4), 1205-1218. <https://www.ncbi.nlm.nih.gov/pubmed/10778943>
- Graudens, E., Boulanger, V., Mollard, C., Mariage-Samson, R., Barlet, X., Gremy, G., Couillault, C., Lajemi, M., Piatier-Tonneau, D., Zaborski, P., Eveno, E., Auffray, C., & Imbeaud, S. (2006). Deciphering cellular states of innate tumor drug responses. *Genome Biol*, 7(3), R19. <https://doi.org/10.1186/gb-2006-7-3-r19>
- Gresa-Arribas, N., Serratos, J., Solà, C., & Saura, J. (2010). *Inhibition of CCAAT/enhancer binding protein δ expression by chrysin in microglial cells results in anti-inflammatory and neuroprotective effects* (Vol. 115).
- Grothey, A., & Goldberg, R. M. (2004). A review of oxaliplatin and its clinical use in colorectal cancer. *Expert Opin Pharmacother*, 5(10), 2159-2170. <https://doi.org/10.1517/14656566.5.10.2159>
- Hagenbuch, B., & Stieger, B. (2013). The SLCO (former SLC21) superfamily of transporters. *Mol Aspects Med*, 34(2-3), 396-412. <https://doi.org/10.1016/j.mam.2012.10.009>
- Hagrman, D., Goodisman, J., & Souid, A.-K. (2004). Kinetic study on the reactions of platinum drugs with glutathione. *Journal of Pharmacology and Experimental Therapeutics*, 308(2), 658-666.
- Hall, M. D., Okabe, M., Shen, D.-W., Liang, X.-J., & Gottesman, M. M. (2008). The role of cellular accumulation in determining sensitivity to platinum-based chemotherapy*. *Annu. Rev. Pharmacol. Toxicol.*, 48, 495-535.
- Hall, M. D., Okabe, M., Shen, D. W., Liang, X. J., & Gottesman, M. M. (2008). The role of cellular accumulation in determining sensitivity to platinum-based chemotherapy. *Annu Rev Pharmacol Toxicol*, 48, 495-535. <https://doi.org/10.1146/annurev.pharmtox.48.080907.180426>
- Haller, D. G., Rothenberg, M. L., Wong, A. O., Koralewski, P. M., Miller, W. H., Jr., Bodoky, G.,

- Habboubi, N., Garay, C., & Olivatto, L. O. (2008). Oxaliplatin plus irinotecan compared with irinotecan alone as second-line treatment after single-agent fluoropyrimidine therapy for metastatic colorectal carcinoma. *J Clin Oncol*, 26(28), 4544-4550. <https://doi.org/10.1200/JCO.2008.17.1249>
- Han, B., Gao, G., Wu, W., Gao, Z., Zhao, X., Li, L., Qiao, R., Chen, H., Wei, Q., & Wu, J. (2011). Association of ABCC2 polymorphisms with platinum-based chemotherapy response and severe toxicity in non-small cell lung cancer patients. *Lung Cancer*, 72(2), 238-243.
- Han, B., Gao, G., Wu, W., Gao, Z., Zhao, X., Li, L., Qiao, R., Chen, H., Wei, Q., Wu, J., & Lu, D. (2011). Association of ABCC2 polymorphisms with platinum-based chemotherapy response and severe toxicity in non-small cell lung cancer patients. *Lung Cancer*, 72(2), 238-243. <https://doi.org/10.1016/j.lungcan.2010.09.001>
- Hector, S., Bolanowska-Higdon, W., Zdanowicz, J., Hitt, S., & Pendyala, L. (2001). In vitro studies on the mechanisms of oxaliplatin resistance. *Cancer Chemotherapy And Pharmacology*, 48(5), 398-406.
- Hediger, M. A., Romero, M. F., Peng, J. B., Rolfs, A., Takanaga, H., & Bruford, E. A. (2004). The ABCs of solute carriers: physiological, pathological and therapeutic implications of human membrane transport proteinsIntroduction. *Pflugers Arch*, 447(5), 465-468. <https://doi.org/10.1007/s00424-003-1192-y>
- Heinemann, V., Boeck, S., Hinke, A., Labianca, R., & Louvet, C. (2008). Meta-analysis of randomized trials: evaluation of benefit from gemcitabine-based combination chemotherapy applied in advanced pancreatic cancer. *BMC Cancer*, 8, 82. <https://doi.org/10.1186/1471-2407-8-82>
- Heinemann, V., Quietzsch, D., Gieseler, F., Gonnermann, M., Schonekas, H., Rost, A., Neuhaus, H., Haag, C., Clemens, M., Heinrich, B., Vehling-Kaiser, U., Fuchs, M., Fleckenstein, D., Gesierich, W., Uthgenannt, D., Einsele, H., Holstege, A., Hinke, A., Schalthorn, A., & Wilkowski, R. (2006). Randomized phase III trial of gemcitabine plus cisplatin compared with gemcitabine alone in advanced pancreatic cancer. *J Clin Oncol*, 24(24), 3946-3952. <https://doi.org/10.1200/JCO.2005.05.1490>
- Hendrik, W. V. V., Koen, V., Henk, B., Irina, O., Jan, K., Bert, P., Arnold, J. M. D., & Wil, N. K. (1996). Multidrug Resistance Mediated by a Bacterial Homolog of the Human Multidrug Transporter MDR1 [research-article]. *Proceedings of the National Academy of Sciences of the United States of America*, 93(20), 10668. <http://ezproxy.aut.ac.nz/login?url=http://search.ebscohost.com/login.aspx?direct=true&db=edsjsr&AN=edsjsr.40211&site=eds-live>
- Heredi-Szabo, K., Kis, E., Molnar, E., Gyorf, A., & Krajcsi, P. (2008). Characterization of 5(6)-carboxy-2,'7'-dichlorofluorescein transport by MRP2 and utilization of this substrate as a fluorescent surrogate for LTC4. *J Biomol Screen*, 13(4), 295-301. <https://doi.org/10.1177/1087057108316702>
- Higgins, C. F. (1992). ABC transporters: from microorganisms to man. *Annu Rev Cell Biol*, 8, 67-113. <https://doi.org/10.1146/annurev.cb.08.110192.000435>

- Hillgren, K. M., Keppler, D., Zur, A. A., Giacomini, K. M., Stieger, B., Cass, C. E., Zhang, L., & International Transporter, C. (2013). Emerging transporters of clinical importance: an update from the International Transporter Consortium. *Clin Pharmacol Ther*, 94(1), 52-63. <https://doi.org/10.1038/clpt.2013.74>
- Hinoshita, E., Uchiumi, T., Taguchi, K., Kinukawa, N., Tsuneyoshi, M., Maehara, Y., Sugimachi, K., & Kuwano, M. (2000). Increased expression of an ATP-binding cassette superfamily transporter, multidrug resistance protein 2, in human colorectal carcinomas. *Clin Cancer Res*, 6(6), 2401-2407.
- Hoffmann, U., & Kroemer, H. K. (2004). The ABC transporters MDR1 and MRP2: multiple functions in disposition of xenobiotics and drug resistance. *Drug Metab Rev*, 36(3-4), 669-701. <https://doi.org/10.1081/DMR-200033473>
- Hong, J., Zhou, J., Fu, J., He, T., Qin, J., Wang, L., Liao, L., & Xu, J. (2011). Phosphorylation of Serine 68 of Twist1 by MAPKs Stabilizes Twist1 Protein and Promotes Breast Cancer Cell Invasiveness. *Cancer Research*, 71(11), 3980-3990. <https://doi.org/10.1158/0008-5472.can-10-2914>
- Huang, X., Wang, M., Zhu, B., Hao, Y., Gao, R., Liu, W., Cheng, J., Hua, G., & Xue, C. (2024). *Unraveling the Mechanism of Curculiginis Rhizoma in Suppressing Cisplatin Resistance in Non-Small Cell Lung Cancer: An Experimental Study* (Vol. 17).
- Huang, Y., Anderle, P., Bussey, K. J., Barbacioru, C., Shankavaram, U., Dai, Z., Reinhold, W. C., Papp, A., Weinstein, J. N., & Sadee, W. (2004). Membrane transporters and channels: role of the transportome in cancer chemosensitivity and chemoresistance. *Cancer Res*, 64(12), 4294-4301. <https://doi.org/10.1158/0008-5472.CAN-03-3884>
- Huang, Y., & Sadee, W. (2006). Membrane transporters and channels in chemoresistance and -sensitivity of tumor cells. *Cancer Lett*, 239(2), 168-182. <https://doi.org/10.1016/j.canlet.2005.07.032>
- Huisman, M. T., Chhatta, A. A., van Tellingen, O., Beijnen, J. H., & Schinkel, A. H. (2005). MRP2 (ABCC2) transports taxanes and confers paclitaxel resistance and both processes are stimulated by probenecid. *Int J Cancer*, 116(5), 824-829. <https://doi.org/10.1002/ijc.21013>
- Institute, G. C. (2023). *Changing outcomes for people with gastro-intestinal cancer since 1991*. AGITG. <https://gicancer.org.au/gi-cancer-explained/>
- International Transporter, C., Giacomini, K. M., Huang, S. M., Tweedie, D. J., Benet, L. Z., Brouwer, K. L., Chu, X., Dahlin, A., Evers, R., Fischer, V., Hillgren, K. M., Hoffmaster, K. A., Ishikawa, T., Keppler, D., Kim, R. B., Lee, C. A., Niemi, M., Polli, J. W., Sugiyama, Y.,...Zhang, L. (2010). Membrane transporters in drug development. *Nat Rev Drug Discov*, 9(3), 215-236. <https://doi.org/10.1038/nrd3028>
- Jedlitschky, G., Burchell, B., & Keppler, D. (2000). The multidrug resistance protein 5 functions as an ATP-dependent export pump for cyclic nucleotides. *The Journal Of Biological Chemistry*, 275(39), 30069-30074. <http://ezproxy.aut.ac.nz/login?url=http://search.ebscohost.com/login.aspx?direct=true>

- Jemnitz, K., Heredi-Szabo, K., Janossy, J., Iojă, E., Vereczkey, L., & Krajcsi, P. (2010). ABC2/Abcc2: a multispecific transporter with dominant excretory functions. *Drug Metab Rev*, 42(3), 402-436. <https://doi.org/10.3109/03602530903491741>
- Jenkins, R., Burton, N., & Cooper, R. (2011). Manuka honey inhibits cell division in methicillin-resistant *Staphylococcus aureus*. *Journal of Antimicrobial Chemotherapy*, 66(11), 2536-2542. <https://doi.org/10.1093/jac/dkr340>
- Jerremalm, E., Eksborg, S., & Ehrsson, H. (2003). Hydrolysis of oxaliplatin—evaluation of the acid dissociation constant for the oxalato monodentate complex. *Journal of pharmaceutical sciences*, 92(2), 436-438.
- Jerremalm, E., Wallin, I., & Ehrsson, H. (2009). New insights into the biotransformation and pharmacokinetics of oxaliplatin. *Journal of pharmaceutical sciences*, 98(11), 3879-3885.
- Jodoin, J., Demeule, M., & Beliveau, R. (2002). Inhibition of the multidrug resistance P-glycoprotein activity by green tea polyphenols. In (Vol. 1542, pp. 149-159).
- Jong, N. N., Nakanishi, T., Liu, J. J., Tamai, I., & McKeage, M. J. (2011). Oxaliplatin transport mediated by organic cation/carnitine transporters OCTN1 and OCTN2 in overexpressing human embryonic kidney 293 cells and rat dorsal root ganglion neurons. *J Pharmacol Exp Ther*, 338(2), 537-547. <https://doi.org/10.1124/jpet.111.181297>
- Jun-Shik, C., Hoo-Kyun, C., & Sang-Chul, S. (2004). Enhanced bioavailability of paclitaxel after oral coadministration with flavone in rats. *International Journal of Pharmaceutics*(1), 165. <https://doi.org/10.1016/j.ijpharm.2004.01.032>
- Jun-Shik, C., & Sang-Chul, S. (2005). Enhanced paclitaxel bioavailability after oral coadministration of paclitaxel prodrug with naringin to rats. *International Journal of Pharmaceutics*(1), 149. <https://doi.org/10.1016/j.ijpharm.2004.11.031>
- K, N., A, K., K, O., K, M., N, N., & Y, T. (2002). *Copper-transporting P-type adenosine triphosphatase (ATP7B) as a cisplatin based chemoresistance marker in ovarian carcinoma: comparative analysis with expression of MDR1, MRP1, MRP2, LRP and BCRP* (Vol. 101).
- K, N., M, T., R, M., S, F., T, I., & H, K. (2023). *Development of multi-drug resistance to anticancer drugs in HepG2 cells due to MRP2 upregulation on exposure to menthol* (Vol. 18).
- Kamiloglu, S., Sari, G., Ozdal, T., & Capanoglu, E. (2020). *Guidelines for cell viability assays* (Vol. 1). John Wiley and Sons Inc.
- Kang, K. A., Wang, Z. H., Zhang, R., Piao, M. J., Kim, K. C., Kang, S. S., Kim, Y. W., Lee, J., Park, D., & Hyun, J. W. (2010). Myricetin protects cells against oxidative stress-induced apoptosis via regulation of PI3K/Akt and MAPK signaling pathways. *Int J Mol Sci*, 11(11), 4348-4360. <https://doi.org/10.3390/ijms11114348>
- Kapse-Mistry, S., Govender, T., Srivastava, R., & Yergeri, M. (2014). Nanodrug delivery in reversing multidrug resistance in cancer cells. *Front Pharmacol*, 5, 159. <https://doi.org/10.3389/fphar.2014.00159>

- Kathawala, R. J., Gupta, P., Ashby, C. R., Jr., & Chen, Z. S. (2015). The modulation of ABC transporter-mediated multidrug resistance in cancer: a review of the past decade. *Drug Resist Updat*, 18, 1-17. <https://doi.org/10.1016/j.drug.2014.11.002>
- Kavallaris, M. (1997). The role of multidrug resistance-associated protein (MRP) expression in multidrug resistance. *Anti-cancer drugs*, 8(1), 17-25. <https://doi.org/10.1097/00001813-199701000-00002>
- Kawabe, T., Chen, Z.-S., Wada, M., Uchiumi, T., Ono, M., Akiyama, S.-i., & Kuwano, M. (1999). Enhanced transport of anticancer agents and leukotriene C 4 by the human canalicular multispecific organic anion transporter (cMOAT/MRP2). *FEBS letters*, 456(2), 327-331.
- Ke, S. Z., Ni, X. Y., Zhang, Y. H., Wang, Y. N., Wu, B., & Gao, F. G. (2013). Camptothecin and cisplatin upregulate ABCG2 and MRP2 expression by activating the ATM/NF-kappaB pathway in lung cancer cells. *Int J Oncol*, 42(4), 1289-1296. <https://doi.org/10.3892/ijo.2013.1805>
- Kell, D. B., Dobson, P. D., & Oliver, S. G. (2011). Pharmaceutical drug transport: the issues and the implications that it is essentially carrier-mediated only. *Drug Discov Today*, 16(15-16), 704-714. <https://doi.org/10.1016/j.drudis.2011.05.010>
- Kelland, L. (2007). The resurgence of platinum-based cancer chemotherapy. *Nat Rev Cancer*, 7(8), 573-584. <https://doi.org/10.1038/nrc2167>
- Keogh, J., Hagenbuch, B., Rynn, C. S., B.; , & Nicholls, G. (2016). *The role of Transporters in ADME* (G. Y. Nicholls, K., Ed. Vol. Drug Transporters: Volume 1). The Royal Society of Chemistry.
- Keppler, D. (2011). Multidrug resistance proteins (MRPs, ABCs): importance for pathophysiology and drug therapy. *Handb Exp Pharmacol*(201), 299-323. https://doi.org/10.1007/978-3-642-14541-4_8
- Khan, M. A. W., Ologun, G., Arora, R., McQuade, J. L., & Wargo, J. A. (2020). Gut Microbiome Modulates Response to Cancer Immunotherapy. In (Vol. 65, pp. 885-896).
- Khine, M., Riya, B., Yan, L., Nancy, J., Stephen, J., Johnson, L., Catherine, H., Christopher, S., Fabrice, M., Jun, L., Takeo, N., Ikumi, T., & Mark, M. (2019). Identification of MRP2 as a targetable factor limiting oxaliplatin accumulation and response in gastrointestinal cancer [article]. *Scientific Reports*(1), 1. <https://doi.org/10.1038/s41598-019-38667-8>
- Khoo, B. Y., Chua, S. L., & Balaram, P. (2010). Apoptotic effects of chrysin in human cancer cell lines. *Int J Mol Sci*, 11(5), 2188-2199. <https://doi.org/10.3390/ijms11052188>
- Kim, B. R., Ha, J., Lee, S., Park, J., & Cho, S. (2019). *Anti-cancer effects of ethanol extract of Reynoutria japonica Houtt. radix in human hepatocellular carcinoma cells via inhibition of MAPK and PI3K/Akt signaling pathways* (Vol. 245). Elsevier Ireland Ltd.
- Kim, J.-W., Kim, J., Lee, S. M., Rim, Y. A., Sung, Y. C., Nam, Y., Kim, H.-J., Kim, H., Jung, S. I., Lim, J., & Ju, J. H. (2024). *Combination of induced pluripotent stem cell-derived motor neuron progenitor cells with irradiated brain-derived neurotrophic factor over-expressing engineered mesenchymal stem cells enhanced restoration of axonal regeneration in a chronic spinal cord injury rat model* (Vol. 15).

- Kinzler, K. W. V., B. (2002). *The Genetic Basis of Human Cancer (2nd edition)*. McGraw-Hill, New York.
- Klopman, G., Shi, L. M., & Ramu, A. (1997). Quantitative structure-activity relationship of multidrug resistance reversal agents. *Molecular Pharmacology*, 52(2), 323-334. <http://ezproxy.aut.ac.nz/login?url=http://search.ebscohost.com/login.aspx?direct=true&db=cmedm&AN=9271356&site=eds-live>
- Kocherova, I., Kempisty, B., Hutchings, G., Janowicz, K., Moncrieff, L., Dompe, C., Petite, J., Shibli, J. A., & Mozdziak, P. (2020). *Cell-based approaches in drug development-a concise review* (Vol. 8). Sciendo.
- Komatsu, M., Sumizawa, T., Mutoh, M., Chen, Z.-S., Terada, K., Furukawa, T., Yang, X.-L., Gao, H., Miura, N., & Sugiyama, T. (2000). Copper-transporting P-type adenosine triphosphatase (ATP7B) is associated with cisplatin resistance. *Cancer Research*, 60(5), 1312-1316.
- Konig, J., Nies, A. T., Cui, Y., Leier, I., & Keppler, D. (1999). Conjugate export pumps of the multidrug resistance protein (MRP) family: localization, substrate specificity, and MRP2-mediated drug resistance. *Biochim Biophys Acta*, 1461(2), 377-394. <https://www.ncbi.nlm.nih.gov/pubmed/10581368>
- Kool, M., De Haas, M., Borst, P., Scheffer, G. L., Scheper, R. J., Van Eijk, M. J. T., Juijn, J. A., & Baas, F. (1997). Analysis of expression of cMOAT (MRP2), MRP3, MRP4, and MRP5, homologues of the multidrug resistance-associated protein gene (MRP1), in human cancer cell lines [Article]. *Cancer Research*, 57(16), 3537-3547. <http://ezproxy.aut.ac.nz/login?url=http://search.ebscohost.com/login.aspx?direct=true&db=edselc&AN=edselc.2-52.0-0030841332&site=eds-live>
- Kool, M., de Haas, M., Scheffer, G. L., Scheper, R. J., van Eijk, M. J., Juijn, J. A., Baas, F., & Borst, P. (1997). Analysis of expression of cMOAT (MRP2), MRP3, MRP4, and MRP5, homologues of the multidrug resistance-associated protein gene (MRP1), in human cancer cell lines. *Cancer Res*, 57(16), 3537-3547. <https://www.ncbi.nlm.nih.gov/pubmed/9270026>
- Kool, M., van der Linden, M., de Haas, M., Baas, F., & Borst, P. (1999). Expression of human MRP6, a homologue of the multidrug resistance protein gene MRP1, in tissues and cancer cells. *Cancer Research*, 59(1), 175-182. <http://ezproxy.aut.ac.nz/login?url=http://search.ebscohost.com/login.aspx?direct=true&db=cmedm&AN=9892204&site=eds-live>
- Koopman, G., Reutelingsperger, C. P., Kuijten, G. A., Keehnen, R. M., Pals, S. T., & van Oers, M. H. (1994). Annexin V for flow cytometric detection of phosphatidylserine expression on B cells undergoing apoptosis. *Blood*, 84(5), 1415-1420. <https://www.ncbi.nlm.nih.gov/pubmed/8068938>
- Korita, P. V., Wakai, T., Shirai, Y., Matsuda, Y., Sakata, J., Takamura, M., Yano, M., Sanpei, A., Aoyagi, Y., Hatakeyama, K., & Ajioka, Y. (2010). Multidrug resistance-associated protein 2 determines the efficacy of cisplatin in patients with hepatocellular carcinoma. *Oncol Rep*, 23(4), 965-972. https://doi.org/10.3892/or_00000721
- Krishna, R., & Mayer, L. D. (2000). Multidrug resistance (MDR) in cancer. Mechanisms, reversal

- using modulators of MDR and the role of MDR modulators in influencing the pharmacokinetics of anticancer drugs. *Eur J Pharm Sci*, 11(4), 265-283. <https://www.ncbi.nlm.nih.gov/pubmed/11033070>
- Kruh, G. D. (2003). Lustrous insights into cisplatin accumulation: copper transporters. *Clin Cancer Res*, 9(16 Pt 1), 5807-5809. <https://www.ncbi.nlm.nih.gov/pubmed/14676099>
- Kruh, G. D., Yanping, G., Hopper-Borge, E., Belinsky, M. G., & Zhe-Sheng, C. (2007). ABCC10, ABCC11, and ABCC12 [Article]. *Pflugers Archiv European Journal of Physiology*, 453(5), 675-684. <https://doi.org/10.1007/s00424-006-0114-1>
- Kumar, S., Sepuhle, N., Bouic, P. J., & Rosenkranz, B. (2018). HPLC/ LC-MS guided phytochemical and in vitro screening of *Astragalus membranaceus* (Fabaceae), and prediction of possible interactions with CYP2B6. In (Vol. 14, pp. 35-47).
- Larson, C. A., Blair, B. G., Safaei, R., & Howell, S. B. (2009). The role of the mammalian copper transporter 1 in the cellular accumulation of platinum-based drugs. *Molecular Pharmacology*, 75(2), 324-330.
- Leslie, E. M., Deeley, R. G., & Cole, S. P. (2005). Multidrug resistance proteins: role of P-glycoprotein, MRP1, MRP2, and BCRP (ABCG2) in tissue defense. *Toxicology and applied pharmacology*, 204(3), 216-237.
- Li, P., Fang, Y. J., Li, F., Ou, Q. J., Chen, G., & Ma, G. (2013). ERCC1, defective mismatch repair status as predictive biomarkers of survival for stage III colon cancer patients receiving oxaliplatin-based adjuvant chemotherapy. *Br J Cancer*, 108(6), 1238-1244. <https://doi.org/10.1038/bjc.2013.83>
- Li, P., Hu, Y., Zhan, L., He, J., Lu, J., Gao, C., Du, W., Yue, A., Zhao, J., & Zhang, W. (2023). *A Natural Glucan from Black Bean Inhibits Cancer Cell Proliferation via PI3K-Akt and MAPK Pathway* (Vol. 28).
- Li, S., Chen, Y., Zhang, S., More, S. S., Huang, X., & Giacomini, K. M. (2011). Role of organic cation transporter 1, OCT1 in the pharmacokinetics and toxicity of cis-diammine(pyridine)chloroplatinum(II) and oxaliplatin in mice. *Pharm Res*, 28(3), 610-625. <https://doi.org/10.1007/s11095-010-0312-6>
- Li, W., Sun, H., Zhang, X., Wang, H., & Wu, B. (2015). Efflux transport of chrysin and apigenin sulfates in HEK293 cells overexpressing SULT1A3: The role of multidrug resistance-associated protein 4 (MRP4/ABCC4). *Biochem Pharmacol*, 98(1), 203-214. <https://doi.org/10.1016/j.bcp.2015.08.090>
- Li, W., Zhang, H., Assaraf, Y. G., Zhao, K., Xu, X., Xie, J., Yang, D. H., & Chen, Z. S. (2016). Overcoming ABC transporter-mediated multidrug resistance: Molecular mechanisms and novel therapeutic drug strategies. *Drug Resist Updat*, 27, 14-29. <https://doi.org/10.1016/j.drug.2016.05.001>
- Li, Y., Revalde, J., & Paxton, J. W. (2017). The effects of dietary and herbal phytochemicals on drug transporters. *Adv Drug Deliv Rev*, 116, 45-62. <https://doi.org/10.1016/j.addr.2016.09.004>
- Li, Y., Revalde, J. L., Reid, G., & Paxton, J. W. (2010). Interactions of dietary phytochemicals with

- ABC transporters: possible implications for drug disposition and multidrug resistance in cancer. *Drug Metab Rev*, 42(4), 590-611. <https://doi.org/10.3109/03602531003758690>
- Li, Y., Revalde, J. L., Reid, G., & Paxton, J. W. (2011). Modulatory effects of curcumin on multi-drug resistance-associated protein 5 in pancreatic cancer cells. *Cancer Chemother Pharmacol*, 68(3), 603-610. <https://doi.org/10.1007/s00280-010-1515-6>
- Li, Y. Q., Yin, J. Y., Liu, Z. Q., & Li, X. P. (2018). Copper efflux transporters ATP7A and ATP7B: Novel biomarkers for platinum drug resistance and targets for therapy. *IUBMB Life*, 70(3), 183-191. <https://doi.org/10.1002/iub.1722>
- Li, Z., Liu, K., Sun, P., Mei, L., Hao, T., Tian, Y., Tang, Z., Li, L., & Chen, D. (2013). Poly(D, L-lactide-co-glycolide)/montmorillonite nanoparticles for improved oral delivery of exemestane. *J Microencapsul*, 30(5), 432-440. <https://doi.org/10.3109/02652048.2012.746749>
- Liedert, B., Materna, V., Schadendorf, D., Thomale, J., & Lage, H. (2003). Overexpression of cMOAT (MRP2/ABCC2) is associated with decreased formation of platinum-DNA adducts and decreased G2-arrest in melanoma cells resistant to cisplatin. *J Invest Dermatol*, 121(1), 172-176. <https://doi.org/10.1046/j.1523-1747.2003.12313.x>
- Lincz, L. F. (1998). Deciphering the apoptotic pathway: all roads lead to death. *Immunol Cell Biol*, 76(1), 1-19. <https://doi.org/10.1046/j.1440-1711.1998.00712.x>
- Linton, K. J. (2007). Structure and function of ABC transporters. *Physiology (Bethesda)*, 22, 122-130. <https://doi.org/10.1152/physiol.00046.2006>
- Litman, T., Druley, T. E., Stein, W. D., & Bates, S. E. (2001). From MDR to MXR: new understanding of multidrug resistance systems, their properties and clinical significance. In (Vol. 58, pp. 931-959).
- Liu, J. J., Jamieson, S. M., Subramaniam, J., Ip, V., Jong, N. N., Mercer, J. F., & McKeage, M. J. (2009). Neuronal expression of copper transporter 1 in rat dorsal root ganglia: association with platinum neurotoxicity. *Cancer Chemother Pharmacol*, 64(4), 847-856. <https://doi.org/10.1007/s00280-009-1017-6>
- Liu, J. J., Kim, Y., Yan, F., Ding, Q., Ip, V., Jong, N. N., Mercer, J. F., & McKeage, M. J. (2013). Contributions of rat Ctr1 to the uptake and toxicity of copper and platinum anticancer drugs in dorsal root ganglion neurons. *Biochem Pharmacol*, 85(2), 207-215. <https://doi.org/10.1016/j.bcp.2012.10.023>
- Liu, J. J., Lu, J., & McKeage, M. J. (2012). Membrane transporters as determinants of the pharmacology of platinum anticancer drugs. *Curr Cancer Drug Targets*, 12(8), 962-986. <https://www.ncbi.nlm.nih.gov/pubmed/22794121>
- Liu, T., Meng, Q., Wang, C., Liu, Q., Guo, X., Sun, H., Peng, J., Ma, X., Liu, K., & Kaku, T. (2012). Changes in expression of renal *Oat1*, *Oat3* and *Mrp2* in cisplatin-induced acute renal failure after treatment of JBP485 in rats (Vol. 264).
- Liu, X. P., Geng, D. Q., Xu, H. X., & Sui, X. H. (2009). The tissue distribution in mice and pharmacokinetics in rabbits of oxaliplatin liposome. *J Liposome Res*, 19(4), 278-286. <https://doi.org/10.3109/08982100902824211>

- Liu, Z., Qiu, M., Tang, Q., Liu, M., Lang, N., & Bi, F. (2010). Establishment and biological characteristics of oxaliplatin-resistant human colon cancer cell lines. *Chin J Cancer*, 29(7), 661-667.
- Liu, Z., Qiu, M., Tang, Q. L., Liu, M., Lang, N., & Bi, F. (2010). Establishment and biological characteristics of oxaliplatin-resistant human colon cancer cell lines. *Chin J Cancer*, 29(7), 661-667. <https://doi.org/10.5732/cjc.009.10666>
- Lorenzer, C., Dirin, M., Winkler, A. M., Baumann, V., & Winkler, J. (2015). Going beyond the liver: progress and challenges of targeted delivery of siRNA therapeutics. *J Control Release*, 203, 1-15. <https://doi.org/10.1016/j.jconrel.2015.02.003>
- Louafi, S., Boige, V., Ducreux, M., Bonyhay, L., Mansourbakht, T., de Baere, T., Asnacios, A., Hannoun, L., Poynard, T., & Taïeb, J. (2007). Gemcitabine plus oxaliplatin (GEMOX) in patients with advanced hepatocellular carcinoma (HCC): results of a phase II study. *Cancer*, 109(7), 1384-1390. <https://doi.org/10.1002/cncr.22532>
- Lu, P., Takai, K., Weaver, V. M., & Werb, Z. (2011). Extracellular Matrix Degradation and Remodeling in Development and Disease. In (Vol. 3).
- Lutsenko, S., Barnes, N. L., Bartee, M. Y., & Dmitriev, O. Y. (2007). Function and regulation of human copper-transporting ATPases. *Physiol Rev*, 87(3), 1011-1046. <https://doi.org/10.1152/physrev.00004.2006>
- M, d. V., AF, K., & LH, d. P. (2024). *Pneumatic extrusion bioprinting-based high throughput fabrication of a melanoma 3D cell culture model for anti-cancer drug screening* (Vol. 19).
- M, M. N., F, M., S, W., A, G., & K, L. (2024). *Dynamic cell culture modulates colon cancer cell migration in a novel 3D cell culture system* (Vol. 14).
- Ma, J. J., Chen, B. L., & Xin, X. Y. (2009). Inhibition of multi-drug resistance of ovarian carcinoma by small interfering RNA targeting to MRP2 gene. *Arch Gynecol Obstet*, 279(2), 149-157. <https://doi.org/10.1007/s00404-008-0690-8>
- Machala, M., Kubínová, R., Horavová, P., & Suchý, V. (2001). Chemoprotective potentials of homoisoflavonoids and chalcones of *Dracaena cinnabari*: modulations of drug-metabolizing enzymes and antioxidant activity. *Phytother Res*, 15(2), 114-118. <https://doi.org/10.1002/ptr.697>
- Mahapatra, E., Sengupta, D., Kumar, R., Dehury, B., Das, S., Roy, M., & Mukherjee, S. (2022a). *Phenethylisothiocyanate Potentiates Platinum Therapy by Reversing Cisplatin Resistance in Cervical Cancer* (Vol. 13).
- Mahapatra, E., Sengupta, D., Kumar, R., Dehury, B., Das, S., Roy, M., & Mukherjee, S. (2022b). *Phenethylisothiocyanate Potentiates Platinum Therapy by Reversing Cisplatin Resistance in Cervical Cancer* (Vol. 13).
- Mahmood, T., & Yang, P. C. (2012). Western blot: technique, theory, and trouble shooting. *N Am J Med Sci*, 4(9), 429-434. <https://doi.org/10.4103/1947-2714.100998>
- Mann, S., Andrews, P., & Howell, S. (1987). Comparison of lipid content, surface membrane

- fluidity, and temperature dependence of cis-diamminedichloroplatinum (II) accumulation in sensitive and resistant human ovarian carcinoma cells. *Anticancer research*, 8(6), 1211-1215.
- Martinez-Balibrea, E., Martinez-Cardus, A., Gines, A., Ruiz de Porras, V., Moutinho, C., Layos, L., Manzano, J. L., Buges, C., Bystrup, S., Esteller, M., & Abad, A. (2015). Tumor-Related Molecular Mechanisms of Oxaliplatin Resistance. *Mol Cancer Ther*, 14(8), 1767-1776. <https://doi.org/10.1158/1535-7163.MCT-14-0636>
- Martinez-Cardus, A., Martinez-Balibrea, E., Bandres, E., Malumbres, R., Gines, A., Manzano, J. L., Taron, M., Garcia-Foncillas, J., & Abad, A. (2009). Pharmacogenomic approach for the identification of novel determinants of acquired resistance to oxaliplatin in colorectal cancer. *Mol Cancer Ther*, 8(1), 194-202. <https://doi.org/10.1158/1535-7163.MCT-08-0659>
- Martins, I. L., Charneira, C., Gandin, V., Ferreira da Silva, J. L., Justino, G. C., Telo, J. P., Vieira, A. J., Marzano, C., & Antunes, A. M. (2015). Selenium-containing chrysin and quercetin derivatives: attractive scaffolds for cancer therapy. *J Med Chem*, 58(10), 4250-4265. <https://doi.org/10.1021/acs.jmedchem.5b00230>
- Masuda, S., Terada, T., Yonezawa, A., Tanihara, Y., Kishimoto, K., Katsura, T., Ogawa, O., & Inui, K. (2006). Identification and functional characterization of a new human kidney-specific H⁺/organic cation antiporter, kidney-specific multidrug and toxin extrusion 2. *J Am Soc Nephrol*, 17(8), 2127-2135. <https://doi.org/10.1681/ASN.2006030205>
- Materna, V., Stege, A., Surowiak, P., Pribsch, A., & Lage, H. (2006). RNA interference-triggered reversal of ABCC2-dependent cisplatin resistance in human cancer cells. *Biochem Biophys Res Commun*, 348(1), 153-157. <https://doi.org/10.1016/j.bbrc.2006.07.022>
- Matsson, P., Pedersen, J., Bergström, C., & Artursson, P. (2009). *Identification of Novel Specific and General Inhibitors of the Three Major Human ATP-Binding Cassette Transporters P-gp, BCRP and MRP2 Among Registered Drugs* (Vol. 26).
- Matsson, P., Pedersen, J. M., Norinder, U., Bergstrom, C. A., & Artursson, P. (2009). Identification of novel specific and general inhibitors of the three major human ATP-binding cassette transporters P-gp, BCRP and MRP2 among registered drugs. *Pharm Res*, 26(8), 1816-1831. <https://doi.org/10.1007/s11095-009-9896-0>
- McKeage, M. J. (2001). Lobaplatin: a new antitumour platinum drug. *Expert Opin Investig Drugs*, 10(1), 119-128. <https://doi.org/10.1517/13543784.10.1.119>
- Medina, J. H., Paladini, A. C., Wolfman, C., Levi de Stein, M., Calvo, D., Diaz, L. E., & Peña, C. (1990). Chrysin (5,7-di-OH-flavone), a naturally-occurring ligand for benzodiazepine receptors, with anticonvulsant properties. *Biochem Pharmacol*, 40(10), 2227-2231. [https://doi.org/10.1016/0006-2952\(90\)90716-x](https://doi.org/10.1016/0006-2952(90)90716-x)
- Michalkiewicz, A., Biesaga, M., & Pyrzynska, K. (2008). *Solid-phase extraction procedure for determination of phenolic acids and some flavonols in honey* (Vol. 1187).
- Minemura, M., Tanimura, H., & Tabor, E. (1999). Overexpression of multidrug resistance genes MDR1 and cMOAT in human hepatocellular carcinoma and hepatoblastoma cell lines. *Int*

J Oncol, 15(3), 559-563. <https://www.ncbi.nlm.nih.gov/pubmed/10427140>

Ministry of Health. (2014). *Cancer: New registrations and deaths 2011*. Retrieved May 25 from <http://www.health.govt.nz/system/files/documents/publications/cancer-new-registrations-deaths-2011-v4sept14.pdf>

Mirakhorli, M., Rahman, S. A., Abdullah, S., Vakili, M., Rozafzon, R., & Khoshzaban, A. (2013). Multidrug resistance protein 2 genetic polymorphism and colorectal cancer recurrence in patients receiving adjuvant FOLFOX-4 chemotherapy. *Mol Med Rep*, 7(2), 613-617. <https://doi.org/10.3892/mmr.2012.1226>

Mirakhorli, M., Shayanfar, N., Rahman, S. A., Rosli, R., Abdullah, S., & Khoshzaban, A. (2012). Lack of association between expression of MRP2 and early relapse of colorectal cancer in patients receiving FOLFOX-4 chemotherapy. *Oncol Lett*, 4(5), 893-897. <https://doi.org/10.3892/ol.2012.889>

Mishima, M., Samimi, G., Kondo, A., Lin, X., & Howell, S. B. (2002). The cellular pharmacology of oxaliplatin resistance. *Eur J Cancer*, 38(10), 1405-1412. <https://www.ncbi.nlm.nih.gov/pubmed/12091073>

Moens, F., Van den Abbeele, P., Basit, A. W., Dodoo, C., Gaisford, S., Chatterjee, R., & Smith, B. (2019). A four-strain probiotic exerts positive immunomodulatory effects by enhancing colonic butyrate production in vitro [Article]. *International Journal of Pharmaceutics*, 555, 1-10. <https://doi.org/10.1016/j.ijpharm.2018.11.020>

Mohammad, I. S., He, W., & Yin, L. (2018). Understanding of human ATP binding cassette superfamily and novel multidrug resistance modulators to overcome MDR. *Biomed Pharmacother*, 100, 335-348. <https://doi.org/10.1016/j.biopha.2018.02.038>

Mohan, A., Quek, S. Y., Gutierrez-Maddox, N., Gao, Y., & Shu, Q. (2017). Effect of honey in improving the gut microbial balance [Article]. *Food Quality and Safety*, 1(2), 107-115. <https://doi.org/10.1093/fqsafe/fyx015>

Mohn, C., Hacker, H. G., Hilger, R. A., Gutschow, M., & Jaehde, U. (2013). Defining the role of MRP-mediated efflux and glutathione in detoxification of oxaliplatin. *Pharmazie*, 68(7), 622-627. <https://www.ncbi.nlm.nih.gov/pubmed/23923647>

Mohn, C., Häcker, H. G., Hilger, R. A., Gütschow, M., & Jaehde, U. (2013). Defining the role of MRP-mediated efflux and glutathione in detoxification of oxaliplatin. *Pharmazie*, 68(7), 622-627.

Mohn, C., Kalayda, G., Häcker, H., Gütschow, M., Metzger, S., & Jaehde, U. (2010). Contribution of glutathione and MRP-mediated efflux to intracellular oxaliplatin accumulation. *International journal of clinical pharmacology and therapeutics*, 48(7), 445.

Mohn, C., Kalayda, G. V., Hacker, H. G., Gutschow, M., Metzger, S., & Jaehde, U. (2010). Contribution of glutathione and MRP-mediated efflux to intracellular oxaliplatin accumulation. *Int J Clin Pharmacol Ther*, 48(7), 445-447. <https://www.ncbi.nlm.nih.gov/pubmed/20557839>

Mohn, C., Kalayda, G. V., Häcker, H. G., Gütschow, M., Metzger, S., & Jaehde, U. (2010). Contribution of glutathione and MRP-mediated efflux to intracellular oxaliplatin

- accumulation. *Int J Clin Pharmacol Ther*, 48(7), 445-447. <https://doi.org/10.5414/cpp48445>
- Moore, M. J., Goldstein, D., Hamm, J., Figer, A., Hecht, J. R., Gallinger, S., Au, H. J., Murawa, P., Walde, D., Wolff, R. A., Campos, D., Lim, R., Ding, K., Clark, G., Voskoglou-Nomikos, T., Ptasynski, M., Parulekar, W., & National Cancer Institute of Canada Clinical Trials, G. (2007). Erlotinib plus gemcitabine compared with gemcitabine alone in patients with advanced pancreatic cancer: a phase III trial of the National Cancer Institute of Canada Clinical Trials Group. *J Clin Oncol*, 25(15), 1960-1966. <https://doi.org/10.1200/JCO.2006.07.9525>
- Moriya, Y., Nakamura, T., Horinouchi, M., Sakaeda, T., Tamura, T., Aoyama, N., Shirakawa, T., Gotoh, A., Fujimoto, S., Matsuo, M., Kasuga, M., & Okumura, K. (2002). Effects of polymorphisms of MDR1, MRP1, and MRP2 genes on their mRNA expression levels in duodenal enterocytes of healthy Japanese subjects. *Biol Pharm Bull*, 25(10), 1356-1359. <https://www.ncbi.nlm.nih.gov/pubmed/12392094>
- Myint, K. (2015). *Multidrug resistance-associated protein 2 (MRP2) and oxaliplatin transport* [The University of Auckland]. Auckland.
- Myint, K., Biswas, R., Li, Y., Jong, N., Jamieson, S., Liu, J., Han, C., Squire, C., Merien, F., Lu, J., Nakanishi, T., Tamai, I., & McKeage, M. (2019). Identification of MRP2 as a targetable factor limiting oxaliplatin accumulation and response in gastrointestinal cancer. *Sci Rep*, 9(1), 2245. <https://doi.org/10.1038/s41598-019-38667-8>
- Myint, K., Li, Y., Paxton, J., & McKeage, M. (2015). Multidrug Resistance-Associated Protein 2 (MRP2) Mediated Transport of Oxaliplatin-Derived Platinum in Membrane Vesicles. *PLoS One*, 10(7), e0130727. <https://doi.org/10.1371/journal.pone.0130727>
- Nakagawa, M., Nomura, Y., Kohno, K., Ono, M., Mizoguchi, H., Ogata, J., & Kuwano, M. (1993). Reduction of drug accumulation in cisplatin-resistant variants of human prostatic cancer PC-3 cell line. *J Urol*, 150(6), 1970-1973. [https://doi.org/10.1016/s0022-5347\(17\)35948-7](https://doi.org/10.1016/s0022-5347(17)35948-7)
- Namisaki, T., Schaeffeler, E., Fukui, H., Yoshiji, H., Nakajima, Y., Fritz, P., Schwab, M., & Nies, A. T. (2014). Differential expression of drug uptake and efflux transporters in Japanese patients with hepatocellular carcinoma. *Drug Metab Dispos*, 42(12), 2033-2040. <https://doi.org/10.1124/dmd.114.059832>
- Naruhashi, K., Tamai, I., Inoue, N., Muraoka, H., Sai, Y., Suzuki, N., & Tsuji, A. (2002). Involvement of multidrug resistance-associated protein 2 in intestinal secretion of grepafloxacin in rats. *Antimicrob Agents Chemother*, 46(2), 344-349. <https://www.ncbi.nlm.nih.gov/pubmed/11796340>
- Neveu, V., Perez-Jimenez, J., Vos, F., Crespy, V., Du Chaffaut, L., Mennen, L., Knox, C., Eisner, R., Cruz, J., Wishart, D., & Scalbert, A. (2010). Phenol-Explorer: an online comprehensive database on polyphenol contents in foods. *Database*, 2010(0), bap024-bap024. <https://doi.org/10.1093/database/bap024>
- Nies, A. T., Konig, J., Pfannschmidt, M., Klar, E., Hofmann, W. J., & Keppler, D. (2001). Expression of the multidrug resistance proteins MRP2 and MRP3 in human hepatocellular carcinoma.

- Int J Cancer*, 94(4), 492-499. <https://www.ncbi.nlm.nih.gov/pubmed/11745434>
- Nies, A. T., König, J., Pfannschmidt, M., Klar, E., Hofmann, W. J., & Keppler, D. (2001). Expression of the multidrug resistance proteins MRP2 and MRP3 in human hepatocellular carcinoma. *Int J Cancer*, 94(4), 492-499. <https://doi.org/10.1002/ijc.1498>
- NIH- Cancer Treatment. (2018). <https://www.cancer.gov/about-cancer/treatment>
- Nolan, V. C., Harrison, J., Wright, J. E. E., & Cox, J. A. G. (2020). Clinical Significance of Manuka and Medical-Grade Honey for Antibiotic-Resistant Infections: A Systematic Review. *Antibiotics (Basel)*, 9(11). <https://doi.org/10.3390/antibiotics9110766>
- Noma, B., Sasaki, T., Fujimoto, Y., Serikawa, M., Kobayashi, K., Inoue, M., Itsuki, H., Kamigaki, M., Minami, T., & Chayama, K. (2008). Expression of multidrug resistance-associated protein 2 is involved in chemotherapy resistance in human pancreatic cancer. *Int J Oncol*, 33(6), 1187-1194. <https://www.ncbi.nlm.nih.gov/pubmed/19020751>
- Nozhat, Z., Khalaji, M. S., Hedayati, M., & Kia, S. K. (2022). Different Methods for Cell Viability and Proliferation Assay: Essential Tools in Pharmaceutical Studies. *Anticancer Agents Med Chem*, 22(4), 703-712. <https://doi.org/10.2174/1871520621999201230202614>
- O'Connor, A., McNamara, D., & O'Morain, C. A. (2013). Surveillance of gastric intestinal metaplasia for the prevention of gastric cancer. *Cochrane Database Syst Rev*(9), CD009322. <https://doi.org/10.1002/14651858.CD009322.pub2>
- Ogawara, K., Un, K., Tanaka, K., Higaki, K., & Kimura, T. (2009). In vivo anti-tumor effect of PEG liposomal doxorubicin (DOX) in DOX-resistant tumor-bearing mice: Involvement of cytotoxic effect on vascular endothelial cells. *J Control Release*, 133(1), 4-10. <https://doi.org/10.1016/j.jconrel.2008.09.008>
- Oostendorp, R. L., Beijnen, J. H., & Schellens, J. H. (2009). The biological and clinical role of drug transporters at the intestinal barrier. *Cancer Treat Rev*, 35(2), 137-147. <https://doi.org/10.1016/j.ctrv.2008.09.004>
- Otsuka, M., Matsumoto, T., Morimoto, R., Arioka, S., Omote, H., & Moriyama, Y. (2005). A human transporter protein that mediates the final excretion step for toxic organic cations. *Proc Natl Acad Sci U S A*, 102(50), 17923-17928. <https://doi.org/10.1073/pnas.0506483102>
- Ozsahin, D. U., Nyakuwanikwa, K., Wallace, T., & Ozsahin, I. (2019). Evaluation and Simulation of Colon Cancer Treatment Techniques with Fuzzy PROMETHEE. In (pp. 1): IEEE.
- Paulusma, C. C., Kool, M., Bosma, P. J., Scheffer, G. L., ter Borg, F., Scheper, R. J., Tytgat, G., Borst, P., Baas, F., & Elferink, R. O. (1997). A mutation in the human canalicular multispecific organic anion transporter gene causes the Dubin-Johnson syndrome. *Hepatology*, 25(6), 1539-1542.
- Perego, P., & Robert, J. (2016). Oxaliplatin in the era of personalized medicine: from mechanistic studies to clinical efficacy. *Cancer Chemother Pharmacol*, 77(1), 5-18. <https://doi.org/10.1007/s00280-015-2901-x>
- Petrioli, R., Roviello, G., Fiaschi, A. I., Laera, L., Marrelli, D., Roviello, F., & Francini, E. (2015).

- Gemcitabine, oxaliplatin, and capecitabine (GEMOXEL) compared with gemcitabine alone in metastatic pancreatic cancer: a randomized phase II study. *Cancer Chemother Pharmacol*, 75(4), 683-690. <https://doi.org/10.1007/s00280-015-2683-1>
- Pichichero, E., Cicconi, R., Mattei, M., & Canini, A. (2011). Chrysin-induced apoptosis is mediated through p38 and Bax activation in B16-F1 and A375 melanoma cells. *Int J Oncol*, 38(2), 473-483. <https://doi.org/10.3892/ijo.2010.876>
- Piet, B., Raymond, E., Marcel, K., & Jan, W. (2000). A Family of Drug Transporters: the Multidrug Resistance-Associated Proteins. *Journal of the National Cancer Institute*(16), 1295. <http://ezproxy.aut.ac.nz/login?url=http://search.ebscohost.com/login.aspx?direct=true&db=edsovi&AN=edsovi.00005042.200008160.00003&site=eds-live>
- Potschka, H., Fedrowitz, M., & Löscher, W. (2003). Multidrug resistance protein MRP2 contributes to blood-brain barrier function and restricts antiepileptic drug activity. *Journal of Pharmacology and Experimental Therapeutics*, 306(1), 124-131.
- Pratt, S., Shepard, R. L., Kandasamy, R. A., Johnston, P. A., Perry, W., & Dantzig, A. H. (2005). The multidrug resistance protein 5 (ABCC5) confers resistance to 5-fluorouracil and transports its monophosphorylated metabolites. In (Vol. 4, pp. 855-863).
- Prime-Chapman, H. M., Fearn, R. A., Cooper, A. E., Moore, V., & Hirst, B. H. (2004). Differential multidrug resistance-associated protein 1 through 6 isoform expression and function in human intestinal epithelial Caco-2 cells [Article]. *Journal of Pharmacology and Experimental Therapeutics*, 311(2), 476-484. <https://doi.org/10.1124/jpet.104.068775>
- Publication of Surgeon General's Report, The Health Consequences of Involuntary Exposure to Tobacco Smoke. (2006). [misc]. *Morbidity and Mortality Weekly Report*, 55(25), 705. <http://ezproxy.aut.ac.nz/login?url=http://search.ebscohost.com/login.aspx?direct=true&db=edsjsr&AN=edsjsr.23316791&site=eds-live>
- Pushpavalli, G., Veeramani, C., & Pugalendi, K. V. (2010). Influence of chrysin on hepatic marker enzymes and lipid profile against d-galactosamine-induced hepatotoxicity rats. *Food and Chemical Toxicology*, 48(6), 1654-1659. <https://doi.org/https://doi.org/10.1016/j.fct.2010.03.040>
- Qu, X., Gao, H., Zhai, J., Sun, J., Tao, L., Zhang, Y., Song, Y., & Hu, T. (2020). *Astragaloside IV enhances cisplatin chemosensitivity in hepatocellular carcinoma by suppressing MRP2* (Vol. 148). Elsevier B.V.
- Quan, E., Wang, H., Dong, D., Zhang, X., & Wu, B. (2015). Characterization of chrysin glucuronidation in UGT1A1-overexpressing HeLa cells: elucidating the transporters responsible for efflux of glucuronide. *Drug Metab Dispos*, 43(4), 433-443. <https://doi.org/10.1124/dmd.114.061598>
- Rabik, C. A., & Dolan, M. E. (2007). Molecular mechanisms of resistance and toxicity associated with platinating agents. *Cancer Treat Rev*, 33(1), 9-23. <https://doi.org/10.1016/j.ctrv.2006.09.006>
- Rabik, C. A., Maryon, E. B., Kasza, K., Shafer, J. T., Bartnik, C. M., & Dolan, M. E. (2009). Role of

- copper transporters in resistance to platinating agents. *Cancer Chemother Pharmacol*, 64(1), 133-142. <https://doi.org/10.1007/s00280-008-0860-1>
- Raymond, E., Chaney, S., Taamma, A., & Cvitkovic, E. (1998). Oxaliplatin: a review of preclinical and clinical studies. *Annals of Oncology*, 9(10), 1053-1071.
- Raymond, E., Chaney, S. G., Taamma, A., & Cvitkovic, E. (1998). Oxaliplatin: a review of preclinical and clinical studies. *Ann Oncol*, 9(10), 1053-1071. <https://www.ncbi.nlm.nih.gov/pubmed/9834817>
- Raymond, E., Faivre, S., Chaney, S., Woynarowski, J., & Cvitkovic, E. (2002a). Cellular and molecular pharmacology of oxaliplatin. In (Vol. 1, pp. 227-235).
- Raymond, E., Faivre, S., Chaney, S., Woynarowski, J., & Cvitkovic, E. (2002b). Cellular and molecular pharmacology of oxaliplatin. *Mol Cancer Ther*, 1(3), 227-235. <https://www.ncbi.nlm.nih.gov/pubmed/12467217>
- Raymond, E., Faivre, S., Woynarowski, J. M., & Chaney, S. G. (1998a). Oxaliplatin: mechanism of action and antineoplastic activity. *Seminars in oncology*, 25(2 Suppl 5), 4-12. <http://europepmc.org/abstract/MED/9609103>
- Raymond, E., Faivre, S., Woynarowski, J. M., & Chaney, S. G. (1998b). Oxaliplatin: mechanism of action and antineoplastic activity. *Semin Oncol*, 25(2 Suppl 5), 4-12. <https://www.ncbi.nlm.nih.gov/pubmed/9609103>
- Rixe, O., Ortuzar, W., Alvarez, M., Parker, R., Reed, E., Paull, K., & Fojo, T. (1996). Oxaliplatin, tetraplatin, cisplatin, and carboplatin: spectrum of activity in drug-resistant cell lines and in the cell lines of the National Cancer Institute's Anticancer Drug Screen panel. *Biochemical Pharmacology*, 52(12), 1855-1865. <http://ezproxy.aut.ac.nz/login?url=http://search.ebscohost.com/login.aspx?direct=true&db=cmedm&AN=8951344&site=eds-live>
- Roberts, A., Brown, H. L., & Jenkins, R. (2015). On the antibacterial effects of manuka honey: mechanistic insights. *Research and Reports in Biology*, 215. <https://doi.org/10.2147/rrb.s75754>
- Roberts, D. L., Williams, K. J., Cowen, R. L., Barathova, M., Eustace, A. J., Brittain-Dissont, S., Tilby, M. J., Pearson, D. G., Ottley, C. J., Stratford, I. J., & Dive, C. (2009). Contribution of HIF-1 and drug penetrance to oxaliplatin resistance in hypoxic colorectal cancer cells. *Br J Cancer*, 101(8), 1290-1297. <https://doi.org/10.1038/sj.bjc.6605311>
- Robey, R. W., Pluchino, K. M., Hall, M. D., Fojo, A. T., Bates, S. E., & Gottesman, M. M. (2018a). Revisiting the role of ABC transporters in multidrug-resistant cancer. *Nat Rev Cancer*. <https://doi.org/10.1038/s41568-018-0005-8>
- Robey, R. W., Pluchino, K. M., Hall, M. D., Fojo, A. T., Bates, S. E., & Gottesman, M. M. (2018b). Revisiting the role of ABC transporters in multidrug-resistant cancer. *Nature Reviews: Cancer*, 18(7), 452-464. <https://doi.org/10.1038/s41568-018-0005-8>
- Rothenberg, M. L., Oza, A. M., Bigelow, R. H., Berlin, J. D., Marshall, J. L., Ramanathan, R. K., Hart, L. L., Gupta, S., Garay, C. A., & Burger, B. G. (2003). Superiority of oxaliplatin and

fluorouracil-leucovorin compared with either therapy alone in patients with progressive colorectal cancer after irinotecan and fluorouracil-leucovorin: interim results of a phase III trial. *Journal of Clinical Oncology*, 21(11), 2059-2069.

- Rothwell, J. A., Perez-Jimenez, J., Neveu, V., Medina-Remon, A., M'Hiri, N., Garcia-Lobato, P., Manach, C., Knox, C., Eisner, R., Wishart, D. S., & Scalbert, A. (2013). Phenol-Explorer 3.0: a major update of the Phenol-Explorer database to incorporate data on the effects of food processing on polyphenol content. *Database*, 2013(0), bat070-bat070. <https://doi.org/10.1093/database/bat070>
- Rothwell, J. A., Urpi-Sarda, M., Boto-Ordoñez, M., Knox, C., Llorach, R., Eisner, R., Cruz, J., Neveu, V., Wishart, D., Manach, C., Andres-Lacueva, C., & Scalbert, A. (2012). Phenol-Explorer 2.0: a major update of the Phenol-Explorer database integrating data on polyphenol metabolism and pharmacokinetics in humans and experimental animals. *Database*, 2012. <https://doi.org/10.1093/database/bas031>
- Ryan, D. P., Hong, T. S., & Bardeesy, N. (2014). Pancreatic adenocarcinoma. *N Engl J Med*, 371(22), 2140-2141. <https://doi.org/10.1056/NEJMc1412266>
- Ryu, J. K., Hong, S. M., Karikari, C. A., Hruban, R. H., Goggins, M. G., & Maitra, A. (2010). Aberrant MicroRNA-155 expression is an early event in the multistep progression of pancreatic adenocarcinoma. *Pancreatology*, 10(1), 66-73. <https://doi.org/10.1159/000231984>
- S, R., C, D., & P, P. (2021). *The rediscovery of platinum-based cancer therapy* (Vol. 21).
- S. L. R. Ellison, & A. Williams. *EURACHEM/CITAC Guide Quantifying Uncertainty in Analytical Measurement* (Third Edition ed.). Eurachem. <https://www.eurachem.org/index.php/publications/guides/quam#translations>
- Salari, N., Faraji, F., Jafarpour, S., Faraji, F., Rasoulpoor, S., Dokaneheifard, S., & Mohammadi, M. (2022). Anti-cancer Activity of Chrysin in Cancer Therapy: a Systematic Review. *Indian J Surg Oncol*, 13(4), 681-690. <https://doi.org/10.1007/s13193-022-01550-6>
- Salphati, L., Lee, L. B., Pang, J., Plise, E. G., & Zhang, X. (2010). Role of P-glycoprotein and breast cancer resistance protein-1 in the brain penetration and brain pharmacodynamic activity of the novel phosphatidylinositol 3-kinase inhibitor GDC-0941. *Drug Metab Dispos*, 38(9), 1422-1426. <https://doi.org/10.1124/dmd.110.034256>
- Saltz, L. B., Clarke, S., Diaz-Rubio, E., Scheithauer, W., Figuer, A., Wong, R., Koski, S., Lichinitser, M., Yang, T. S., Rivera, F., Couture, F., Sirzen, F., & Cassidy, J. (2008). Bevacizumab in combination with oxaliplatin-based chemotherapy as first-line therapy in metastatic colorectal cancer: a randomized phase III study. *J Clin Oncol*, 26(12), 2013-2019. <https://doi.org/10.1200/JCO.2007.14.9930>
- Samimi, G., Katano, K., Holzer, A. K., Safaei, R., & Howell, S. B. (2004). Modulation of the cellular pharmacology of cisplatin and its analogs by the copper exporters ATP7A and ATP7B. *Mol Pharmacol*, 66(1), 25-32. <https://doi.org/10.1124/mol.66.1.25>
- Samimi, G., Safaei, R., Katano, K., Holzer, A. K., Rochdi, M., Tomioka, M., Goodman, M., & Howell, S. B. (2004). Increased expression of the copper efflux transporter ATP7A mediates

- resistance to cisplatin, carboplatin, and oxaliplatin in ovarian cancer cells. *Clin Cancer Res*, 10(14), 4661-4669. <https://doi.org/10.1158/1078-0432.CCR-04-0137>
- Samimi, G., Safaei, R., Katano, K., Holzer, A. K., Rochdi, M., Tomioka, M., Goodman, M., & Howell, S. B. (2004). Increased expression of the copper efflux transporter ATP7A mediates resistance to cisplatin, carboplatin, and oxaliplatin in ovarian cancer cells. *Clinical Cancer Research*, 10(14), 4661-4669.
- Sandusky, G. E., Mintze, K. S., Pratt, S. E., & Dantzig, A. H. (2002). Expression of multidrug resistance-associated protein 2 (MRP2) in normal human tissues and carcinomas using tissue microarrays. *Histopathology*, 41(1), 65-74. <https://www.ncbi.nlm.nih.gov/pubmed/12121239>
- Saris, C., van de Vaart, P. M., Rietbroek, R., & Bloramaert, F. (1996). In vitro formation of DNA adducts by cisplatin, lobaplatin and oxaliplatin in calf thymus DNA in solution and in cultured human cells. *Carcinogenesis*, 17(12), 2763-2769.
- Sarkadi, B., Homolya, L., Szakács, G., & Váradi, A. (2006). Human multidrug resistance ABCB and ABCG transporters: participation in a chemoimmunity defense system. *Physiological reviews*, 86(4), 1179-1236.
- Schick, S., & Glantz, S. (2005). Philip Morris toxicological experiments with fresh sidestream smoke: more toxic than mainstream smoke. *Tobacco Control*, 14(6), 396. <http://ezproxy.aut.ac.nz/login?url=http://search.ebscohost.com/login.aspx?direct=true&db=edb&AN=19298004&site=eds-live>
- Schinkel, A. H., & Jonker, J. W. (2003). Mammalian drug efflux transporters of the ATP binding cassette (ABC) family: an overview. *Advanced drug delivery reviews*, 55(1), 3-29.
- Schwarz, U., Gramatte, T., Krappweis, J., Oertel, R., & Kirch, W. (2000). P-Glycoprotein inhibitor erythromycin increases oral bioavailability of talinolol in humans. *Inter J Clin Pharmacol Ther*, 38(4), 161-167.
- Screnci, D., McKeage, M. J., Galettis, P., Hambley, T. W., Palmer, B. D., & Baguley, B. C. (2000). Relationships between hydrophobicity, reactivity, accumulation and peripheral nerve toxicity of a series of platinum drugs. *Br J Cancer*, 82(4), 966-972. <https://doi.org/10.1054/bjoc.1999.1026>
- SEER Cancer Statistics Review (CSR) 1975-2015. (2018). https://seer.cancer.gov/csr/1975_2015/
- Sekine, T., Miyazaki, H., & Endou, H. (2006). Molecular physiology of renal organic anion transporters. *Am J Physiol Renal Physiol*, 290(2), F251-261. <https://doi.org/10.1152/ajprenal.00439.2004>
- Selby-Pham, S. N. B., Howell, K. S., Dunshea, F. R., Ludbey, J., Lutz, A., & Bennett, L. (2018). Statistical modelling coupled with LC-MS analysis to predict human upper intestinal absorption of phytochemical mixtures. In (Vol. 245, pp. 353-363).
- Sell, S. A., Wolfe, P. S., Spence, A. J., Rodriguez, I. A., McCool, J. M., Petrella, R. L., Garg, K., Ericksen, J. J., & Bowlin, G. L. (2012). A Preliminary Study on the Potential of Manuka Honey and Platelet-Rich Plasma in Wound Healing. *International Journal of Biomaterials*, 2012,

1-14. <https://doi.org/10.1155/2012/313781>

- Seraglio, S. K. T., Schulz, M., Gonzaga, L. V., Fett, R., & Costa, A. C. O. (2021). Current status of the gastrointestinal digestion effects on honey: A comprehensive review. *Food Chemistry*, 357, 129807. <https://doi.org/https://doi.org/10.1016/j.foodchem.2021.129807>
- Shamsudin, S., Selamat, J., Abdul Shomad, M., Ab Aziz, M. F., & Haque Akanda, M. J. (2022). *Antioxidant Properties and Characterization of Heterotrigona itama Honey from Various Botanical Origins according to Their Polyphenol Compounds*.
- Sharma, S., Shah, N. A., Joiner, A. M., Roberts, K. H., & Canman, C. E. (2012). DNA polymerase zeta is a major determinant of resistance to platinum-based chemotherapeutic agents. *Mol Pharmacol*, 81(6), 778-787. <https://doi.org/10.1124/mol.111.076828>
- Shen, D. W., Goldenberg, S., Pastan, I., & Gottesman, M. M. (2000). Decreased accumulation of [14c] carboplatin in human cisplatin-resistant cells results from reduced energy-dependent uptake. *Journal of cellular physiology*, 183(1), 108-116.
- Shen, K., Cui, D., Sun, L., Lu, Y., Han, M., & Liu, J. (2012). Inhibition of IGF-IR increases chemosensitivity in human colorectal cancer cells through MRP-2 promoter suppression. *J Cell Biochem*, 113(6), 2086-2097. <https://doi.org/10.1002/jcb.24080>
- Shitara, Y., Horie, T., & Sugiyama, Y. (2006). Transporters as a determinant of drug clearance and tissue distribution. *Eur J Pharm Sci*, 27(5), 425-446. <https://doi.org/10.1016/j.ejps.2005.12.003>
- Shuzhong, Z., & Marilyn E, M. (2003). Effect of the Flavonoids Biochanin A and Silymarin on the P-Glycoprotein-Mediated Transport of Digoxin and Vinblastine in Human Intestinal Caco-2 Cells. *Pharmaceutical Research*(8), 1184. <http://ezproxy.aut.ac.nz/login?url=http://search.ebscohost.com/login.aspx?direct=true&db=edsovi&AN=edsovi.00006623.200320080.00012&site=eds-live>
- Siddik, Z. H. (2003). Cisplatin: mode of cytotoxic action and molecular basis of resistance. *Oncogene*, 22(47), 7265-7279. <https://doi.org/10.1038/sj.onc.1206933>
- Siegel, R. L., Miller, K. D., & Jemal, A. (2018). Cancer statistics, 2018. *CA Cancer J Clin*, 68(1), 7-30. <https://doi.org/10.3322/caac.21442>
- Siissalo, S., Hannukainen, J., Kolehmainen, J., Hirvonen, J., & Kaukonen, A. M. (2009). A Caco-2 cell based screening method for compounds interacting with MRP2 efflux protein. *Eur J Pharm Biopharm*, 71(2), 332-338. <https://doi.org/10.1016/j.ejpb.2008.08.010>
- Sikic, B. I., Fisher, G. A., Lum, B. L., Halsey, J., Beketic-Oreskovic, L., & Chen, G. (1997). Modulation and prevention of multidrug resistance by inhibitors of P-glycoprotein. *Cancer Chemotherapy And Pharmacology*, 40 Suppl, S13-S19. <http://ezproxy.aut.ac.nz/login?url=http://search.ebscohost.com/login.aspx?direct=true&db=cmedm&AN=9272128&site=eds-live>
- Society, A. C. (2018). *Cancer Statistics Center*. American Cancer Society. https://cancerstatisticscenter.cancer.org/?_ga=2.97211231.1917096062.1531790933-1790028610.1519871633#!/

- Song, I.-S., Savaraj, N., Siddik, Z. H., Liu, P., Wei, Y., Wu, C. J., & Kuo, M. T. (2004). Role of human copper transporter Ctr1 in the transport of platinum-based antitumor agents in cisplatin-sensitive and cisplatin-resistant cells. *Molecular cancer therapeutics*, 3(12), 1543-1549.
- Šošić, D., Richardson, J. A., Yu, K., Ornitz, D. M., & Olson, E. N. (2003). Twist Regulates Cytokine Gene Expression through a Negative Feedback Loop that Represses NF- κ B Activity. *Cell*, 112(2), 169-180. [https://doi.org/10.1016/s0092-8674\(03\)00002-3](https://doi.org/10.1016/s0092-8674(03)00002-3)
- Souglakos, J., Androulakis, N., Syrigos, K., Polyzos, A., Ziras, N., Athanasiadis, A., Kakolyris, S., Tsousis, S., Kouroussis, C., Vamvakas, L., Kalykaki, A., Samonis, G., Mavroudis, D., & Georgoulas, V. (2006). FOLFOXIRI (folinic acid, 5-fluorouracil, oxaliplatin and irinotecan) vs FOLFIRI (folinic acid, 5-fluorouracil and irinotecan) as first-line treatment in metastatic colorectal cancer (MCC): a multicentre randomised phase III trial from the Hellenic Oncology Research Group (HORG). *Br J Cancer*, 94(6), 798-805. <https://doi.org/10.1038/sj.bjc.6603011>
- Sprowl, J. A., Ness, R. A., & Sparreboom, A. (2013). Polymorphic transporters and platinum pharmacodynamics. *Drug Metab Pharmacokinet*, 28(1), 19-27. <https://www.ncbi.nlm.nih.gov/pubmed/22986709>
- St-Pierre, M., Serrano, M., Macias, R., Dubs, U., Hoechli, M., Lauper, U., Meier, P., & Marin, J. (2000). Expression of members of the multidrug resistance protein family in human term placenta. *American Journal of Physiology-Regulatory, Integrative and Comparative Physiology*, 279(4), R1495-R1503.
- Stein, A., & Arnold, D. (2012). Oxaliplatin: a review of approved uses. *Expert Opin Pharmacother*, 13(1), 125-137. <https://doi.org/10.1517/14656566.2012.643870>
- Stompor-Goracy, M., Bajek-Bil, A., & Machaczka, M. (2021). *Chrysin: Perspectives on Contemporary Status and Future Possibilities as Pro-Health Agent* (Vol. 13).
- Surowiak, P., Materna, V., Kaplenko, I., Spaczynski, M., Dolinska-Krajewska, B., Gebarowska, E., Dietel, M., Zabel, M., & Lage, H. (2006). ABCC2 (MRP2, cMOAT) can be localized in the nuclear membrane of ovarian carcinomas and correlates with resistance to cisplatin and clinical outcome. *Clinical Cancer Research*, 12(23), 7149-7158.
- Suzuki, H., & Sugiyama, Y. (2002). Single nucleotide polymorphisms in multidrug resistance associated protein 2 (MRP2/ABCC2): its impact on drug disposition. *Adv Drug Deliv Rev*, 54(10), 1311-1331. <https://www.ncbi.nlm.nih.gov/pubmed/12406647>
- Synold, T. W., Takimoto, C. H., Doroshow, J. H., Gandara, D., Mani, S., Remick, S. C., Mulkerin, D. L., Hamilton, A., Sharma, S., & Ramanathan, R. K. (2007). Dose-escalating and pharmacologic study of oxaliplatin in adult cancer patients with impaired hepatic function: a National Cancer Institute Organ Dysfunction Working Group study. *Clinical Cancer Research*, 13(12), 3660-3666.
- Szakacs, G., Paterson, J. K., Ludwig, J. A., Booth-Genthe, C., & Gottesman, M. M. (2006). Targeting multidrug resistance in cancer. *Nat Rev Drug Discov*, 5(3), 219-234. <https://doi.org/10.1038/nrd1984>

- Tadini-Buoninsegni, F., Bartolommei, G., Moncelli, M. R., Inesi, G., Galliani, A., Sinisi, M., Losacco, M., Natile, G., & Arnesano, F. (2014). Translocation of platinum anticancer drugs by human copper ATPases ATP7A and ATP7B. *Angewandte Chemie International Edition*, 53(5), 1297-1301.
- Takacs, D., Csonka, A., Horvath, A., Windt, T., Gajdacs, M., Riedl, Z., Hajos, G., Amaral, L., Molnar, J., & Spengler, G. (2015). Reversal of ABCB1-related Multidrug Resistance of Colonic Adenocarcinoma Cells by Phenothiazines. *Anticancer Res*, 35(6), 3245-3251. <https://www.ncbi.nlm.nih.gov/pubmed/26026084>
- Tamai, I., & Safa, A. R. (1991). Azidopine noncompetitively interacts with vinblastine and cyclosporin A binding to P-glycoprotein in multidrug resistant cells [Article]. *Journal of Biological Chemistry*, 266(25), 16796-16800. <http://ezproxy.aut.ac.nz/login?url=http://search.ebscohost.com/login.aspx?direct=true&db=edselc&AN=edselc.2-52.0-0025991731&site=eds-live>
- Tan, B., Piwnica-Worms, D., & Ratner, L. (2000). Multidrug resistance transporters and modulation. *Curr Opin Oncol*, 12(5), 450-458. <https://www.ncbi.nlm.nih.gov/pubmed/10975553>
- Tanaka, M., Okazaki, T., Suzuki, H., Abbruzzese, J. L., & Li, D. (2011). Association of multi-drug resistance gene polymorphisms with pancreatic cancer outcome. *Cancer*, 117(4), 744-751. <https://doi.org/10.1002/cncr.25510>
- Taniguchi, K., Wada, M., Kohno, K., Nakamura, T., Kawabe, T., Kawakami, M., Kagotani, K., Okumura, K., Akiyama, S., & Kuwano, M. (1996). A human canalicular multispecific organic anion transporter (cMOAT) gene is overexpressed in cisplatin-resistant human cancer cell lines with decreased drug accumulation. *Cancer Res*, 56(18), 4124-4129. <https://www.ncbi.nlm.nih.gov/pubmed/8797578>
- Tashiro, A., Tatsumi, S., Takeda, R., Naka, A., Matsuoka, H., Hashimoto, Y., Hatta, K., Maeda, K., & Kamoshida, S. (2014). High expression of organic anion transporter 2 and organic cation transporter 2 is an independent predictor of good outcomes in patients with metastatic colorectal cancer treated with FOLFOX-based chemotherapy. *Am J Cancer Res*, 4(5), 528-536. <https://www.ncbi.nlm.nih.gov/pubmed/25232494>
- Taur, J. S., & Rodrigue-Proteau, R. (2008). Effects of dietary flavonoids on the transport of cimetidine via P-glycoprotein and cationic transporters in Caco-2 and LLC-PK1 cell models. In (Vol. 38, pp. 1536-1550).
- Theile, D., Grebhardt, S., Haefeli, W. E., & Weiss, J. (2009). Involvement of drug transporters in the synergistic action of FOLFOX combination chemotherapy. *Biochem Pharmacol*, 78(11), 1366-1373. <https://doi.org/10.1016/j.bcp.2009.07.006>
- Thomas, H., & Coley, H. M. (2003). Overcoming multidrug resistance in cancer: an update on the clinical strategy of inhibiting p-glycoprotein. *Cancer Control*, 10(2), 159-165. <https://doi.org/10.1177/107327480301000207>
- Thomas, S. (2022). *Human microbiome : clinical implications and therapeutic interventions*. Springer. <https://ezproxy.aut.ac.nz/login?url=https://link.springer.com/10.1007/978->

- Tian, C., Ambrosone, C. B., Darcy, K. M., Krivak, T. C., Armstrong, D. K., Bookman, M. A., Davis, W., Zhao, H., Moysich, K., Gallion, H., & DeLoia, J. A. (2012). Common variants in ABCB1, ABCC2 and ABCG2 genes and clinical outcomes among women with advanced stage ovarian cancer treated with platinum and taxane-based chemotherapy: a Gynecologic Oncology Group study. *Gynecol Oncol*, 124(3), 575-581. <https://doi.org/10.1016/j.ygyno.2011.11.022>
- Toh, S., Wada, M., Uchiumi, T., Inokuchi, A., Makino, Y., Horie, Y., Adachi, Y., Sakisaka, S., & Kuwano, M. (1999). Genomic structure of the canalicular multispecific organic anion-transporter gene (MRP2/cMOAT) and mutations in the ATP-binding-cassette region in Dubin-Johnson syndrome. *Am J Hum Genet*, 64(3), 739-746. <https://doi.org/10.1086/302292>
- Torres-Piedra, M., Ortiz-Andrade, R., Villalobos-Molina, R., Singh, N., Medina-Franco, J. L., Webster, S. P., Binnie, M., Navarrete-Vázquez, G., & Estrada-Soto, S. (2010). A comparative study of flavonoid analogues on streptozotocin-nicotinamide induced diabetic rats: quercetin as a potential antidiabetic agent acting via 11beta-hydroxysteroid dehydrogenase type 1 inhibition. *Eur J Med Chem*, 45(6), 2606-2612. <https://doi.org/10.1016/j.ejmech.2010.02.049>
- Tsuji, S., Midorikawa, Y., Takahashi, T., Yagi, K., Takayama, T., Yoshida, K., Sugiyama, Y., & Aburatani, H. (2012). Potential responders to FOLFOX therapy for colorectal cancer by Random Forests analysis. *Br J Cancer*, 106(1), 126-132. <https://doi.org/10.1038/bjc.2011.505>
- Tusnády, G. E., Bakos, É., Váradi, A., & Sarkadi, B. (1997). Membrane topology distinguishes a subfamily of the ATP-binding cassette (ABC) transporters. *FEBS letters*, 402(1), 1-3.
- Uchida, Y., Ohtsuki, S., Katsukura, Y., Ikeda, C., Suzuki, T., Kamiie, J., & Terasaki, T. (2011). Quantitative targeted absolute proteomics of human blood-brain barrier transporters and receptors. *J Neurochem*, 117(2), 333-345. <https://doi.org/10.1111/j.1471-4159.2011.07208.x>
- V, G., C. N, S., L, N., A, R., M. C, A., T. V, K., P. A, P., D, V., K, H., S. C, W., A. P, C., L, Z., C. W, H., D. S, H., T, M., M, P. d. M., T, C., T, K., W. S, C.,...J. A, W. (2018). Gut microbiome modulates response to anti-PD-1 immunotherapy in melanoma patients. *Science*, 359(6371), 97-103. <https://doi.org/10.1126/science.aan4236>
- Vaisman, A., Varchenko, M., Chaney, S. G., Umar, A., Kunkel, T. A., Risinger, J. I., Barrett, J. C., & Hamilton, T. C. (1998). The role of hMLH1, hMSH3, and hMSH6 defects in cisplatin and oxaliplatin resistance: Correlation with replicative bypass of platinum-DNA adducts [Article]. *Cancer Research*, 58(16), 3579-3585. <http://ezproxy.aut.ac.nz/login?url=http://search.ebscohost.com/login.aspx?direct=true&db=edselc&AN=edselc.2-52.0-0032529467&site=eds-live>
- Vaisman, A., Varchenko, M., Umar, A., Kunkel, T. A., Risinger, J. I., Barrett, J. C., Hamilton, T. C., & Chaney, S. G. (1998). The role of hMLH1, hMSH3, and hMSH6 defects in cisplatin and

- oxaliplatin resistance: correlation with replicative bypass of platinum-DNA adducts. *Cancer Res*, 58(16), 3579-3585. <https://www.ncbi.nlm.nih.gov/pubmed/9721864>
- van Engeland, M., Nieland, L. J., Ramaekers, F. C., Schutte, B., & Reutelingsperger, C. P. (1998). Annexin V-affinity assay: a review on an apoptosis detection system based on phosphatidylserine exposure. *Cytometry*, 31(1), 1-9. <https://www.ncbi.nlm.nih.gov/pubmed/9450519>
- Velásquez, P., Valenzuela, L. M., Montenegro, G., Giordano, A., Cabrera-Barjas, G., & Martin-Belloso, O. *k-carrageenan edible films for beef: Honey and bee pollen phenolic compounds improve their antioxidant capacity* (Vol. 124). Elsevier B.V.
- Versantvoort, C. H. M., Broxterman, H. J., Lankelma, J., feller, N., & Pinedo, H. M. (1994). Competitive inhibition by genistein and ATP dependence of daunorubicin transport in intact MRP overexpressing human small cell lung cancer cells. *Biochemical Pharmacology*, 48(6), 1129-1136. [https://doi.org/https://doi.org/10.1016/0006-2952\(94\)90149-X](https://doi.org/https://doi.org/10.1016/0006-2952(94)90149-X)
- Versantvoort, C. H. M., Rhodes, T., & Twentyman, P. R. (1996). Acceleration of MRP-associated efflux of rhodamine 123 by genistein and related compounds. *British Journal of Cancer*, 74(12), 1949-1954. <https://doi.org/10.1038/bjc.1996.658>
- Versantvoort, C. H. M., Schuurhuis, G. J., Pinedo, H. M., Eekman, C. A., Kuiper, C. M., Lankelma, J., & Broxterman, H. J. (1993). Genistein modulates the decreased drug accumulation in non-p-glycoprotein mediated multidrug resistant tumour cells [Article]. *British Journal of Cancer*, 68(5), 939-946. <https://doi.org/10.1038/bjc.1993.458>
- Villar, I. C., Jiménez, R., Galisteo, M., Garcia-Saura, M. F., Zarzuelo, A., & Duarte, J. (2002). *Effects of chronic chrysin treatment in spontaneously hypertensive rats* (Vol. 68).
- Von Hoff, D. D., Ervin, T., Arena, F. P., Chiorean, E. G., Infante, J., Moore, M., Seay, T., Tjulandin, S. A., Ma, W. W., & Saleh, M. N. (2013). Increased survival in pancreatic cancer with nab-paclitaxel plus gemcitabine. *New England Journal of Medicine*, 369(18), 1691-1703.
- Vyara, M., Jessica, F., Riyue, B., Tara, C., Yuanyuan, Z., Maria-Luisa, A., Jason J, L., & Thomas F, G. (2018). The commensal microbiome is associated with anti-PD-1 efficacy in metastatic melanoma patients. *Science*, 359(6371), 104-108. <https://doi.org/10.1126/science.aao3290>
- W, Z., H, Z., Y, Y., J, L., H, L., D, J., Z, C., D, Y., Z, X., & Z, Y. (2016). *Combination of gambogic acid with cisplatin enhances the antitumor effects on cisplatin-resistant lung cancer cells by downregulating MRP2 and LRP expression* (Vol. 2016).
- Wahdan, H. (1998). Causes of the antimicrobial activity of honey. *Infection*, 26(1), 26. <http://ezproxy.aut.ac.nz/login?url=http://search.ebscohost.com/login.aspx?direct=true&db=edb&AN=49979644&site=eds-live>
- Walle, U. K., Galijatovic, A., & Walle, T. (1999). Transport of the flavonoid chrysin and its conjugated metabolites by the human intestinal cell line Caco-2. *Biochem Pharmacol*, 58(3), 431-438. [https://doi.org/10.1016/s0006-2952\(99\)00133-1](https://doi.org/10.1016/s0006-2952(99)00133-1)

- Wang, D., & Lippard, S. J. (2005). Cellular processing of platinum anticancer drugs. *Nat Rev Drug Discov*, 4(4), 307-320. <https://doi.org/10.1038/nrd1691>
- Wang, E. J., Barecki-Roach, M., & Johnson, W. W. (2002). Elevation of P-glycoprotein function by a catechin in green tea. In (Vol. 297, pp. 412-418).
- Wang, H., Li, X., Chen, T., Wang, W., Liu, Q., Li, H., Yi, J., & Wang, J. (2013). Mechanisms of verapamil-enhanced chemosensitivity of gallbladder cancer cells to platinum drugs: glutathione reduction and MRP1 downregulation. *Oncol Rep*, 29(2), 676-684. <https://doi.org/10.3892/or.2012.2156>
- Wang, J., Qiu, J., Dong, J., Li, H., Luo, M., Dai, X., Zhang, Y., Leng, B., Deng, X., Niu, X., & Zhao, S. (2011). *Chrysin protects mice from Staphylococcus aureus pneumonia* (Vol. 111).
- Wang, Y., Kim, N. S., Haince, J.-F., Kang, H. C., David, K. K., Andrabi, S. A., Poirier, G. G., Dawson, V. L., & Dawson, T. M. (2011). Poly(ADP-Ribose) (PAR) Binding to Apoptosis-Inducing Factor Is Critical for PAR Polymerase-1-Dependent Cell Death (Parthanatos). *Science Signaling*, 4(167), ra20-ra20. <https://doi.org/10.1126/scisignal.2000902>
- Washington, C. B., Duran, G. E., Man, M. C., Sikic, B. I., & Blaschke, T. F. (1998). Interaction of anti-HIV protease inhibitors with the multidrug transporter P-glycoprotein (P-gp) in human cultured cells. *Journal Of Acquired Immune Deficiency Syndromes And Human Retrovirology: Official Publication Of The International Retrovirology Association*, 19(3), 203-209. <http://ezproxy.aut.ac.nz/login?url=http://search.ebscohost.com/login.aspx?direct=true&db=cmedm&AN=9803961&site=eds-live>
- WebMD. (2018). *Colorectal cancer Health Center* <https://www.webmd.com/colorectal-cancer/default.htm>
- Weickhardt, A., Wells, K., & Messersmith, W. (2011). Oxaliplatin-induced neuropathy in colorectal cancer. *J Oncol*, 2011, 201593. <https://doi.org/10.1155/2011/201593>
- Wen, X., Buckley, B., McCandlish, E., Goedken, M. J., Syed, S., Pelis, R., Manautou, J. E., & Aleksunes, L. M. (2014). Transgenic expression of the human MRP2 transporter reduces cisplatin accumulation and nephrotoxicity in Mrp2-null mice. *Am J Pathol*, 184(5), 1299-1308. <https://doi.org/10.1016/j.ajpath.2014.01.025>
- Wen, X., Goedken, M. J., Syed, S., Aleksunes, L. M., Buckley, B., McCandlish, E., Pelis, R., & Manautou, J. E. (2014). *Transgenic expression of the human MRP2 transporter reduces cisplatin accumulation and nephrotoxicity in Mrp2-Null mice* (Vol. 184). Elsevier Inc.
- Weng, M. S., Ho, Y. S., & Lin, J. K. (2005). Chrysin induces G1 phase cell cycle arrest in C6 glioma cells through inducing p21Waf1/Cip1 expression: involvement of p38 mitogen-activated protein kinase. *Biochem Pharmacol*, 69(12), 1815-1827. <https://doi.org/10.1016/j.bcp.2005.03.011>
- Wersto, R. P., Chrest, F. J., Leary, J. F., Morris, C., Stetler-Stevenson, M. A., & Gabrielson, E. (2001). Doublet discrimination in DNA cell-cycle analysis. *Cytometry*, 46(5), 296-306. <https://www.ncbi.nlm.nih.gov/pubmed/11746105>

- White, J. W., Jr. (1978). Honey. *Adv Food Res*, 24, 287-374. [https://doi.org/10.1016/s0065-2628\(08\)60160-3](https://doi.org/10.1016/s0065-2628(08)60160-3)
- Wijnholds, J., Mol, C. A. A. M., Deemter, L. v., Haas, M. d., Scheffer, G. L., Baas, F., Beijnen, J. H., Scheper, R. J., Hatse, S., Clercq, E. D., Balzarini, J., & Borst, P. (2000). Multidrug-Resistance Protein 5 Is a Multispecific Organic Anion Transporter Able to Transport Nucleotide Analogs [research-article]. *Proceedings of the National Academy of Sciences of the United States of America*, 97(13), 7476. <http://ezproxy.aut.ac.nz/login?url=http://search.ebscohost.com/login.aspx?direct=true&db=edsjsr&AN=edsjsr.122838&site=eds-live>
- Woynarowski, J. M., Chapman, W. G., Napier, C., Herzig, M. C., & Juniewicz, P. (1998). Sequence and region-specificity of oxaliplatin adducts in naked and cellular DNA. *Molecular Pharmacology*, 54(5), 770-777. <http://ezproxy.aut.ac.nz/login?url=http://search.ebscohost.com/login.aspx?direct=true&db=cmedm&AN=9804612&site=eds-live>
- Wu, C.-P., Calcagno, A. M., Hladky, S. B., Ambudkar, S. V., & Barrand, M. A. (2005). Modulatory effects of plant phenols on human multidrug-resistance proteins 1, 4 and 5 (ABCC1, 4 and 5). *The FEBS Journal*(18), 4725. <http://ezproxy.aut.ac.nz/login?url=http://search.ebscohost.com/login.aspx?direct=true&db=edsovi&AN=edsovi.01217111.200509180.00016&site=eds-live>
- Wu, T., Zhang, Q., Li, J., Chen, H., Wu, J., & Song, H. (2016). Up-regulation of BSEP and MRP2 by Calculus Bovis administration in 17alpha-ethynylestradiol-induced cholestasis: Involvement of PI3K/Akt signaling pathway. *J Ethnopharmacol*, 190, 22-32. <https://doi.org/10.1016/j.jep.2016.05.056>
- Xavier, J. B., Young, V. B., Skufca, J., Ginty, F., Testerman, T., Pearson, A. T., Macklin, P., Mitchell, A., Shmulevich, I., Xie, L., Caporaso, J. G., Crandall, K. A., Simone, N. L., Godoy-Vitorino, F., Griffin, T. J., Whiteson, K. L., Gustafson, H. H., Slade, D. J., Schmidt, T. M.,...Wargo, J. A. (2020). The Cancer Microbiome: Distinguishing Direct and Indirect Effects Requires a Systemic View. *Trends Cancer*, 6(3), 192-204. <https://doi.org/10.1016/j.trecan.2020.01.004>
- Xiang, D., Wang, C.-g., Wang, W.-q., Shi, C.-y., Xiong, W., Wang, M.-d., & Fang, J.-g. (2017). Gastrointestinal stability of dihydromyricetin, myricetin, and myricitrin: an in vitro investigation. *International Journal of Food Sciences & Nutrition*, 68(6), 704-711. <http://ezproxy.aut.ac.nz/login?url=http://search.ebscohost.com/login.aspx?direct=true&db=s3h&AN=123914360&site=eds-live>
- Xie, S. M., Fang, W. Y., Liu, Z., Wang, S. X., Li, X., Liu, T. F., Xie, W. B., & Yao, K. T. (2008). Lentivirus-mediated RNAi silencing targeting ABCC2 increasing the sensitivity of a human nasopharyngeal carcinoma cell line against cisplatin. *J Transl Med*, 6, 55. <https://doi.org/10.1186/1479-5876-6-55>
- Xuan, H. Z., Zhang, J. H., Wang, Y. H., Fu, C. L., & Zhang, W. (2016). Anti-tumor activity evaluation of novel chrysin-organotin compound in MCF-7 cells. *Bioorg Med Chem Lett*, 26(2), 570-574. <https://doi.org/10.1016/j.bmcl.2015.11.072>

- Xue, C., Chen, Y., Hu, D. N., Iacob, C., Lu, C., & Huang, Z. (2016). Chrysin induces cell apoptosis in human uveal melanoma cells via intrinsic apoptosis. *Oncol Lett*, 12(6), 4813-4820. <https://doi.org/10.3892/ol.2016.5251>
- Yang, B., Ma, Y. F., & Liu, Y. (2015). Elevated Expression of Nrf-2 and ABCG2 Involved in Multi-drug Resistance of Lung Cancer SP Cells. *Drug Res (Stuttg)*, 65(10), 526-531. <https://doi.org/10.1055/s-0034-1390458>
- Yang, J., Parsons, J., Nicolay, N. H., Caporali, S., Harrington, C. F., Singh, R., Finch, D., D'Atri, S., Farmer, P. B., Johnston, P. G., McKenna, W. G., Dianov, G., & Sharma, R. A. (2010). Cells deficient in the base excision repair protein, DNA polymerase beta, are hypersensitive to oxaliplatin chemotherapy. *Oncogene*, 29(3), 463-468. <https://doi.org/10.1038/onc.2009.327>
- Yang, S., Wu, S., Huang, Y., Shao, Y., Chen, X. Y., Xian, L., Zheng, J., Wen, Y., Chen, X., Li, H., & Yang, C. (2012). Screening for oesophageal cancer. *Cochrane Database Syst Rev*, 12, CD007883. <https://doi.org/10.1002/14651858.CD007883.pub2>
- Yates, M. S., & Kensler, T. W. (2007). Keap1 eye on the target: chemoprevention of liver cancer. *Acta Pharmacol Sin*, 28(9), 1331-1342. <https://doi.org/10.1111/j.1745-7254.2007.00688.x>
- Yilmaz, M. A., Temel, H., Cakir, O., Ertas, A., Yener, I., Akdeniz, M., Altun, M., Demirtas, I., & Boga, M. (2018). A comprehensive LC-MS/MS method validation for the quantitative investigation of 37 fingerprint phytochemicals in Achillea species: A detailed examination of *A. coarctata* and *A. monocephala* [Article]. *Journal of Pharmaceutical and Biomedical Analysis*, 154, 413-424. <https://doi.org/10.1016/j.jpba.2018.02.059>
- Yin, M., Yan, J., Martinez-Balibrea, E., Graziano, F., Lenz, H. J., Kim, H. J., Robert, J., Im, S. A., Wang, W. S., Etienne-Grimaldi, M. C., & Wei, Q. (2011). ERCC1 and ERCC2 polymorphisms predict clinical outcomes of oxaliplatin-based chemotherapies in gastric and colorectal cancer: a systemic review and meta-analysis. *Clin Cancer Res*, 17(6), 1632-1640. <https://doi.org/10.1158/1078-0432.CCR-10-2169>
- Yokoo, S., Yonezawa, A., Masuda, S., Fukatsu, A., Katsura, T., & Inui, K. (2007). Differential contribution of organic cation transporters, OCT2 and MATE1, in platinum agent-induced nephrotoxicity. *Biochem Pharmacol*, 74(3), 477-487. <https://doi.org/10.1016/j.bcp.2007.03.004>
- Yokooji, T., Murakami, T., Yumoto, R., Nagai, J., & Takano, M. (2007). Site-specific bidirectional efflux of 2,4-dinitrophenyl-S-glutathione, a substrate of multidrug resistance-associated proteins, in rat intestine and Caco-2 cells. *J Pharm Pharmacol*, 59(4), 513-520. <https://doi.org/10.1211/jpp.59.4.0005>
- Yonezawa, A., Masuda, S., Yokoo, S., Katsura, T., & Inui, K.-i. (2006). Cisplatin and oxaliplatin, but not carboplatin and nedaplatin, are substrates for human organic cation transporters (SLC22A1-3 and multidrug and toxin extrusion family). *Journal of Pharmacology and Experimental Therapeutics*, 319(2), 879-886.
- Yonezawa, A., Masuda, S., Yokoo, S., Katsura, T., & Inui, K. (2006). Cisplatin and oxaliplatin, but not carboplatin and nedaplatin, are substrates for human organic cation transporters

- (SLC22A1-3 and multidrug and toxin extrusion family). *J Pharmacol Exp Ther*, 319(2), 879-886. <https://doi.org/10.1124/jpet.106.110346>
- Yoshitomi, S., Ikemoto, K., Takahashi, J., Miki, H., Namba, M., & Asahi, S. (2001). Establishment of the transformants expressing human cytochrome P450 subtypes in HepG2, and their applications on drug metabolism and toxicology. *Toxicol In Vitro*, 15(3), 245-256. <https://www.ncbi.nlm.nih.gov/pubmed/11377097>
- Yupanqui Mieves, J., Vyas, C., Aslan, E., Humphreys, G., Diver, C., & Bartolo, P. (2022). Honey: An Advanced Antimicrobial and Wound Healing Biomaterial for Tissue Engineering Applications. *Pharmaceutics*, 14(8). <https://doi.org/10.3390/pharmaceutics14081663>
- Zaanan, A., Williet, N., Hebbar, M., Dabakuyo, T. S., Fartoux, L., Mansourbakht, T., Dubreuil, O., Rosmorduc, O., Cattan, S., Bonnetain, F., Boige, V., & Taïeb, J. (2013). Gemcitabine plus oxaliplatin in advanced hepatocellular carcinoma: a large multicenter AGEO study. *J Hepatol*, 58(1), 81-88. <https://doi.org/10.1016/j.jhep.2012.09.006>
- Zahid H, S. (2003). Cisplatin: mode of cytotoxic action and molecular basis of resistance. *Oncogene*(47), 7265. <http://ezproxy.aut.ac.nz/login?url=http://search.ebscohost.com/login.aspx?direct=true&db=edsovi&AN=edsovi.00006374.200322470.00003&site=eds-live>
- Zamek-Gliszczyński, M. J., Xiong, H., Patel, N. J., Turncliff, R. Z., Pollack, G. M., & Brouwer, K. L. (2003). Pharmacokinetics of 5 (and 6)-carboxy-2',7'-dichlorofluorescein and its diacetate promoiety in the liver. *J Pharmacol Exp Ther*, 304(2), 801-809. <https://doi.org/10.1124/jpet.102.044107>
- Zaniboni, A., & Meriggi, F. (2005). The emerging role of oxaliplatin in the treatment of gastric cancer. *J Chemother*, 17(6), 656-662. <https://doi.org/10.1179/joc.2005.17.6.656>
- Zelcer, N., Huisman, M. T., Reid, G., Wielinga, P., Breedveld, P., Kuil, A., Knipscheer, P., Schellens, J. H., Schinkel, A. H., & Borst, P. (2003). Evidence for two interacting ligand binding sites in human multidrug resistance protein 2 (ATP binding cassette C2). *J Biol Chem*, 278(26), 23538-23544. <https://doi.org/10.1074/jbc.M303504200>
- Zhang, S., Lovejoy, K. S., Shima, J. E., Lagpacan, L. L., Shu, Y., Lapuk, A., Chen, Y., Komori, T., Gray, J. W., Chen, X., Lippard, S. J., & Giacomini, K. M. (2006). Organic cation transporters are determinants of oxaliplatin cytotoxicity. *Cancer Res*, 66(17), 8847-8857. <https://doi.org/10.1158/0008-5472.CAN-06-0769>
- Zhang, S., & Morris, M. E. (2003). Effect of the Flavonoids Biochanin A and Silymarin on the P-Glycoprotein-Mediated Transport of Digoxin and Vinblastine in Human Intestinal Caco-2 Cells. *Pharmaceutical Research*(8), 1184. <http://ezproxy.aut.ac.nz/login?url=http://search.ebscohost.com/login.aspx?direct=true&db=edsovi&AN=edsovi.00006623.200320080.00012&site=eds-live>
- Zhong, D. T., Wu, R. P., Wang, X. L., Huang, X. B., Lin, M. X., Lan, Y. Q., & Chen, Q. (2015). Combination Chemotherapy with S-1 and Oxaliplatin (SOX) as First-Line Treatment in Elderly Patients with Advanced Gastric Cancer. *Pathol Oncol Res*, 21(4), 867-873. <https://doi.org/10.1007/s12253-015-9903-1>

Zhou, S.-F., Wang, L.-L., Di, Y. M., Xue, C. C., Duan, W., Li, C. G., & Li, Y. (2008). Substrates and Inhibitors of Human Multidrug Resistance Associated Proteins and the Implications in Drug Development. *Current Medicinal Chemistry*, 15(20), 1981-2039. <https://doi.org/10.2174/092986708785132870>

Appendix

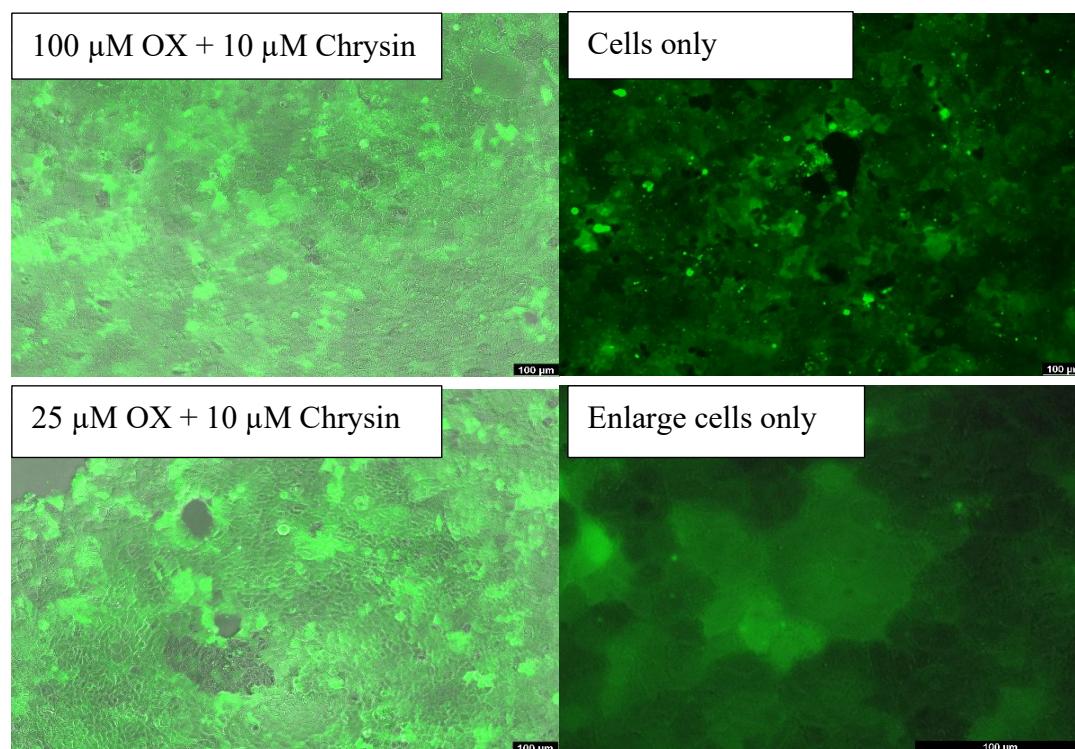


Figure A1 Fluorescent images for CDCF accumulation in Caco-2 cell lines

Caco-2 cells were treated with 10 μM chrysin for 30 mins before adding oxaliplatin of different concentrations (0, 25, 100 μM), after coincubation 2 hours, cells were incubated with drug free complete medium for 24 hours. Following incubation, the cells were washed once with warm phosphate-buffered saline (PBS) and subsequently treated in triplicate with 100 μL of phenol red-free RPMI medium containing chrysin at increasing concentrations; control wells received only phenol red-free RPMI medium. After a 30-minute incubation period, 100 μL of 3 μM CellEvent™ Caspase-3/7 Detection Reagent solution was added to each well, and the plates were incubated for an additional 30 minutes while protected from light to prevent photobleaching. The cells were then placed on ice and washed twice with 200 μL of ice-cold PBS to remove excess dye and inhibitors, followed by fixation with 100 μL of 1% paraformaldehyde (PFM) added to each well. Fluorescent images were captured utilizing a Leica DMI8 inverted fluorescence microscope (Leica Microsystems, GmbH) equipped with a GFP filter and a SPOT RT digital camera to visually assess intracellular fluorescence distribution.



Figure A2. Original chemiluminescent western blotting image to detect ABCC2 in HEK293-ABCC2 cells.